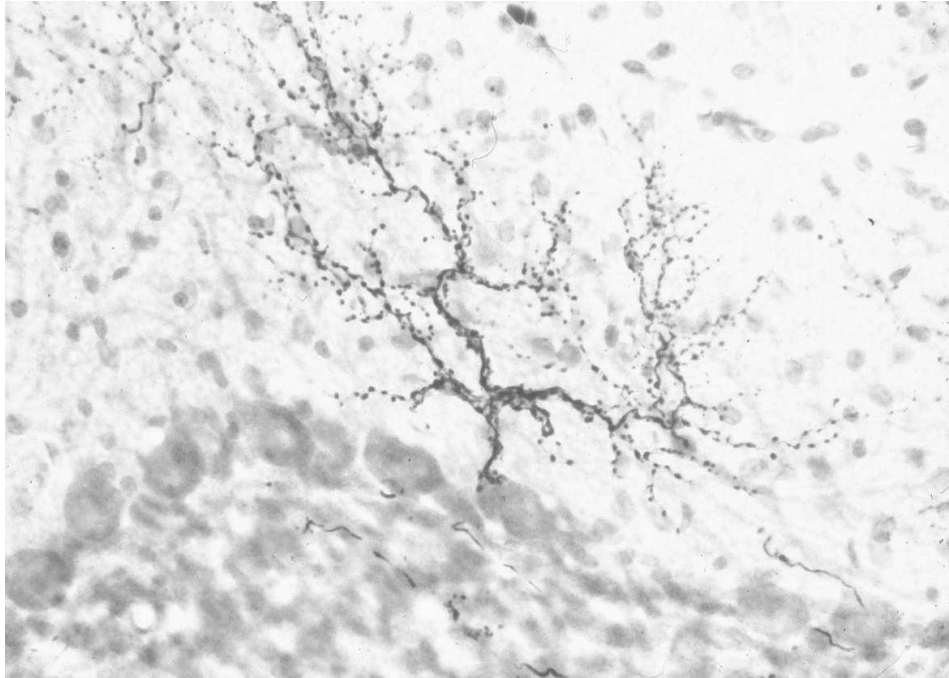


Functional Anatomy Of The Intermediate Cerebellum In The Rat



Angelique Pijpers

Functional Anatomy Of The Intermediate Cerebellum In The Rat

Functionele anatomie van het intermediaire cerebellum van de rat

Proefschrift

ter verkrijging van de graad van doctor aan de
Erasmus Universiteit Rotterdam
op gezag van de rector magnificus
Prof.dr. S.W.J. Lamberts
en volgens het besluit van het College voor Promoties.

De openbare verdediging zal plaatsvinden op
woensdag 10 januari 2007 om 15.45 uur

door

Wilhelmina Catharina Theodora Maria Pijpers

geboren te Nieuw - Ginneken

Promotiecommissie:

Promotor: Prof.dr. C.I. de Zeeuw

Overige leden: Prof.dr. M.A. Frens
Prof.dr. G. van Rij
Dr. R. Apps

Copromotor: Dr. T.J.H. Ruigrok

Voor tante Duul

Table of contents

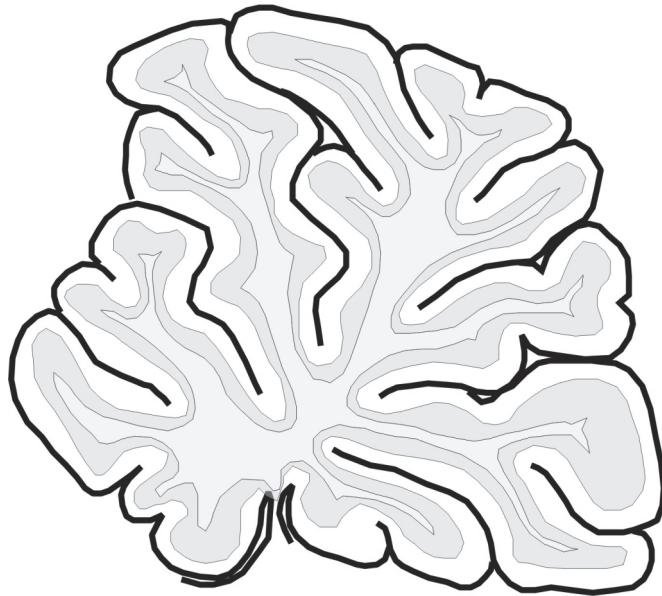
Chapter 1	General introduction	7
	1.1 Introducing the cerebellum	
	1.2 The cells that make up the cerebellum	
	1.3 Afferent connections to the cerebellum	
	1.4 Efferent connections from the cerebellum	
	1.5 Cerebellar organization, modules and function	
	1.6 Aims of this thesis	
Chapter 2	Topography of olivo-cortico-nuclear modules in the intermediate cerebellum of the rat	25
Chapter 3	Organization of pontocerebellar projections to identified climbing fiber zones in the rat	61
Chapter 4	Precise spatial relationships between mossy fibers and climbing fibers in rat cerebellar cortical zones	91
Chapter 5	Cerebellar zones involved in rat hind limb control; a retrograde transneuronal tracing study with rabies virus	125
Chapter 6	Selective impairment of the C1 module involved in rat hind limb control has specific effects on locomotion	165
Chapter 7	General discussion	197
	7.1 Introduction	
	7.2 Organization of olivo-cortico-nuclear projections in the intermediate cerebellum	
	7.3 Relation of mossy fiber organization with the cerebellar modular concept	

- 7.4 Cerebellar modules associated to single muscles
- 7.5 The C1 module and adaptive control of reflex modulation
- 7.6 Future experiments and final conclusion

Summary	209
Samenvatting	213
Dankwoord	217
Curriculum Vitae	219
List of publications	221

Chapter 1

General Introduction



1.1 Introducing the cerebellum

The cerebellum is situated in the posterior part of the skull, dorsal to the brainstem and pontine nuclei (Fig.1). Despite the fact that it is called “little brain” it harbors about half of the total number of neurons within the central nervous system (Kandel, 2003). The cerebellum is divided into an anterior lobe and a posterior lobe by the deep primary fissure. In addition, the posterior lobe is separated from the flocculonodular lobe by the posterolateral fissure. Transverse (interlobular) fissures divide the cerebellum further into 10 lobules (numbered I to X; Larsell, 1952; Larsell and Jansen, 1970). These lobules can be further sub divided by a various amount of foliation according to species (Figure 1). From medial to lateral, the cerebellum is divided into a vermis and a laterally positioned hemisphere. Amongst the two the paravermis or intermediate cerebellum is located, the organization and function of which will be the focus of this thesis.

The cerebellum consists of a superficially located cortex, which, due to the impressive foliations reaches an enormous surface in the human. Deep in the white matter of the cerebellum the cerebellar nuclei are located which provide the output of the cerebellum. The cerebellum is connected to the brainstem by three cerebellar peduncles (superior, middle and inferior). Afferent connections (see 1.3) are found in all three peduncles and contact neurons located in the cerebellar cortex and/or the cerebellar nuclei (see 1.2 and 1.4). Efferent fibers leave the cerebellum via the superior cerebellar peduncle or via the uncinata tracts. The Purkinje cell layer of the flocculonodular lobe projects directly to the vestibular nuclei.

Functionally, the cerebellum is divided into three regions; the phylogenetically oldest one presumably is the vestibulocerebellum, which more or less equals the flocculonodular lobe, and is involved in controlling balance and eye movements. The second part anatomically consists of the vermis and paravermis and is referred to as the spinocerebellum due to the fact that it receives abundant somatosensory input from the spinal cord. It is thought to be mostly involved in reflexive and/or unconsciously executed motor control of the striated muscles. Finally, the cerebrocerebellum, consisting of most of the hemispheres, is phylogenetically the youngest addition to the cerebellum and receives its input almost exclusively related to and from the cerebral cortex. It is concerned with the planning, coordination and learning of complex movements but has also been implicated in cognitive functions (Schmahmann, 1991; Gao et al., 1996).

In the following paragraphs the cells that make up the cerebellum, their in- and output relations and their possible functions will be addressed.

1.2 The cells that make up the cerebellum

The cerebellar cortex

The cerebellar cortex (Fig. 2) has a remarkably uniform internal structure, which is divided into three layers with a core of white matter. From superficial to deep, these are the molecular layer, the Purkinje cell layer and the granular layer. Each of these layers contains specific type(s) of neurons and Santiago Ramon y Cajal (1888; 1911), using Golgi's staining techniques, was the first to provide a complete description of the histology of the cerebellar cortex.

The molecular layer predominantly consists of the distal T-parts of the bifurcation of ascending segments of the axons of granule cells, which themselves, are located in the granular layer, a.k.a. the parallel fibers. These parallel fibers run along the long axis of the folia, and in the rat, the length of a parallel fiber may be as long as up to 4.6-5.0mm (Brand et al, 1976; Schild, 1980; Mugnaini, 1983). In addition, two types of inhibitory interneurons are found in the molecular layer; the stellate- and basket cells. Both of these cell types receive excitatory input from the parallel fibers. However, whereas the stellate cells have short axons that contact the more distal dendrites of nearby Purkinje cells (PCs), the basket cells have longer axons that contact the proximal parts of PCs (particularly of its soma and axon hillock) that are located anterior and posterior to the parallel fiber beam (Ito, 1984). Basket cells furthermore receive recurrent collaterals from PCs, climbing fibers, and other stellate- and basket cells (Palay and Chan Palay, 1977). Together with the Golgi cells (see below), these small-type interneurons are thought to act as inhibitory feedback and feedforward loops regulating activity levels of the granule- and Purkinje cells.

The Purkinje cells are the largest neurons found within the cerebellar cortex and are arranged into a single layer. They constitute the sole output cells of the cerebellar cortex. The dendritic tree of the PC extends into the molecular layer and is oriented perpendicular to the course of the parallel fibers. The soma and the proximal dendrites of the PCs are relatively smooth and the distal dendrites bear long-necked spines (Fox and Barnard, 1957). Each PC of the rat receives excitatory inputs from up to 175,000 parallel fibers, from one or two ascending segments of granule cell axons (Napper and Harvey, 1988; Gundappa-Sulur et al., 1999) and from a single climbing fiber (the latter originating from the contralateral inferior olive see 1.3). Parallel fibers synapse on the spiny branchlets whereas the climbing fiber terminates (climbs into) on the cell body and main dendrite. Purkinje cell axons are myelinated and course through the granular layer to terminate within the cerebellar nuclei or, in case of the PCs of the vestibulocerebellum, on the vestibular nuclei, both on the ipsilateral side (Klimhoff, 1899). A single PC is likely to contact approximately 30-50 different cerebellar nucleus cells (Chan-Palay, 1977). In addition to these projections, they give rise to recurrent collaterals terminating on neighboring PCs in a so-called plexiform layer and on basket cells in the molecular layer. Most of these collateral

arborizations are located in the same plane as the dendritic tree of the PC (so perpendicular to the long axis of the folia). The PCs are inhibitory and use GABA as a transmitter (Ito et al., 1964). Wedged between the somata of the PCs are the candelabrum cells. Although, little is known about these cells they appear to influence the dendritic trunks of neighboring PCs (Laine and Axelrad, 1994). The physiological characteristics of PCs are well studied. To an important extent this is due to the fact that they respond in a very characteristic way (i.e. the complex spike) to discharges of their climbing fiber. Activation by way of the parallel fibers result in normal or so-called simple spikes. The average resting discharge of simple spikes is quite high (about 50 Hz and up to 100 Hz), whereas the complex spike rate averages only 1-2 Hz. Interactions between parallel fiber and climbing fiber systems have been shown to result in long term changes in synaptic efficacy of both systems and may form the basis of cerebellar learning (Ito, 1998; Hansel and Linden, 2000).

The inner most granular layer consists of a large amount of various neurons. By far, the most abundant are the small, densely packed, granule cells. Together with the unipolar brush cells (another type of interneuron, located predominantly in the vestibulocerebellum) they are the only excitatory interneurons in the cerebellar cortex. The 3-4 short dendrites of granule cells receive excitatory input from several mossy fibers (see 1.3) and, when present, from mossy fiber-like terminals derived from unipolar brush cells. They receive inhibitory inputs from recurrent PC collaterals and Golgi cells. Its axon can be divided into two (possibly functional distinct) parts that both contact the PCs; It consists of an ascending segment and bifurcates in the molecular layer to give rise to the two ends of a parallel fiber that run in opposite direction. Each granule cell therefore contacts hundreds of PCs. In addition, axon collaterals synaps on Lugaro cells and basket neurons.

The Lugaro cells are another type of interneurons located mainly just below the Purkinje cell layer (Lugaro, 1894; Voogd et al, 1994). They receive excitatory, serotonergic input and appear to inhibit mainly the interneurons in the molecular layer (Laine and Axelrad, 1998; Dieudonne, 2001). In addition, they receive inhibitory input by recurrent PC collaterals. Lugaro cells further contact virtually every other type of cell found in the cerebellar cortex (Dieudonne and Dumoulin, 2000; Melik-Musyan and Fanardzhyan, 2004).

This uniform pattern of basic cerebellar architecture indicates that the cerebellum performs its role in quite different functions using a similar operation and that the specific identity of a particular part of the cerebellum is mainly if not exclusively determined by highly organized input-output relations. Therefore, the topographical relations of in- and outputs will determine the functional identity of different cerebellar areas.

The cerebellar nuclei

The cerebellar nuclei are situated in the roof of the fourth ventricle and form, apart from those Purkinje cells that target the vestibular nuclei, the sole output station of the cerebellum. For the rat they were originally described by Goodman et al. (1963) and further detailed by Korneliussen (1968) and by Buisseret-Delmas and Angaut (1993). In general they are divided into three main parts, which can be referred to as the medial, interposed and lateral cerebellar nuclei. Each can be further subdivided, but here the description will be limited to the nuclei that are relevant for this thesis (e.g. connected to the paravermis). The dorsolateral protuberance (DLP) is a part of the medial cerebellar nucleus (MCN) and it receives some PC input from the paravermis. The interposed nucleus is usually further divided into an anterior and posterior part (AIN and PIN), as they have different connections and functions. Wedged in the white matter between MCN and both interposed nuclei are the interstitial cell groups (ICG). Finally, the dorsolateral hump (DLH) more or less forms a conspicuous bulge that marks the transition between the interposed nuclei and the lateral cerebellar nucleus (LCN).

The cerebellar nuclei consist of small, inhibitory neurons and excitatory neurons of various sizes, which show a mixed distribution (Batini et al., 1992; Teune et al., 1995). The inhibitory neurons, project predominantly to the inferior olive (De Zeeuw et al., 1989; Fredette and Mugnaini, 1991; Batini et al., 1992; Teune et al., 1995). On the other hand, the larger excitatory neurons project to all other targets but the inferior olive (Tolbert et al., 1980; Teune et al., 1995; Teune et al., 2000, also see 1.4). Some of these neurons in addition send collaterals to the cerebellar cortex (Tolbert et al., 1976; Buisseret-Delmas and Angaut, 1988).

As mentioned earlier, the input from to the cerebellar nuclei is mostly derived from the PCs. A single PC can innervate both non-GABAergic as well as GABAergic projection neurons (Teune et al., 1998). Apart from the inhibitory input from PCs, excitatory inputs are provided by collaterals of the mossy and climbing fibers (van der Want et al., 1987; van der Want et al., 1989b; van der Want et al., 1989a; Ruigrok and Voogd, 2000).

1.3 Afferent connections to the cerebellum

Input to the cerebellum is provided by three afferent systems. The mossy fiber and climbing fiber systems are generally regarded as the major afferent systems. They are supplemented by monoaminergic inputs, which are likely to play important modulatory roles.

The climbing fiber system; the olivary connection

The inferior olive (IO), located ventromedially in the caudal part of the medulla oblongata, is the sole source of climbing fibers (Desclin, 1974). Each olivary axon branches into 8-10 terminal

branches that each 'climb' into a single PC (Sugihara et al., 2001). In addition, collaterals are sent to the cerebellar and part of the vestibular nuclei (Ruigrok, 1997; Ruigrok and Voogd, 2000). The inferior olivary complex is assembled of several subnuclei, which was first noted by Kooy (1916). However, here the descriptions of the rat olivary complex as provided by Bernard (1987) and Azizi and Woodward (1987) are used to give an overview of its structure (also see Ruigrok, 2004). The subdivisions of the rat inferior olive (IO) are schematically shown in Figure 3. The IO can be divided into three major subdivisions; the medial accessory olive (MAO), the dorsal accessory olive (DAO) and the principle olive (PO), each of which can be further subdivided. These subnuclei each receive their own specific (direct or indirect) ascending and descending inputs from many different sources, such as the spinal cord, several brain stem nuclei, and the cerebral cortex (see Fig. 3, based on Azizi and Woodward, 1987; also see: Ruigrok, 2004; Sugihara and Shinoda, 2004). In addition, all receive recurrent collaterals from the cerebellar- or specific parts of the vestibular nuclei (Ruigrok and Voogd, 1990). The efferent connections of the inferior olive show a highly specific and conspicuous organization that will be further detailed in 1.5.

Although a complete description of the ultra structure of the IO goes beyond the scope of this thesis, some aspects will be pointed out here (for review see De Zeeuw et al., 1989; De Zeeuw et al., 1998). In the rat two morphologically distinct types of olivary neurons can be found, each with a specific dendritic architecture that is covered with simple and complex appendages. These dendritic spines of up to six different neurons form clusters, that are contacted by axon terminals and the whole is called a glomerulus. Through dendrodendritic gap junctions olivary neurons are electrotonically coupled to each other (Bernardo and Foster, 1986; Sotelo et al., 1986). The interplay of a number of highly specific voltage-dependent ion channels that are likely to be unevenly distributed over the cellular membrane, the glomerular substrate, and electrotonic coupling, warrants highly complex electrophysiological characteristics (e.g. see Crill, 1970; Llinás and Yarom, 1981; Ruigrok and Voogd, 1995). Furthermore, activation of a climbing fiber results in strong excitations of the PCs they innervate, which respond with a complex spike and a change in the interaction with other PC inputs. Although normally, parallel fiber input to the PC elicits simple spikes, this response is suppressed after climbing fiber activation (Armstrong et al., 1979).

Despite detailed knowledge of the structure and connections of the IO and its effect on PCs, its functional role is still open to debate (e.g. see Simpson et al., 1996; Apps and Garwicz, 2005).

The mossy fiber system

The other major input to the cerebellar cortex is provided by the mossy fibers, which derive their name from the conspicuously shaped terminals (mossy fiber rosettes) that terminate on granule cells and local interneurons. The organization of the mossy fiber system appears less structured

than that of the climbing fiber system. For example they originate from many parts of the central nervous system such as the pontine nuclei, trigeminal complex, lateral reticular nucleus, dorsal column nuclei and the spinal cord (for review see Ruigrok, 2004). Also, individual fibers are characterized by a diverging pattern of projections, e.g. single mossy fibers not only collateralize along the parasagittal axis, but also in the mediolateral direction and even to the contralateral side (Mihailoff, 1993; Wu et al., 1999; Serapide et al., 2001; Sultan, 2001; Ruigrok, 2003). Mossy fiber receptive fields are usually described in terms of patches or short stripes, which are arranged as multiple somatotopically related aggregates over the cerebellar cortex. This concept has become known as the fractionated somatotopy of the cerebellar cortex (Welker, 1987). As yet, the relation between the organization of the mossy fiber systems and that of the climbing fibers remains unclear and was one of the topics of this thesis.

Monoaminergic afferents

The monoaminergic inputs to the cerebellum predominantly make use of serotonergic and noradrenergic projections, although possibly a dopaminergic input might be present as well (Panagopoulos et al., 1991). In the rat, the serotonergic fibers originating from the medullary and pontine reticular formation (two brainstem structures) terminate predominantly as a layer beneath the PC layer (Anden et al., 1967; Bishop et al., 1985). Noradrenergic fibers terminate in all layers of the cerebellar cortex and originate from the dorsal part of the locus coeruleus (Grzanna and Fritschy, 1991). In addition, the serotonergic system, and possibly the noradrenergic system, provides an input to the cerebellar nuclei and inferior olive (Landis et al., 1975; Takeuchi et al., 1982). All monoaminergic inputs are most likely involved in modulatory processes (van Neerven et al., 1990; Strahlendorf et al., 1991; André et al., 1993; André et al., 1995).

1.4 Efferent connections from the cerebellum

As mentioned in paragraph 1.2, apart from those Purkinje cells projecting to the vestibular nuclei, the cerebellar nuclei form the sole output stations of the cerebellum. In general, they target various structures in the brain stem, spinal cord and thalamus (Teune et al., 2000; Voogd, 2004). Again, a detailed description will be limited to those nuclei that are relevant to the paravermis (see Fig. 3).

The DLP in general projects to the thalamus and the reticular formation where the projections extend into the pons and the mesencephalon, contacting the deep mesencephalic nucleus, the interstitial nucleus, the periaqueductal gray matter and the superior colliculus (Bentivoglio and Kuypers, 1982; Teune et al., 2000).

The ICG has overlapping projections with other cerebellar nuclei to the medial reticular formation, vestibular nuclei, spinal cord and thalamus (Bentivoglio and Kuypers, 1982; Buisseret-Delmas et al., 1998; Teune et al., 2000; Voogd, 2004). Olivary projections are directed to the intermediate part of the MAO (Ruigrok and Voogd, 1990).

The PIN has a very prominent projection to the rostral part of the MAO (Ruigrok and Voogd, 2000). Furthermore, it projects to the red nucleus, periaqueductal gray matter, the deep mesencephalic nucleus, superior colliculus, the subparafascicular nucleus, the zona incerta and several thalamic areas (Daniel et al., 1988; Teune et al., 2000).

The AIN projects predominantly to the magnocellular part of the red nucleus, the nucleus reticularis tegmentum pontis as well as to the basilar pons, various thalamic nuclei, and to the ipsilateral bulbar reticular formation. Connections to the inferior olive reach the DAO (Daniel et al., 1988; Ruigrok and Voogd, 1990; Teune et al., 2000).

The DLH is specifically well developed in rodents (Voogd, 2004) and is connected to the lateral parvicellular formation, the pontine reticular formation, the trigeminal nucleus, the red nucleus, the nucleus reticularis tegmentum pontis, the deep mesencephalic nucleus, the anterior pretectal nucleus, the thalamus and the DM group of the inferior olive (Woodson and Angaut, 1984; Teune et al., 2000; Ruigrok 2004).

1.5 Cerebellar organization, modules and function

As has been mentioned in paragraph 1.2 the basic cerebellar architecture is characteristically uniform (Ramón y Cajal, 1888). However, it is also known for quite some time that the functional diversity of the cerebellum is related to specific cerebellar regions (Dow and Moruzzi, 1958). Therefore, the functions of the cerebellum in its different roles, for instance in motor movements, classical conditioning or cognition, are likely to be governed by a similar set of operations (Holmes, 1939; Ito, 1984; Middleton and Strick, 1998; Yeo and Hesslow, 1998; Gottwald et al., 2004; Ito, 2006). Consequently, highly organized input-output relations mainly, if not exclusively, determine the specific identity of a particular part of the cerebellum. Jan Voogd was the first to recognize that longitudinally arranged zones of the cerebellar Purkinje cells, termed A, B, C1, C2, C3 and D, project to specific parts of the cerebellar nuclei (Voogd, 1964). This scheme was validated by observations that within the organization of olivocerebellar climbing fibers a similar zonal pattern could be recognized (Groenewegen and Voogd, 1977; Groenewegen et al., 1979). Hence, longitudinal arrays of matching olivo-cortico-nuclear projections gave rise to the concept of cerebellar modules (Voogd and Bigaré, 1980). Nuclear collaterals of the climbing fibers as well as the olivary projections from the cerebellar nuclei seem to fully follow the olivo-cortico-nuclear organization (Ruigrok and Voogd, 1990; Ruigrok, 1997; Ruigrok and Voogd, 2000). Further

validation of the modular concept was found in the near-identical organization of receptive fields characteristics of the climbing fiber system (Oscarsson, 1980; for recent review, see Apps and Garwicz, 2005). Later studies also provided definitions of additional zones such as the X zone and CX zone (Buisseret-Delmas et al., 1993) or of subzones (Voogd and Ruigrok, 2004). Although initially the modular organization was mostly studied in cat, recent studies in rat are in full accordance with this concept and appear to provide additional detail (e.g. see Pardoe and Apps, 2002; Sugihara and Shinoda, 2004; Voogd and Ruigrok, 2004). It will be obvious that the cerebellar (and to some extent also vestibular) nuclei are actually at the heart of the modular concept. Since these nuclei all have a specific combination of targets in the brain stem and thalamus (Teune et al., 2000) they constitute the specific output stations of the various modules (see Fig. 4).

The basic modular arrangement as observed in the rat is shown in Figures 3 and 4. In the vermis, the A, X, and B zones are distinguished that, by definition project to MCN, ICG and lateral vestibular nucleus, respectively. They receive climbing fiber input from respectively the caudal part of MAO, the intermediate part of MAO and the dorsal fold of DAO (Voogd and Ruigrok, 2004). In the paravermis, the C1, CX, C2 and C3 zones are located and in the hemispheres the D zones (D1, D0 and D2) are found but their precise relation with inferior olive and cerebellar nuclei are debated (Ruigrok and Voogd, 1990; Buisseret-Delmas and Angaut, 1993; Buisseret-Delmas et al., 1993; Ruigrok, 1997; Ruigrok and Voogd, 2000). Concluding, the highly organized input-output relations of each of these zones determine their functional roles and as a whole they are called modules, which possibly reflect the functional entities of the cerebellum (Oscarsson, 1980). Individual modules are supposedly linked by the parallel fibers, which run perpendicular to these modules (see Fig.4).

The interactions between the transversally oriented parallel fibers and the longitudinally oriented climbing fibers at the Purkinje cell dendrite, would allow parallel processing of information derived from different mossy fiber inputs (either from local or non-local mossy fibers via the granule cell-parallel fiber system) with a supposed 'error' or 'teaching' signal from the inferior olive. These interactions may result in long-term changes in synaptic efficacy of these inputs and are thought to be at the heart of cerebellar functioning (Marr, 1969; Albus, 1971; Ito, 1984). In the paravermis, both afferent systems that converge on a PC to a point have similar or related peripheral receptive fields from the extremities (Brown and Bower, 2001; Ekerot and Jorntell, 2001). However, mossy fiber input is usually modality related, whereas climbing fiber input is multi-modal (i.e. no convergence vs. convergence of tactile and nociceptive skin afferents and muscle afferents (Ekerot et al., 1987b; Ekerot et al., 1987a; Bloedel and Bracha, 1995; Jorntell et al., 1996; Bosco and Poppele, 2001). Together, they are thought to control sequences of muscle activations and to detect errors in a motor frame of reference (Bastian et al., 2000; Cooper et al., 2000; Martin et al., 2000). However, the specific functions of individual modules are still unclear.

1.6 Aims of this thesis

Although a lot is already known about cerebellar architecture and its partition into modules and mechanisms of cortical information processing, available data is still not sufficient to explain their function(s) (e.g. see Ito, 2006). Open questions are mainly concern:

- 1) To what extent do climbing fibers branch to different rostrocaudal parts within the same zone, or to different mediolateral zones that belong to the same modular group?
- 2) What is the relation of the mossy fiber system with the modular system of olivo-cortico-nuclear connections?
- 3) What is the relation between cerebellar modular output and peripheral structures such as individual muscles?
- 4) What do individual cerebellar modules control?

In this thesis several new techniques were used to investigate these problems in the paravermis of the rat. In all experiments, the intrinsic and fixed pattern of zebrin-positive and –negative Purkinje cells (Hawkes and Leclerc, 1987) proved to be extremely useful as a frame of reference (Voogd et al., 2003; Voogd and Ruigrok, 2004). By preparing a detailed unfolded surface reconstruction of the cerebellar cortex that included this pattern of zebrin-banding connectivity patterns could be evaluated between animals. E.g. using this standard pattern, the resultant climbing fiber collateral labeling and branching was investigated that resulted from small injections with biotinilated dextran amine (BDA) into those parts of the inferior olivary complex that give rise to climbing fiber projections to the paravermal zones of the cerebellum, thus providing detailed information on open question 1. Furthermore, by combining olivary injections with BDA with injections of gold-lectin into the interposed nuclei and zebrin immunohistochemistry, this triple labeling technique provided the first direct anatomical evidence of cerebellar modular connectivity (*Chapter 2: Pijpers et al., 2005*).

In order to better understand the relation between the organizations of mossy fiber and climbing fiber systems (question 2), small injections of cholera toxin subunit b (CTb) were made in the cerebellar cortex of the posterior lobe. Many of these injections were placed under physiological guidance (Atkins and Apps, 1997). By correlating the distribution of retrogradely labeled neurons in the inferior olive and basal pontine nuclei, lobular and to a certain extent also zonal differences in pontocerebellar projections were established (*Chapter 3: Pijpers and Ruigrok, 2006*). The above mentioned injections of CTb into physiologically- and zebrin- identified zones within the posterior cerebellum also enables labeling of the collaterals of mossy and climbing fibers that terminate within the injection site (Voogd et al., 2003). Using this technique we have examined the precise relation of mossy and climbing fiber collateral branching and also related them to the zebrin-banding pattern. These studies clearly show that the mossy fiber system also has a high

level of organization that in many ways, but not completely, resembles the climbing fiber organization (*Chapter 4: Pijpers et al. accepted*).

From the above, the modular concept of cerebellar connections has gained further validation, specifically for the paravermal zones. However, which and how these modules participate in the control of muscles is still not clear. To study which cerebellar modules are involved in the control of individual muscles (question 3) we have, in collaboration with Patrice Coulon (Marseille) injected rabies virus into selected hind limb muscles. Rabies virus is able to distribute itself through connected neurons by retrograde transport and multiplication. In this way, we have shown for the first time that specific and identified complete and partial cerebellar zones located in vermal, paravermal and hemispherical parts of the cerebellum all are involved in the control of a single muscle (*Chapter 5: Ruigrok et al, submitted*). These data suggest that individual zones may control separate qualities of muscle control.

In order to begin assessing these qualities (question 4), we have developed a new technique to lesion selective modules with a targeted toxin (CTb-Saporin). Subsequently, we have investigated the effects on hind limb locomotion after lesions of the C1 zone of the copula pyramidis that is known to be involved in hind limb control and show that this module may be specifically involved in controlling modulation of reflexes during locomotion (*Chapter 6: Pijpers et al., in preparation*).

References

- Albus JS (1971) A theory on cerebellar function. *Math Biosci* 10:25-61.
- Anden NE, Fuxe K, Ungerstedt U (1967) Monoamine pathways to the cerebellum and cerebral cortex. *Experientia* 23:838-839.
- André P, Pompeiano O, White S (1993) Activation of muscarinic receptors induces a long-lasting enhancement of purkinje cell responses to glutamate. *Brain Res* 617:28-36.
- André P, Pompeiano O, White SR (1995) Role of muscarinic receptors in the cerebellar control of the vestibulospinal reflex gain: cellular mechanisms. *Acta Otolaryngol* 520:87-91.
- Apps R, Garwicz M (2005) Anatomical and physiological foundations of cerebellar information processing. *Nat Rev Neurosci* 6:297-311.
- Armstrong DM, Cogdell B, Harvey RJ (1979) Discharge patterns of Purkinje cells in cats anaesthetized with alpha-chloralose. *J Physiol* 291:351-366.
- Atkins MJ, Apps R (1997) Somatotopical organisation within the climbing fibre projection to the paramedian lobule and copula pyramidis of the rat cerebellum. *J Comp Neurol* 389:249-263.
- Azizi SA, Woodward DJ (1987) Inferior olivary nuclear complex of the rat: morphology and comments on the principles of organization within the olivocerebellar system. *J Comp Neurol* 263:467-484.
- Batini C, Compoin C, Buisseret-Delmas C, Daniel H, Guegan M (1992) Cerebellar nuclei and the nucleocortical projections in the rat: retrograde tracing coupled to GABA and glutamate immunohistochemistry. *J Comp Neurol* 315:74-84.
- Bentivoglio M, Kuypers HGJM (1982) Divergent axon collaterals from rat cerebellar nuclei to diencephalon, mesencephalon, medulla oblongata and cervical cord. *Exp Brain Res* 46:339-356.
- Bernard J-F (1987) Topographical organization of olivocerebellar and corticonuclear connections in the rat - An WGA-HRP study: I. Lobules IX, X and the flocculus. *J Comp Neurol* 263:241-258.
- Bishop GA, Ho RH, King JS (1985) An immunohistochemical study of serotonin development in the opossum cerebellum. *Anat Embryol* 171:325-338.
- Bloedel JR, Bracha V (1995) On the cerebellum, cutaneomuscular reflexes, movement control and the elusive engrams of memory. *Behavioural Brain Research* 68:1-44.
- Bosco G, Poppele RE (2001) Proprioception from a spinocerebellar perspective. *Physiol Rev* 81:539-568.
- Brown IE, Bower JM (2001) Congruence of mossy fiber and climbing fiber tactile projections in the lateral hemispheres of the rat cerebellum. *J Comp Neurol* 429:59-70.
- Buisseret-Delmas C, Angaut P (1988) The cerebellar nucleo-cortical projections in the rat. A retrograde labeling study using horseradish peroxidase combined to a lectin. *Neurosci Letters* 84:255-260.
- Buisseret-Delmas C, Angaut P (1993) The cerebellar olivo-cortico-nuclear connections in the rat. *Progr Neurobiol* 40:63-87.
- Buisseret-Delmas C, Yatim N, Buisseret P, Angaut P (1993) The X zone and CX subzone of the cerebellum in the rat. *Neurosci Res* 16:195-207.
- Buisseret-Delmas C, Angaut P, Compoin C, Diagne M, Buisseret P (1998) Brainstem efferents from the interface between the nucleus medialis and the nucleus interpositus in the rat. *J Comp Neurol* 402:264-275.
- Chan-Palay V (1977) Cerebellar dentate nucleus: organization, cytology and transmitters. Berlin: Springer-Verlag.
- Crill WE (1970) Unitary multiple-spiked responses in cat inferior olivary nucleus. *J Physiol (Lond)* 199-209.
- Daniel H, Angaut P, Batini C, Billard JM (1988) Topographic organization of the interpositorubral connections in the rat. A WGA-HRP study. *Behav Brain Res* 28:69-70.
- De Zeeuw CI, Holstege JC, Ruigrok TJH, Voogd J (1989) Ultrastructural study of the GABAergic, cerebellar and mesodiencephalic innervation of the cat medial accessory olive: anterograde tracing combined with immunocytochemistry. *J Comp Neurol* 284:12-35.
- De Zeeuw CI, Simpson JI, Hoogenraad CC, Galjart N, Koekkoek SKE, Ruigrok TJH (1998) Microcircuitry and function of the inferior olive. *Trends Neurosci* 21:391-400.
- Desclin JC (1974) Histological evidence supporting the inferior olive as the major source of cerebellar climbing fibers in the rat. *Brain Res* 77:365-388.
- Dieudonne S (2001) Serotonergic neuromodulation in the cerebellar cortex: cellular, synaptic, and molecular basis. *Neuroscientist* 7:207-219.
- Dieudonne S, Dumoulin A (2000) Serotonin-driven long-range inhibitory connections in the cerebellar cortex. *J Neurosci* 20:1837-1848.
- Dow RS, Moruzzi G (1958) The physiology and pathology of the cerebellum. Minneapolis: University of Minnesota Press.
- Ekerot CF, Jorntell H (2001) Parallel fibre receptive fields of Purkinje cells and interneurons are climbing fibre-specific. *Eur J Neurosci* 13:1303-1310.
- Ekerot C-F, Oscarsson O, Schouenborg J (1987a) Stimulation of cat cutaneous nociceptive C fibres causing tonic and synchronous activity in climbing fibres. *J Physiol (Lond)* 386:539-546.
- Ekerot C-F, Gustavsson P, Oscarsson O, Schouenborg J (1987b) Climbing fibres projecting to cat cerebellar anterior lobe activated by cutaneous A and C fibres. *J Physiol (Lond)* 386:529-538.
- Fredette BJ, Mugnaini E (1991) The GABAergic cerebello-olivary projection in the rat. *Anat Embryol* 184:225-243.
- Gao J-H, Parsons L, Bower JM, Xiong J, Li J, Fox PT (1996) Cerebellum implicated in sensory acquisition and discrimination rather than motor control. *Science* 272:545-547.
- Gottwald B, Wilde B, Mihajlovic Z, Mehdorn HM (2004) Evidence for distinct cognitive deficits after focal cerebellar lesions. *J Neurol Neurosurg Psychiatry* 75:1524-1531.
- Groenewegen HJ, Voogd J (1977) The parasagittal zonation within the olivocerebellar projection. I. Climbing fiber distribution in the vermis of cat cerebellum. *J Comp Neurol* 174:417-488.

- Groenewegen HJ, Voogd J, Freedman SL (1979) The parasagittal zonation within the olivocerebellar projection. II. Climbing fiber distribution in the intermediate and hemispheric parts of cat cerebellum. *J Comp Neurol* 183:551-601.
- Grzanna R, Fritschy JM (1991) Efferent projections of different subpopulations of central noradrenaline neurons. *Prog Brain Res* 88:89-101.
- Gundappa-Sulur G, De Schutter E, Bower JM (1999) Ascending granule cell axon: an important component of cerebellar cortical circuitry. *J Comp Neurol* 408:580-596.
- Hansel C, Linden DJ (2000) Long-term depression of the cerebellar climbing fiber-Purkinje neuron synapse. *Neuron* 26:473-482.
- Hawkes R, Leclerc N (1987) Antigenic map of the rat cerebellar cortex: the distribution of parasagittal bands as revealed by monoclonal anti-Purkinje cell antibody mabQ113. *J Comp Neurol* 256:29-41.
- Holmes G (1939) The cerebellum of man. *Brain* 62:1-30.
- Ito M (1984) The cerebellum and neural control. New York: Raven press.
- Ito M (1998) Cerebellar learning in the vestibulo-ocular reflex. *Trends Cogn Sci* 2:313-321.
- Ito M (2006) Cerebellar circuitry as a neuronal machine. *Prog Neurobiol* 78:272-303.
- Ito M, Yoshida M, Obata K (1964) Monosynaptic inhibition of the intracerebellar nuclei induced from the cerebellar cortex. *Experientia* 20:575-576.
- Jorntell H, Garwicz M, Ekerot CF (1996) Relation between cutaneous receptive fields and muscle afferent input to climbing fibres projecting to the cerebellar C3 zone in the cat. *Eur J Neurosci* 8:1769-1779.
- Kooy FH (1916) The inferior olive in vertebrates. *Folia Neurobiol* 10:205-369.
- Korneliusson HK (1968) On the morphology and subdivision of the cerebellar nuclei of the rat. *J Hirnsforsch* 10:109-122.
- Laine J, Axelrad H (1994) The candelabrum cell: a new interneuron in the cerebellar cortex. *J Comp Neurol* 339:159-173.
- Laine J, Axelrad H (1998) Lugaro cells target basket and stellate cells in the cerebellar cortex. *Neuroreport* 9:2399-2403.
- Landis SC, Shoemaker WJ, Schlumpf M, Bloom FE (1975) Catecholamines in mutant mouse cerebellum: fluorescence microscopic and chemical studies. *Brain Res* 93:253-266.
- Larsell O (1970) The comparative anatomy and histology of the cerebellum from Monotremes through Apes. Minneapolis: The University of Minnesota Press.
- Llinás R, Yarom Y (1981) Properties and distribution of ionic conductances generating electroresponsiveness of mammalian inferior olivary neurones *in vitro*. *J Physiol (Lond)* 315:569-584.
- Marr D (1969) A theory of cerebellar cortex. *J Physiol (Lond)* 202:437-470.
- Melik-Musyan AB, Fanardzhyan VV (2004) Morphological characteristics of Lugaro cells in the cerebellar cortex. *Neurosci Behav Physiol* 34:633-638.
- Middleton FA, Strick PL (1998) The cerebellum: an overview. *Trends Neurosci* 21:367-369.
- Mihailoff G (1993) Cerebellar nuclear projections from the basilar pontine nuclei and nucleus reticularis tegmenti pontis as demonstrated with PHA-L tracing in the rat. *J Comp Neurol* 330:130-146.
- Napper RM, Harvey RJ (1988) Number of parallel fiber synapses on an individual Purkinje cell in the cerebellum of the rat. *J Comp Neurol* 274:168-177.
- Oscarsson O (1980) Functional organization of olivary projections to the cerebellar anterior lobe. In: The inferior olivary nucleus, anatomy and physiology (Courville J, de Montigny C, Lamarre Y, eds), pp 279-289. New York: Raven Press.
- Panagopoulos NT, Papadopoulos GC, Matsokis NA (1991) Dopaminergic innervation and binding in the rat cerebellum. *Neurosci Lett* 130:208-212.
- Pardoe J, Apps R (2002) Structure-function relations of two somatotopically corresponding regions of the rat cerebellar cortex: olivo-cortico-nuclear connections. *Cerebellum* 1:165-184.
- Pijpers A, Ruigrok TJ (2006) Organization of pontocerebellar projections to identified climbing fiber zones in the rat. *J Comp Neurol* 496:513-528.
- Pijpers A, Voogd J, Ruigrok TJ (2005) Topography of olivo-cortico-nuclear modules in the intermediate cerebellum of the rat. *J Comp Neurol* 492:193-213.
- Ramón y Cajal S (1888) Sobre las fibras nerviosas de la capa molecular del cerebelo. *Rev Trimest Histol* 2:33-41.
- Ramón y Cajal S (1911) *Histologie du système nerveux de l'homme et des vertébrés*. Paris: Maloine.
- Ruigrok TJ (2003) Collateralization of climbing and mossy fibers projecting to the nodulus and flocculus of the rat cerebellum. *J Comp Neurol* 466:278-298.
- Ruigrok TJ, Voogd J (2000) Organization of projections from the inferior olive to the cerebellar nuclei in the rat. *J Comp Neurol* 426:209-228.
- Ruigrok TJH (1997) Cerebellar nuclei: the olivary connection. In: The cerebellum: from structure to control (De Zeeuw CI, Strata P, Voogd J, eds), pp 162-197. Elsevier Science B.V.
- Ruigrok TJH (2004) Precerebellar nuclei and red nucleus. In: The rat nervous system, third edition (Paxinos G, ed), pp 167-204. San Diego: Elsevier Academic Press.
- Ruigrok TJH, Voogd J (1990) Cerebellar nucleo-olivary projections in rat. An anterograde tracing study with *Phaseolus vulgaris*-leucoagglutinin (PHA-L). *J Comp Neurol* 298:315-333.
- Ruigrok TJH, Voogd J (1995) Cerebellar influence on olivary excitability in the cat. *Eur J Neurosci* 7:679-693.
- Schmahmann JD (1991) An emerging concept. The cerebellar contribution to higher function. *Arch Neurol* 48:1178-1187.
- Serapide MF, Panto MR, Parenti R, Zappala A, Cicirata F (2001) Multiple zonal projections of the basilar pontine nuclei to the cerebellar cortex of the rat. *J Comp Neurol* 430:471-484.
- Simpson JI, Wylie DR, De Zeeuw CI (1996) On climbing fiber signals and their consequence(s). *Behav Brain Sci* 19:384-398.
- Strahlendorf JC, Lee M, Strahlendorf HK (1991) Serotonin modulates muscimol- and baclofen-elicited inhibition of cerebellar Purkinje cells. *Eur J Pharmacol* 201:239-242.
- Sugihara I, Shinoda Y (2004) Molecular, topographic, and functional organization of the cerebellar cortex: a study with combined aldolase C and olivocerebellar labeling. *J Neurosci* 24:8771-8785.

- Sugihara I, Wu HS, Shinoda Y (2001) The entire trajectories of single olivocerebellar axons in the cerebellar cortex and their contribution to Cerebellar compartmentalization. *J Neurosci* 21:7715-7723.
- Sultan F (2001) Distribution of mossy fibre rosettes in the cerebellum of cat and mice: evidence for a parasagittal organization at the single fibre level. *Eur J Neurosci* 13:2123-2130.
- Takeuchi Y, Kimura H, Sano Y (1982) Immunohistochemical demonstration of serotonin-containing nerve fibers in the cerebellum. *Cell Tissue Res* 226:1-12.
- Teune TM, Van der Burg J, Ruigrok TJH (1995) Cerebellar projections to the red nucleus and inferior olive originate from separate populations of neurons in the rat. A non-fluorescent double labeling study. *Brain Res* 673:313-319.
- Teune TM, van der Burg J, De Zeeuw CI, Voogd J, Ruigrok TJH (1998) Single Purkinje cell can innervate multiple classes of projection neurons in the cerebellar nuclei of the rat: a light microscopic and ultrastructural triple-tracer study in the rat. *J Comp Neurol* 392:164-178.
- Teune TM, van der Burg J, van der Moer J, Voogd J, Ruigrok TJH (2000) Topography of cerebellar nuclear projections to the brain stem in the rat. In: *Cerebellar modules: molecules, morphology and function* (Gerrits NM, Ruigrok TJH, De Zeeuw CI, eds), pp 141-172. Amsterdam: Elsevier Science B.V.
- Tolbert DL, Bantli H, Bloedel JR (1976) Anatomical and physiological evidence for a cerebellar nucleocortical projection in the cat. *Neuroscience* 1:205-217.
- Tolbert DL, Bantli H, Hames EG, Ebner TJ, McMullen TA, Bloedel JR (1980) A demonstration of the dentato-reticulospinal projection in the cat. *Neuroscience* 5:1479-1488.
- van der Want JLL, Gerrits NM, Voogd J (1987) Autoradiography of mossy fiber terminals in the fastigial nucleus of the cat. *J Comp Neurol* 258:70-80.
- van der Want JLL, Wiklund L, Guegan M, Ruigrok T, Voogd J (1989a) Anterograde tracing of the rat olivocerebellar system with *Phaseolus vulgaris*-leucoagglutinin (PHA-L). Demonstration of climbing fiber collateral innervation of the cerebellar nuclei. *J Comp Neurol* 288:1-18.
- van der Want JLL, Guegan M, Wiklund L, Buisseret-Delmas C, Ruigrok TJH, Voogd J (1989b) Climbing fibre "collateral" innervation of the central cerebellar nuclei studied with anterograde *Phaseolus vulgaris*-leucoagglutinin (PHA-L) labelling. In: *The olivocerebellar system in motor control* (Strata P, ed), pp 82-85. Berlin: Springer-Verlag.
- van Neerven J, Pompeiano O, Collewyn H, van der Steen J (1990) Injections of beta-noradrenergic substances in the flocculus of rabbits affect adaptation of the VOR gain. *Exp Brain Res* 79:249-260.
- Voogd J (1964) The cerebellum of the cat: Structure and fiber connections. Assen: Van Gorcum.
- Voogd J (2004) Cerebellum. In: *The rat nervous system, third edition* (Paxinos G, ed), pp 205-242. San diego: Elsevier Academic Press.
- Voogd J, Bigaré F (1980) Topographical distribution of olivary and cortico nuclear fibers in the cerebellum: a review. In: *The inferior olivary nucleus. Anatomy and physiology* (Courville J, de Montigny C, Lamarre Y, eds), pp 207-234. New York: Raven Press.
- Voogd J, Ruigrok TJ (2004) The organization of the corticonuclear and olivocerebellar climbing fiber projections to the rat cerebellar vermis: the congruence of projection zones and the zebrin pattern. *J Neurocytol* 33:5-21.
- Voogd J, Pardoe J, Ruigrok TJ, Apps R (2003) The distribution of climbing and mossy fiber collateral branches from the copula pyramidis and the paramedian lobule: congruence of climbing fiber cortical zones and the pattern of zebrin banding within the rat cerebellum. *J Neurosci* 23:4645-4656.
- Welker W (1987) Spatial organization of somatosensory projections to granule cell cerebellar cortex: functional and connectional implications of fractured somatotopy (summary of Wisconsin studies). In: *New concepts in cerebellar neurobiology* (King JS, ed), pp 239-280. New York: Alan R. Liss, Inc.
- Wu HS, Sugihara I, Shinoda Y (1999) Projection patterns of single mossy fibers originating from the lateral reticular nucleus in the rat cerebellar cortex and nuclei. *J Comp Neurol* 411:97-118.
- Yeo CH, Hesslow G (1998) Cerebellum and conditioned responses. *Trends Neurosci* 2:322-330.

Figures

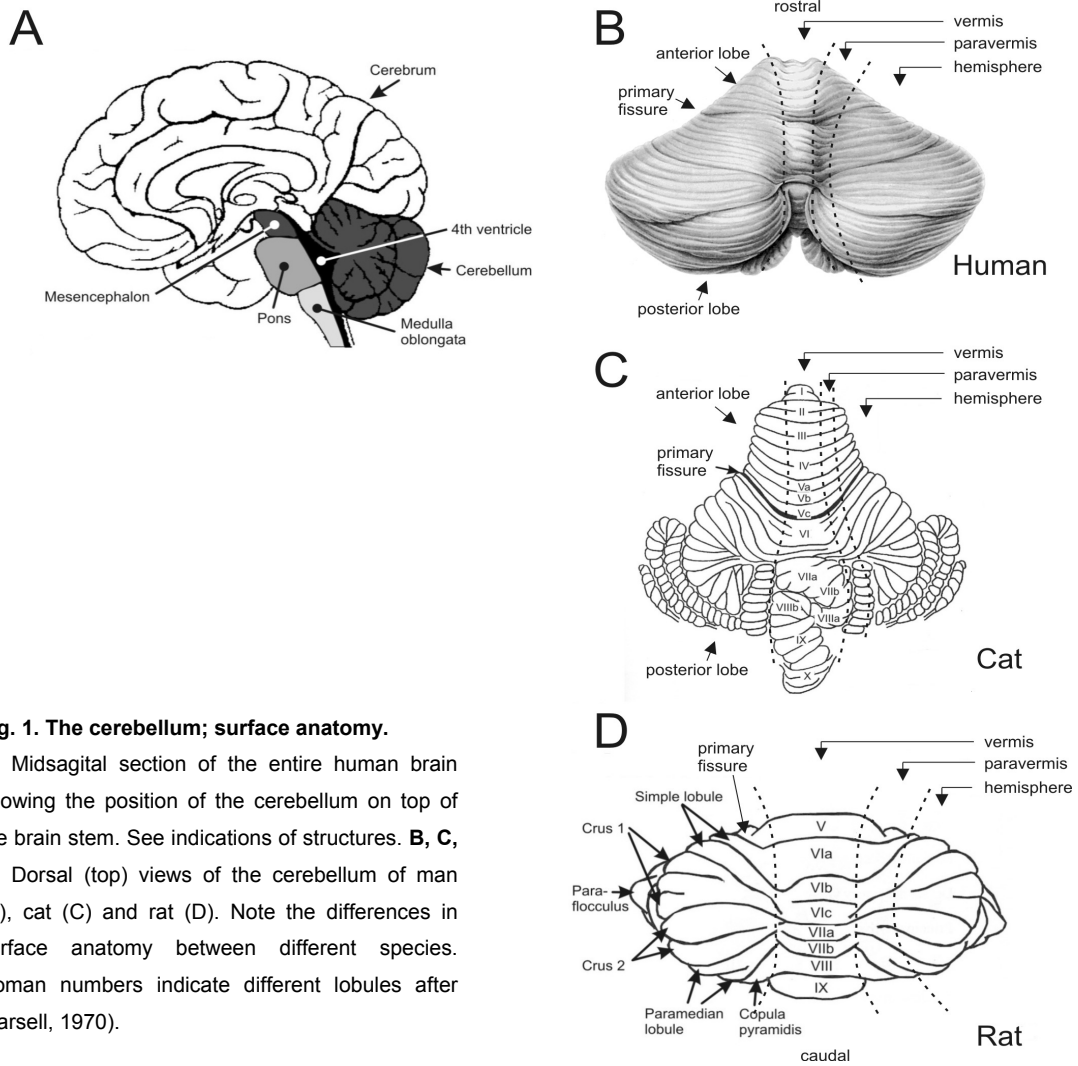


Fig. 1. The cerebellum; surface anatomy.

A: Midsagittal section of the entire human brain showing the position of the cerebellum on top of the brain stem. See indications of structures. **B, C, D:** Dorsal (top) views of the cerebellum of man (B), cat (C) and rat (D). Note the differences in surface anatomy between different species. Roman numbers indicate different lobules after (Larsell, 1970).

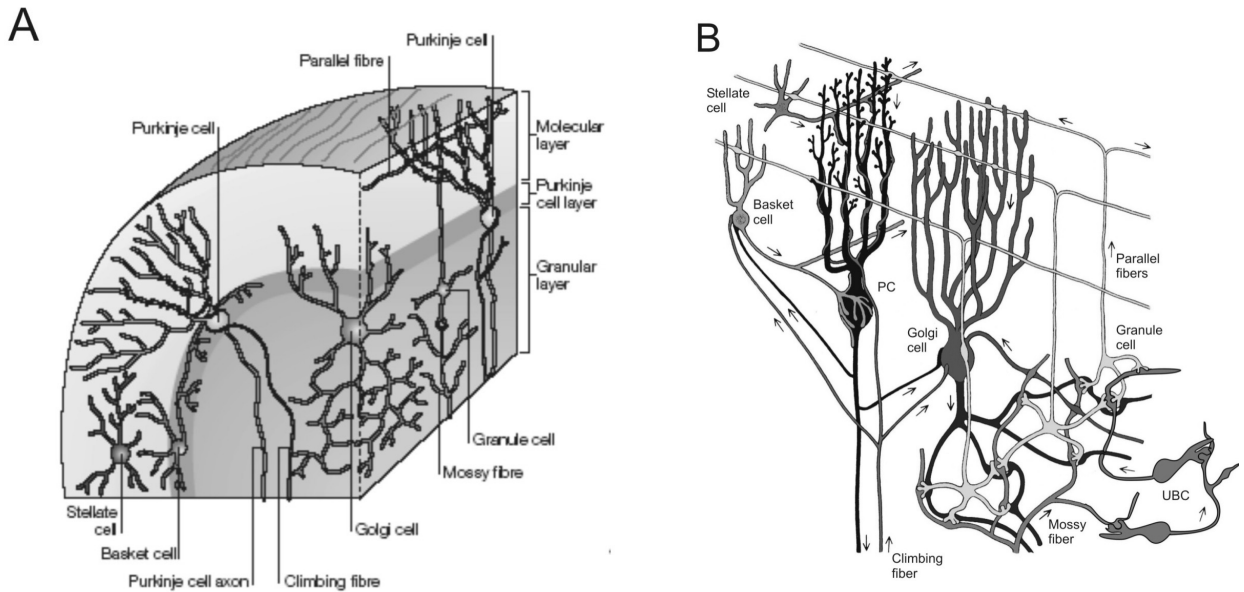


Fig. 2

Fig. 2. Detailed anatomy of the cerebellar cortex.

A. Global anatomy of the layers of the cerebellar cortex (from Apps and Garwicz, 2005). **B.** Schematic diagram of the cerebellar cortex showing the connections with the interneurons (after Ruigrok and Simpson, unpublished data).

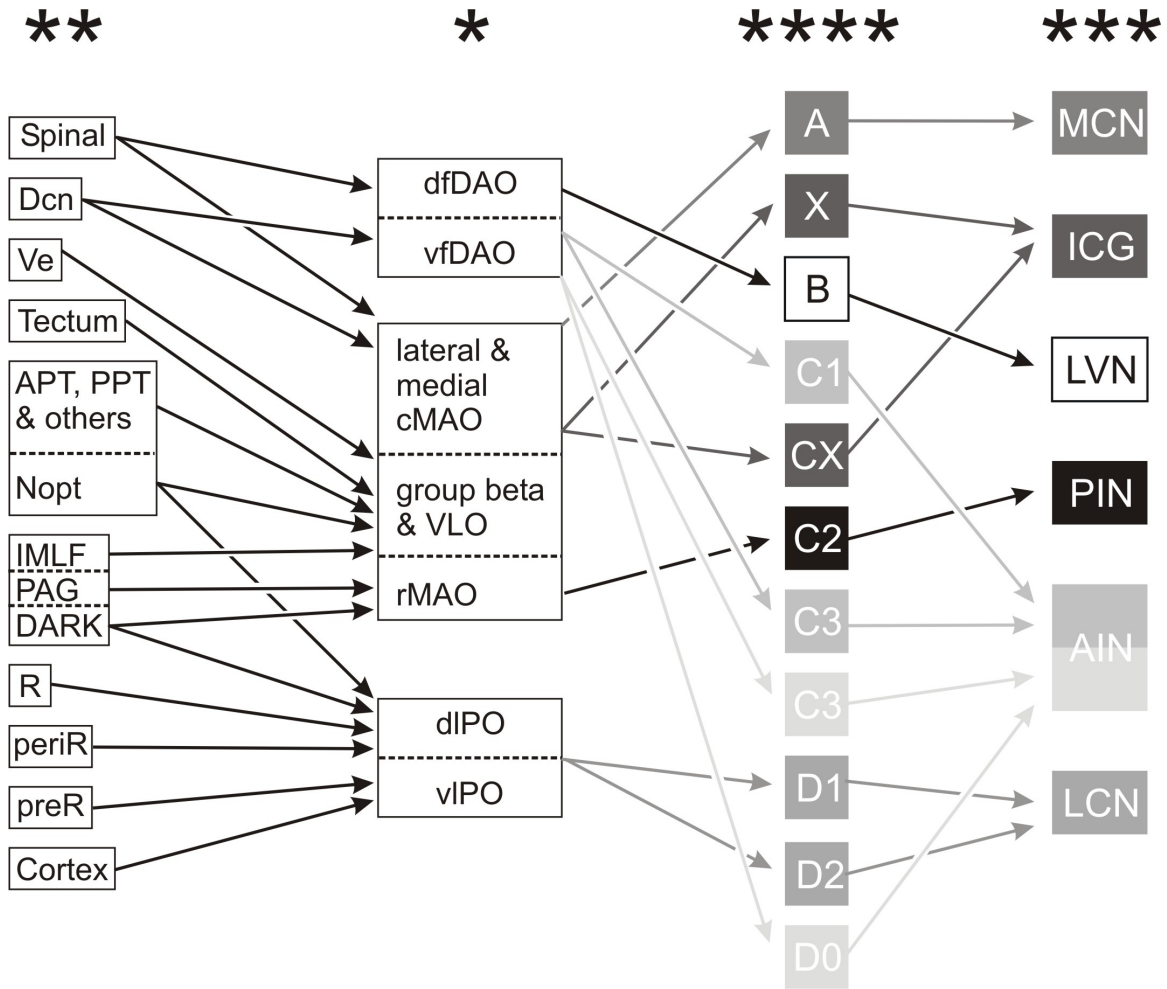


Fig. 3. Afferent olivocerebellar connections and cerebellar cortical zones.

*: Subdivisions of the inferior olive (IO). The black arrows on the left indicate the ascending and descending inputs to the IO. **: Origin of afferent connection to the inferior olive, except for the nucleo-olivary projections. ***: Subdivisions of the cerebellar nuclei and their cortical input, note that each in addition receives corresponding olivary input. ****: Longitudinal zones of Purkinje cells in the cerebellar cortex. A, X, B, C1, CX, C2, C3, D1, D2, D0; AIN, anterior interposed nucleus; APT, anterior pretectal nucleus; cMAO, caudal medial accessory olive; cortex, cerebral cortex; DCn, dorsal column nuclei; DARK, nucleus Darkschewitsch; dfDAO, dorsal fold of the dorsal accessory olive; diPO, dorsal leaf of the principle olive; ICG, interstitial cell group; IMLF, interstitial nucleus of the medial longitudinal fasciculus; MCN, medial cerebellar nucleus; LCN, lateral cerebellar nucleus; LVN, lateral vestibular nucleus; Nopt, nucleus of the optic tract; PAG, periaqueductal gray; periR, prerubral area; PIN, posterior interposed nucleus; preR, prerubral area; PPT, posterior pretectal nucleus; R, red nucleus; rMAO, rostral medial accessory olive; Spinal, spinal cord; Ve, vestibular nuclei; VLO, ventrolateral outgrowth; viPO, ventral leaf of the principle olive.

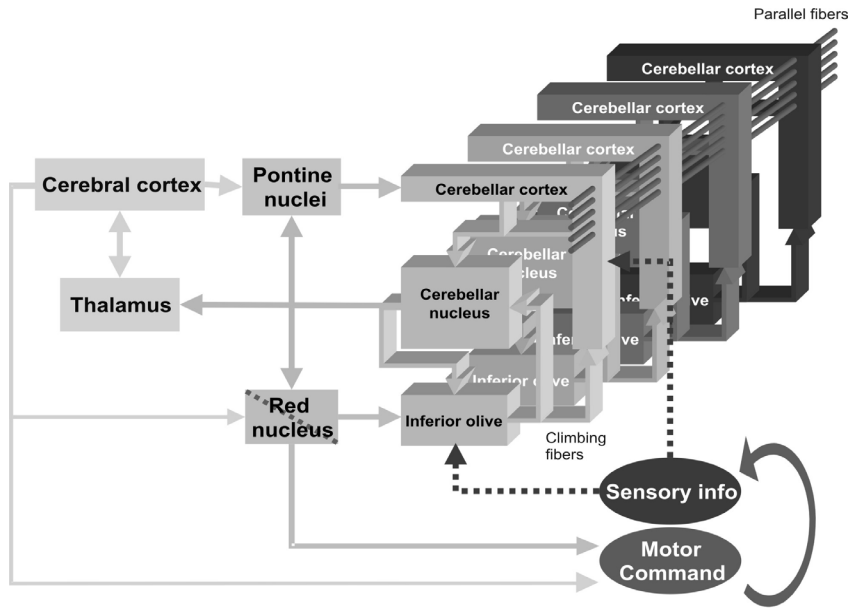


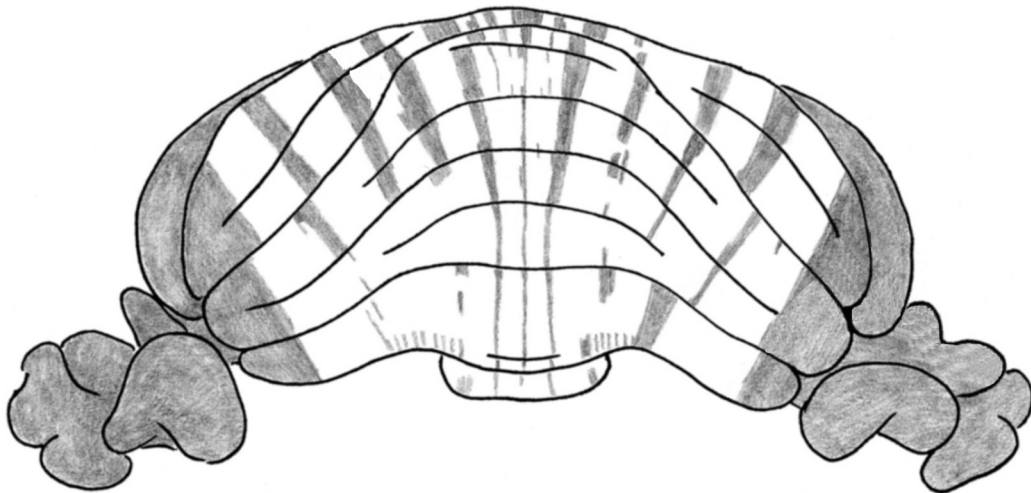
Fig. 4

Fig. 4. Modular organization of the cerebellum.

Each module, indicated in gray scale, has its own specific in- and output relations. The modules are connected by the parallel fibers.

Chapter 2

Topography Of Olivo-Cortico-Nuclear Modules In The Intermediate Cerebellum Of The Rat



Adapted from:

Pijpers A, Voogd J, Ruigrok TJH (2005): *Topography of olivo-cortico-nuclear modules in the intermediate cerebellum of the rat*. J Comp Neurol, 492 (2): 193-213

Abstract

This study provides a detailed anatomical description of the relation between olivo-cortico-nuclear modules of the intermediate cerebellum of the rat and the intrinsic zebrin pattern of the Purkinje cells. Strips of climbing fibers were labeled using small injections of biotinylated dextran amine into either the medial or dorsal accessory olives, while, in some cases, simultaneous retrograde labeling of Purkinje cells was obtained using gold-lectin injections into selected parts of the interposed nuclei. Our data are represented in a new, highly detailed, cortical surface reconstruction of the zebrin pattern and in relation to the collateral labeling of the climbing fibers to the cerebellar nuclei. We show that the somatotopic regions of the dorsal accessory olive behave differently in their projections to essentially zebrin-negative regions that represent the C1 and C3 zones of the anterior and posterior parts of the cortex. The rostral part of the medial accessory olive projects to zebrin-positive areas, in particular to the P4+ band of the anterior lobe and lobule VI, and to the P5+ band of the posterior lobe, indicating that C2 has two non-contiguous representations in the SL and crus 1. By relating the areas of overlap that resulted from the injections in the accessory olives, i.e. labeling of climbing fiber strips and patches of climbing fiber nuclear collaterals, with the results from the injections in the interposed nuclei, i.e. retrograde labeling of Purkinje cells and of inferior olivary neurons, direct verification of the concept of modular cerebellar connections was obtained.

Introduction

Although the structure of the cerebellar cortex is uniform, it exerts its actions on quite different functional systems. This functional heterogeneity is probably based on specific in- and output relations (Llinás and Sasaki, 1989; Bloedel, 1992; Voogd and Ruigrok, 1997; Jörntell et al. 2000; Brown and Bower, 2001). The organization of the afferent and efferent connections of the cerebellar cortex allows the distinction of a number of parasagittal units or modules (Voogd and Bigaré, 1980; Buisseret-Delmas and Angaut, 1993). One of the biochemical markers supporting this organization pattern of the rodent cerebellar cortex is the distribution of zebrin II (MaBQ 113, aldolase-C) in alternating bands of zebrin-positive and -negative Purkinje cells (Ahn et al., 1994; Hawkes and Leclerc, 1987). This pattern is highly reproducible between animals and can therefore be used as a reference pattern (Voogd et al., 2003; Sugihara and Shinoda, 2004).

In the past, extensive research has been done on the distribution and branching patterns of the climbing fibers, which arise from the inferior olive. Different subnuclei of this nuclear complex have been shown to project in a specific pattern of 50 – 1000 μm wide zones in the contralateral

cerebellar cortex and to provide a collateral innervation of the cerebellar target nuclei of the Purkinje cells located in these zones (Buisseret-Delmas and Angaut, 1993; Ruigrok and Voogd, 2000). In addition, the GABAergic nucleo-olivary pathway connects the cerebellar nuclei with the appropriate subnuclei of the inferior olive (Ruigrok and Voogd, 1990; Ruigrok, 1997; De Zeeuw et al., 1998). These olivocerebellar and corticonuclear connections and recurrent loops together, form a series of cerebellar modules, subserving the output of the cerebellar cortex. Some of these modules, which receive a somatosensory input from the periphery, have been shown to be constructed of narrower functional units in the cat and ferret (Andersson and Oscarsson, 1978; Ekerot and Larson, 1980, Garwicz, 1997). A microzone consists of a narrow strip of Purkinje cells innervated by climbing fibers sharing the same peripheral receptive field. Microzones in the somatosensory zones of the cerebellum have been demonstrated to be arranged in somatotopical patterns (Brown and Bower, 2002; Jörntell et al., 2003). Recently, Sugihara et al (2001) showed that the terminal axonal arborizations of individual olivary neurons were confined to narrow ~200-300 μm wide strips in the anterior and posterior cerebellum, which may represent the anatomical substrate of the microzones in the rat. Indeed, it proved possible to correlate the organization of climbing fiber zones to the patterning of zebrin bands in increasing detail (Gravel et al., 1987; Voogd et al., 2003; Sugihara and Shinoda, 2004; Voogd and Ruigrok, 2004). However, no detailed information is available on the projections of the rostral parts of the medial and dorsal accessory olives and the dorsomedial group (r-MAO, DAO and DM, respectively), and their possible microzonal organization to the intermediate regions of the cerebellum. In this paper we report on small injections of biotinylated-dextran-amine (BDA) in the r-MAO, the DAO and in the DM of the rat. Moreover, in several cases, an additional injection with wheat-germ-agglutinin bovine-serum- albumin complex conjugated to gold particles (WGA-BSA-gold, hereafter referred to as gold-lectin) was made in the contralateral cerebellar nuclei in order to trace the corticonuclear projections (Ruigrok et al., 1995). In this way, we could compare olivocortical and olivonuclear projections with corticonuclear projections in the same and between animals, using the zebrin-banding pattern as a reference. These descriptions will be necessary in order to enable and evaluate future manipulation of selected cerebellar modules.

To present our data, a new, detailed, two-dimensional surface reconstruction of the entire cerebellar cortex displaying the zebrin pattern was used, based on reconstructions of individual lobules as originally developed by Ruigrok (2003).

The results agree well with studies done by Voogd et al (2003) investigating the collateralization of climbing fibers to the paramedian lobule (PMD) and the copula pyramidis (COP), representing the hemispheres of lobule VII and VIII, respectively and with those conducted by Sugihara and Shinoda (2004) who investigated climbing fiber projections to the cerebellar cortex in relation to the zebrin pattern. The present study, however, provides new insight into the interrelation of the C zones between the anterior and posterior parts of the cerebellar cortex. In addition, our study

relates the zonal climbing fiber patterns to the terminal arborizations of the climbing fiber collaterals within the cerebellar nuclei and, together with the gold-lectin injections, provides anatomical evidence of the existence of interrelated olivo-cortico-nuclear modules.

Materials and methods

Surgical procedures

Thirty male adult Wistar rats (Harlan, Horst, the Netherlands) were used in this study. All procedures adhered to the NIH Guide for the Care and Use of Laboratory Animals according to the principles expressed in the declaration of Helsinki and were approved by a National Committee overseeing animal welfare.

Animals were anesthetized with a ketamin / xylazine mixture (100 mg/kg + 3mg/kg) administered intraperitoneally (i.p.). Surgical levels of anesthesia were monitored by the absence of rhythmic whisker movements and pinch withdrawal reflex. When necessary, supplementary doses were administered to maintain surgical levels of anesthesia. During surgery body temperature was monitored and kept within physiological limits. Postoperative analgesia was provided by a single subcutaneous dose of buprenorphine (0,05 mg/kg). All animals received at least one BDA injection (Molecular Probes, Leiden, the Netherlands, mol. weight 10.000, 10% solution in 0,05M phosphate buffer (PB)) aimed at the rostral part of the inferior olive. Because the olivocerebellar projections are strictly contralateral, bilateral BDA injections were made in several animals (Ruigrok and Voogd, 2000; Sugihara et al., 2001). In addition, selected cases received an injection of gold-lectin in the contralateral anterior or posterior interposed nucleus (AIN or PIN respectively, n=19). The gold-lectin is a strictly retrograde transported tracer (for details the reader is referred to the original paper of Ruigrok et al. (1995)). Surgical procedures can be recapitulated as follows: All animals were placed in a stereotactical head holder (Paxinos and Watson, 1986). Skin and neck musculature were cleaved in the midline exposing the dura. In the case of an additional gold-lectin injection in the cerebellar nuclei a small craniotomy was performed exposing cerebellar lobules IX, VIII and VII. Subsequently, the atlanto-occipital membrane and dura were cut and the flaps were folded to the side. All injections were placed under guidance of stereotactical coordinates and extracellular recordings, using obex as a reference point. Once position was determined, an electrode (tip diameter ~8 μ m) filled with 10 μ l, 10% BDA was advanced into the brainstem at an angle of 45⁰ with the vertical axis. The site of injection was chosen as judged by the depth of the pipette and the number of encountered layers showing the specific firing pattern of olivary neurons and an ensuing iontophoretic BDA injection was made (4 μ Amp, 7 sec on, 7 sec off, for 10 minutes). A similar procedure was followed for

injections in the interposed nuclei except that a double-barrel electrode was used (tip diameter ~15µm). The sealed part of the electrode was filled with 4,0 M NaCl to obtain extracellular recordings to distinguish between Purkinje cell layer, white matter and cerebellar nuclear neurons. The open barrel was filled with the conjugate and connected to a pressure injection device (Ruigrok et al., 1995). Alignment of the gold-lectin injection site with the placement of the olivary injection was attempted by knowledge on the relation of the organization of olivary projections to the cerebellar nuclei (Ruigrok and Voogd, 2000). Nevertheless, only 5 out of 19 cases with double injections could be used in the present study. When the typical cerebellar nuclear firing pattern was recorded at the appropriate depth, a small pressure injection of 10-50 nl was made, after which the electrode was withdrawn. Subsequently, the dura was replaced, overlying layers were sutured and the animals were allowed to recover.

After a 7-day survival period the animals were sacrificed under deep anesthesia with pentobarbital (240 mg/kg i.p.). After an initial transcardial flush of 500 ml saline (0,9% NaCl in 0,05M PB), 1 L of fixative was used (4% paraformaldehyde, 0,05% glutaraldehyde and 4% sucrose, in 0,05 M PB, pH 7,4). The brains were collected and post-fixed for an additional 3 hours, after which they were stored overnight in 0,05M PB, containing 10% sucrose at 4⁰C. Subsequently, the brains were embedded in 11% gelatin, 10 % sucrose. The blocks were hardened in 30% formalin, 30% sucrose solution for 3 hours and were stored overnight in 0,05M PB containing 30% sucrose at 4⁰C.

Histochemical procedures

Transverse sections were cut at 40 µm on a freezing microtome and collected serially in 8 glass vials containing 0,05M PB. Of each animal, two vials were processed in a BDA protocol and two additional vials were processed for a combined BDA- zebrin – immunostaining, thus yielding a complete one out of four series of sections. All 4 vials were rinsed with phosphate buffered saline (PBS). The sections were incubated, freefloating, overnight at 4⁰C in ABC-elite™ solution (Vector, PK6100 1 drop A and 1 drop B in 10 ml PBS containing 0,5% Triton X-100). Subsequently, sections were rinsed in 0,05M PB. The two vials for BDA staining only were incubated in 3,3'-diaminobenzidine tetrahydrochloride (DAB: 37,5 mg DAB, 25µl H₂O₂ 30%, in 150 ml 0,05M PB) for 20 minutes. The other two vials were incubated in DAB-cobalt (1,5 ml CoSO₄ 1% and 1,5 ml NiSO₄ 1% added to the DAB protocol). All vials were rinsed in 0,05 M PB. Next, the vials processed for zebrin staining, were rinsed in Tris buffered saline (TBS, 0,05M Tris, 0,9% NaCl, pH 7,6) and the sections were incubated, free floating, for 48-72 hours in Zebrin II (antibody kindly provided by Dr. R. Hawkes, Calgary, 1:150 in Tris-buffered high saline, 0,05M Tris, 0,5M NaCl, 0,05% Triton X-100 (TBS+) containing 2% normal horse serum (NHS)) at 4⁰C. After rinsing in TBS+, sections were incubated for 2 hours in rabbit anti-mouse HRP (p260 Dako, 1:200 in

TBS+, containing 2% NHS). Subsequently, sections were thoroughly rinsed in 0,05M PB and incubated in a second DAB staining for 15-20 min and rinsed in 0,05M PB. In case of an additional gold-lectin injection, the sections were processed, 2 times 10 minutes, for silver intensification of the gold label (Aurion, 1:1, R- Gent enhancer and R- Gent developer). All sections were mounted on slides in a chromic alum solution, air dried, and counterstained with thionin. Subsequently, slides were dehydrated in graded alcohol and xylene, and coverslipped with Permount.

Analysis

In all cases, injection sites were assessed in the non-zebrin-stained sections by examining the inferior olive and contralateral cerebellar nuclei. Some cases had injections into the right and left olivary complex, and are referred to by their case number and the addition of R or L, respectively. However, for convenience, all injections are represented in standardized diagrams representing the left inferior olive and its projection in diagrams of the right cerebellar nuclei and a reconstruction of the right cerebellar cortical surface (Ruigrok, 2003; Fig. 1A,B,C,D). Terminology of divisions of the cerebellar nuclei was adapted from Korneliussen (1968; also see Voogd, 2004) and for the inferior olive it was based on descriptions by Bernard (1987; also see Azizi and Woodward, 1987, and Ruigrok, 2004).

A general map of the zebrin-banding pattern was reconstructed out of three animals. The reconstruction was performed along the lines of earlier cerebellar cortex reconstructions made by Ruigrok (2003). Figure 1E shows a cortical surface reconstruction indicating the unfolded and outstretched Purkinje cell layer with superimposed the zebrin-banding pattern. Roman numbers indicate individual lobules and arrows are used to indicate their apices. The zebrin-positive bands are presented in gray and the numbers and letters in these bands refer to the zebrin-positive compartments from the nomenclature of Hawkes and Leclerc (1987) and modified by Voogd and Ruigrok (2004) and by Sugihara and Shinoda (2004). The corresponding negative compartments lie immediately lateral to the positive compartments. In the rostral half of lobule II, IV, VI and VIII, the caudal half of lobule VII and in lobule V some indistinct zebrin-positive compartments were observed that were not named because they were not clearly present in all our cases. Some of these bands were identified by Sugihara and Shinoda (2004), who used a different zebrin marker. All other bands were highly reproducible between animals. Hence, this reconstruction could be reliably used to accurately indicate the climbing fiber labeling resulting from the various BDA injections (see below). We have used the term “buried folium” for a folium that is completely covered by crus 1c (Welker, 1987). Sugihara and Shinoda (2004) indicated this folium as crus 1c. Based on the size of the injection and verification of olivo-nuclear (BDA injections) or nucleo-olivary (gold-lectin injections) projections, the location of tracer uptake was determined (Ruigrok and Voogd, 1990, 2000). On the outcome of these results, animals were either in- or excluded

from the present study. Inclusion criteria were; injection site restricted to the rostral parts of the inferior olive (level 8 or higher); injection site restricted to only one subnucleus or only slight involvement of a second. All zebrin sections of two series were photographed with a digital camera (Leica DC300) and printed on A-4 paper, while preserving relative size. On these prints, the zebrin pattern, labeled climbing fiber collaterals and in several cases gold-lectin labeled Purkinje cells were depicted using sections from all four series and a Leica-microscope (objectives 20x and 40x). The intersection interval therefore was 80 μm . To indicate data of individual cases into our standard diagram of the zebrin pattern, the photographs of all sections were matched and subsequently labeling was drawn into the unfolded cerebellar surface reconstruction. Photo panels were constructed in CorelDrawTM 11.0 using digitally obtained microphotographs that were saved in TIF format. Some correction for brightness and contrast was performed in Corel PhotopaintTM 11.0.

Results

The effective BDA injection site in the inferior olive was found to be limited to the dark-stained core as defined by Ruigrok and Voogd (1990, 2000). This view was supported by the distribution of anterograde-labeled terminal arborizations within the cerebellar nuclei. In most of our cases the effective injection site had an approximate diameter of 200-400 μm . Figure 2A shows the injection in a case where it was centered on the rostral part of the medial accessory olive (r-MAO) and resulted in a fine varicose plexus of terminal arborizations of collaterals in the medial part of the contralateral posterior interposed nucleus (PIN; Fig. 2B). In addition to the collateral labeling in the cerebellar nuclei, all cases resulted in anterogradely labeled climbing fibers, which were usually arranged in longitudinal strips in multiple lobules in both the anterior and posterior parts of the contralateral cerebellar cortex (Fig. 2C-F).

Injections centered on the rostral part of the medial accessory olive

Nine cases were selected in which the BDA injection was mostly or completely confined to the r-MAO. In two of these cases an additional injection with gold-lectin was centered on the PIN (Fig. 6D). They are divided into four sets of surface reconstructions, which are illustrated in Fig. 3. The first set consists of case 877L only, with an injection at the rostral border of the intermediate MAO (i-MAO; olivary level 8 and 9, Fig. 3A, B1); its cortical labeling is shown in Fig. 3E. In the cerebellar nuclei, varicose terminal labeling was found in the interstitial cell groups (ICG: Buisseret-Delmas et al. 1993) and in the rostrolateral part of PIN (Fig. 3C1, D1). Climbing fiber labeling was located in two main strips located in lobules V and VI, i.e. one directly adjacent to

the P2+ band within the P2- band, and the other in the P3- band, adjacent to and, at times somewhat within, the P4+ band. In the posterior lobe climbing fiber labeling was present in the P3- and P5a- bands of the caudal paramedian lobule (PMD), where it extended into the rostral part of the copula pyramidis (COP). In contrast to all other cases with r-MAO injections, no labeled climbing fibers were observed in the paraflocculus.

The injections of the next three sets of cases, illustrated in Fig. 3, were located at successively more rostral levels of the r-MAO. The first of these set (cases 883R and 881L) were centered at levels 9 and 10 of the r-MAO (Fig. 3A, B1). The more caudal injection (case 883R) produced collateral labeling in the caudomedial PIN (Fig. 3C1, D1) and climbing fiber labeling in the zebrin-positive anterior P4+ and the posterior P5+ bands (Fig. 3F). The labeling in P4+ extends from lobule IV into the simple lobule (SL); P5+ labeling is present in the COP and the caudal PMD but also involves crus 1 and SL. Both in P4+ and P5+, the labeled climbing fibers occupy a medial position. Case 881L forms a transition with the next set of three cases in which the injections extended more rostrally into levels 11 to 13 of the r-MAO (003R, 880R, 891R: Fig. 3A, B2, C2, D2, G). The collateral projections to the PIN now occupied central and more caudolateral portions of the PIN. In the cerebellar cortex one main band of labeling can be recognized located in the P4+ zebrin-band of the anterior lobe and the SL and in the P5+ band of the posterior lobe from the crus 1a to the PMD and extending in P5/7+ of lobule VIII (Fig. 3G). Labeled climbing fibers generally took up more lateral positions compared to case 881L. Like cases 881L and 883R labeling was also seen in the caudal part of the paraflocculus.

Injections in the rostral-most tip of MAO form the last set of cases (879R, 001R and 871R; olivary levels 12 to 15, Fig. 3A, B3) and gave rise to collateral labeling in largely overlapping areas in the caudolateral part of the PIN (Fig. 3C3,D3). Note that in case 871R there was some involvement of the ventral leaf of the principal olive (vl-PO), resulting in collateral labeling in the ventromedial part of the lateral cerebellar nucleus. In the cerebellar cortex (Fig.3 H), labeled climbing fibers predominated in the SL and the crura of the ansiform lobule. Here, in cases 879R and 001R, labeling was restricted to P5+, where they took up a lateral position. Climbing fiber labeling in case 871R was more widespread and included both zebrin-negative compartments flanking P5+ and the zebrin-positive P6+ and P7+ band in the posterior lobe. Climbing fiber labeling in the central lobules of the paraflocculus had shifted to a more caudolateral position.

In figure 6A, B, C, D, K, two of the above-described cases are shown. However, here the BDA injection was combined with a gold-lectin injection in the cerebellar nuclei (cases 891L and 001L). The, rather small, injection in case 891L gave rise to Purkinje cell labeling in the anterior P4+ and posterior P5+ bands, which overlapped with the climbing fiber labeling in these bands (Fig.6K). The gold-lectin injection in case 001L covers a large portion of the PIN and resulted in labeling of the P3+, P4+, P4- and P5+ bands in the anterior lobe as well as some labeling lateral to and within the P2+ band. Within the posterior lobe, most retrograde-labeled Purkinje cells were

confined to P4+ and P5+, and incorporated patch e of the COP. Overlap with the climbing fiber labeling was restricted to P5+ in the posterior lobe. Both injections gave rise to retrogradely labeled neurons in the r-MAO, which were largely (case 891) or only partially (case 001) coexisting with the BDA injection site. In case 001L, labeled cells were also found in the vl-PO and within the dorsomedial group (DM) of the PO, suggesting that some of the gold-lectin tracer had spread beyond PIN into the lateral cerebellar nucleus (LCN) and the dorsolateral hump (DLH). The involvement of these nuclei may be responsible for the additional Purkinje cell labeling in the uvula and lateral nodulus in case 001L (Voogd et al., 1996).

In summary, five key observations can be derived from these results: 1) injections located at the border of i-MAO and r-MAO label two stripes of climbing fibers, mostly within zebrin-negative territory, immediately lateral to the P2+ and medial to P4+ in lobules V and VI and lateral to P3+ and medial to P5+ in PMD and COP; 2) injections into the r-MAO label the anterior P4+ and posterior P5+ bands; 3) more rostral injections result in shifts of climbing fiber labeling to more lateral positions within the P4+ and P5+ bands and, in SL and crus 1, also from P4+ to P5+; 4) a rostral shift in r-MAO results in lateral shift in the position of collaterals to PIN; 5) Purkinje cells in anterior P4+ and posterior P5+ project to the PIN.

Injections centered on the dorsal accessory olive

Seventeen cases were selected in which the BDA injection was mostly or completely restricted to the DAO (Fig. 4). In three of these cases an additional gold-lectin injection in the anterior interposed nucleus (AIN) was made (Fig 6,E-I, L). In some cases there was a slight involvement of the dorsal leaf of the PO.

All cases were grouped in three sets of injections. The first set incorporates 5 cases with injections centered on the caudal half of the DAO (954L, 016R, 881R, 015L and 875L: olivary levels 6 – 10; Fig. 4A1, A3). In the cases with involvement of the dorsal fold of the DAO (df-DAO; all cases except 875L) collateral labeling of climbing fibers was present in the lateral vestibular nucleus (LVN) and resulted in climbing fiber labeling in the anterior P2- band of lobules I-VI and in the posterior P4- band of the COP and caudal PMD. This typical projection pattern is particularly evident in case 954L, where the injection was restricted to the df-DAO. Close inspection of the labeling in the anterior P2- revealed that it remained separated from P2+ in lobules IV-V by a narrow, zebrin-negative space. Climbing fibers originating from the i-MAO occupy this space (cf. Fig. 3E: also see Voogd and Ruigrok, 2004). P2- labeling in cases 015L, 016R and 881R was overlapping with those seen in case 954L (Fig.4D) and, thus, was taken to originate from the df-DAO also. Therefore, additional labeling in these cases and in case 875L must have resulted from the involvement of the vf-DAO. The vf-DAO climbing fiber labeling in this group of experiments shares several features. They all provided a collateral projection to the caudomedial part of the AIN (Fig. 4A2, A4). Furthermore, they invariably supplied, possibly collateral, labeling

to the two zebrin-negative bands that flanked the anterior P4+ (i.e. P3- and P4-) as well as the posterior P5+ bands (P4-/P5a- and P5-). Moreover, labeling in anterior P4- always extended more rostrally compared to the labeling in anterior P3- (to lobule II and IV, respectively). Similarly, in the posterior lobe, labeling from the two medial-most injection sites (cases 875L and 881R) expanded further rostrally in P5- than in P4-. Finally, only scant labeling was observed in the caudal SL and both crura.

The second set involves five cases where the injection was centered on the rostralateral part of the vf-DAO (884R, 950R, 001L, 950L and 009R: olivary levels 11-16, Fig. 4B1, B3). In the AIN labeling had shifted to its rostromedial tip (Fig. 4B2, B4). Climbing fiber labeling extended into lobule II, but mostly spared the crura and rostral PMD (Fig. 4E). Again, labeling was distributed at both sides of the anterior P4+ band and extended more anteriorly in P4- (most clearly seen in cases 001L and 884R). The two rostromedial-most cases of this group (950L and 009R) were remarkable, because labeled climbing fibers were situated on both sides of anterior P5+ in the zebrin-negative bands P4- and P5- and, in the posterior lobe, focused on the buried folium, flanking P5+. A potential origin of the labeled climbing fibers from the principal olive, which is slightly involved in both experiments, seems unlikely, because the principal olive is known to project to the zebrin-positive anterior P5+ and P6+, and the posterior P6+ and P7+ bands (Voogd et al., 2003; Sugihara and Shinoda, 2004).

The final set of injections includes seven cases, which were centered on the medial aspect of the vf-DAO (002L, 003L, 884L, 868L, 880L, 871L and 896R: olivary levels 8-13; Fig. 4C1, C3). Their respective cortical projections are visualized in two diagrams (Fig. 4F,G). This set resulted in collateral labeling in the caudolateral part of the AIN, bordering on the dorsolateral hump (DLH: Fig. 4C2, C4). Note that the rostral-most injections projected to the rostral-most part of the lateral AIN. Climbing fiber projections to the cerebellar cortex were most abundantly found within the P4- of the caudal half of lobule V and the SL, where they took up more lateral positions compared to the previously described injections. Several cases also showed some labeling in P5- (884L, 868L, 871L: Fig. 4F,G), but this projection may, at least partly, be due to involvement of the DM group into the injection site (Fig. 4 C1-4). Spread of the injection into the principal olive in cases 009R, 950L, 871L and 884L is consistent with the presence of labeled climbing fibers in the P6+ and P7+ bands of the posterior lobe. When comparing all sets of cases, and apart from the particulars described above, a general tendency was noted that climbing fibers labeled from more medial injection sites took up more lateral positions within the anterior P3- and P4- bands and the posterior P5- band than more lateral injection sites (compare figure 4E, F, G).

In Fig. 6 E-I, L, the results of three cases with gold-lectin injections that were centered on the AIN are shown (cases 001R, 002R and 896L), as well as their accompanying BDA injections placed in the vf-DAO (cases 001L, 002L and 896R, respectively). In all three cases zebrin-negative Purkinje cells were retrogradely labeled in P3- and P4-, flanking anterior P4+. The gold-lectin

injection of 002R in the rostralateral part of the AIN and the more medial injection of 896L, resulted in continuous strips of retrograde labeled Purkinje cells which, similar to the climbing fiber bands, reached more rostrally in P4- (in case 002R into lobule III), than in P3- (in case 002R into lobule V: Fig. 6I). In the posterior cerebellum, labeled Purkinje cells were found in the P4-band of the PMD and the rostral COP. A small patch of labeled Purkinje cells was present in P5- in case 002R. In agreement with the positioning of the gold-lectin injection sites, retrograde labeled olivary cells were found in the appropriate locations of the vf-DAO. In case 002R the gold-lectin injection site did clearly not encompass the PIN, yet a number of retrogradely labeled neurons was found throughout the r-MAO (Fig. 6I) and PO (not shown). This labeling is likely to be related to the observation that the injection also involved the fibers directly dorsal to the AIN (Fig. 6H) and, as a pressure injection, may have caused some damage to the climbing fibers that course directly around the interposed nuclei (Ruigrok and Voogd, 2000; van der Want et al., 1989; Sugihara et al., 2001), resulting in inadvertent labeling of some olivary neurons.

It will be obvious that the location of the gold-lectin injections and of the BDA injection are related. E.g. in case 001R the retrograde gold-lectin labeling in the vf-DAO overlaps with the BDA injection site of case 015L (Fig. 4A) coinciding with apparent overlap of the gold-lectin injection site with the collateral labeling of climbing fiber collaterals in the AIN in case 015L. This conforms rather well to the distribution of retrogradely labeled Purkinje cells of case 001R and to the distribution of labeled climbing fibers in case 015L. Similar parallels can be drawn between e.g. cases 896L and 002R with gold-lectin injections and the cases 001L and 003L with BDA injections of the vf-DAO, respectively.

Obviously, in this material, matching of injection sites and projections can be directly evaluated within the same animal. Hence, it is specifically relevant to notice that in case 896L partial overlap was observed between the DAO territory containing gold-lectin retrogradely labeled neurons and the BDA injection deposit (Fig. 6I). Indeed, a corresponding area in the cerebellar nuclei that fell both within the gold-lectin injection site and received labeled climbing fiber collaterals was present (Fig. 6I). Finally, in the cerebellar cortex a region of overlap was found between the strips of gold-lectin labeled Purkinje cells and strips of labeled climbing fibers (Fig. 6G, L). In case 001L-BDA and 001R-gold-lectin no overlap in injection and resultant labeling was present either in the inferior olive or in the cerebellar nuclei. Hence, no overlap in the labeling of Purkinje cells and climbing fibers could be observed in the cerebellar cortex (Fig. 6I,L). A similar observation can be made for the injection pairs 002R-gold-lectin and 002L-BDA.

The following conclusions can be drawn from these results: 1) olivary neurons of the DAO supply climbing fibers to Purkinje cells of zebrin-negative areas only; 2) for the df-DAO these zebrin-negative zones involve the P2- band from lobules I through VI and medial P4- in posterior VII and VIII, for the vf-DAO they are located medial and lateral to P4+ (P3- and P4-) in the anterior lobe and SL, but on either side of P5+ in the posterior lobe; (3) the caudal and lateral vf-DAO projects

to a single band in lobule VIII (lateral to P4+) and to two bands on either side of P4+ in the anterior lobe, whereas the medial vf-DAO projects to two bands in PMD and crus 2 (located on either side of P5+) but predominantly to a single band (P4-) in caudal lobule V, SL and rostral crus 1. (4) Double injections confirm the modular and submodular organization of olivo-cortico-nuclear connections.

Injections centered on the rostral part of the dorsomedial group

In Fig. 5 three cases (002R, 008R and 013R) in which the BDA injection was restricted to the rostral DM will be presented (olivary levels 13-16; Fig. 5A, B). Collateral labeling in the cerebellar nuclei was mostly restricted to the rostral part of the DLH (Fig. 5C, D) such that the injection in the rostral-most tip of the DM (case 002R) resulted in the rostral-most labeling within the DLH (levels 5-9 Fig. 5C, D). Labeled climbing fiber collaterals were found in the anterior P5- band in lobule II, III, IV, V, SL, crus 1a and in the posterior P5- and P6- of the caudal half of buried folium and the rostral half of crus 2a (Fig. 5E). In cases 884L and 871L (Fig. 4A), the injection sites encroached upon the DM. Collateral labeling was found in small patches in caudal DLH. In the cortex strips of labeled climbing fibers were present in the zebrin-negative area medial to the P6/7+ band of SL and in case 871L in the posterior P6- compartment. It should be noticed that climbing fiber labeling in the medial anterior P5- was also present in cases 009R and 950L (Fig. 4B).

Summary

The projections of the accessory olives to the cerebellar nuclei and cortex, as established in this study, are summarized in Fig. 6J and M. Projections from the i-MAO (green) are located in the ICG of the cerebellar nuclei and in the cortical X and CX zones that border the anterior P2+ and P4+ bands and posterior P3+ and P5+ bands. Projections from the r-MAO (blue) include the PIN and the C2 zone, which corresponds to the anterior P4+ band and the posterior P5+ band, and extends in the caudal paraflocculus. Projections from successively more rostral levels of the r-MAO are indicated in lighter shades of blue. Note that both P4+ and P5+ receive climbing fibers in SL and crus 1. The projection of the df-DAO to the LVN and the B zone is indicated in yellow. Projections from the vf-DAO to the AIN and to the C1 and C2 zones, occupy the zebrin-negative areas flanking anterior P4+ and posterior P5+. Different shades of red and orange indicate the topographical relations between the vf-DAO and its projection area. Arrows provide additional gradients in the relation between DAO and AIN. The projection of the DM to the DLH and the anterior P5- and posterior P6- bands (corresponding to the D0 zone) are indicated in pink. Projections from the vf-DAO to this zone have not been included in the diagram, and will be considered in the discussion.

Discussion

The present study extends and integrates data from our previous studies in the rat on the topography of climbing fiber branching (Ruigrok, 2003; Voogd et al., 2003, Voogd and Ruigrok, 2004) and the interrelation between connections of the inferior olive and the cerebellar nuclei (Ruigrok and Voogd, 1990, 2000) by providing a detailed account of the projections of the accessory olives to the intermediate cerebellum. The cortical topography of climbing fiber projections in the rat has recently been the subject of a study by Sugihara and Shinoda (2004), but they did not consider the collateral innervation of the cerebellar nuclei, which provides important additional information on the organization of the olivocerebellar system, nor did they consider the relation with the corticonuclear projection. Moreover, their experimental material on the connections of the rostral MAO and DAO was incomplete.

The zebrin pattern proved to be essential as a reference frame for the identification of zonal climbing fiber patterns (also see Voogd and Ruigrok, 2004; Sugihara and Shinoda, 2004). Obviously, the zebrin pattern does not reveal the borders of all topographical or functional units. Indeed, Armstrong and Hawkes (2000) already showed that expression patterns of various other antigens (HNK-1, GP65, Map-1a and α -dystrophin) revealed higher levels of complexity in the organization of the cerebellar cortex. Therefore, input originating from a specific subnucleus of the inferior olive, is not necessarily restricted to either a zebrin-positive or -negative band and within each band further subdivisions can be made. In our study this could be noted by labeled strips of climbing fibers, located at the border of a zebrin band and that seemingly shifted from positions within the band to adjacent zebrin-negative areas (e.g. case 877L, Fig. 3E).

Topography of the X and CX zones

The relatively simple subdivision of the vermis and the intermediate cerebellum into the A, B, C1, C2 and C3 zones, established in the anatomical and electrophysiological studies of Voogd (1964; Voogd et al., 1969) and Oscarsson (1969) was changed by the identification of the x- and cx zone¹ in the anterior lobe of the cat (Ekerot and Larson 1982; Campbell and Armstrong 1985). The X zone is located between the A and B zones, whereas the CX zone is situated between the C1 and C2 zones. Like the C1 and C3 zones, these zones receive short-latency somatosensory information. However, in contrast to the C1 and C3 zones, this information is not relayed via the DAO, but through intermediate levels of the MAO (Trott and Armstrong, 1987; also see Pardoe

¹Lower case lettering indicates that the zones were identified by electrophysiological techniques whereas upper case lettering refers to anatomically defined zones. Although many of these zones have been shown to be identical, in some cases the relationships between both types of zones are still discussed (e.g. see Pardoe and Apps, 2002, Voogd et al. 2003).

and Apps, 2002). The X and CX zones have been found to be innervated by branching climbing fibers, but the amount of this collateralization was considered not to be extensive (Apps et al., 1991). Later, Buisseret-Delmas and co-workers (1993) found evidence for the existence of an X and CX zone of the rat, which, for the anterior lobe, was partially confirmed electrophysiologically by Jörntel et al. (2000). The X zone was found to extend from lobule IV to lobule VIa and to be wedged between the A and B zones. The CX zone runs from lobule V to VIa lateral to the C1 zone, but the presence of X and CX zones in the posterior cerebellum is still controversial (see below). The origin of the climbing fiber afferents of these zones was found as an oblique band in the i-MAO. The X and CX zones have been proposed to project to the interstitial cell groups (ICG), which includes small groups of neurons that are located between the interposed nuclei and the medial cerebellar nucleus (Trott and Armstrong, 1987; Buisseret-Delmas et al., 1993).

In the present study, as in previous studies, the identification of the X- and CX- zones in relation to the zebrin pattern was based on the localization of the climbing fiber projections of the i-MAO in combination with climbing fiber collateral or corticonuclear projections to the ICG (Voogd et al., 2003; Voogd and Ruigrok, 2004). The X and CX zones were located in the medial part of the zebrin-negative P2- band and in the lateral P3- in lobules IV, V and the SL, immediately adjacent to P2+ and P4+, respectively. In the posterior lobe the X zone occupies P3- in the lobules VII and VIII, whereas CX is located laterally in the COP, adjacent to P5+. In case 877L the posterior CX zone was found to extend more rostrally into the PMD. It should be noted that, since the i-MAO and r-MAO, which projects to the adjacent zebrin-positive P4+ or P5+ bands (see below), as well as the ICG and medial PIN are directly adjacent, it is impossible to indicate an absolute border between CX and C2 based on a pure anatomical signature.

Sugihara and Shinoda (2004) found labeled climbing fibers in the position of the X and CX zones, stemming from injections of the rostral pole of their medial and lateral subnuclei b of the caudal MAO, respectively, but the collateral projection to the ICG was not verified and a projection to both populations from a single injection site, as observed in our experiments, was not observed. The presence or absence of climbing fiber branching to the X and CX zones may depend on the localization of the injection site in the transverse zone in the intermediate MAO. In the cat this zone consists of lateral and medial portions, which project to the X and CX zones respectively, and a central portion with double-projecting cells (Apps et al., 1991).

Topography of the B zone

The B zone is located in the lateral vermis of the anterior lobe and SL. It was defined in the cat by its projection to the LVN (Voogd, 1964). The physiological equivalent of the B zone is characterized by short latency bilateral climbing fiber activation upon stimulation of peripheral nerves (Oscarsson and Sjölund, 1977). Its climbing fibers were shown to be derived from the caudal part of the DAO, which, in the rat, is known as the dorsal fold of the DAO (df-DAO: Voogd

et al., 1969; Azizi and Woodward, 1987; Groenewegen and Voogd, 1977; Buisseret-Delmas and Angaut, 1993; Voogd and Ruigrok, 2004). Recently, the B zone was related to the zebrin pattern and was shown to occupy the zebrin-negative region lateral to anterior P2+ in the lobules I-VI (Voogd and Ruigrok, 1997; 2004; Sugihara and Shinoda, 2004). In the posterior lobe the B zone is located in the COP (lobule VIII), where it forms a narrow zone within the P4-band directly adjacent to the P4+ (Voogd and Ruigrok, 2004). Sugihara and Shinoda (2004) designated the anterior zebrin band b+, innervated by the lateral-most aspect of the df-DAO (and directly bordering on the main body of the DAO), as the lateral border of the B zone. However, since they did not identify the collateral projections of these climbing fibers, they were unable to define the precise border of the B with the C1 zone. Both zones receive a projection from the DAO, but C1 emits collaterals to the AIN. Our data on the B zone are in agreement with Voogd and Ruigrok (2004) and exclude the b+ band from the B zone. When the injection site included the caudal vf-DAO (e.g. 016R and 881R), additional strips of climbing fibers were labeled lateral to P3+ and collateral labeling appeared in the AIN. In the posterior lobe the B zone was found to extend somewhat more rostrally into lobule VII, than reported by Voogd and Ruigrok (2004).

Topography of the C1, C3 and D0 zones

Some of the features, which characterize the C1 and C3 zones as established in the original studies in the cat, also can be recognized in our experiments in the rat. These zones project to the AIN, receive climbing fibers from the rostral DAO, which, in the rat, is termed ventral fold of the DAO (vf-DAO: Azizi and Woodward, 1987). Through this relay, they receive somatotopically organized sensory information. For the rat, and based on retrograde tracing of cortical injections, the C1 and C3 zones were described by Buisseret-Delmas (1988). In accordance with her schemes, our material also indicates a C1 zone running from the anterior lobe to the COP whereas the C3 zone is found from anterior lobe to PMD. Both zones are interrupted in crus 1. With regard to the corticonuclear projections there is some discrepancy between the scheme proposed by Buisseret-Delmas and Angaut (1993) and the classical studies in the cat. In particular, their claim that C1 (as well as C2) project to both the AIN and the PIN was not supported by Voogd et al. (2003) and by the experiments in the present study, which document an exclusive projection of C1 and C3 to the AIN. Moreover, this relationship is supported by the collateral projection of climbing fibers from the vf-DAO to the AIN, reported by Ruigrok and Voogd (2000) and in the present study and by the termination of the nucleo-olivary pathway from the AIN in the vf-DAO (Ruigrok and Voogd, 1990).

Buisseret-Delmas and Angaut (1989) described another zone, D0, in the lateral cerebellum of the rat. D0 projects to the dorsolateral hump (DLH), a subnucleus located between the AIN and the lateral cerebellar nucleus, and which receives its climbing fibers from the dorsomedial group (DM)

of the principal olive. Originally Buisseret and Angaut (1989, 1993) located the D0 zone between C3 and D1. However, Sugihara and Shinoda (2004) recently showed that the D0 is located between the D1 and D2 zones, as suggested earlier by Voogd (Voogd et al. 1993; Voogd et al. 2003). The present study was in accordance with this notion and supports the identification of a D0 climbing fiber zone from the DM group by the presence of collateral labeling within the rostral DLH. Like the C1 and C3 zones, D0 is interrupted in crus 1.

Recently, Voogd et al. (2003) and Sugihara and Shinoda (2004) related the C1, C3 and D0 zones in the rat to the zebrin pattern. Our results on the topography of the C1, C3 and D0 zones are in general accordance with their results. However, with respect to the possibility and the topography of interzonal branching of climbing fibers and the topical relations between the vf-DAO, the AIN and the C1 and C3 zones, our data differ somewhat from those reported by Sugihara and Shinoda (2004). All three zones occupied zebrin-negative bands. In the anterior cerebellum, C1 and C3 flank the P4+ zebrin band, however, caudal of crus 1, they are found medially and laterally to P5+, respectively. The position of the usually only vague zebrin-positive anterior P3+ band remains enigmatic. It received exclusive collateral labeling from climbing fibers terminating in the zebrin-positive patch e of the COP, originating from the junction of the df- and vf-DAO (Voogd et al., 2003). An injection located in this region of the DAO, published by Sugihara and Shinoda (2004) also produced labeling in anterior P3+ and patch e. Purkinje cell labeling in P3+ was present after injections of retrograde tracers in the ICG and/or the PIN (Voogd and Ruigrok, 2004; this study), whereas Purkinje cell labeling was restricted to zebrin-negative zones and never included P3+ in our cases with gold-lectin injections in the AIN. The D0 zone was located in the P5- band of the anterior lobe extending from lobule II well into crus 1. Leaving the rest of crus 1 devoid of labeled climbing fibers, the labeling of D0 appeared again in the lateral half of the P5- band in the dorsal leaf of buried folium. In crus 2 and the PMD labeling is present in P6-.

The anterior D0 zone is suggestive of the electrophysiologically defined y zone in the anterior lobe of the cat (Ekerot and Larson, 1979, 1982). Both are separated from the C3 zone by a zone projecting to the lateral cerebellar nucleus and that receives climbing fibers from the principal olive. A characteristic feature of the y zone relates to the branching of climbing fibers between the c3 and y zones. Indeed, some of our injections in the medial and rostral vf-DAO, resulted in labeling of climbing fibers in P5- of the anterior lobe (e.g. cases 009R and 871L of Fig. 4E and G, respectively). We therefore presume that the rostral continuation of the D0 zone in P5- involves a rat equivalent of the cat y zone and will, at least partly, receive its climbing fibers from the vf-DAO in addition to those of the DM group. In accordance with the data of Sugihara and Shinoda (2004), this y-part of D0 may be located within a thin medial strip in P5- band of lobules III to crus 1a. Although a D0 zone has been noted in P6- of the posterior cerebellum, a DAO contribution was not observed and a y component in the posterior cerebellum of the cat, likewise, has not been reported.

Single injections of the vf-DAO resulted in combinations of labeled climbing fiber strips belonging to C1, C3 and D0 zones in anterior and posterior parts of the cerebellum. Similar combinations of Purkinje cell labeling in the different zones were present in cases with gold-lectin injections in the AIN. The question can be raised whether climbing fiber labeling in rostral and caudal compartments of the same zone or in different zones is due to branching of individual climbing fibers. Although our material does not allow a definite answer, rostrocaudal branching within a single zone seems highly likely in view of the small size of our injection sites, the original observations in the cat of Armstrong et al. (1971, 1973) and Oscarsson and Sjölund (1977), and the rostrocaudal branching patterns of individual climbing fibers (cat: Rosina and Provini, 1983; rat: Sugihara et al., 2001; Voogd et al., 2003). With respect to collateralization to different zones, our injections in the caudal and lateral parts of the vf-DAO usually resulted in simultaneous labeling of the C1 and C3 zones (i.e. P3- and P4, respectively) in the anterior lobe and rostral SL and of C1 (P4-) in COP and caudal PMD. In contrast, medial injections invariably resulted in labeling of C3 (i.e. P4-) of SL and of C1 and C3 (i.e. P4- and P5-, respectively), in PMD and crus 2. These results are in line with early observations in the cat by Ekerot and Larson (1982; also see Apps et al., 1991; Voogd et al., 2003). Sugihara and Shinoda (2004), however, only rarely reported mediolateral branching between C1 and C3 with their injections of the vf-DAO (also see Sugihara et al., 2001).

Topography of the C2 zone

Both in the rat and other species the C2 zone extends over the entire cerebellum, from lobule II to the flocculus, projects to the PIN and receives climbing fibers from the r-MAO. (Voogd, 1964; Voogd et al., 1969; Voogd and Bigaré, 1980; Buisseret-Delmas, 1988; Buisseret-Delmas and Angaut, 1993; Ruigrok et al. 1992; Groenewegen et al., 1979; Apps, 1990). Here, we could confirm the correspondence between the C2 zone and the anterior P4+ and posterior P5+ bands (Voogd and Ruigrok, 1997, 2004; Voogd et al., 2003; Sugihara and Shinoda, 2004). However, the connections of the r-MAO and the intrinsic organization of the C2 zone were underexposed in the latter studies. The rostrocaudal extent of the climbing fiber labeling with injections at the caudal and middle levels of the r-MAO is very similar. However, with successively more rostral injections, the labeling shifts laterally in P4+ and P5+. This translocation coincides with a caudolateral shift in the collateral projection to the PIN (cf. Ruigrok and Voogd, 2000). The lateral displacement of the projection in these rostral injections ultimately results in the labeling of anterior P5+ in the SL and the anterior crus 1. When P5+, representing the posterior C2 zone was followed into crus 1 it proved to be continuous with anterior P5+ of crus 1a and the SL (cf. case 879R and 871R of Fig. 3). Indeed, in some folia both P4+ and P5+ contained labeled climbing fibers that originating from the r-MAO (see cases 883R and 881L of Fig. 3). Hence, rather than joining each other within crus

1, we propose that the anterior and posterior C2 zone are discontinuous and exist next to one another in SL and crus 1 (see Fig. 6M). Labeling of C2 in the paraflocculus is limited to its caudal half, which is in accordance with Sugihara and Shinoda (2004).

Functional considerations

A universal feature of the topography of projections from the presently studied regions of the inferior olive to the cerebellar cortex is that single olivary regions are mapped in multiple, non-contiguous zones in the cerebellar cortex. However, in each cerebellar target nucleus only a single map of the collateral projections from these olivary nuclei is produced. Apparently multiple cortical maps converge upon a single representation in the nuclei (Garwicz and Ekerot, 1994; Apps and Garwicz, 2000). Within the zones that receive somatosensory information from the periphery through the olivocerebellar system, the olive is mapped in long and narrow strips of climbing fibers, which share the same receptive field: the microzones. Together, the microzones in each of the cat's B, C1, C3 and γ zones seem to produce continuous body maps. Rostrocaudal branching of climbing fibers would duplicate these maps in the anterior and posterior C1 and C3 zones (Oscarsson and Sjölund, 1977; Andersson and Oscarsson, 1978; Ekerot and Larson, 1979; Ekerot and Larson, 1982; Garwicz, 1997). The longitudinal strips of climbing fibers terminal arborizations, originating from individual or from small groups of olivary neurons, described by Sugihara et al. (2001, 2004) and in this study probably are the substrate of these microzones. They occur in all olivocerebellar projection areas and allow the distinction of medio-lateral and rostrocaudal topical patterns in the projection of accessory olives. In the projection of the df-DAO to the anterior P2- band (the B zone) the localization of the different climbing fiber strips is a medio-lateral one, no rostrocaudal shift in their localization is apparent. This would be in accordance with the mediolateral somatotopy in the B zone, as described for the cat (Oscarsson and Sjölund, 1977).

More distinct rostrocaudal gradients in the projection of the vf-DAO can be discussed when considering the somatotopical relations of different parts of the vf-DAO. Unfortunately, no complete map of the somatotopical organization of the vf-DAO is available for the rat, but the detailed map of Gellman et al. (1983) for the cat may be applied, since it seems to be in accordance with available data in the rat (Atkins and Apps, 1997; Pardoe and Apps, 2002). In Gellman's scheme, the caudal and lateral vf-DAO (i.e. our first group of vf-DAO injections Fig. 4A) would represent the hindlimb; rump and tail region would be located in the rostralateral vf-DAO (our second group: Fig. 4B) while forelimb and face area are represented in the medial vf-DAO (our third group: Fig. 4C). It can be noted that mediolateral branching (i.e. simultaneous labeling) between the C1 and C3 zones in the anterior lobe and SL mainly occurred in the putative tail, rump and hindlimb regions of these zones, but not in their forelimb representation. In contrast

branching in the caudal aspects of the C1 and C3 zones, mediolateral branching between C1 and C3 may occur in PMD and crus 2 for the forelimb/face representations but not, or only sparsely, for the hindlimb/rump/tail regions in COP and posterior PMD. According to Jörntell et al. (2000) the forelimb was represented in the c1 zone of the lobules V and VI. The presumed absence of c3 and y zones in the anterior cerebellum of the rat was interpreted by these authors as a reflection of differences in the organization of motor systems in the rat as compared with the cat. Neither of these observations could be confirmed in our material. The absence of a forelimb representation (i.e. resulting from our injections in the medial vf-DAO) in C1 of the SL (i.e. in P3-) is at odds with physiological data from Pardoe and Apps (2002). Future research will have to determine whether their recordings were made within P3- or P4-. The representation of hind- and forelimb in, respectively, the C1 zone of the COP and the PMD (Atkins and Apps, 1997) was confirmed in our study, although the border between these representations was less distinct. A tail representation to the medial C1 zone of COP might be represented by injections 884R and 015L (Fig. 4A, D and Fig. 4B,E, respectively) and is also in line with the anatomical data provided by Atkins and Apps (1997).

It is possible to transpose the somatotopical map of the vf-DAO to the AIN by evaluating the climbing fiber collateral labeling. Hence, the hind limb region would be represented in the caudomedial AIN, rump/tail region in its rostromedial tip, whereas forelimb/face receptive areas are found in the caudolateral part of the AIN. This general scheme is in line with known projections from the AIN to the spinal cord via the magnocellular red nucleus (Daniel et al., 1987; Teune et al., 2000; for review see: Ruigrok, 2004).

Subdivisions of the C2 zone have not been reported before. However, with rostrally shifting injections of the r-MAO we have noted a medio-lateral shift of the labeling in the P4+ and labeling within the P5+ band of the SL and the crus 1 becomes more prominent. The electrophysiological equivalent of the C2 zone (i.e. the c2 zone) has been shown to receive long latency input from the ipsi- and contralateral forelimb in both cat and rat (Ekerot and Larson, 1979; Atkins and Apps, 1997; Pardoe and Apps, 2002), but the functional meaning of the topical patterns in the projection of the r-MAO remains unknown (also see description of afferents to their group I by Sugihara and Shinoda, 2004).

As yet, it is not known if the breaking up of the cortical zones is related to developmental (e.g. Hashimoto and Mikoshiba, 2003) or to functional aspects (or both). Indeed, it is not known if zones in the anterior and posterior cerebellum that receive climbing fiber input from the same olivary cells (Sugihara et al., 2001; Voogd et al, 2003) function in a similar way. Observations by Apps and collaborators (Apps and Lee, 1999; Apps, 2000; also see Pardoe and Apps, 2002) have indicated that gating of climbing fiber excitability of C1 zones in SL and PMD behave differently. However, as outlined above, our results show that the olivary regions supplying C1 of PMD preferably reach C3 of the SL rather than C1 (also see Voogd et al., 2003). Furthermore, in

order to understand the functional implications of the multiple and essentially discontinuous organization of the olivocortical projections it will be important to gain more detailed information on the identity and patterning of the specific mossy fiber inputs to these regions (Pijpers et al., 2003, Voogd et al, 2003).

Zones and modules

The notion of matching olivocortical and corticonuclear, as well as of olivonuclear and nucleo-olivary connections, has resulted in the concept of the modular organization of the cerebellum. However, a detailed study correlating the collateral projections of the olive to the cerebellar nuclei directly with the corticonuclear projection is still lacking. In the present study combinations of injections of anterograde tracers within the inferior olive and retrograde tracers in the cerebellar nuclei of the same animal were used to study this problem. In this way, by analyzing the topography of retrogradely labeled Purkinje cells and anterogradely labeled climbing fibers, we were able to directly verify the complementary nature of corticonuclear and olivocortical projections. The modular nature of the interconnectivity of the injected areas was specifically highlighted by the observation that overlap of injection site and transported label in olive coincided with overlap in the cerebellar nuclei. Only in these instances it was possible to find congruence of retrogradely labeled Purkinje cells and BDA labeled climbing fibers. Although, as yet, it cannot be excluded that some mismatch between parts of the entities of olivocortical, olivonuclear, corticonuclear and nucleo-olivary projections may exist, the present data strongly suggest that the modular extension of cerebellar cortical zonal organization presents a key feature of cerebellar functioning.

Acknowledgements

The authors would like to thank Ms E. Sabel-Goedknecht and J. van der Burg for their excellent technical assistance. This study would not have been possible without the generous gifts of zebrin II antibody by dr. R. Hawkes (Univ. of Calgary, Canada). Supported by the Dutch Organization for Scientific Research (NOW-ALW: project number 810.37.005) and the Dutch Ministry of Health, Welfare, and Sports.

Abbreviations used in text

AIN anterior interposed nucleus
β subnucleus beta
BDA biotinylated-dextran-amine
BSA bovine serum albumin
COP copula pyramidis
DAB 3,3'-diaminobenzidinetetrahydrochloride
DAO dorsal accessory olive
DC dorsal cap
df-DAO dorsal fold of DAO
dl-LCN dorsolateral part of LCN
DLH dorsolateral hump
DLP dorsolateral protuberance
dl-PO dorsal leaf of PO
DM dorsomedial group
DMCC dorsomedial cell column
ICG interstitial cell groups
i-MAO intermediate medial accessory olive
L left
LCN lateral cerebellar nucleus
LVN lateral vestibular nucleus
MCN medial cerebellar nucleus
NHS normal horse serum
PB phosphate buffer
PBS phosphate buffered saline
PIN posterior interposed nucleus
PMD paramedian lobule
PO principle olive
R right
r-MAO rostral medial accessory olive
SL simple lobule
SVN superior vestibular nucleus
TBS tris buffered saline
vl-PO ventral leaf of PO
VLO ventrolateral outgrowth
Vm-LCN ventromedial part of LCN
WGA wheat germ agglutinin

References

- Ahn AH, Dziennis S, Hawkes R, Herrup K. 1994. The cloning of zebrin II reveals its identity with aldolase C. *Development* 120:2081-2090.
- Andersson G, Oscarsson O. 1978. Climbing fiber microzones in cerebellar vermis and their projection to different groups of cells in the lateral vestibular nucleus. *Exp Brain Res* 32:565-579.
- Apps R. 1990. Columnar organisation of the inferior olive projection to the posterior lobe of the rat cerebellum. *J Comp Neurol* 302:236-254.
- Apps R. 2000. Gating of climbing fibre input to cerebellar cortical zones. *Prog Brain Res* 124:201-211.
- Apps R, Lee S. 1999. Gating of transmission in climbing fibre paths to cerebellar cortical C1 and C3 zones in the rostral paramedian lobule during locomotion in the cat. *J Physiol* 516:875-883.
- Apps R, Garwicz M. 2000. Precise matching of olivo-cortical divergence and cortico-nuclear convergence between somatotopically corresponding areas in the medial C1 and medial C3 zones of the paravermal cerebellum. *Europ J Neurosci* 12:205-214.
- Apps R, Trott JR, Dietrichs E. 1991. A study of branching in the projection from the inferior olive to the x and lateral c1 zones of the cat cerebellum using a combined electrophysiological and retrograde fluorescent double labeling technique. *Exp Brain Res* 87:141-152.
- Armstrong DM, Harvey RJ, Schild RF. 1971. Distribution in the anterior lobe of the cerebellum of branches from climbing fibers to the paramedian lobule. *Brain Res* 25:203-206.
- Armstrong DM, Harvey RJ, Schild RF. 1973. Branching of the inferior olivary axons to terminate in different folia, lobules or lobes of the cerebellum. *Brain Res* 54:365-371.
- Armstrong CL, Hawkes R. 2000. Pattern formation in the cerebellar cortex. *Biochem Cell Biol* 78:551-562.
- Atkins MJ, Apps R. 1997. Somatotopical organisation within the climbing fibre projection to the paramedian lobule and copula pyramidis of the rat cerebellum. *J Comp Neurol* 389:249-263.
- Azizi SA, Woodward DJ. 1987. Inferior olivary nuclear complex of the rat: morphology and comments on the principles of organization within the olivocerebellar system. *J Comp Neurol* 263:467-484.
- Bernard J-F. 1987. Topographical organization of olivocerebellar and corticonuclear connections in the rat - An WGA-HRP study: I. Lobules IX, X and the flocculus. *J Comp Neurol* 263:241-258.
- Bloedel JR. 1992. Functional heterogeneity with structural homogeneity: How does the cerebellum operate? *Behav Brain Sci* 15:666-678.
- Brown IE, Bower JM. 2001. Congruence of mossy fiber and climbing fiber tactile projections in the lateral hemispheres of the rat cerebellum. *J Comp Neurol* 429:59-70.
- Brown IE, Bower JM. 2002. The influence of somatosensory cortex on climbing fiber responses in the lateral hemispheres of the rat cerebellum after peripheral tactile stimulation. *J Neurosci* 22:6819-6829.
- Buisseret-Delmas C. 1988. Sagittal organization of the olivocerebellonuclear pathway in the rat. II. Connections with the nucleus interpositus. *Neurosci Res* 5:494-512.
- Buisseret-Delmas C, Angaut P. 1989. Anatomical mapping of the cerebellar nucleo-cortical projections in the rat: a retrograde labeling study. *J Comp Neurol* 288:297-310.
- Buisseret-Delmas C, Angaut P. 1993. The cerebellar olivo-cortico-nuclear connections in the rat. *Progr Neurobiol* 40:63-87.
- Buisseret-Delmas C, Yatim N, Buisseret P, Angaut P. 1993. The X zone and CX subzone of the cerebellum in the rat. *Neurosci Res* 16:195-207.
- Campbell NC, Armstrong DM. 1985. Origin in the medial accessory olive of climbing fibers to the x and lateral c1 zones of the cat cerebellum: a combined electrophysiological / WGA-HRP investigation. *Exp Brain Res* 58:520-531.
- Daniel H, Billard JM, Angaut P, Batini C. 1987. The interposito-rubrospinal system. Anatomical tracing of a motor control pathway in the rat. *Neurosci Res* 5:87-112.
- De Zeeuw CI, Simpson JI, Hoogenraad CC, Galjart N, Koekkoek SKE, Ruigrok TJH. 1998. Microcircuitry and function of the inferior olive. *Trends Neurosci* 21:391-400.
- Ekerot CF, Larson B. 1979. The dorsal spino-olivocerebellar system in the cat. II. Somatotopical organization. *Exp Brain Res* 36:219-232.
- Ekerot C-F, Larson B. 1980. Termination in overlapping sagittal zones in cerebellar anterior lobe of mossy and climbing fiber paths activated from dorsal funiculus. *Exp Brain Res* 38:163-172.
- Ekerot C-F, Larson B. 1982. Branching of olivary axons to innervate pairs of sagittal zones in the cerebellar anterior lobe of the cat. *Exp Brain Res* 48:185-198.
- Garwicz M. 1997. Sagittal zonal organization of climbing fibre input to the cerebellar anterior lobe of the ferret. *Exp Brain Res* 117:389-398.
- Garwicz M, Ekerot C-F. 1994. Topographical organization of the cerebellar cortical projection to nucleus interpositus anterior in the cat. *J Physiol* 474:245-260.
- Garwicz M, Jorntell H, Ekerot CF. 1998. Cutaneous receptive fields and topography of mossy fibres and climbing fibres projecting to cat cerebellar C3 zone. *J Physiol* 512 (Pt 1):277-293.
- Gellman R, Houk JC, Gibson AR. 1983. Somatosensory properties of the inferior olive of the cat. *J Comp Neurol* 215:228-243.
- Gravel C, Eisenman LM, Sasseville R, Hawkes R. 1987. Parasagittal organization of the rat cerebellar cortex: direct correlation between antigenic Purkinje cell bands revealed by mabQ113 and the organization of the olivocerebellar projection. *J Comp Neurol* 265:294-310.

- Groenewegen HJ, Voogd J, Freedman SL. 1979. The parasagittal zonation within the olivocerebellar projection. II. Climbing fiber distribution in the intermediate and hemispheric parts of cat cerebellum. *J Comp Neurol* 183:551-602.
- Groenewegen HJ, Voogd J. 1977. The parasagittal zonation within the olivocerebellar projection. I. Climbing fiber distribution in the vermis of cat cerebellum. *J Comp Neurol* 174:417-488.
- Hawkes R, Leclerc N. 1987. Antigenic map of the rat cerebellar cortex: the distribution of parasagittal bands as revealed by monoclonal anti-Purkinje cell antibody mabQ113. *J Comp Neurol* 256:29-41.
- Hashimoto M, Mikoshiba K. 2003. Mediolateral compartmentalization of the cerebellum is determined on the "birth date" of Purkinje cells. *J Neurosci* 23:11342-11351.
- Jornfell H, Ekeröt CF, Garwicz M, Luo XL. 2000. Functional organization of climbing fibre projection to the cerebellar anterior lobe of the rat. *J Physiol (Lond)* 522 Pt 2:297-309.
- Jornfell H, Ekeröt CF. 2003. Receptive field plasticity profoundly alters the cutaneous parallel fiber synaptic input to cerebellar interneurons in vivo. *J Neurosci* 23:9620-9631.
- Korneliusson HK. 1968. On the morphology and subdivision of the cerebellar nuclei of the rat. *J Hirnforsch* 10:109-122.
- Llinás R, Sasaki K. 1989. The functional organization of the olivo-cerebellar system as examined by multiple Purkinje cell recording. *Eur J Neurosci* 1:587-603.
- Oscarsson O. 1969. Termination and functional organization of the dorsal spino-olivocerebellar path. *J Physiol* 200:129-149.
- Oscarsson O, Sjolund B. 1977. The ventral spino-olivocerebellar system in the cat. I. Identification of five paths and their termination in the cerebellar anterior lobe. *Exp Brain Res* 28:469-486.
- Pardoe J, Apps R. 2002. Structure-function relations of two somatotopically corresponding regions of the rat cerebellar cortex: olivo-cortico-nuclear connections. *Cerebellum* 1:165-184.
- Paxinos G, Watson C. 1986. The rat brain in stereotaxic coordinates. Sydney: Academic Press.
- Pijpers A, Pardoe J, Apps R, Voogd J, Ruigrok TJH. 2003. Partial congruence of climbing and mossy fiber projections to the rat cerebellum. Program No. 274.14. 2003 Abstract Viewer/Itinerary Planner. Washington, DC: Soc Neurosci Online.
- Rosina A, Provini L. 1983. Somatotopy of climbing fiber branching to the cerebellar cortex in cat. *Brain Res* 289:45-63.
- Ruigrok TJH. 1997. Cerebellar nuclei: the olivary connection. In: De Zeeuw CI, Strata P, Voogd J, Editors. The cerebellum: from structure to control. Elsevier Science B.V. pp 162-197.
- Ruigrok TJ. 2003. Collateralization of climbing and mossy fibers projecting to the nodulus and flocculus of the rat cerebellum. *J Comp Neurol* 466:278-298.
- Ruigrok TJH. 2004. Precerebellar nuclei and red nucleus. In: Paxinos G, Editor. The rat nervous system, third edition. San Diego: Elsevier Academic Press. pp 167-204.
- Ruigrok TJH, Osse R-J, Voogd J. 1992. Organization of inferior olivary projections to the flocculus and ventral paraflocculus of the rat cerebellum. *J Comp Neurol* 316:129-150.
- Ruigrok TJH, Teune TM, van der Burg J, Sabel-Goedknecht H. 1995. A retrograde double labeling technique for light microscopy. A combination of axonal transport of cholera toxin B-subunit and a gold-lectin conjugate. *J Neurosci Meth* 61:127-138.
- Ruigrok TJH, Voogd J. 1990. Cerebellar nucleo-olivary projections in rat. An anterograde tracing study with *Phaseolus vulgaris*-leucoagglutinin (PHA-L). *J Comp Neurol* 298:315-333.
- Ruigrok TJH, Voogd J. 2000. Organization of projections from the inferior olive to the cerebellar nuclei in the rat. *J Comp Neurol* 426:209-228.
- Sugihara I, Ebata S, Shinoda Y. 2004. Functional compartmentalization in the flocculus and the ventral dentate and dorsal group y nuclei: an analysis of single olivocerebellar axonal morphology. *J Comp Neurol* 470:113-133.
- Sugihara I, Shinoda Y. 2004. Molecular, topographic, and functional organization of the cerebellar cortex: a study with combined aldolase C and olivocerebellar labeling. *J Neurosci* 24:8771-8785.
- Sugihara I, Wu HS, Shinoda Y. 2001. The entire trajectories of single olivocerebellar axons in the cerebellar cortex and their contribution to Cerebellar compartmentalization. *J Neurosci* 21:7715-7723.
- Teune TM, van der Burg J, van der Moer J, Voogd J, Ruigrok TJH. 2000. Topography of cerebellar nuclear projections to the brain stem in the rat. In: Gerrits NM, Ruigrok TJH, De Zeeuw CI, Editors. Cerebellar modules: molecules, morphology and function. Amsterdam: Elsevier Science B.V. pp 141-172.
- Trott JR, Armstrong DM. 1987. The cerebellar corticonuclear projection from lobule Vb/c of the cat anterior lobe: a combined electrophysiological and autoradiographic study. I. Projections from the intermediate region. *Exp Brain Res* 66:318-338.
- Van der Want JLL, Wiklund L, Guegan M, Ruigrok TJH, Voogd J. 1989. Anterograde tracing of the rat olivocerebellar system with *Phaseolus vulgaris* leucoagglutinin (PHA-L). Demonstration of climbing fiber collateral innervation of the cerebellar nuclei. *J Comp Neurol* 288: 1-18.
- Voogd J. 1964. The cerebellum of the cat: Structure and fiber connections. Assen: Van Gorcum.
- Voogd J. 2004. Cerebellum. In: Paxinos G, Editor. The rat nervous system, third edition. San diego: Elsevier Academic Press. pp 205-242.
- Voogd J, Bigaré F. 1980. Topographical distribution of olivary and cortico nuclear fibers in the cerebellum: a review. In: Courville J, de Montigny C, Lamarre Y, Editors. The inferior olivary nucleus. Anatomy and physiology. New York: Raven Press. pp 207-234.
- Voogd J, Broere G, van Rossum J. 1969. The medio-lateral distribution of the spinocerebellar projection in the anterior lobe and the simple lobule in the cat and a comparison with some other afferent fibre systems. *Psychiatr Neurol Neurochir* 72:137-151.
- Voogd J, Eisenman LM, Ruigrok TJH. 1993. Relation of olivocerebellar projection zones to zebrin pattern in rat cerebellum. *Soc Neurosci Abstr* 19:1216.
- Voogd J, Gerrits NM, Ruigrok TJH. 1996. Organization of the vestibulocerebellum. *Ann New York Acad Sci* 781:553-579.

- Voogd J, Pardoe J, Ruigrok TJH, Apps R. 2003. The distribution of climbing and mossy fiber collateral branches from the copula pyramidis and the paramedian lobule: congruence of climbing fiber cortical zones and the pattern of zebrin banding within the rat cerebellum. *J Neurosci* 23:4645-4656.
- Voogd J, Ruigrok TJH. 1997. Transverse and longitudinal patterns in the mammalian cerebellum. In: De Zeeuw CI, Strata P, Voogd J, Editors. *The cerebellum: From structure to control*. Amsterdam: Elsevier. pp 21-37.
- Voogd J, Ruigrok TJH. 2004. The organization of the corticonuclear and olivocerebellar climbing fiber projections to the rat cerebellar vermis: the congruence of projection zones and the zebrin pattern. *J Neurocytol* 33:5-21.
- Welker W. 1987. Spatial organization of somatosensory projections to granule cell cerebellar cortex: functional and connective implications of fractured somatotopy (summary of Wisconsin studies). In: King JS, Editor. *New concepts in cerebellar neurobiology*. New York: Alan R. Liss, Inc. pp 239-280.

Figures

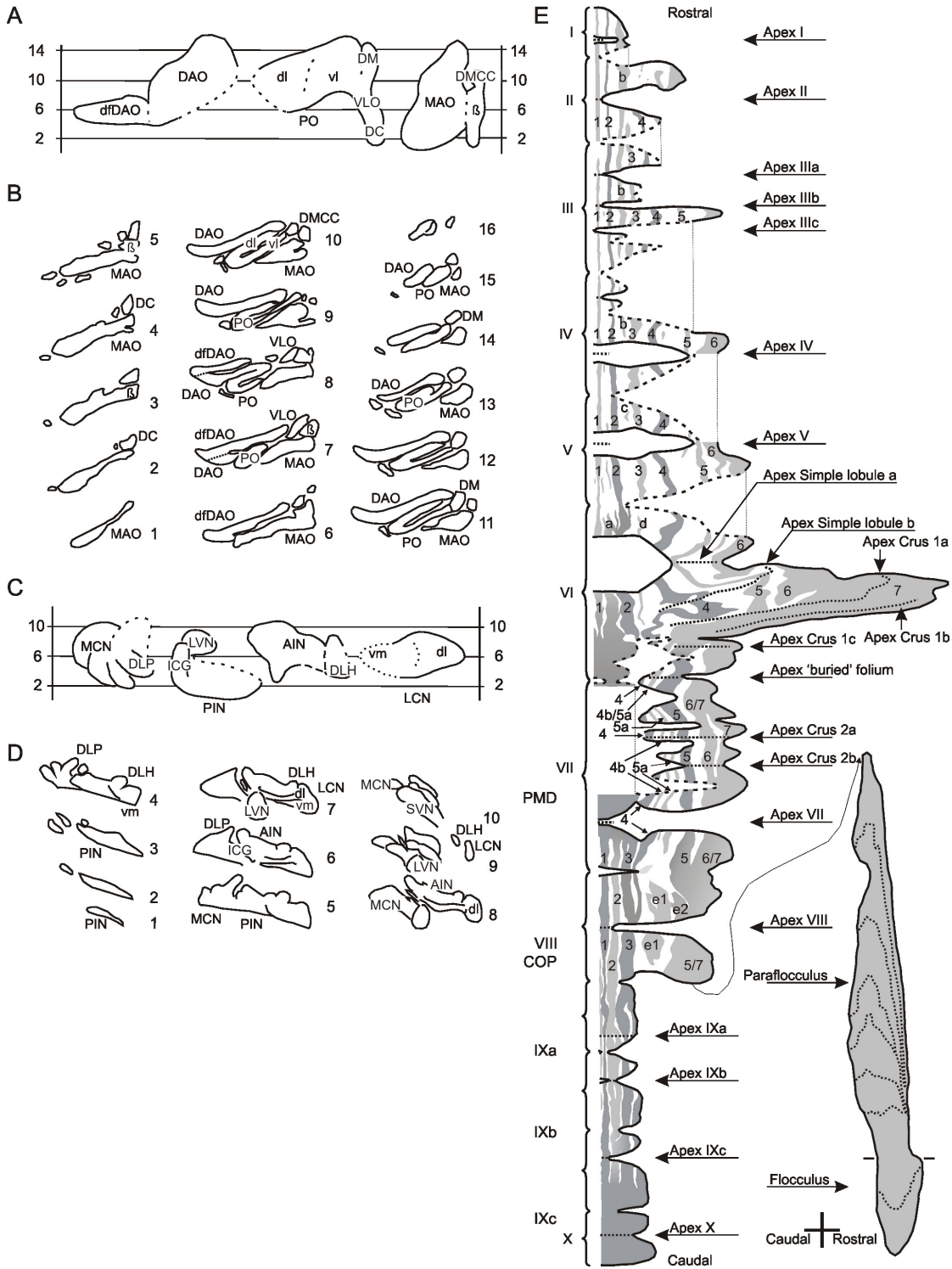


Fig. 1. Standardized diagrams of the inferior olive, cerebellar nuclei and cerebellar cortex with zebrin pattern.

These diagrams were used to indicate injections (solid contours) into the inferior olive (BDA) and cerebellar nuclei (gold-lectin) and projections (stippled contours in the inferior olive and/or cerebellar nuclei, and colored lines in the cortex). **A:** The 'unfolded' and flattened dorsal view of the left inferior olivary complex, numbers refer to the level of the corresponding transverse sections (see B). **B:** Transverse diagrams of sections through the left inferior olivary complex, numbered from caudal (1) to rostral (16) at 160 μ m intervals. **C:** The 'unfolded' and flattened dorsal view of the right cerebellar nuclei, based on the transverse series shown in D. **D:** Transverse diagrams of sections through the right cerebellar nuclei, numbered from caudal (1) to rostral (10) at 160 μ m intervals. A-D are adapted from Ruigrok and Voogd, 2000). **E:** Standardized diagram of the unfolded and flattened right half of the cerebellar cortex in which the zebrin-positive bands are indicated. Note that the orientation of the paraflocculus and flocculus is rotated 90° clockwise and both lobules are separated from the hemispherical part of lobule VIII (copula). At the midline the vermal lobules I to X are indicated, hemispherical lobules are indicated to the right. The apexes of the lobules are indicated with fine-hatched lines. For method of unfolding see 'Material and Methods' and Ruigrok, 2003). For abbreviations, see list.

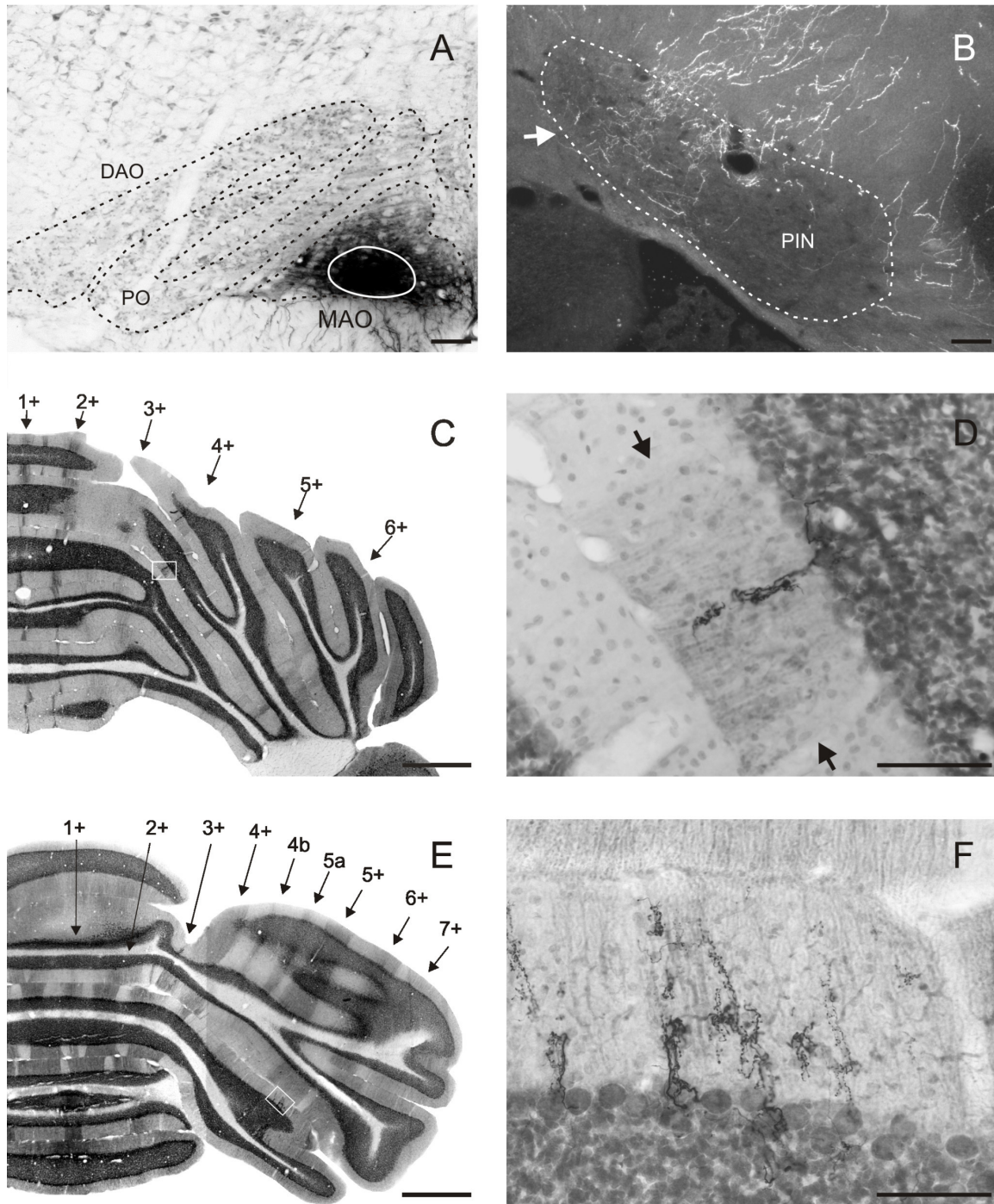


Fig. 2. Microphotographs showing examples of BDA injection site, terminal labeling in the cerebellum and the zebrin pattern. **A:** BDA injection site in the rostral MAO of case 883R. The presumed area from which tracer uptake and transport originated is indicated by the white oval. **B:** Resultant fine varicose terminal labeling in the medial part of the PIN (arrow). **C:** Overview of a zebrin-immunostained section through the anterior part of the cerebellum, the zebrin-positive bands are indicated and the boxed-in area is enlarged in **D**. **D:** Double labeling of BDA-labeled climbing fiber (black) and zebrin-positive Purkinje cells (between arrows) belonging to the P4+ band of lobule IV. **E,F:** As **C** and **D** for the posterior part of the cerebellum. Note that the labeled climbing fibers are found within the Pe2+ zebrin band. For abbreviations see list. Scale bar = 100 μ m in **A**, **B**, **D**, **F**; 1 mm in **C**, **E**.

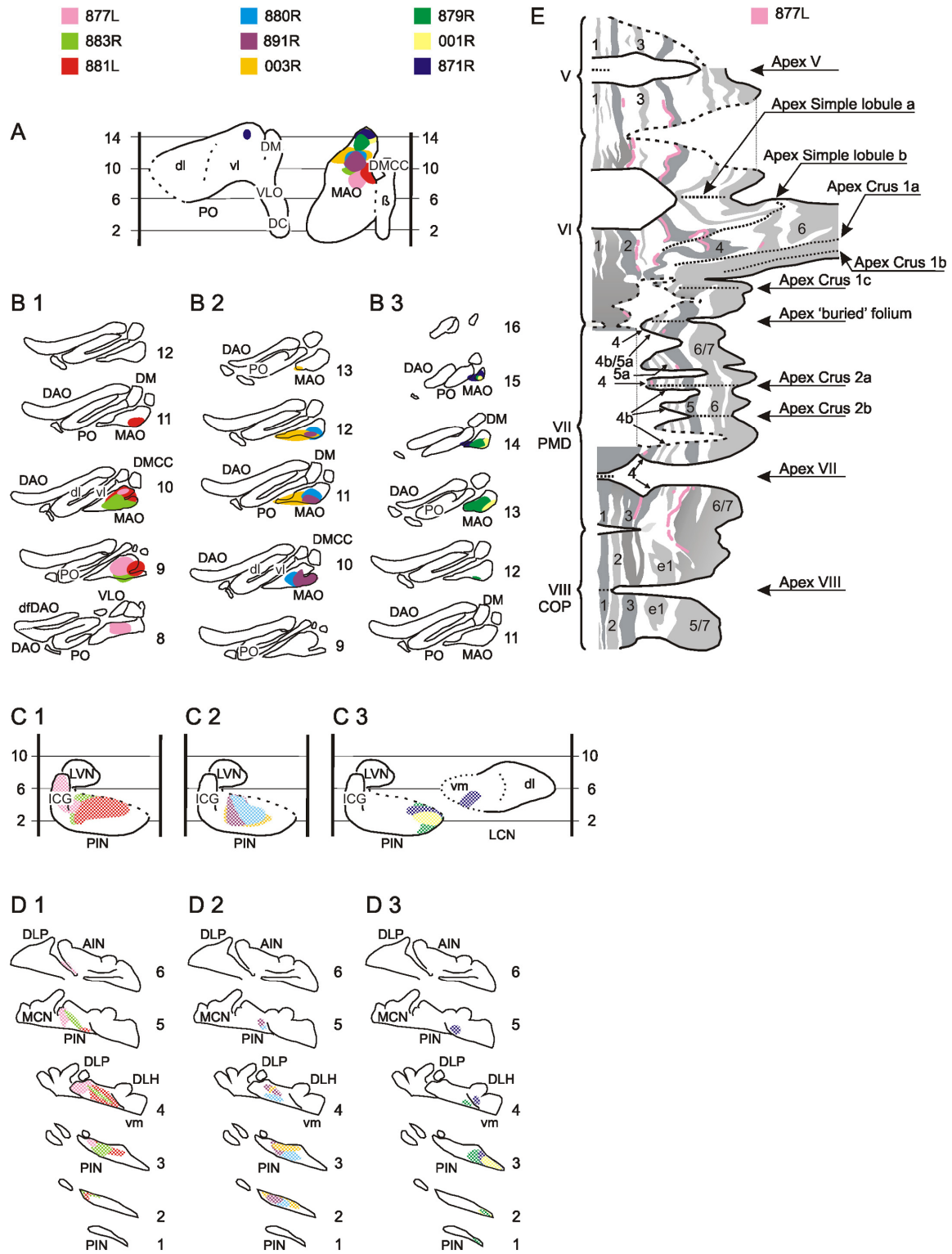


Figure 3 (Continued)

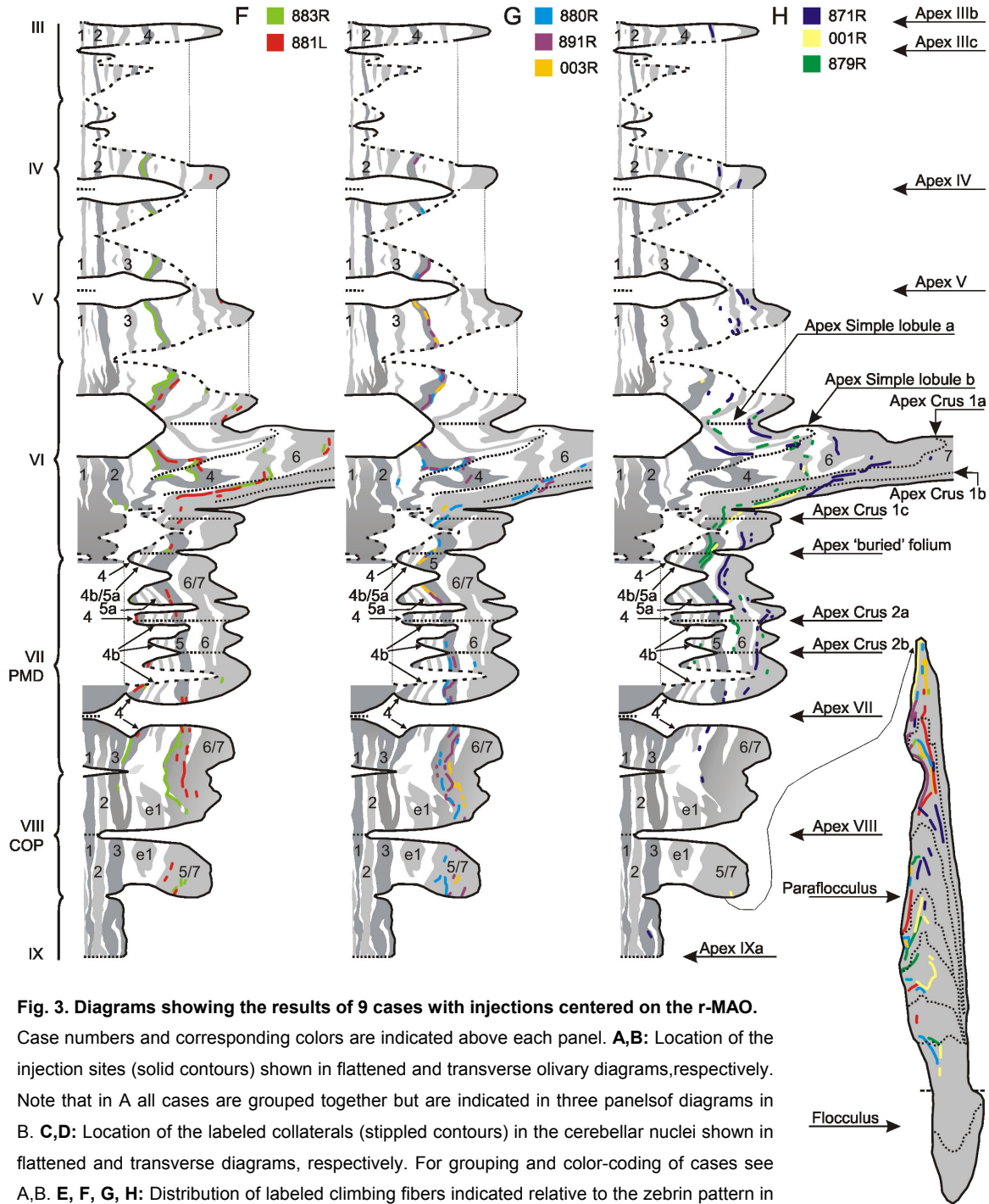


Fig. 3. Diagrams showing the results of 9 cases with injections centered on the r-MAO.

Case numbers and corresponding colors are indicated above each panel. **A,B:** Location of the injection sites (solid contours) shown in flattened and transverse olivary diagrams, respectively. Note that in A all cases are grouped together but are indicated in three panels of diagrams in B. **C,D:** Location of the labeled collaterals (stippled contours) in the cerebellar nuclei shown in flattened and transverse diagrams, respectively. For grouping and color-coding of cases see A,B. **E, F, G, H:** Distribution of labeled climbing fibers indicated relative to the zebrin pattern in the unfolded and flattened diagram of the cerebellar cortex (see Fig. 2). For all cases labeling to the paraflocculus has been entered in H. Note that the rostral-most r-MAO injections give rise to varicose terminal labeling in the lateral half of the PIN and labeled climbing fibers are mostly distributed within or directly adjacent to the P5+ band of lobules III-VI. See text for further explanation. For abbreviations, see list.

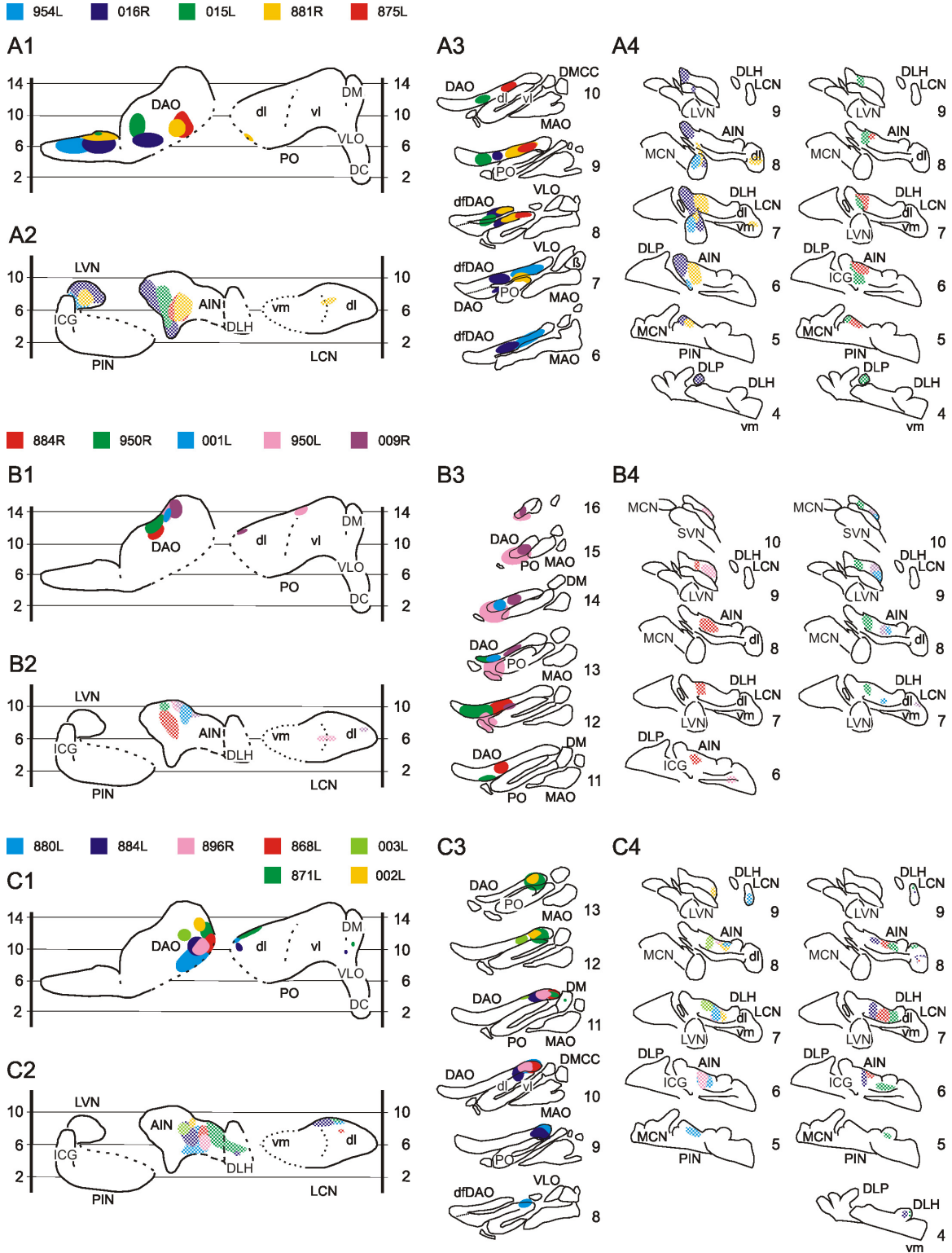


Figure 4 (Continued)

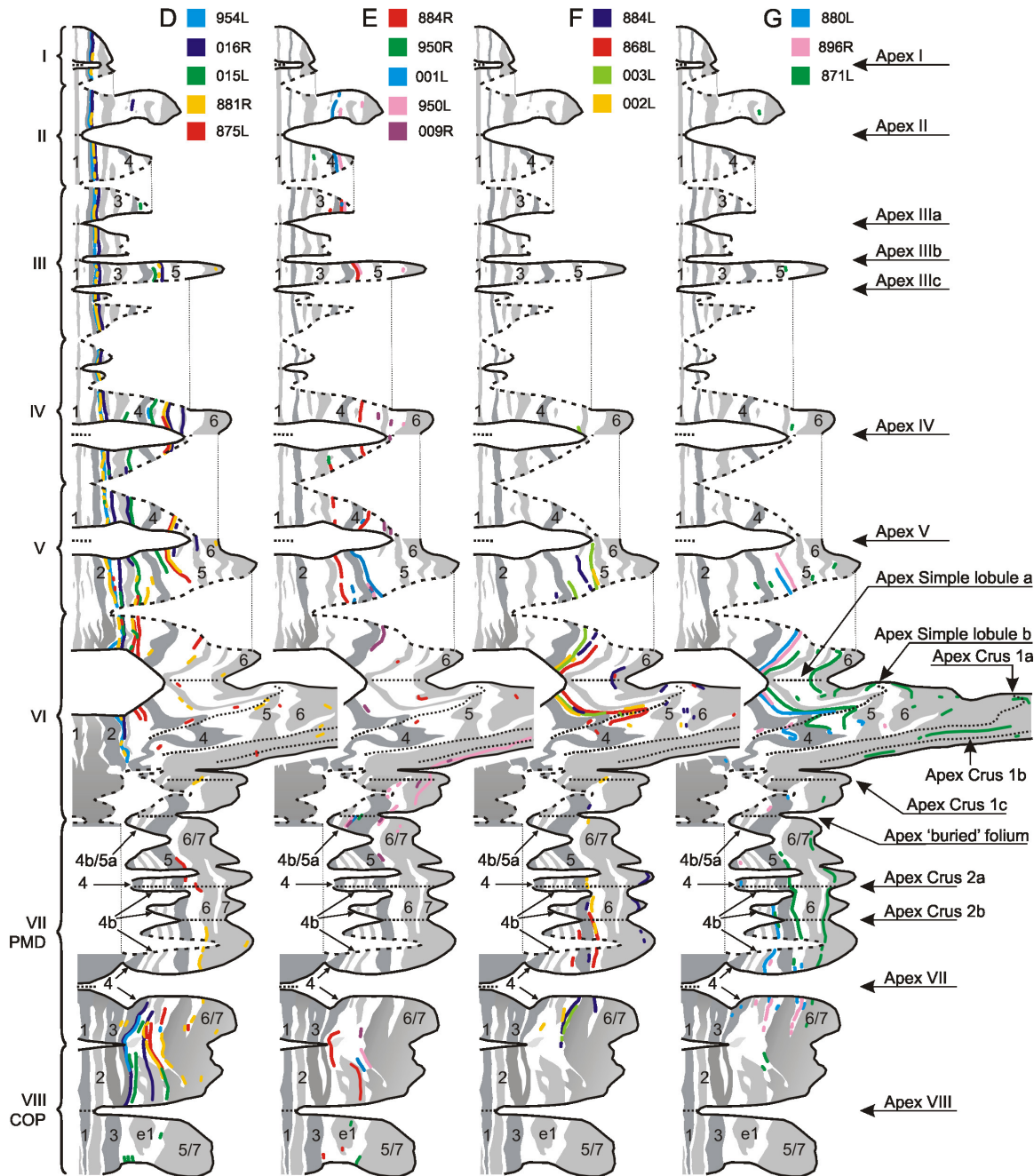


Fig. 4. Diagrams showing the injections of 17 cases with injections centered on the DAO. Case numbers and corresponding colors are indicated above each panel. **A1,B1,C1** and **A3,B3,C3**: Location of the injection sites shown in flattened and transverse olivary diagrams, respectively. **A2,B2,C2** and **A4,B4,C4**: Location of labeled collaterals in the cerebellar nuclei shown in flattened and transverse diagrams, respectively. For grouping of cases see A,B,C. **E,F,G,H**: Distribution of labeled climbing fibers indicated relative to the zebrin pattern in the unfolded and flattened diagram of the cerebellar cortex (see Fig. 2). Figure A and E represent the caudal group, B and F represent the rostrolateral group and C and G and H represent the rostromedial group. Note that between these three groups varicose terminal labeling generally shifts from medial to rostrolateral AIN and corresponds with a shift from medial positions in rostral and caudal cortex to more lateral positions in the central cerebellar cortex. See text for further explanation. For abbreviations, see list.

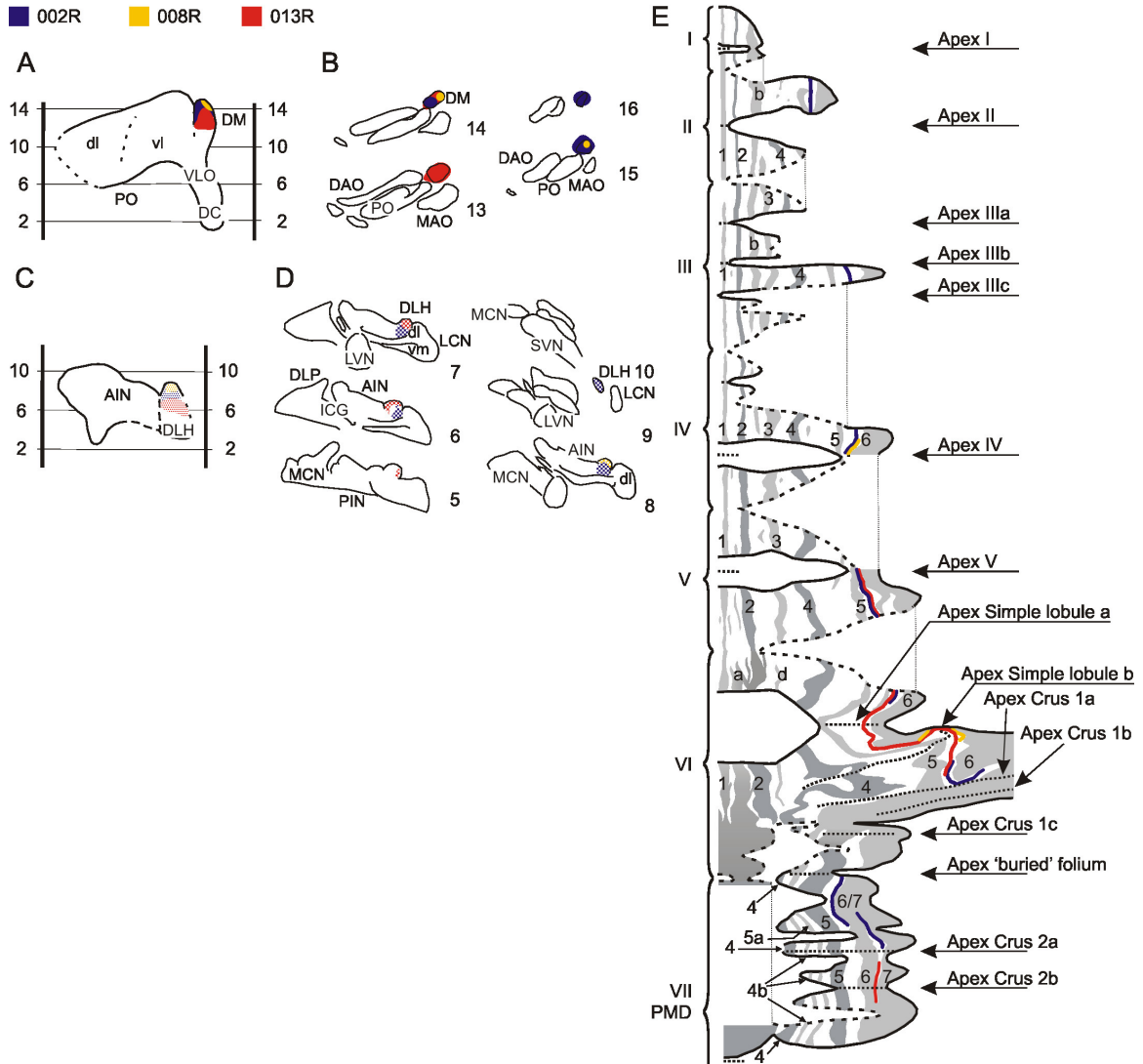


Fig. 5. Diagrams showing the injections of 3 cases with injections centered on the rostral DM group of the principal olive. Case numbers and corresponding colors are indicated above each panel. **A,B:** Location of the injection sites shown in flattened and transverse olivary diagrams, respectively. **C,D:** Location of labeled collaterals in the cerebellar nuclei shown in flattened and transverse diagrams, respectively. **E:** Distribution of labeled climbing fibers indicated relative to the zebrin pattern in the unfolded and flattened diagram of the cerebellar cortex (see Fig. 2). See text for further explanation. For abbreviations, see list.

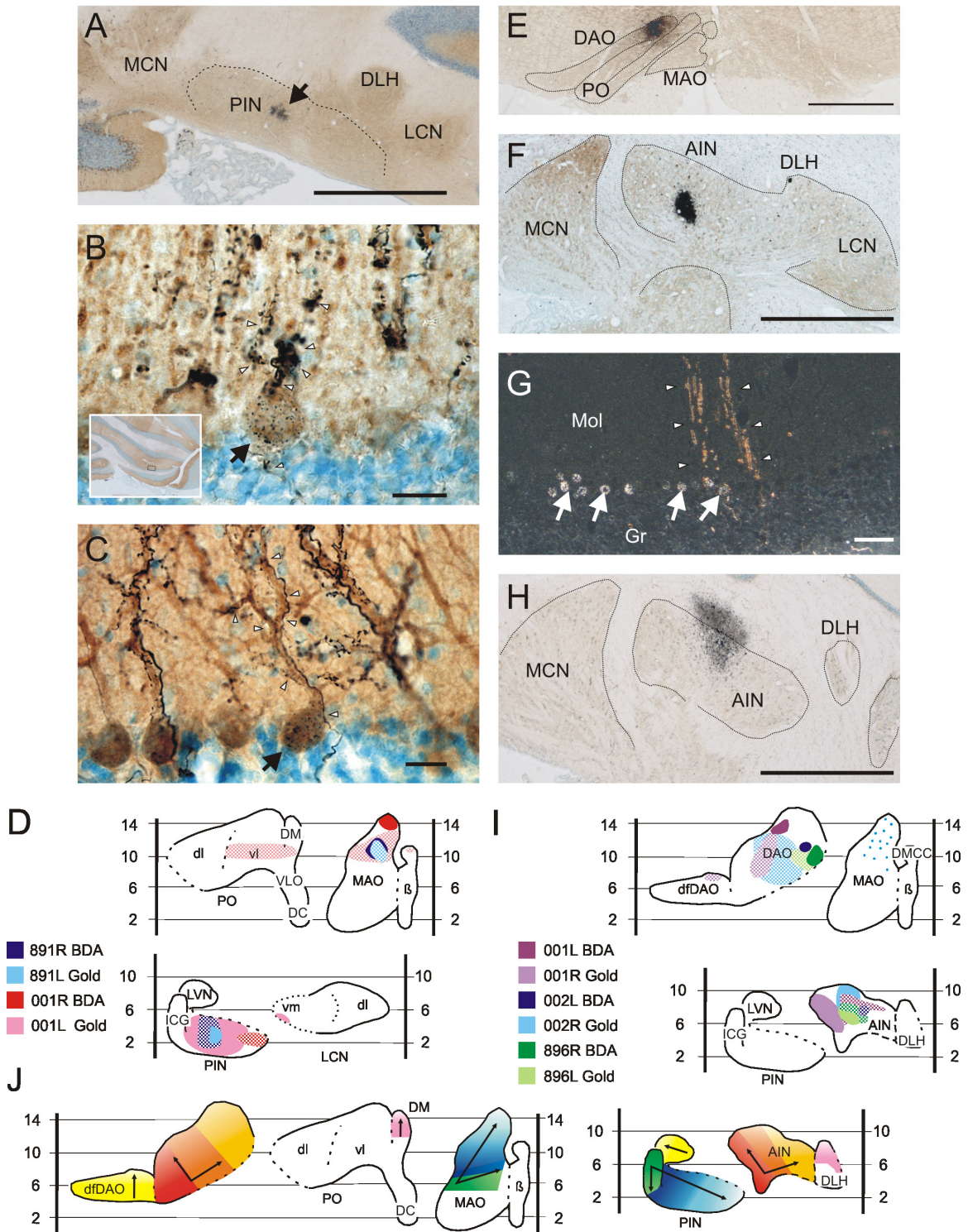


Figure 6 (Continued)

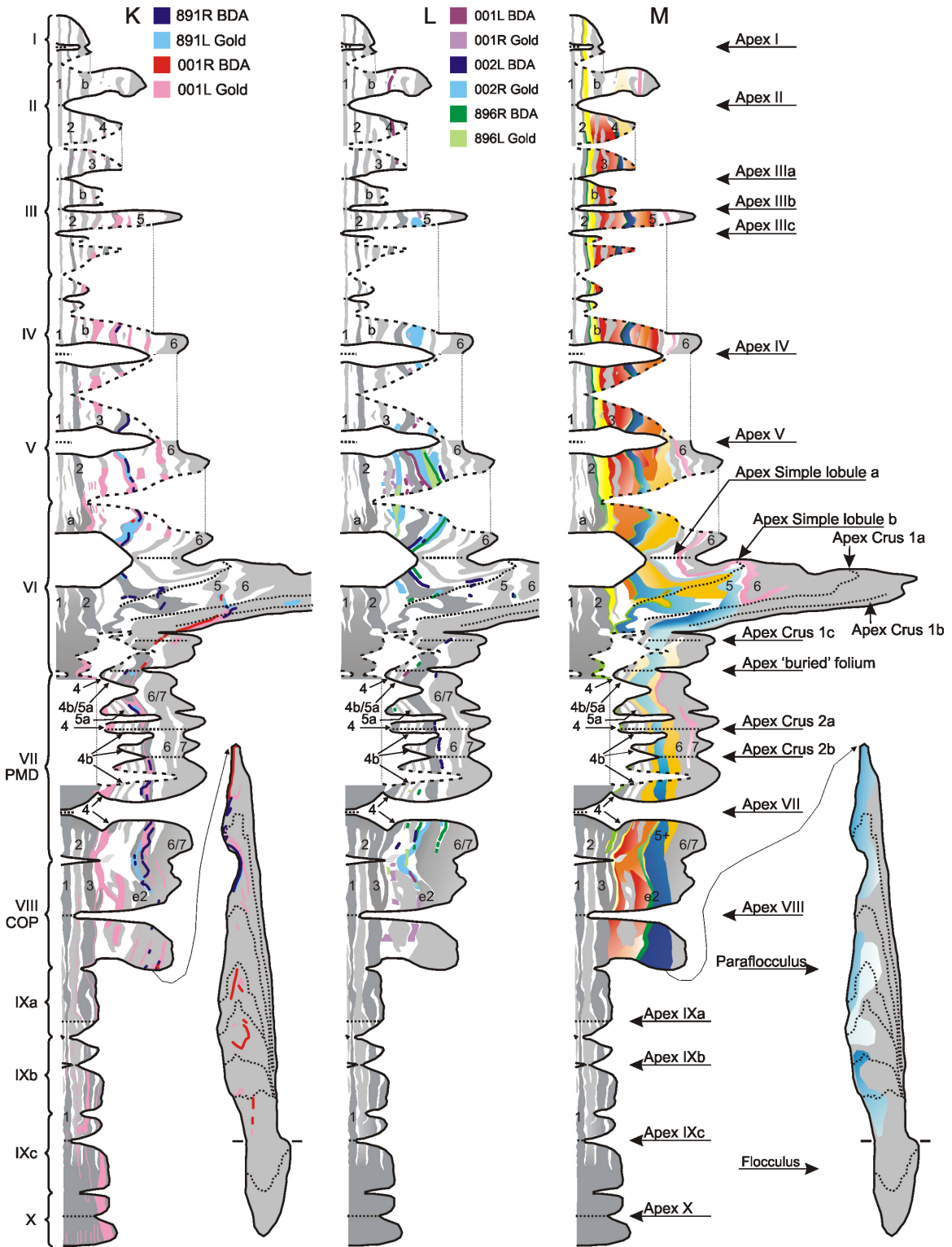


Fig. 6. Double tracing and triple labeling experiments and summary figure. A, B, C, D, and K represent two with cases injections involving the r-MAO and PIN. E, F, G, H, and L represent three cases involving DAO and AIN injections. J and M represent the summary diagrams.

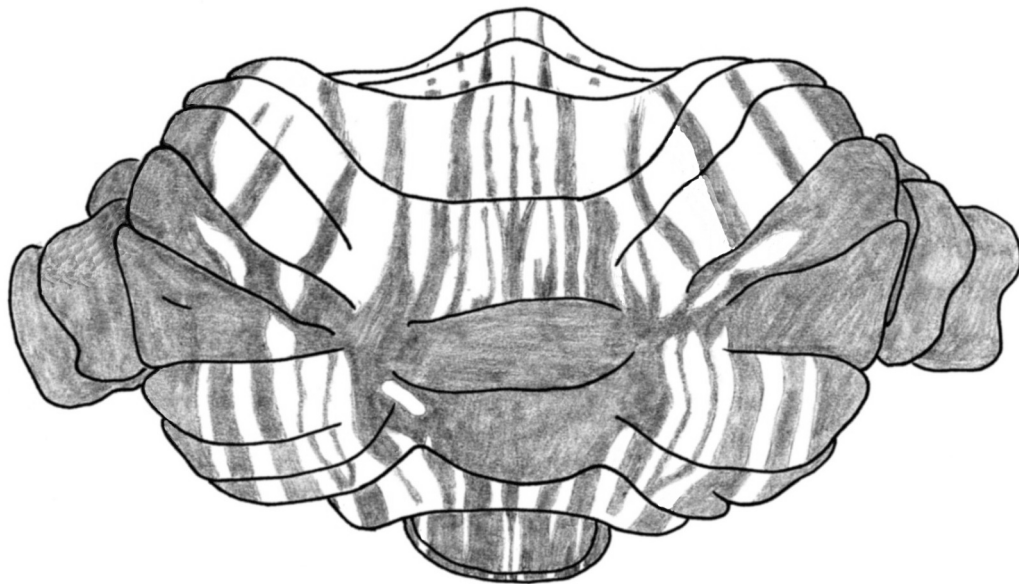
A: detail of the gold-lectin injection site in PIN in case 891L (black arrow). **B, C:** high magnification photographs of triple labeled Purkinje cells in the cerebellar cortex (PMD); Zebrin II immuno-reactivity (DAB: brown) of the P5+ band, silver-intensified gold particles in the Purkinje cell body (black arrow) and labeled climbing fiber collaterals (DAB-Cobalt: black, white arrow heads). The inset (box) in B shows a lower magnification of the PMD indicating exposed area in black box **D:** plots demonstrating location and the results of 2 cases with an injection of BDA centered on the rostral half of the MAO (solid colors) and a simultaneously placed injection with gold-lectin in the contralateral PIN (solid colors). Respective anterograde labeling in the PIN and retrograde labeling in the MAO are shown in color-matched hatching pattern. **K:** Distribution labeled climbing fibers and Purkinje cell bodies indicated relative to the zebrin pattern in the unfolded and flattened diagram of the cerebellar cortex (see Fig. 2). Note the areas of overlap between the two tracers.

E: photograph of the BDA injection in the medial DAO at level 11 (case 896R). **F:** photograph of the gold-lectin injection in the medial part of AIN at level 7 (case 896L). **G:** high magnification photograph (darkfield illumination) of lobule V showing silver-intensified gold particles in the Purkinje cell body (white arrows), labeled climbing fiber collaterals (white arrow heads). **H:** Gold-lectin injection site in case 002R. Note that in this case the injection site incorporates the fibers directly dorsal to the AIN. Here, many climbing fibers course over and towards the interposed nuclei. Damage to these fibers most likely caused the retrograde uptake by scattered olivary neurons in the rostral MAO as seen in I.I: Diagrams demonstrating location and the results of the three cases with an injection with BDA centered on the rostral half of the DAO (solid colors) and a simultaneously placed injection with gold-lectin in the contralateral AIN (solid colors). Respective anterograde labeling in the AIN and retrograde labeling in the DAO are shown in color-matched hatching pattern. Note that the gold-lectin injection in case 002R was centered on the central part of the rostral AIN and did not involve the PIN. Nevertheless, scattered retrograde labeling was noted throughout the rostral MAO (also see H and text). **L:** Distribution labeled climbing fibers and Purkinje cell bodies indicated relative to the zebrin pattern in the unfolded and flattened diagram of the cerebellar cortex (see Fig. 2). Note the areas of overlap between the two tracers.

J: Summary figure of projections within the flattened inferior olive reconstruction and its relation with the flattened cerebellar nuclei reconstruction. **M:** Summary figure of projections to the cerebellar cortex of the r-MAO, DAO and DM relative to the zebrin pattern. See text for further explanation. For abbreviations, see list. Scale bar = 1mm in A,E,F,H; 25 μ m in B,C; 100 μ m in G.

Chapter 3

Organization Of Pontocerebellar Projections To Identified Climbing Fiber Zones In The Rat



Adapted from:

Pijpers A and Ruigrok TJH (2006): *Organization of pontocerebellar projections to identified climbing fiber zones in the rat*. J Comp Neurol, 464 (4): 513-528.

Abstract

The organization of pontocerebellar projections to the paravermis and hemisphere of the posterior cerebellum of the rat was studied in relation to the organization of climbing fibers. Small injections with cholera toxin subunit b were placed in the cerebellar cortex at locations predetermined by evoked climbing fiber potentials from selected body parts or based on coordinates. The injection site was characterized with respect to the zebrin pattern and by the distribution of retrogradely labeled neurons in the inferior olive. The following zones were studied: hindlimb-related zones C1 and C2 of lobule VIII; forelimb-related zones C1, C2 and D0/D1 of the paramedian lobule; face-related zones A2 of the paramedian lobule, and C2 and D0 of crus 2B.

The results show that the distribution of pontine neurons is closely related to the climbing fiber somatotopy. Injections centered on face-related zones result in distribution of pontine neurons within the pontine core region. Forelimb regions surround this core while hindlimb regions are mostly supplied by caudal pontine regions and by a single patch of more rostrally located neurons. This distribution fits well with published data on the somatotopy of the cortico-pontine projection from the rat primary somatosensory cortex. However, apart from differences in the participation of ipsilaterally projecting cells, the distribution of pontine neurons does not change significantly when the injection covers different zones of the same lobule such as C1 and C2 of lobule VIII; C1, C2 and D0/D1 of paramedian lobule; A2 of PMD and C2 and D0 of crus 2B.

Introduction

The cerebro-cerebellar connection represents one of the most powerful pathways in the mammalian brain. The basilar pontine nuclei (Pn) essentially form the intermediary in this pathway (Brodal and Bjaalie, 1992). They receive their major input from the cerebral cortex and project as mossy fibers to the cerebellar cortex. One of the most interesting questions in the organization of this massive corridor relates to the how and why the somatotopic pattern of cerebrum (e.g. see Leergaard et al., 2000c) is transposed to a fractured cerebellar map (Welker, 1987), which supposedly results from combining peripheral and cerebro-cerebellar tactile receptive fields (Morissette and Bower, 1996). Also, as yet, it is far from clear how the organization of the other main afferent system of the cerebellum, i.e. the climbing fibers, relates to the cerebro-ponto-cerebellar system. Some of these questions will be addressed in the present study performed in the Wistar rat as they were in a very recent study by Odeh et al. (2005).

In the rat, the ipsilaterally organized corticopontine projection has been shown to originate from layer V neurons located throughout most of the cerebral cortex (Legg et al., 1989). However, clear regional differences have been described and the densest projections seem to originate

from the sensorimotor and visual cortices (for review, see Ruigrok, 2004). Although initially a clear somatotopic pattern could not be detected in the corticopontine projections that arise from the somatosensory cortex (SI), recent studies by Leergaard and collaborators have shown that the SI map is converted to concentric shells in the Pn (Leergaard et al., 2000c). A description of the translation from the concentric somatosensory pontine maps onto the somatotopic cerebellar maps described for peripherally-induced climbing fiber and mossy fiber activations (Atkins and Apps, 1997; Brown and Bower, 2001) will obviously help to understand the anatomical substrate of the fractured cerebellar somatotopy (Bower, 1996) and provide significant clues to general cerebellar functioning. Indeed, a recent study by Odeh et al. (2005) showed that the organization of the pontocerebellar projection not only is in line with previously described aspects of the corticopontine projection from the somatosensory cortex (Leergaard et al., 2000b) but also adheres to the somatotopic and zonal pattern of the climbing fiber system. In this respect it is important to note that recent studies by Cicirata and his group (Serapide et al., 1994; 2001; 2002b) also have shown that small injections with anterogradely transported tracers result in multiple longitudinally oriented strip-like patterns of mossy fibers. In the anterior cerebellum a spatial correspondence of climbing fiber zones and subjacent positioned mossy fiber rosettes both labeled from the posterior cerebellum has been suggested by Voogd et al. (2003). Similar observations have been made in the vestibulocerebellum (Ruigrok, 2003).

The zonal pattern of the organization of the climbing fibers adheres well to the organization of the Purkinje cell projections to the cerebellar nuclei (Voogd and Glickstein, 1998; Voogd, 2004; Pijpers et al., 2005). For the cat these zonal relations can be subdivided to a microzonal level which may constitute the entities of cerebellar functioning (for review see Apps and Garwicz, 2005). Somatotopic relations have also been documented for the rat concerning the connections between the dorsal accessory olive (DAO) and the C1 zone of the cerebellar cortex (Atkins and Apps, 1997; Pardoe and Apps, 2002; Voogd et al., 2003; Odeh et al., 2005). I.e. a strip of ipsilateral hindlimb responsive climbing fibers terminates within the C1 zone of the copula pyramidis (COP; lobule VIII), whereas the ipsilateral forelimb is represented by climbing fibers in both the C1 and C3 zones of the paramedian lobule (PMD; lobule VII); face-receptive fields are found within the A2 zone of the PMD. However, receptive fields of the anatomically-defined C2 zone encompass both sides of the body (Atkins and Apps, 1997).

In the present study we have examined the relation between several identified climbing fiber zones in the paravermal and hemispherical cortex of lobules VII and VIII and the organization of the pontine origin of the mossy fiber projections to these zones. Small injections with a retrograde tracer covering both the molecular and granular layer resulted in retrogradely labeled neurons in Pn as well as in the olivary subnuclei. The latter enabled identification of the zonal location of the injection and, thus, allowed studying directly the relation between the (pontine) mossy fiber projection and the climbing fiber zones. In line with results presented by Odeh et al. (2005) we

show that the pontine origin of pontocerebellar projections is related to the somatotopy of climbing fiber zones as well as to the organization of the somatosensory corticopontine projections. However, apart from differences in the amount of ipsilaterally located pontine neurons a clear distinction in distribution of pontine cells that could be related to different climbing fiber zones within the same lobule was not revealed in the present study.

From selected sections photomicrographs were prepared using a Leica DMR microscope equipped with a digital camera (Leica DC-300) was used to obtain photomicrographs. Photo panels were constructed in CorelDraw™ 11.0, after some correction for brightness and contrast in Corel Photopaint™ 11.0.

Material and Methods

For this study experiments performed in ten male Wistar rats were selected out of a batch of 16 cases with cholera toxin b subunit (CTb) injections in the posterior cerebellum. All procedures adhered to the NIH Guide for the Care and Use of Laboratory Animals according to the principles expressed in the declaration of Helsinki and were approved by a national committee overseeing animal welfare. Animals were anesthetized with a ketamine/xylazine mixture (100 mg/kg + 3mg/kg) or with pentobarbital (40 mg/kg) administered intraperitoneally (i.p.). Surgical levels of anesthesia were monitored by the absence of rhythmic whisker movements and pinch withdrawal reflex. When necessary, supplementary doses were administered to maintain surgical levels of anesthesia. During surgery body temperature was monitored and kept within physiological limits. After inducing anesthesia, the animals were placed in a stereotactic head holder and the posterior cerebellum was accessed as described earlier (Ruigrok et al., 1995; Voogd et al., 2003). Subsequently, a single iontophoretic injection was made with CTb in selected places of the right hemisphere of lobule VIII (copula pyramidis: COP), lobule VII (paramedian lobule: PMD) or crus 2B. In most cases the actual place of injection was determined by prior mapping of field potentials resulting from stimulation of the ipsilateral hindlimb, forelimb or contralateral or ipsilateral face by percutaneous stimulation with pairs of fine needles (see Table 1). The stimulation and recording paradigm has been described by Atkins and Apps (1997; also see Voogd et al., 2003). In these cases, pentobarbital was used as the anesthetic of choice. Depending on the site of maximum response, or based on coordinates, CTb (#104, lot #10426A, low salt: List Biological Laboratories, 1% w/v in 0.2 M phosphate buffer, pH 7.4) was injected at the apex of the lobule using a glass pipette (with filament, tip 10-15 µm: see Ruigrok et al., 1995; Voogd et al., 2003) and applying 7 sec on, 7 sec off pulses of 4 nA anodal current for 5 to 10 minutes. After injection, muscles and skin were sutured, and the animal was allowed to recover. Postoperative analgesia was provided by a single dose of subcutaneously administered buprenorphine (0,05 mg/kg). All

animals recovered uneventfully and were checked daily but additional analgesic therapy was not considered necessary.

After a survival time of 7 days, rats were given a lethal dose of sodium pentobarbital (240 mg/kg), and the rats were perfusion-fixed by cannulation of the ascending aorta and by subsequent infusion of 500 ml of saline, 1000 ml of fixative, made up of 4% freshly prepared paraformaldehyde and 0.1% glutaraldehyde in 0.05M phosphate buffer (PB) containing 4% sucrose. After perfusion, the brains were extracted, blocked, and post-fixed in the same fixative for 3-5 hours. They were rinsed and stored overnight in 0.05 M PB containing 10% sucrose, embedded in 11% gelatin containing 10 % sucrose. The gelatin block was hardened for 3 hours in a 4 % formaldehyde solution (containing 30% sucrose) and again stored overnight in 0.05M PB containing 30% sucrose.

Histology

Histological procedures have been detailed elsewhere (Ruigrok et al., 1995; Voogd et al., 2003). Briefly, sections were cut at 40 μ m on a freezing microtome and serially collected in glass vials containing 0.05 M PB. CTb immunohistochemistry was carried out on free floating sections within selected glass vials using subsequent incubations in a high titer polyclonal anti-cholera toxin B subunit (CTb) raised in goat (goat anti-CTb: lot #703: List Biological Laboratories, 1:15,000 in PB buffered saline, PBS, and containing 0.4% Triton X-100 for 48-72 hours at 4 °C), biotinylated donkey anti-goat (List Biological Laboratories, 1:2000 for 1½ hours at room temperature), avidin-biotin complex (ABC Elite, Vector Laboratories for 1½ hours at room temperature) and, finally, with 3,3'-diaminobenzidine tetrahydrochloride (0.025% DAB and 0.005% H₂O₂ in PB at room temperature). This procedure resulted in dense staining of CTb present at the injection site and within neuronal profiles throughout brainstem and cerebellar regions that have been known to be related to the injection site (Luppi et al., 1990; Voogd et al., 2003; Ruigrok, 2004; Voogd, 2004). Some vials were selected for double staining with zebrin II immunohistochemistry. In these vials, cobalt (0.01 %) and nickel (0.01%) ions supplemented the DAB incubation bath resulting in a black deposit of reaction product, and sections were subsequently incubated with the mouse monoclonal anti-zebrin II, which was produced by immunization with a crude cerebellar homogenate of the weakly electric fish *Apteronotus* and recognizes a single polypeptide antigen with a molecular weight of approximately 36 kD (Brochu et al., 1990). This antibody was kindly provided by Dr. R. Hawkes, Calgary, Canada. Briefly, sections were incubated, free floating, for 48-72 hours in anti Zebrin II, 1:150 in Tris-buffered saline containing 0.4% Triton X-100 (TBS) and 2% normal horse serum at 4°C. After thorough rinsing, sections were incubated for 2 hours in rabbit anti-mouse conjugated to HRP (p260 Dako, 1:200 in TBS and 2% normal horse serum). Subsequently, sections were thoroughly rinsed in phosphate buffer, incubated in a second DAB

staining (without heavy metal ions) for 15-20 min and rinsed in 0,05M PB resulting in brown staining of zebrin positive Purkinje cells in a pattern that was identical to that described in detail earlier (Voogd et al., 2003; Voogd and Ruigrok, 2004; Pijpers et al., 2005). No cellular zebrin II staining was found in the brainstem and no zebrin staining of Purkinje cells resulted when the primary antiserum was omitted. All sections were mounted on slides in a chromic alum solution, air-dried and counterstained with thionin. Subsequently, slides were dehydrated in graded alcohol and xylene, and coverslipped with Permount.

Analysis

Sections were analyzed with an Olympus microscope equipped with a Lucivid™ miniature monitor, and using NeuroLucida™ software (MicroBrightfield, Williston, VT). Brain stem and nuclear contours were plotted at low magnification (2.5x objective) and retrogradely labeled cells were subsequently indicated at high power magnification (10-20x objective). Maps of the labeling in the inferior olive as well as of the Pn were based on sequential series of 1 out of 4 sections (i.e. every 160 μm), resulting in a series of 12 coronal plots throughout the Pn. Width and height of the sections were adjusted with respect to a standard series of sections, enabling comparison of the results between animals (Brevik et al., 2001). Subsequently, a 160 μm x 160 μm grid overlay was used to count the number of labeled neurons within every grid square and served as a measure of the density of labeled neurons. Using standard Matlab™ routines and interpolation (The Mathworks Inc, Natick, MA) this density was visualized in color-coded density plots. In addition, by rearranging the grids, the same data could also be used to obtain horizontal and sagittal planes. By summation of grids, summed plots of the coronal, dorsal and sagittal views were obtained. The 12 coronal plots also served as the basis of the 3D-plots of the Pn. Section by section alignment was performed using the NeuroLucida software. The midline ventral surface of the pons was used as a reference and new sections were shifted and rotated to obtain a best fit of contours. Three-point smoothing of contours was performed before final 3D rendering by NeuroLucida.

The photomicrographs of Figure 2 were made with a Leica DMR microscope equipped with a digital camera (Leica DC-300). Photo panels were constructed in CorelDraw™ 11.0, after some correction for brightness and contrast in Corel Photopaint™ 11.0.

Results

Key objective of the present study was to relate the pontocerebellar projection to the organization of climbing fiber input to the cerebellar cortex. Because the relation between the zebrin pattern and the organization of the olivary projections to the cerebellar cortex has recently been established (Sugihara and Shinoda, 2004; Voogd and Ruigrok, 2004; Pijpers et al., 2005), an accurate classification of injection sites as based on their position relative to the zebrin pattern (see below) as well as with respect to the resultant retrograde labeling in the contralateral inferior olive was possible. Within the posterior part of the paravermal, or intermediate, cerebellar cortex three parasagittally oriented climbing fiber zones have been identified (Buisseret-Delmas and Angaut, 1993; Voogd et al., 2003; Sugihara and Shinoda, 2004). Most medially, the C1 zone is located, which receives its climbing fiber input from the ventral fold of the dorsal accessory olive (vfDAO). Directly lateral to the C1 zone, the C2 zone is found, which is innervated by climbing fibers that are derived from the rostral part of the medial accessory olive (rMAO); the C3 zone laterally borders C2 and is again supplied by the vfDAO. Lateral to the C zones, the hemispherical D zones are located and they receive their climbing fiber input from the principal olive (PO). Medial to the C zones, a vermal B zone is found in lobule VIII, whereas a vermal A2 zone is noted in lobule VII (Atkins and Apps, 1997; Sugihara and Shinoda, 2004; Voogd and Ruigrok, 2004). Identification of the C zones as well as of the A2 zone was possible prior to injection by determining the location of the receptive fields of these climbing fiber zones (Atkins and Apps, 1997; Voogd et al., 2003). However, although most of the injections (n=6) were based on the latency and laterality of the evoked climbing fiber responses from different body parts, in all cases the ultimate classification of the injection site was based on the resulting labeling in the inferior olivary complex (Table 1).

Classification of injection sites

Figure 1 presents the location of ten injections that were analyzed in detail together with their resultant labeling within the contralateral inferior olivary complex. The injections are shown relative to their position with respect to the zebrin pattern banding as examined in the double-labeled sections. Terminology of zebrin-banding is adapted from Voogd and Ruigrok (2004; also see Sugihara and Shinoda, 2004; Pijpers et al., 2005). Three of these cases were centered on the C1 zone. In case GR03, the injection was placed in the copula pyramidis (COP) where it covered part of the zebrin-positive patch 'e' (Fig. 2A). It resulted in retrogradely labeled neurons that were located in the caudolateral aspect of the vfDAO (Fig. 2B). In the COP, climbing fiber evoked potentials in C1, usually referred to as c1 (Voogd et al., 2003), can be triggered by percutaneous stimulation of the ipsilateral hindlimb and tail (Atkins and Apps, 1997). In the

paramedian lobule (PMD), two injections (cases AP03 and 979, respectively) involved the ventral and dorsal aspects of C1. Both injections were centered on the zebrin-negative zone directly medial to P5+ and resulted in labeling of olivary neurons in the rostromedial aspects of the vfDAO. In case AP03 evoked climbing fiber potentials could be triggered by percutaneous stimulation of the ipsilateral forelimb and which are typical for the C1 zone in PMD (Atkins and Apps, 1997). Medial to the C1 injections, the A2 zone was targeted in case A40. As described by Atkins and Apps (1997), contralaterally evoked responses from the face could be recorded at this site (not shown) and the subsequent CTb injection involved both the P4+ and P4- zebrin bands. The resultant olivary labeling was noted in the b/c groups of the caudal MAO, but also included neurons in the caudal part of the DM group of the PO.

Three injections were centered on the C2 zone. In case 981, the injection was positioned within the COP and was found within the medial part of the lateral-most zebrin-positive zone (P5/6/7+). Olivary labeling was restricted to the lateral aspect of the rostral part of the medial accessory olive (rMAO), thus confirming the C2 location of the injection site (Pijpers et al., 2005). In addition, in case AP09, the injection site was located within the P5+ band of PMD and labeled neurons were found within rMAO at a more medial position as compared to case 981. Finally, the injection in case A41 involved the P5+ band in crus 2B and resulted in labeling of neurons within the dorsal aspect of the rMAO. Receptive fields of c2 are typically found bilaterally on the hindlimbs for COP and on both forelimbs for PMD (Atkins and Apps, 1997) as was confirmed for case AP09, but was not tested in case 981 (Table 1). For case A41 ipsilateral face responses could be recorded prior to injection, however, the contralateral face was not tested (inset in Fig. 1A).

Three injections resulted in olivary labeling that was exclusively or mostly confined to the principal olive (PO). Labeling was specifically found in its ventral leaf and within the dorsomedial group (DM), which forms a dorsomedial extension of the ventral leaf of the PO (vIPO). The injections of cases 978 and AP02 were both located in the ventral part of the PMD and covered to varying extent zebrin zones P5- and P6/7+. In case 978, the injection was placed somewhat lateral and ventral to case AP02. In addition to the PO labeling, this resulted in several labeled neurons within the rMAO. Since no involvement of C1 or C3 was apparent due to the lack of olivary labeling in vfDAO, it is likely that the rMAO labeling resulted from a small lateral extension of the main C2 zone (present within the P5+ zebrin band) within the medial aspect of the P6/7+ zone (cf. Sugihara and Shinoda, 2004). PO labeling in case AP02 was rather similar to that obtained in case 978 but here additional labeling was not observed in rMAO but rather in vfDAO. This identified the injection site as centered on the D1 zone (vIPO) and involving the D0 zone (DM group) laterally and the zebrin-negative C3 zone (vfDAO) medially. The third injection involving the D zones (case A39) was placed in crus 2B, in a region where stimulation of the ipsilateral face (whiskerpad and upper lip region) resulted in short latency evoked climbing fiber potentials (see Fig. 1A). In this case, the resulting olivary labeling was confined to the DM group, establishing the

D0 location of the injection site (Buisseret-Delmas and Angaut, 1993; Voogd et al., 2003; Sugihara and Shinoda, 2004; Pijpers et al., 2005).

Pontine labeling

Figure 2 shows the results of the CTb injection placed in the medial aspect of COP (case GR03). As indicated above, this case resulted in labeled olivary neurons that were confined to the caudolateral aspect of vfDAO, thereby demonstrating the C1 locus of the injection site (Fig. 2A,B, also see Fig. 1). In this particular case, retrogradely labeled cells in the Pn were mostly, but not exclusively, located in their caudal aspect at the contralateral side (Fig. 2C,D). An additional cluster of labeled neurons, dissociated from the main body of labeling, was found at the rostral aspect of the Pn. Three-dimensional (3D) plots, based on a 1 out of 4 series of sections and showing both dorsal and caudal views, provide additional information on the overall distribution of labeled neurons throughout the Pn. These plots were constructed for all ten cases, thus enabling direct comparison of the Pn labeling resulting from the different zonal injections (Fig. 3). From these plots it can be appreciated that the injection in the C2 region of COP (case 981) resulted in a rather similar general distribution of pontine labeling as in case GR03 (Fig. 3, lower panels).

The middle row of panels in Figure 3 shows 3D-reconstructions of three cases with injections in the C1, C2 and D0/D1 zones of the PMD, respectively. In these cases, labeling was found at distinctively more central regions compared to the COP injections (cases GR03 and 981), although, in case of the injections of the C1 and C2 zones (cases 979 and AP09), the focus point of the labeling could still be found in the caudal half of the contralateral Pn. Projections to D0/D1 regions of the PMD originated from a medioventral sheath of cells at the center of the pons. Finally, 3D reconstructions of the A2 zone injection (case A40) in PMD and the C2 and D0 injections of crus 2B, which all receive face-triggered climbing fiber evoked potentials, show that in all these cases a fairly circumscribed patch of neurons was found at the center of the Pn. Within this center area no clear caudal or rostral bias of distribution was noted which is in contrast to all formerly described cases. The latter three cases, however, did show differences with respect to the amount of labeled neurons within the ipsilateral Pn (see below).

In order to further facilitate comparing differences in the distributions and densities of labeled neurons in the various cases, the results were quantified and represented in color-coded density distributions (Fig. 4). Note that the resulting interpolated diagrams of Pn labeling, such as shown in Figure 4C, provide both a quick and visually attractive way to evaluate the plot of the same section shown in Figure 4A. By rearranging the grids of consecutive transverse sections (1 out of 4 series of 40 μm sections), horizontally as well as sagittally oriented sectional views of similarly color-coded diagrams could be constructed (Fig. 5A). In this way, the distribution of labeled cells can be readily appraised in all three dimensions and the most optimal view for comparing the

resulting distribution of labeled neurons between cases could be chosen (Fig. 5B). For the present analysis both sliced (Fig. 6A) as well as summed horizontal views (Fig. 6B) were constructed for all cases.

Figure 6A provides sliced diagrams arranged into horizontal sections at different dorsoventral levels of eight representative cases (cf. middle column of Fig. 5A). These diagrams clearly show that the labeling resulting from COP injections (cases GR03 and 981) not only was focused in the caudal part of the Pn, but also at their ventral-most levels. In contrast, the patch of labeling in the rostral pons in both cases was noted at distinctively more dorsal levels. The highest densities of labeled neurons after PMD injections into C1/C2 cases were not only found more rostrally, but also more dorsally compared to cases GR03 and 981. The injection aimed for the forelimb c3 zone but resulting in coverage of mostly the D0/D1 zones (case AP02), also showed a pontine distribution quite similar to that of the C1 and C2 related zones and related region. Finally, the injections in face-related regions of both PMD and crus 2B (cases A40, A41 and A39) appear to be centered in the rostrocaudal as well as the dorsoventral axes.

From these horizontal views, it can be appreciated that in several cases a considerable amount of labeled neurons was located within the ipsilateral Pn (Fig. 6). A further quantification of the distribution of contra- and ipsilateral labeling is shown in Table 1. Note that the case involving the contralateral face regions (A2 of PMD) resulted in the highest percentage of ipsilaterally labeled neurons, followed by both cases that were centered on the C1 zone of the PMD. This contrasts with especially the C1 injection in COP (GR03) and the three hemispherical injections that all resulted in less than 5% of ipsilaterally located pontine neurons.

Figure 6B displays a summary figure of the results where figurines of the summed dorsal views of the pontine labeling are shown on the approximate locations of their respective injection sites on the posterior cerebellum and with respect to their zonal positions. In this view, it can be appreciated that the distribution of pontine cells resulting from injections that were made in the same lobule (e.g. COP) were rather similar whereas the results from injections made in the same zone (e.g. C2) but in different lobules were not. Also note that the distribution of neurons in the contralateral pons after injection into the A2 zone of PMD was quite confined and was rather similar to that resulting from the C2 and D0 cases of crus 2B. In fact, the most striking difference between these injections related to the amount of ipsilaterally labeled neurons that rapidly decreased after more laterally placed injections. A similar tendency was observed in the other injections of the PMD, but was not evident in the two COP cases (Table 1). The injection into the D0 zone of crus 2 resulted in the most confined distribution of labeled neurons that were all located in the center of the contralateral Pn.

Discussion

Pontocerebellar projection and its relation with the corticopontine projection

The cerebrocerebellar connection by way of the Pn is likely to be the largest extracerebral connection in most mammalian species. However, only recently detailed insight into the fine anatomical organization of the first leg, i.e. the cerebro-pontine projection from the primary sensory cortex (SI), has been obtained using small electrophysiologically guided cortical injections of multiple anterogradely transported tracers and 3-dimensional reconstruction techniques (Leergaard et al., 2000a; 2000b). In these, and earlier studies that investigated the ontogeny of the cerebropontine projections (Leergaard et al., 1995), it was shown that the spatial relations that exist within SI essentially are maintained in a more clustered form within the Pn. However here, the rather clearly recognizable cortical somatosensory map of the rat is transposed in sphere-like concentric rings with the head in the center and surrounded by the forelimbs, body and, finally, the hindlimbs and tail (Leergaard et al., 2000b).

Here, we show that the topography of corticopontine projections is generally maintained in the pontocerebellar projection (Fig. 7). Indeed, our injections in lobule VIII, which is considered to be involved in the control of the hindlimb (for review, see Manni and Petrosini, 2004), mostly labeled pontine neurons in a location that was very similar to the corticopontine projections from the hindlimb region of SI (Leergaard et al., 2000b). Likewise, the origin of the pontine projections to the PMD, controlling the forelimb, is overlapping with cerebral projections from the forelimb SI. Finally, the injections into crus 2B, as well as the medial-most injection in PMD, all in a face responsive area, only resulted in labeled pontine neurons that took up rather central positions in the contralateral Pn, hence at a position where terminals from the face-region of the somatosensory cortex are likely to terminate. Similar conclusions were reached in a recent study by Odeh and collaborators (2005), who studied the distribution of retrogradely labeled neurons in the Pn after injections of fluorescent beads in the C1 and A2 zones of PMD and the C1 zone of COP. However, it should be noted that the C1 zone has climbing fiber receptive fields located on body parts ipsilateral of the cerebellar zone, whereas the A2 zone is mostly activated from contralateral face regions (Atkins and Apps, 1997). Nevertheless, as in our material, the pontine distribution of retrogradely labeled cells after an injection in A2 seems to overlap with the distribution after our crus 2B injection in C2 or D0. This suggests that all face-related regions of the cerebellar cortex may receive their pontine 'face' information from essentially the same region but receive their climbing fiber input from rather different parts of the inferior olivary complex.

The observed coincidence between patterns of corticopontine terminations from SI and distribution of pontocerebellar neurons to these regions suggests that at least aspects of the organization of corticopontine projection patterns are maintained in the organization of

pontocerebellar connections. This seems at odds with the general notion that the mossy fiber projections in general and the pontocerebellar projection in particular are characterized by a rather divergent and patchy organization that ultimately results in the transformation of a single cortical somatosensory map into multiple non-continuous or fractured somatosensory regions on the cerebellar cortical surface (Brodal, 1982; Welker, 1987; Bower, 1996; Voogd et al., 1996; Wu et al., 1999). The regions investigated in the present paper are selected and classified with respect to the origin of their climbing fiber input from either hindlimb, forelimb or face rather than with the fine, and fractured, topographic relations that have been described for mossy fibers inputs to these regions (Bower et al., 1981; Welker, 1987; Manni and Petrosini, 2004). Nevertheless, in agreement with Odeh et al. (2005), we are able to make statements on the correlation between the organization of pontocerebellar and olivocerebellar systems.

Pontocerebellar projection and climbing fiber zones

By relating retrograde labeling within the Pn and the inferior olivary complex after individual injections into the cerebellar cortex, it was possible to verify the relation between the cortico-ponto-cerebellar input and the climbing fiber receptive fields in COP, PMD and crus 2B. For the rat, climbing fiber receptive fields in COP and PMD were first described by Atkins and Apps (1997) and were later confirmed by others (Teune et al., 1998; Pardoe and Apps, 2002; Voogd et al., 2003). In these studies, the C1 zone of lobule VIII was shown to respond to short latency stimulation of the ipsilateral hindlimb (i.e. physiological c1 zone) and to receive its climbing fibers from the lateral part of the dorsal accessory olive (DAO). The C2 zone of lobule VIII, by definition, receives its climbing fibers from the rostral part of the medial accessory olive (rMAO) and can be activated from both hindlimbs at a longer latency. In between, a small CX zone or lateral c1 zone is located, which is characterized by short latency hindlimb receptive fields corresponding with climbing fibers that are derived from the intermediate part of the medial accessory olive (iMAO: Atkins and Apps, 1997; Voogd et al., 2003). This latter zone was not specifically studied in the present study.

Although both COP injections were not placed using prior determination of the receptive fields, by relating the injection site to the cortical pattern of zebrin II (Sugihara and Shinoda, 2004) and, more importantly, to the resultant labeling in the inferior olive, it was inferred that our two COP injections typically were centered on the C1 (GR03) and C2 (981) zones. However, no obvious differences were noted in the overall distribution of labeled neurons within the contralateral Pn, although the more or less separated rostral patch of neurons seems to take up a somewhat larger area in case 981 (C2) compared to case GR03 (C1). The observation that the percentage of ipsilaterally labeled neurons was more than twice as high in case 981 (C2) as compared to GR03 (C1: Table 1) may correspond with the notion that the climbing fiber receptive fields of C2 involve both hindlimbs, rather than solely the ipsilateral hindlimb in C1 (Atkins and Apps, 1997).

Within the PMD, six injections were described in the present study that, based on both its location with respect to the zebrin pattern as well as their distribution of retrogradely labeled cells within the inferior olivary complex, were judged to be located in either the A2, C1, C2 or D0/D1 zones. Furthermore, four of these injections had been placed based on the size and distribution of evoked potentials triggered from electrical stimulation of the ipsi- or contralateral forelimbs or contralateral face. Despite the fact that the zonal location of these injections was rather different, the distribution of pontine cells appeared to be remarkably similar with the exception of the A2 injection (case A40). Peak density in all other cases was noted in a focused region, approximately 500-600 μm rostral to the caudal pontine border. This distribution is similar to that observed by Odeh et al. (2005) after selective injections of the C1 zone in PMD. Since these authors also noted a systematic difference in pontine labeling between A2 and C1 zone injections of the PMD they concluded that a precise cerebro-ponto-cerebellar topography exists which can be defined by climbing fiber somatotopy. The present study is in general agreement with this conclusion, provided that the term climbing fiber somatotopy specifically refers to the general part of the body from which climbing fiber responses may be elicited rather than to a more detailed relation with a zonal topography as based on differences between ipsi- and bilateral representation of body parts and related to origin of the climbing fibers within the olivary complex (i.e. C1 or C2 of either COP or PMD). In line with this notion was the observation that although all three cases with injections of the face-responsive regions in PMD and crus 2B, were localized, based on their resultant olivary labeling, within different climbing fiber zones (i.e. A2 of PMD, and C2 and D0 of crus 2B, respectively), most labeling was confined to a central core of the contralateral Pn in all three cases. Hence, the general distribution of pontine neurons that send mossy fiber rosettes to areas subjacent to the characterized climbing fiber zones depends more on the body region from which climbing fiber evoked potentials can be generated (i.e. face, forelimb, hindlimb) than on the zonal location of these regions as based on the olivary origin of these climbing fibers (i.e. A2, C1, C2, or D0/D1 zone).

Although the general pontine distribution was rather similar, conspicuous differences between injections covering different zones were also noted. They concern the percentages of ipsilaterally labeled Pn cells. Quite contrary to the injections in the C1 zone of the COP, PMD injections of C1 resulted in rather high densities of ipsilaterally located neurons, while the highest ipsilateral percentage was noted after the A2 injection (Table 1). These numbers were quite similar to the observations of Odeh et al. (2005). However, although with respect to the predisposition of ipsilaterally located neurons, C1 of COP and PMD were markedly different, this was not the case after injection into C2 of PMD (case AP09) and COP (981). C2 of crus 2B resulted in labeling of twice as many neurons in the ipsilateral Pn as the other C2 cases (Table 1). Finally, injections involving D-zones resulted in very few ipsilaterally localized pontine neurons. Indeed, the ipsilateral face-related region of D0 in case A39 clearly contrasts the contralateral face-related

region of A2 in case A40. In this respect it is interesting to note that the micromapping studies of Welker and his group (1987) show that in the medial regions of crus 2 and PMD (both probably covered by the A2 zone: Voogd and Ruigrok, 2004), patches of granule cells are found that respond to either contralateral or bilateral regions of the face. If indeed, a close correspondence is present between the organization of the climbing fiber system and that of the mossy fibers (Brown and Bower, 2001; Ruigrok, 2003; Voogd et al., 2003; Apps and Garwicz, 2005), a more refined mapping of climbing fiber receptive fields in these regions likewise might reveal a different location for contralaterally and bilaterally located receptive fields. This could be related to the fact that within this region several narrow zebrin zones are located (i.e. P4+, P4-, P4a+, P4a- etc.), which have been shown to receive their climbing fibers from separate olivary subnuclei (Sugihara and Shinoda, 2004). Indeed, our injection A40 covered both the P4+ region as well as the adjacent P4- zone and resulted in retrograde labeling in the caudal DM group (which was shown to project selectively to the P4+ band) and the b/c group of the caudal MAO (projecting to several narrow zones lateral to P4+). Since bilateral projections from the trigeminal nucleus to especially the b/c groups of MAO have been well documented in rabbit (Van Ham and Yeo, 1992), the P4- region could very well be involved in processing information from both sides of the face, whereas other, adjacent, zones might be more selectively involved in processing either ipsi- or contralateral face information.

In conclusion, the location of the pontine neurons that project to the granular layer subjacent to either the A2, C1, C2 or D0/D1 climbing fiber zones of the posterior cerebellum is not simply based on this zonal identification but correlates quite well with the general part of the body that can activate these climbing fibers. Zone-dependent differences that were noted mostly concerned the laterality of retrogradely labeled pontine neurons which, taken together, suggests a highly structured organization of pontocerebellar projections (Mihailoff et al., 1981; Serapide et al., 2002b).

Modular organization of climbing and mossy fiber connections

One of the main questions of this study was to see if the cerebellar cortical regions that receive a characteristic climbing fiber input also differ with respect to the origin of their mossy fiber inputs from the basal Pn. This possibility was suggested by the work of Serapide and collaborators (1994; 2002a), who showed in the rat that small injections with anterograde tracers in the Pn or the reticular tegmental nucleus of the pons resulted in a number of longitudinal zones of mossy fibers. Indeed, Voogd and colleagues (2003) have noted that collaterals of climbing fibers, labeled from localized CTb injections in the caudal cerebellum and arranged in longitudinal patterns, were always accompanied by mossy fiber rosettes labeled from the same injection. However, the origin of the participating mossy fibers was not specified in that study. Congruence of peripherally triggered mossy fibers and climbing fibers has been shown by comparing the receptive fields of

peripheral mossy and climbing fibers responses in a selected region of crus 2 (Brown and Bower, 2001) and by relating this to the zonal distribution of the zebrin pattern of Purkinje cells (Hallem et al., 1999). Cerebrally evoked somatosensory mossy fiber responses have been shown to be in register with the peripherally evoked patterning (Bower et al., 1981).

So, if one accepts a close correlation between the receptive fields of climbing and mossy fibers and most people agree that the climbing fiber organization follows zonal, or at least elongated, patterns (Sugihara and Shinoda, 2004; Voogd and Ruigrok, 2004; Apps and Garwicz, 2005; Pijpers et al., 2005), it follows that the mossy fiber organization is also likely to generally adhere to these patterns. However, our results in this retrograde study do not seem to endorse this conclusion. Apart from the differences in the contribution of ipsilaterally projecting pontine neurons, no conspicuous differences could be noted between the distribution of pontine neurons that supply mossy fibers to C1 or C2 zones of COP and PML. This could imply that within the pontine regions that supply afferents to either the COP or PML, differences in distribution may exist but escape the present level of analysis. Indeed, Eisenman has noted small regional differences of pontine projections to medial, intermediate and lateral parts of lobule VIII, but it appeared not possible to make positive correlations with the olivocerebellar patterning (Eisenman, 1981b; Eisenman, 1981a; also see Mihailoff et al., 1981). A similar conclusion has been made for pontine projections to zonal regions of PMD in the cat (Hoddevik and Walberg, 1979) and for projections of the reticular tegmental nucleus of the pons to the PMD in the rabbit (Grottel et al., 1989). Recently, Herrero et al. (2002) studying collateralization of pontine and olivary projections to c1 zones of both the simple lobule and PMD in the rat noted that there was no correlation in the incidence of double labeled neurons between both cell groups, although one was noted between olivary labeling and labeling in the lateral reticular nucleus. They concluded that the mossy fiber projections from the pons are not zonally organized. Finally, Morissette and Bower (1996) provided evidence that the spatial distribution of cortico-ponto-cerebellar mediated peripheral responses measured within crus 2B have a wider spatial distribution as compared to the direct trigeminocerebellar responses. Therefore, it is quite possible that the zonal distribution of mossy fiber collaterals and their relation to climbing fiber collaterals (Voogd et al., 2003; Pijpers et al., 2005) is primarily based on collateralization of mossy fibers from non-pontine regions such as the spinal cord and lateral reticular formation (King et al., 1998; Herrero et al., 2002). However, in that case the zonal patterning observed after making small injections into the pons as well as the zonal differences in ipsilateral pontine labeling could not be easily explained (Serapide et al., 2001; Voogd et al., 2003). Hence, it is also possible that subtle differences in location of the retrogradely labeled Pn neurons escape the level of the currently used analysis. Indeed, the considerable differences noted in the percentage of ipsilaterally located neurons suggest that zone-related differences in Pn location indeed are possible. Double or triple retrograde tracer

studies employing climbing fiber zone (or mossy fiber patch) -characterized injections into the same cerebellar lobule, may help to establish such patterning.

Functional considerations

Cerebellar modules and their underlying micromodules are thought to act as the functional units of the cerebellum (Apps and Garwicz, 2005). The organization of the climbing fiber input system and the corticonuclear output seems to be perfectly related (Pijpers et al., 2005). However, a climbing fiber-related, modular organization of the mossy fiber system is much less obvious. Only recently have studies in cat and rat suggested that different parts of the mossy fiber input system (e.g. lateral reticular nucleus and Pn) are connected in a distinctive way to the cerebellar modular system (King et al., 1998; Herrero et al., 2002). The present study shows that the organization of pontine projections to the posterior parts of the intermediate cerebellum of the rat can be characterized by patterns of body representations of the overlying climbing fibers and seems to be less obviously related to the olivary origin of the climbing fiber zones. Nevertheless, more subtle zonal differences may still be present as was indicated by zonal differences in ipsilateral projections.

Highly structured patterning of mossy fibers within the cerebellar cortex will have to be taken into account in models of cerebellar functioning. I.e. a potential narrow spatial correlation between the functional identity of mossy and climbing fibers suggests that when both systems are (near-) simultaneously active, local interactions with other constituents of the cerebellar cortex, i.e. granule cells, interneurons and of course the Purkinje cells, are likely to be of a quite different nature when compared to regions receiving mossy fiber collaterals without related climbing fibers (Jorntell and Ekerot, 2003; Apps and Garwicz, 2005). These findings suggest that our knowledge on the spatial and temporal interrelations between the cerebellar afferents and the cortical network (Simpson et al., 2005) has only just begun to deepen.

Acknowledgements

We thank Mrs E. Sabel-Goedknecht, Mr J. van der Burg and Mr E. Dalm for their excellent technical assistance. Support contributed by: Neth Org Sci Res grant nr. 810.37.005 and the Dutch Ministry of Health, Welfare, and Sports.

Abbreviations used in text

β beta subnucleus
BSA bovine serum albumin
COP copula pyramidis
CTb cholera toxin b-subunit
DAB 3,3'-diaminobenzidinetetrahydrochloride
DAO dorsal accessory olive
DC dorsal cap
dfDAO dorsal fold of DAO
dlPO dorsal leaf of PO
DM dorsomedial group
DMCC dorsomedial cell column
lfp longitudinal fascicle of pons
iMAO intermediate part of MAO
PB phosphate buffer
PBS phosphate buffered saline
PMD paramedian lobule
Pn pontine nuclei
PO principal olive
Py pyramidal tract
rMAO rostral medial accessory olive
SI primary somatosensory cortex
TBS tris buffered saline
vfDAO ventral fold of DAO
vlPO ventral leaf of PO

References

- Apps R, Garwicz M. 2005. Anatomical and physiological foundations of cerebellar information processing. *Nat Rev Neurosci* 6:297-311.
- Atkins MJ, Apps R. 1997. Somatotopical organisation within the climbing fibre projection to the paramedian lobule and copula pyramidis of the rat cerebellum. *J. Comp. Neurol.* 389:249-263.
- Bower JM. 1996. Perhaps it's time to completely rethink cerebellar function. *Behav Brain Sci* 19:438.
- Bower JM, Beermann DH, Gibson JM, Shambes GM, Welker W. 1981. Principles of organization of a cerebro-cerebellar circuit. Micromapping the projections from cerebral (SI) to cerebellar (granule cell layer) tactile areas of rats. *Brain Behav Evol* 18:1-18.
- Brevik A, Leergaard TB, Svanevik M, Bjaalie JG. 2001. Three-dimensional computerised atlas of the rat brain stem precerebellar system: approaches for mapping, visualization, and comparison of spatial distribution data. *Anat Embryol (Berl)* 204:319-332.
- Brochu G, Maler L, Hawkes R. 1990. Zebrin II: a polypeptide antigen expressed selectively by Purkinje cells reveals compartments in rat and fish cerebellum. *J. Comp. Neurol.* 291:538-552.
- Brodal P. 1982. The cerebropontocerebellar pathway: Salient features of its organization. In: Chan-Palay V, Palay S, Editors. *The cerebellum-New vistas*. Berlin, Heidelberg: Springer-Verlag. p 108-132.
- Brodal P, Bjaalie JG. 1992. Organization of the pontine nuclei. *Neurosci Res* 13:83-118.
- Brown IE, Bower JM. 2001. Congruence of mossy fiber and climbing fiber tactile projections in the lateral hemispheres of the rat cerebellum. *J Comp Neurol* 429:59-70.
- Buisseret-Delmas C, Angaut P. 1993. The cerebellar olivo-cortico-nuclear connections in the rat. *Progr. Neurobiol.* 40:63-87.
- Eisenman LM. 1981a. Olivocerebellar projections to the pyramis and copula pyramidis in the rat: Differential projections to parasagittal zones. *J. Comp. Neurol.* 199:65-76.
- Eisenman LM. 1981b. Pontocerebellar projections to the pyramis and copula pyramidis in the rat: evidence for a mediolateral topography. *J Comp Neurol* 199:77-86.
- Grottell K, Zimny R, Jakielska D. 1989. Do the same subdivisions of the nucleus reticularis tegmenti pontis project onto longitudinal zones of the paramedian lobule? An anatomical study in the rabbit with retrograde tracing technique (HRP). *J Hirnforsch* 30:107-112.
- Hallem JS, Thompson JH, Gundappa-Sulur G, Hawkes R, Bjaalie JG, Bower JM. 1999. Spatial correspondence between tactile projection patterns and the distribution of the antigenic Purkinje cell markers anti-zebrin I and anti-zebrin II in the cerebellar folium crus IIA of the rat. *Neuroscience* 93:1083-1094.
- Herrero L, Pardoe J, Apps R. 2002. Pontine and lateral reticular projections to the c1 zone in lobulus simplex and paramedian lobule of the rat cerebellar cortex. *Cerebellum* 1:185-199.
- Hoddevik GH, Walberg F. 1979. The pontine projection onto longitudinal zones of the paramedian lobule in the cat. *Exp Brain Res* 34:233-240.
- Jorntell H, Ekerot CF. 2003. Receptive field plasticity profoundly alters the cutaneous parallel fiber synaptic input to cerebellar interneurons in vivo. *J Neurosci* 23:9620-9631.
- King VM, Armstrong DM, Apps R, Trott JR. 1998. Numerical aspects of pontine, lateral reticular, and inferior olivary projections to two paravermal cortical zones of the cat cerebellum. *J Comp Neurol* 390:537-551.
- Leergaard TB, Alloway KD, Mutic JJ, Bjaalie JG. 2000a. Three-dimensional topography of corticopontine projections from rat barrel cortex: correlations with corticostriatal organization. *J Neurosci* 20:8474-8484.
- Leergaard TB, Lakke EA, Bjaalie JG. 1995. Topographical organization in the early postnatal corticopontine projection: a carbocyanine dye and 3-D computer reconstruction study in the rat. *J Comp Neurol* 361:77-94.
- Leergaard TB, Lyngstad KA, Thompson JH, Taeymans S, Vos BP, De Schutter E, Bower JM, Bjaalie JG. 2000b. Rat somatosensory cerebropontocerebellar pathways: spatial relationships of the somatotopic map of the primary somatosensory cortex are preserved in a three-dimensional clustered pontine map. *J Comp Neurol* 422:246-266.
- Leergaard TB, Lyngstad KA, Thompson JH, Taeymans S, Vos BP, De Schutter E, Bower JM, Bjaalie JG. 2000c. Rat somatosensory cerebropontocerebellar pathways: spatial relationships of the somatotopic map of the primary somatosensory cortex are preserved in a three-dimensional clustered pontine map. *J Comp Neurol* 422:246-266.
- Legg CR, Mercier B, Glickstein M. 1989. Corticopontine projection in the rat: the distribution of labelled cortical cells after large injections of horseradish peroxidase in the pontine nuclei. *J. Comp. Neurol.* 286:427-441.
- Luppi P-H, Fort P, Jouvet M. 1990. Ionophoretic application of unconjugated cholera toxin B subunit (CTb) combined with immunohistochemistry of neurochemical substances: a method for transmitter identification of retrogradely labeled neurons. *Brain Res.* 534:209-224.
- Manni E, Petrosini L. 2004. A century of cerebellar somatotopy: a debated representation. *Nat Rev Neurosci* 5:241-249.
- Mihailoff GA, Burne RA, Azizi SA, Norell G, Woodward DJ. 1981. The pontocerebellar system in the rat: an HRP study. II. Hemispherical components. *J Comp Neurol* 197:559-577.
- Morissette J, Bower JM. 1996. Contribution of somatosensory cortex to responses in the rat cerebellar granule cell layer following peripheral tactile stimulation. *Exp Brain Res* 109:240-250.
- Odeh F, Ackerley R, Bjaalie JG, Apps R. 2005. Pontine maps linking somatosensory and cerebellar cortices are in register with climbing fiber somatotopy. *J Neurosci* 25:5680-5690.
- Pardoe J, Apps R. 2002. Structure-function relations of two somatotopically corresponding regions of the rat cerebellar cortex: olivo-cortico-nuclear connections. *Cerebellum* 1:165-184.

- Pijpers A, Voogd J, Ruigrok TJH. 2005. Topography of olivo-cortico-nuclear modules in the intermediate cerebellum of the rat. *J Comp Neurol* 493.
- Ruigrok TJ. 2003. Collateralization of climbing and mossy fibers projecting to the nodulus and flocculus of the rat cerebellum. *J Comp Neurol* 466:278-298.
- Ruigrok TJH. 2004. Precerebellar nuclei and red nucleus. In: Paxinos G, Editor. *The rat nervous system*, third edition. San Diego: Elsevier Academic Press. p 167-204.
- Ruigrok TJH, Teune TM, van der Burg J, Sabel-Goedknecht H. 1995. A retrograde double labeling technique for light microscopy. A combination of axonal transport of cholera toxin B-subunit and a gold-lectin conjugate. *J. Neurosci. Meth.* 61:127-138.
- Serapide MF, Cicirata F, Sotelo C, Panto MR, Parenti R. 1994. The pontocerebellar projection: longitudinal zonal distribution of fibers from discrete regions of the pontine nuclei to vermal and parafloccular cortices in the rat. *Brain Res* 644:175-180.
- Serapide MF, Panto MR, Parenti R, Zappala A, Cicirata F. 2001. Multiple zonal projections of the basilar pontine nuclei to the cerebellar cortex of the rat. *J Comp Neurol* 430:471-484.
- Serapide MF, Parenti R, Panto MR, Zappala A, Cicirata F. 2002a. Multiple zonal projections of the nucleus reticularis tegmenti pontis to the cerebellar cortex of the rat. *Eur J Neurosci* 15:1854-1858.
- Serapide MF, Zappala A, Parenti R, Panto MR, Cicirata F. 2002b. Laterality of the pontocerebellar projections in the rat. *Eur J Neurosci* 15:1551-1556.
- Simpson JI, Hulscher HC, Sabel-Goedknecht E, Ruigrok TJ. 2005. Between in and out: linking morphology and physiology of cerebellar cortical interneurons. *Prog Brain Res* 148:329-340.
- Sugihara I, Shinoda Y. 2004. Molecular, topographic, and functional organization of the cerebellar cortex: a study with combined aldolase C and olivocerebellar labeling. *J Neurosci* 24:8771-8785.
- Teune TM, van der Burg J, De Zeeuw CI, Voogd J, Ruigrok TJH. 1998. Single Purkinje cell can innervate multiple classes of projection neurons in the cerebellar nuclei of the rat: a light microscopic and ultrastructural triple-tracer study in the rat. *J. Comp. Neurol.* 392:164-178.
- Van Ham JJ, Yeo CH. 1992. Somatosensory trigeminal projections to the inferior olive, cerebellum and other precerebellar nuclei in rabbits. *Eur. J. Neurosc.* 4:302-317.
- Voogd J. 2004. Cerebellum. In: Paxinos G, Editor. *The rat nervous system*, third edition. San diego: Elsevier Academic Press. p 205-242.
- Voogd J, Glickstein M. 1998. The anatomy of the cerebellum. *Trends Neurosci.* 2:305-371.
- Voogd J, Jaarsma D, Marani E. 1996. The cerebellum: chemoarchitecture and anatomy. In: Swanson LW, Björklund A, Hökfelt T, Editors. *Handbook of Chemical Neuroanatomy*. Elsevier Science B.V. p 1-369.
- Voogd J, Pardoe J, Ruigrok TJ, Apps R. 2003. The distribution of climbing and mossy fiber collateral branches from the copula pyramidis and the paramedian lobule: congruence of climbing fiber cortical zones and the pattern of zebrin banding within the rat cerebellum. *J Neurosci* 23:4645-4656.
- Voogd J, Ruigrok TJ. 2004. The organization of the corticonuclear and olivocerebellar climbing fiber projections to the rat cerebellar vermis: the congruence of projection zones and the zebrin pattern. *J Neurocytol* 33:5-21.
- Welker W. 1987. Spatial organization of somatosensory projections to granule cell cerebellar cortex: functional and connectional implications of fractured somatotopy (summary of Wisconsin studies). In: King JS, Editor. *New concepts in cerebellar neurobiology*. New York: Alan R. Liss, Inc. p 239-280.
- Wu HS, Sugihara I, Shinoda Y. 1999. Projection patterns of single mossy fibers originating from the lateral reticular nucleus in the rat cerebellar cortex and nuclei. *J Comp Neurol* 411:97-118.

Tables

Table 1. List of experiments and distribution and number of labeled cells in Inferior Olive and Basal Pontine Nuclei ¹

Exp. no.	Lobule	Evoked potentials	Olivary region with labeling	Corresponding cortical zone	Labeled olivary cells (n)	Labeled pontine cells (n)	Ipsilateral pontine cells (%)
GR03	COP	Not tested	vfDAO	C1	167	790	2,51
981	COP	Not tested	rMAO	C2	24	276	6,16
A40	PMD	Contralateral face	MAO b/c + DM	A2 + ?	27	488	47,95
AP03	PMD	Ipsilateral forelimb	vfDAO	C1	105	631	12,97
979	PMD	Not tested	vfDAO	C1	89	709	16,22
AP09	PMD	Ipsi- and contralateral forelimb	rMAO	C2	40	612	6,37
978	PMD	Not tested	viPO/DM	D0/D1	17	459	2,83
AP02	PMD	Ipsilateral forelimb	viPO/DM	D0/D1	59	1093	3,84
A41	Crus 2B	Ipsilateral face	rMAO	C2	29	389	13,37
A39	Crus 2B	Ipsilateral face	DM	DM	33	146	3,42

¹ For abbreviations, see list

Figures

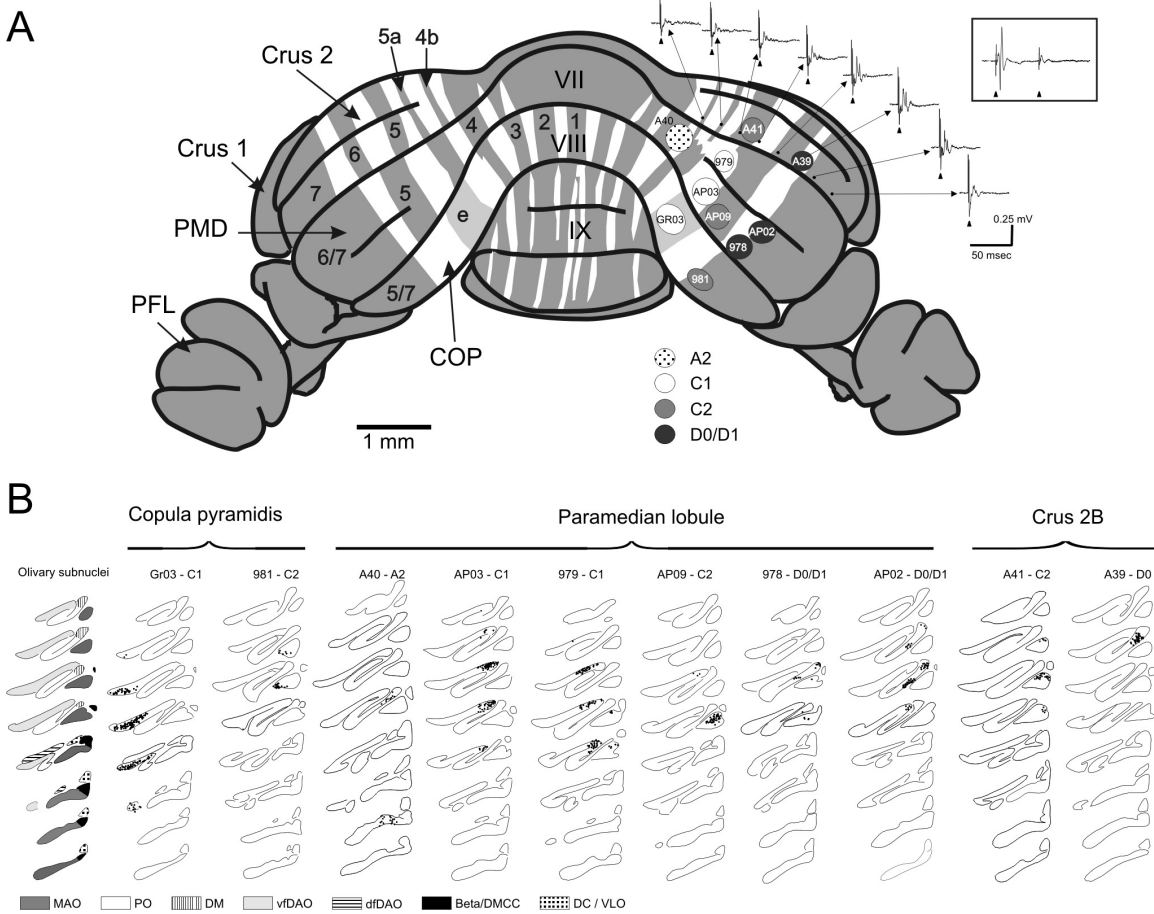


Fig. 1. A: Diagram depicting the site and size of the CTb injections described in this study. Approximate positions of the injections are indicated on a reconstruction of the posterior view of a sectioned rat cerebellum stained for zebrin (Voogd and Ruigrok, 2004). Injections are gray-scale coded to indicate their zonal position as based on the retrograde labeling of neurons in the inferior olive. For case A39 averaged evoked potentials (10 sweeps) triggered from electrical stimulation of the ipsilateral whiskerpad and upper lip region at 300 μA are shown as recorded from the indicated positions on folium B of crus 2. Arrowheads indicate time of stimulation and short arrows point to the sharp positive deflections suggested to be related to climbing fiber activation. Latency of the peak response at the place where the injection was made measured 6.6 msec. Inset shows paired pulse stimulation (interval of 50 msec) in another experiment (A40). Note that the second pulse failed to trigger an evoked response (arrows), which is highly indicative that the evoked potentials indeed reflect climbing fiber activation (Atkins and Apps, 1997). At the indicated positions no responses could be evoked from ipsi- or contralateral hindlimb or forelimb stimulation. **B:** Plots of retrograde labeling in the inferior olive at 160 μm intervals. Each dot indicates a single labeled olivary neuron. Cases are grouped according to their lobular location and distribution of most of the retrogradely labeled cells in the inferior olivary complex. Key to different subdivisions of inferior olive is shown on the far left. For abbreviations see list.

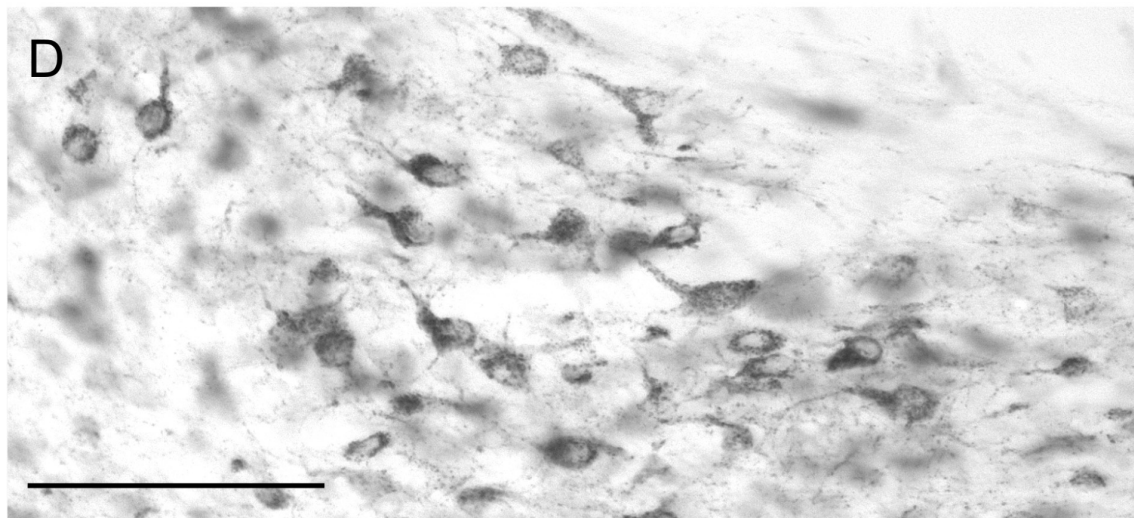
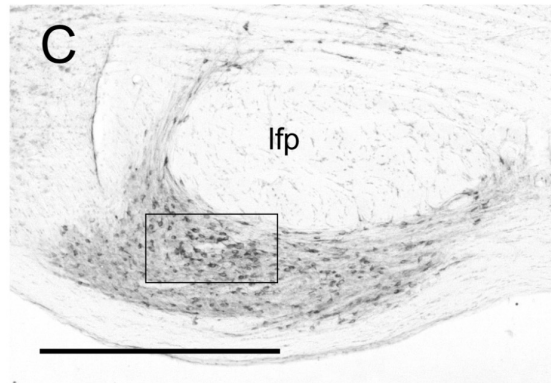
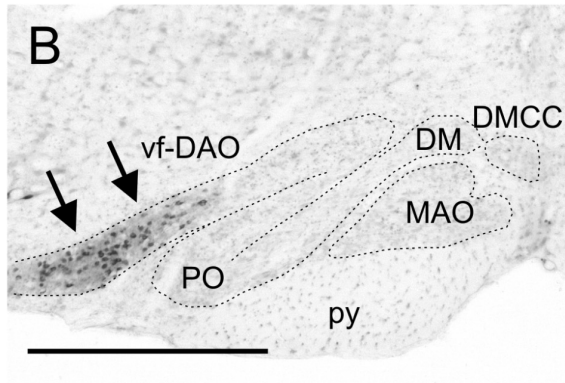
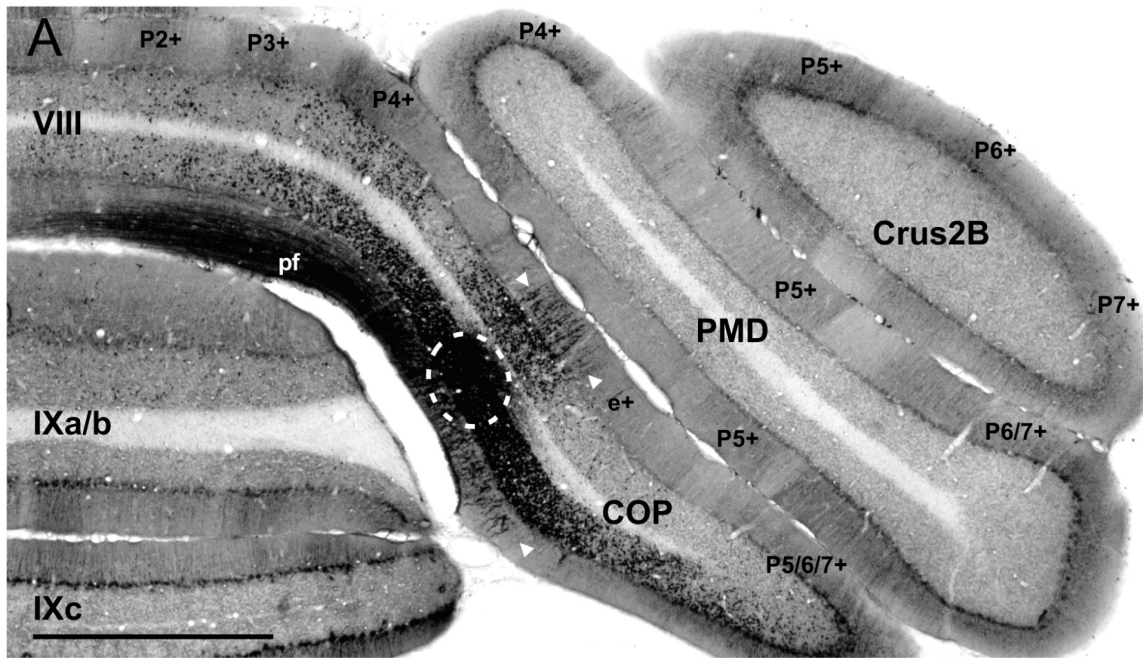


Fig. 2. Microphotographs showing results from case GR03. **A:** Transverse section of the posterior cerebellum incubated for zebrin showing the CTb injection centered at the COP (white hatched circle). Zebrin-positive bands are indicated according to Voogd and Ruigrok (2004). Note that collaterals of labeled mossy fibers are visible throughout the granular layer of lobule VIII as are labeled parallel fibers (pf) and climbing fibers in the molecular layer (arrowheads). **B:** Retrogradely labeled olivary neurons (arrows) are confined to the lateral aspect of the contralateral vfDAO. **C:** retrogradely labeled neurons in the contralateral Pn. **D:** Higher magnification of labeled neurons shown in the boxed area of C. All sections were counterstained with thionin. For abbreviations see list. Scale bar equals 1mm in A, B and C and 100 μ m in D.

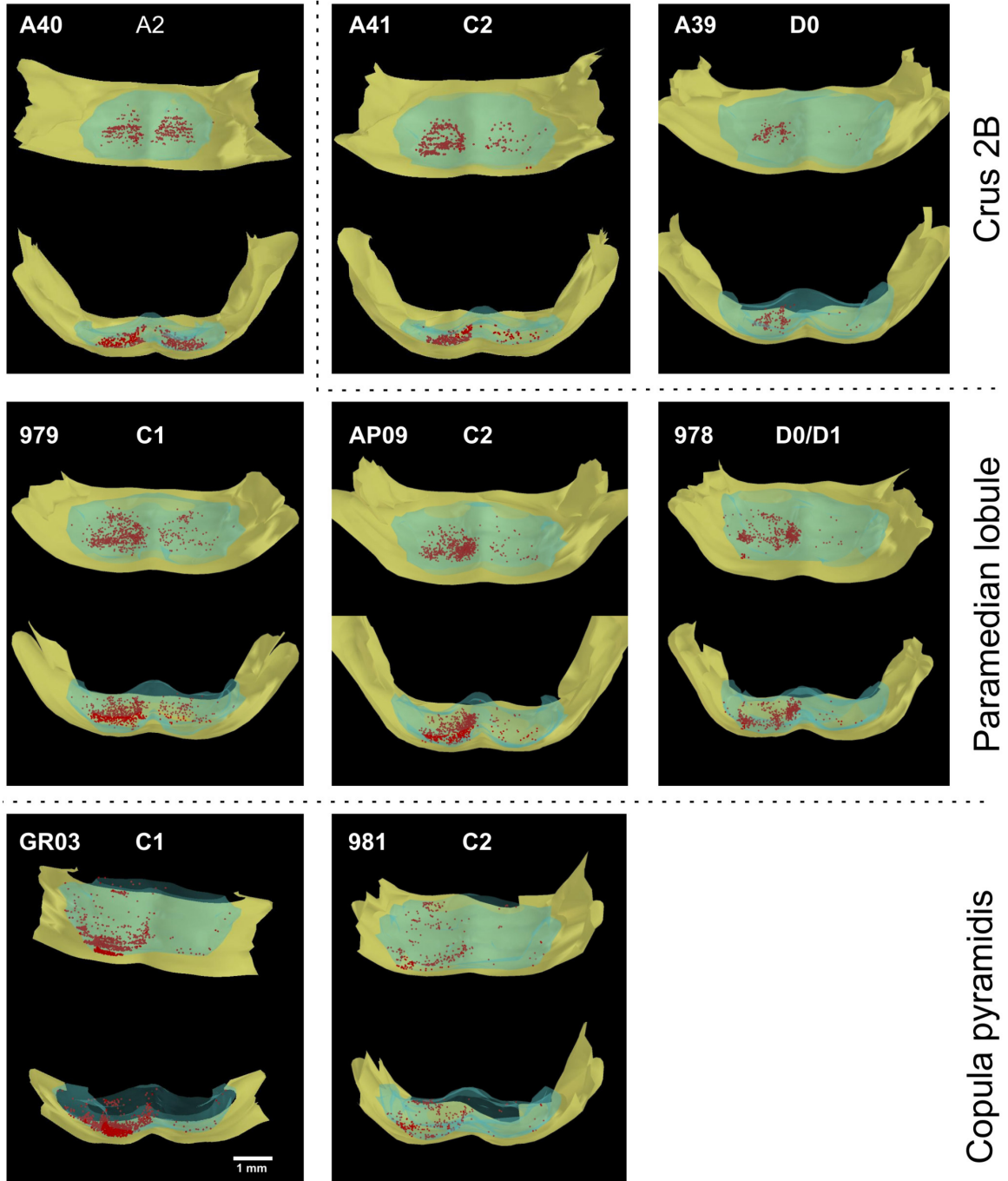


Fig. 3. Three-dimensional (3D) reconstructions of eight cases showing the distribution of retrogradely labeled neurons in the basal pons. Cases are arranged according to position of the injection site. In the top row right-most two panels reflect the 3-D reconstructions of cases A41 and A39 in which the injection was placed in C2 and D0 of crus 2B, respectively. Top row, left hand panel shows pontine labeling in case A40 with an injection involving the A2 zone of PMD. Middle row shows other PMD injections, from left to right cases 979, AP09 and 978 with an injection in C1, C2, and D0/D1, respectively. Refer to Figure 1 for location of injections and determination of climbing fiber zone. Bottom row shows the pontine reconstructions of cases GR03 and 981 with injections in C1 and C2 of the COP, respectively. Both a dorsal (top) and a caudal (bottom) 3D view are shown of the Pn (blue), the pial surface (yellow) and all labeled neurons (red dots) as plotted using a 1 out of 4 series of consecutive sections.

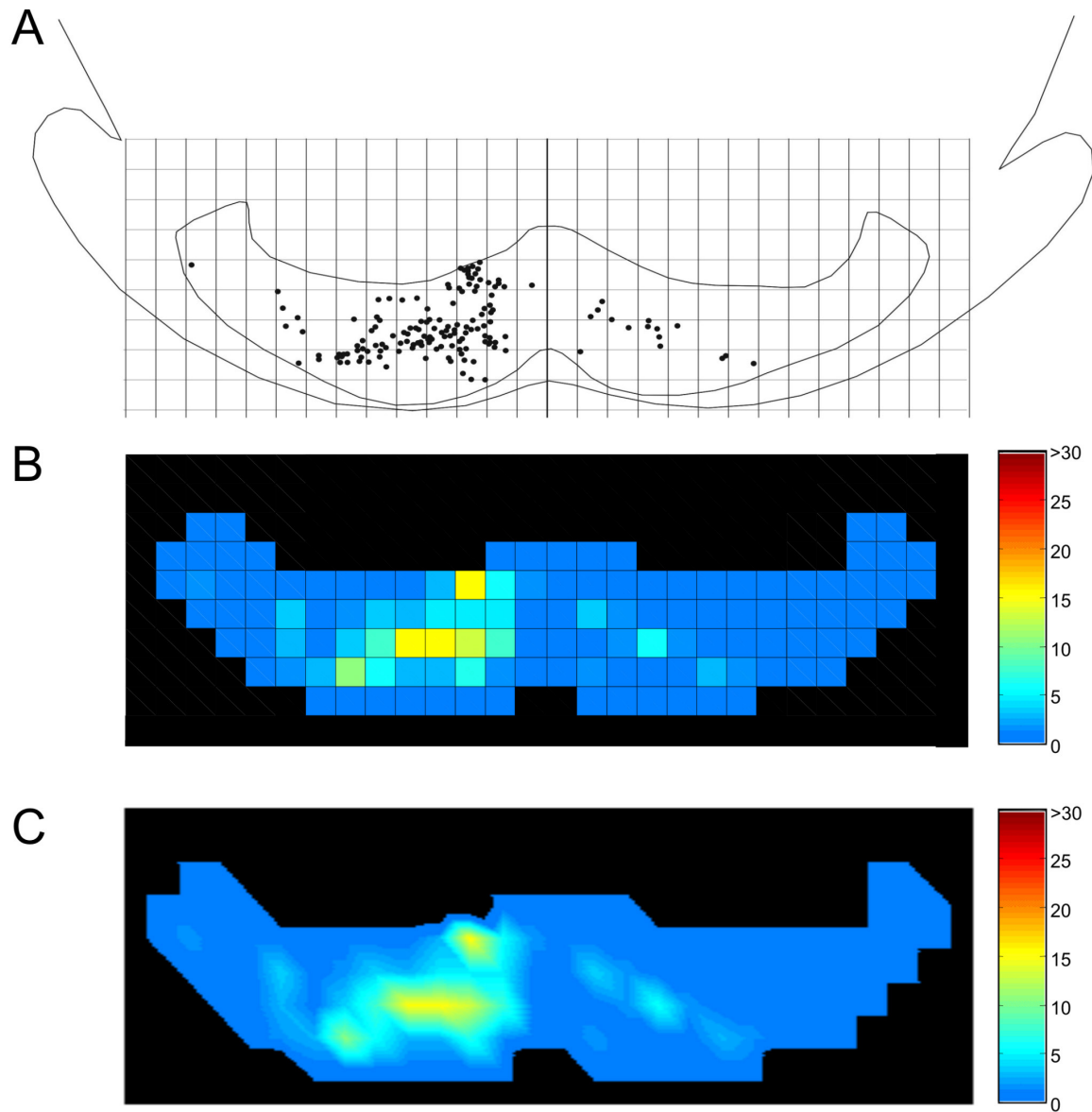
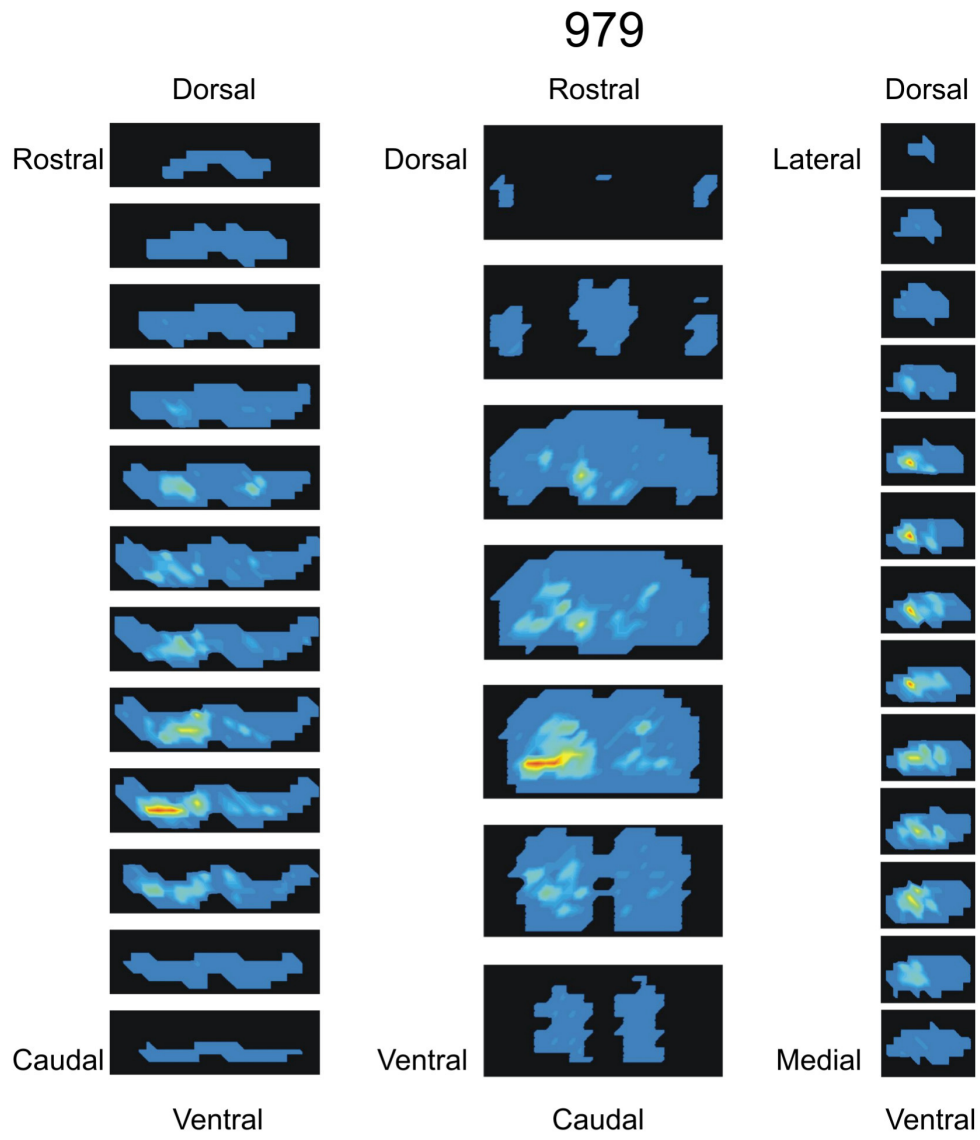


Fig. 4. Conversion of plotted reconstruction of individual sections into color-coded density plots in order to obtain an objective measure of the distribution of pontine labeling (case 979). A: plot of a pontine section indicating borders of the nucleus and position of labeled neurons (using NeuroLucida software). The plot is overlain with a $160\mu\text{m} \times 160\mu\text{m}$ grid and number of dots is counted within every grid square. The ensuing matrix is visualized using Matlab software (**B**) using interpolation (**C**). Color-coding reflects the number of labeled cells within a grid square (i.e. density of labeled neurons).

A



B

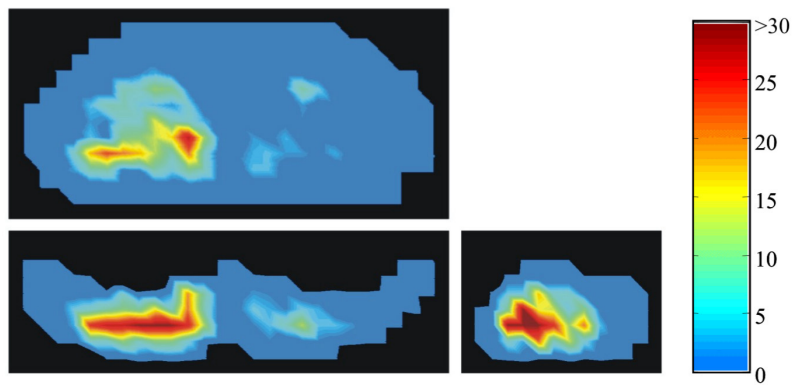


Fig. 5. Color-coded density profiles of the Pn of case 979 as constructed from a series of one out of four transverse sections (of 40 μm each). **A:** Original conversions of transverse series are shown in the left column. By rearranging the 160 x 160 μm grids it was possible to obtain horizontal (middle column) and sagittal (right column) cross-sectional views of the Pn and distribution of labeled cells. **B:** Summing all grids into either the transverse, horizontal or sagittal direction, result in color-coded views of the density profiles in rostrocaudal (top), dorsoventral (bottom left) and lateral-medial (bottom right) views, respectively. Together they provide a 3D-indication of the distribution of labeled neurons. Note that the dorsoventral summed view seems to provide the most useful information on the distribution of labeled neurons. Also note that the sagittal sections in A and sagittal summation in B only involve the contralateral side of the Pn.

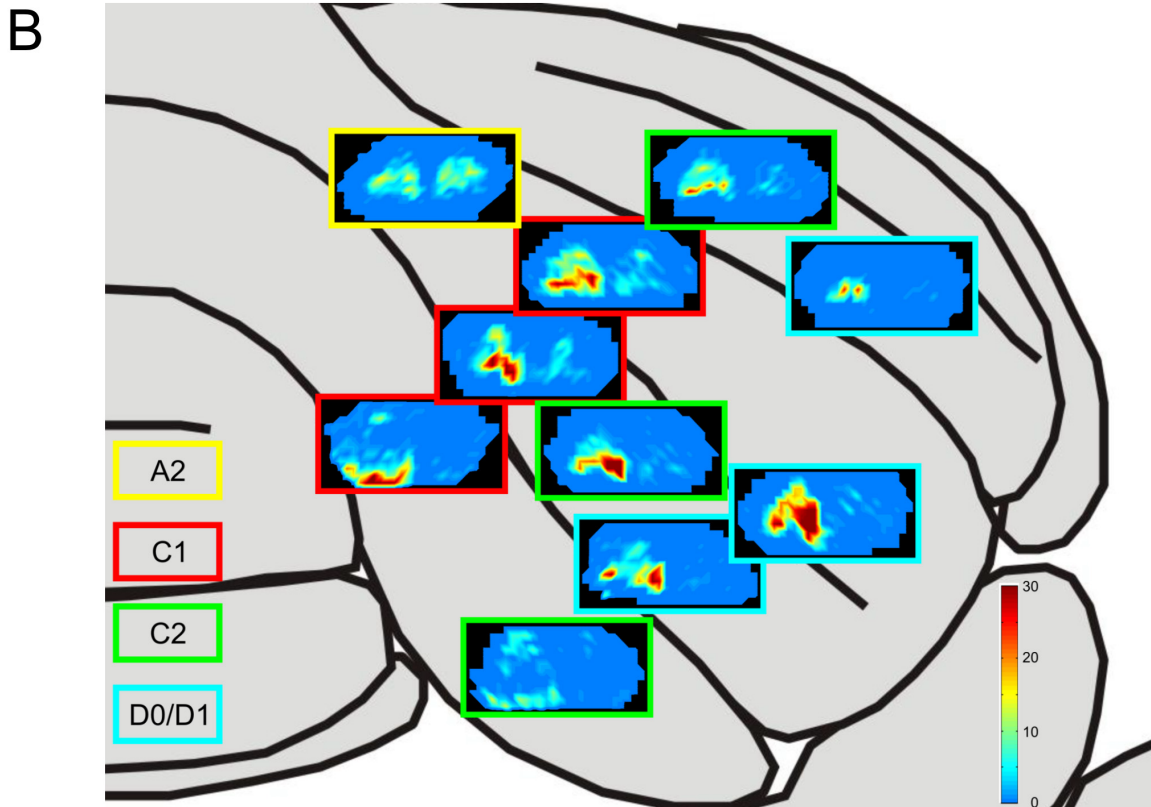
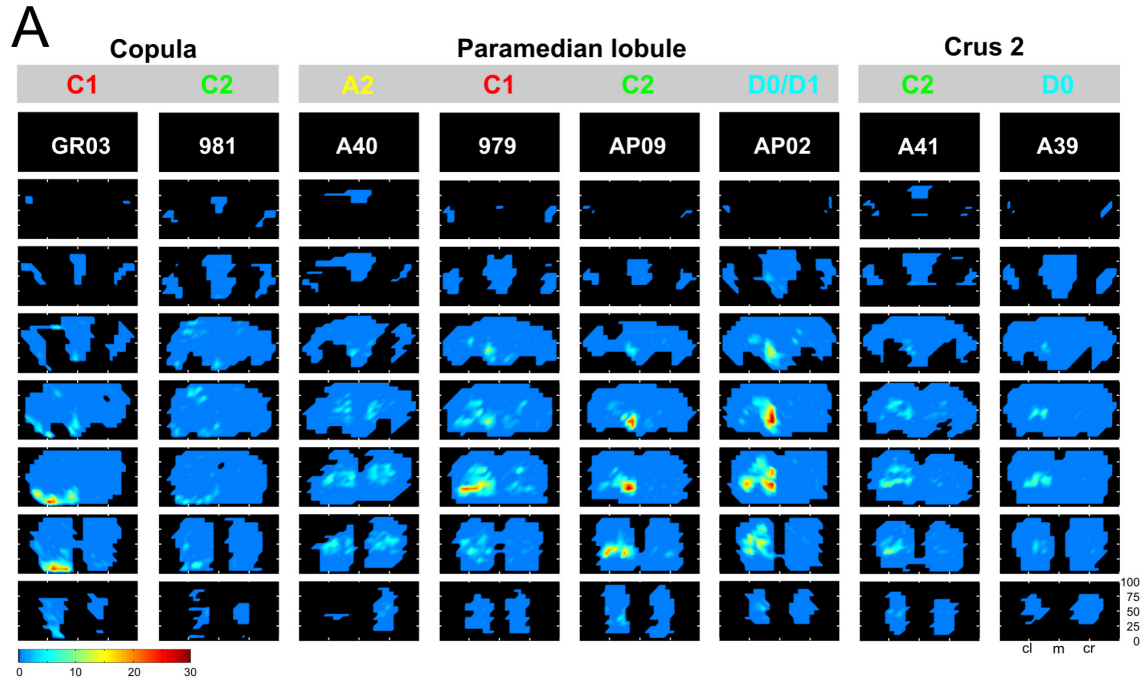


Fig. 6. A: Color-coded density profiles of the distribution of retrogradely labeled neurons in the basal pons viewed with horizontal sections taken at 160 μm intervals in eight cases with injections into identified zonal regions of the posterior cerebellum. Note the similarity in distribution patterns resulting from injections into the COP (hindlimb: cases GR03 and 981), zones C and D zones of PMD (forelimb: cases 979, AP09 and AP03), and zones A2 of PMD and C2 and D0 of crus 2B (face: cases A40, A41 and A39), respectively. However, also note the differences in the contribution of ipsilaterally labeled neurons (cf Table 1). Conventions of representing figurines are similar to Figure 5. In addition, tic marks have been introduced to facilitate comparison between cases and indicated center left (cl), midline (m) and center right (cr) on the horizontal axis and caudorostral extent of the Pn in percentage on the vertical axis. B: Color-coded density profiles of the summed diagrams depicting the dorsoventral distribution of retrogradely labeled neurons in ten cases with CTb injections in the posterior part of the intermediate cerebellum. Diagrams are placed at the approximate position of the injection site on the surface of the posterior cerebellum (also see Fig. 1) and the zonal identification has been indicated by yellow (A2), red (C1), green (C2) or blue (mostly D0/D1) borders.

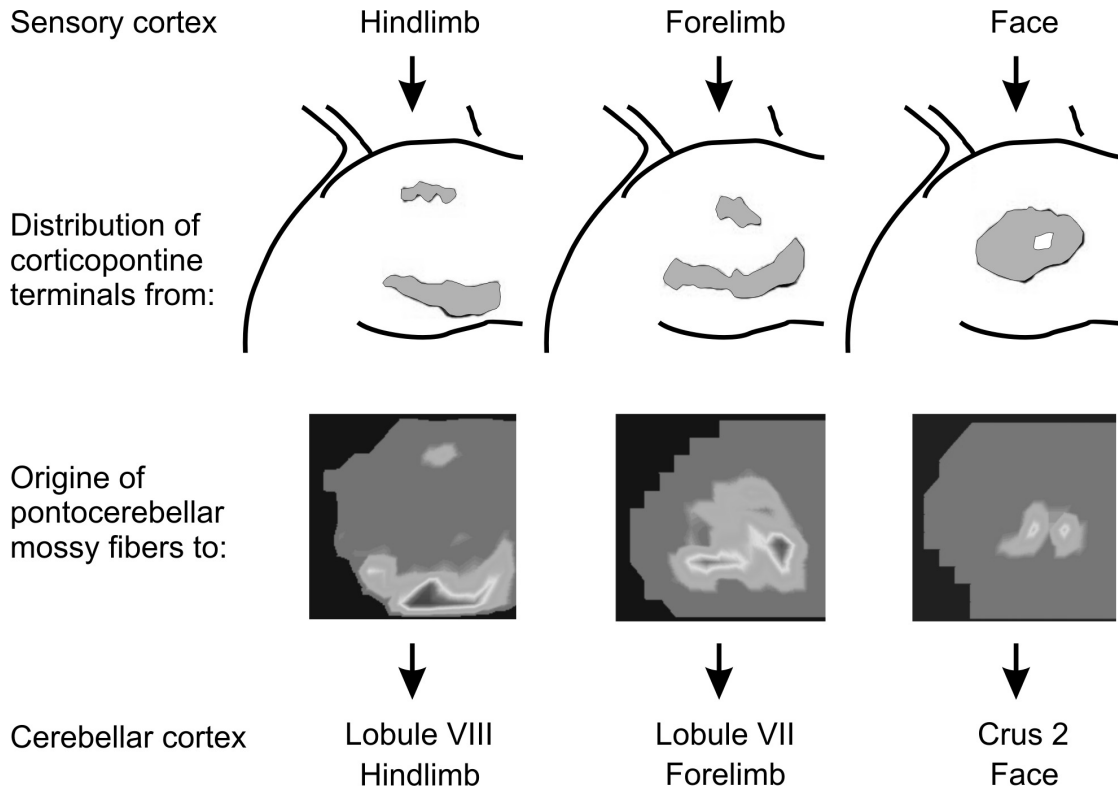
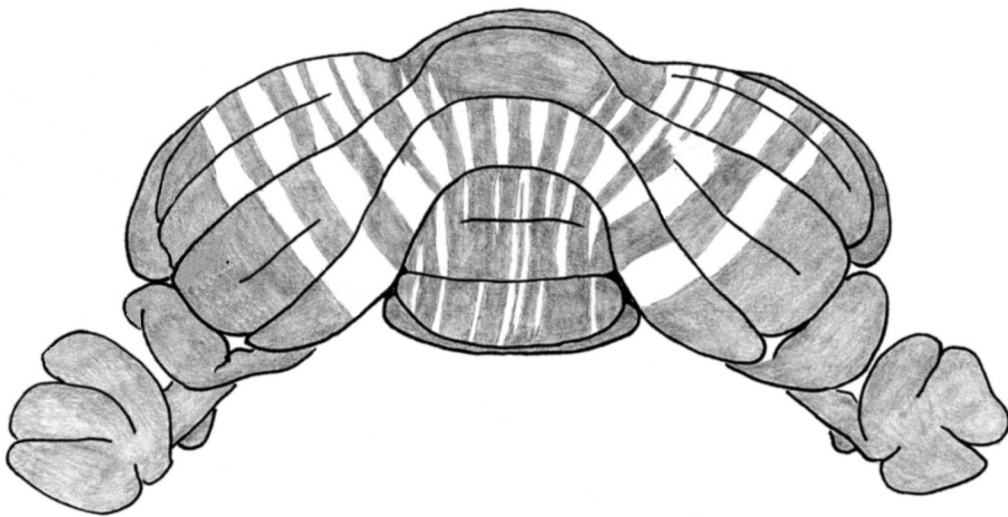


Fig. 7. Similarity in the organization of corticopontine projection from the primary somatosensory cortex and pontocerebellar projection to regions with climbing fiber receptive fields from either hindlimb (ipsi- or bilateral), forelimb (ipsi- or bilateral) and face (ipsilateral). Distribution of corticopontine terminals is redrawn from Leergaard et al. (2000b). Distribution of pontocerebellar neurons is based on average density (in percentages of total number present in contralateral Pn) calculated for cases GR03 and 981 (hindlimb), AP03, 979, AP09 and AP02 (forelimb), AP40, AP41 and A39 (face).

Chapter 4

Precise Spatial Relationships Between Mossy Fibers And Climbing Fibers In Rat Cerebellar Cortical Zones



Adapted from:



Pijpers A, Pardoe J, Apps R, Voogd J, Ruigrok TJH. *Precise spatial relationships between mossy fibers and climbing fibers in rat cerebellar cortical zones*. Accepted for publication, J Neurosci.

Abstract

Classically, mossy fiber (MF) and climbing fiber (CF) terminals are regarded as having very different spatial distributions in the cerebellar cortex. However, previous anatomical studies have not studied these two major cerebellar inputs with sufficient resolution to confirm this assumption. Here, we examine the detailed pattern of collateralization of both types of cerebellar afferent using small injections of the bi-directional tracer cholera toxin b-subunit into the posterior cerebellum. The cortical and zonal location of these injections was characterized by mapping CF field potentials; the distribution of retrogradely labeled olivary neurons; and the intrinsic zebrin-pattern of Purkinje cells.

Labeled CF collaterals were distributed as longitudinal strips and were always accompanied by clusters of labeled MF rosettes in the subjacent granular layer. 2D and 3D reconstructions and quantitative analysis showed that MFs also collateralized to other stripe-like regions usually below Purkinje cells with the same zebrin-positive or zebrin-negative characteristics as that of the injection site and associated CF collaterals. The distribution of retrogradely labeled neurons in two major sources of MFs, the lateral reticular and basilar pontine nuclei, revealed inter-lobular and some inter-zonal differences.

These data indicate that non-adjacent cerebellar zones, sharing the same CF input and zebrin identity also share a common MF input. Other cerebellar cortical regions that receive collaterals from the same MFs usually also have the same zebrin signature. Taken together with the distribution of neurons in precerebellar centers, the findings suggest a revision of the modular hypothesis for information processing in the cerebellar cortex.-

Introduction

The two major afferent systems of the cerebellum, the climbing fiber and mossy fiber systems, are characterized by marked morphological, anatomical and physiological differences (Ito, 1984). Neurons from specific parts of the inferior olive send their climbing fibers to narrow, longitudinally arranged, strips of Purkinje cells (Voogd and Glickstein, 1998; Sugihara and Shinoda, 2004). These strips of Purkinje cells project to specific regions of the cerebellar nuclei that also receive direct input from collaterals of the same climbing fibers, thus resulting in a modular arrangement of olivo-cortico-nuclear connections (Pijpers et al., 2005). Since the cerebellar nuclei constitute the output of the cerebellum, these modules are considered to act as functional entities (Voogd and Bigaré, 1980; Apps and Garwicz, 2005).

The organization of the mossy fibers, which synapse with granule cells and local cortical interneurons, appears much less well structured. They originate from many parts of the central nervous system such as the pontine nuclei, trigeminal complex, lateral reticular nucleus, dorsal

column nuclei and the spinal cord (Yatim et al., 1996; Alisky and Tolbert, 1997; Serapide et al., 2001; Odeh et al., 2005). Individual mossy fibers are characterized by a divergent pattern of projections, i.e. they distribute collaterals along both the rostrocaudal and mediolateral axes (Mihailoff, 1993; Wu et al., 1999; Sultan, 2001; Ruigrok, 2003). The wide divergence of mossy fiber-based information is further magnified by the granule cell-parallel fiber system.

The organizational differences between the mossy fiber/parallel fiber system and the climbing fiber system have been central to all major theories of cerebellar function (Marr, 1969; Albus, 1971; Ito, 1984). Nevertheless, the anatomical interrelation between mossy and climbing fiber systems has not, so far, been studied with sufficient detail to evaluate the structural relationships underpinning these hypotheses. Such an investigation should also provide an anatomical basis for understanding recent physiological observations on receptive field characteristics of climbing fibers and mossy fibers (Brown and Bower, 2001; Ekerot and Jorntell, 2001; Apps and Garwicz, 2005; Ito, 2006).

We have therefore charted the detailed topographical relationship of mossy and climbing fiber afferents by analyzing the distribution of their collateral terminations as labeled from small injections of cholera toxin b-subunit into specific climbing fiber-defined zones of the posterior cerebellar cortex. In addition, these patterns were related to the intrinsic bands of zebrin-positive and -negative Purkinje cells (Hawkes and Leclerc, 1987; Voogd et al., 2003). We show that labeled mossy fiber collaterals are always present in the granular layer directly below labeled collaterals of climbing fibers. In addition, mossy fibers also terminate in strip-like clusters at other cortical locations. 2D and 3D reconstructions and quantitative analysis show that these locations may be functionally linked to the site of injection because they often have the same zebrin signature. These findings, in combination with analyses of the distribution of labeled neurons in two major brainstem sources of mossy fibers suggest that the mossy fiber system makes use of highly organized projection patterns that relate closely to the topography of the climbing fiber system.

Materials and Methods

Eleven adult, male Wistar rats (weight 200-300 g) were used for the present study (see Table 1). Most experiments (n=9) were carried out at the Department of Neuroscience, Erasmus MC Rotterdam, in accordance with the NIH guide for the care and use of laboratory animals and with permission from the national committee overseeing animal experiments. In three of these experiments the injections were guided by electrophysiological recording and the others (n=6) were guided by anatomical landmarks alone (see Table 1). The initial stage of the two additional experiments in which the injections were guided by electrophysiological recording, were carried

out at the Department of Physiology, University of Bristol in accordance with the UK Animals (Scientific Procedures) Act, 1986, and were approved by the institutional animal license advisory group. Six additional cases from Bristol and two from Rotterdam were consulted but their injection sites were found to involve multiple cerebellar cortical zones and were not included in the present paper.

Surgical procedures

In the electrophysiologically-guided experiments animals were initially anesthetized by an intraperitoneal (i.p.) injection of 60 mg/kg pentobarbital (Sagatal, Rhône Merieux, Harlow, UK, or Nembutal, Ceva Sante Animale B.V., Maasluis, Netherlands). In all other cases animals were anesthetized by an i.p. injection of a ketamine/xylazine mixture (40 - 60 mg/kg and 3 mg/kg; ketamine, Alfasan, Woerden, the Netherlands; xylazine: Rompun, Bayer AG, Leverkusen, Germany). In all experiments, supplementary doses were given i.p. in order to maintain a deep level of anesthesia as monitored by absence of the pinch withdrawal reflex and loss of muscle tone. Body temperature was maintained and regulated within physiological limits with a thermostatically controlled heating blanket ($37 \pm 1^{\circ}\text{C}$). All animals were placed in a stereotaxic head holder and a small craniotomy exposed part of the posterior lobe of the cerebellum on one side, allowing access to crus 2, paramedian lobule (PMD) and copula pyramidis (COP). The atlanto-occipital membrane and the dura were opened and the exposed cerebellar surface was kept moist by periodic flushing with sterile saline solution.

In experiments guided by electrophysiology ($n=5$), evoked climbing fiber field potentials were recorded extracellularly with glass-coated tungsten microelectrodes (tip approximately $50\mu\text{m}$; impedance, 50-140 k Ω). The responses were recorded on the cerebellar surface as the result of brief (0.1 ms) electrical percutaneous stimulation of the ipsi- or contralateral forelimb or hindlimb (for detailed description see (Atkins and Apps, 1997)). In these experiments the paravermal part of PMD, COP or crus 2b was mapped at 0.1 mm intervals in a mediolateral direction. In this way the C zones located within these lobules were electrophysiologically identified. Field potentials were amplified and band pass filtered (30 Hz-5 kHz) and a Humbug device (Quest Scientific, North Vancouver, British Columbia, Canada) was used to eliminate 50 Hz electrical interference. Evoked cerebellar responses were recorded and stored for off-line analysis with customized trigger-sampled software (Spike 2TM CED, Cambridge UK) running a CED (Cambridge electronic Design) 1401 plus A/D converter (Pardoe and Apps, 2002). After localization of the desired cortical zone by mapping response amplitude, an iontophoretic injection ($4\mu\text{Amp}$ anodal, 7 sec on, 7 sec off, 10 min) was made of cholera toxin b subunit (CTb, 1% in 0.1 M phosphate buffer, pH 7.4: List Biological Laboratories, Campbell, CA) using a glass micropipette (tip 10-15 μm) attached to a custom-made iontophoresis device (Ruigrok et al., 1995; Teune et al., 1998). Microinjections were made at a depth of 200-300 μm at sites where Purkinje cell activity could be

recorded. This procedure was followed for cases AP02, AP03; AP09, AP10 and A41. The remaining 6 experiments (cases 864, 978, 979, 980, 981, and GR03) were performed in Rotterdam using cerebellar surface coordinates (derived from Atkins and Apps, 1997) to guide the iontophoretic CTb injections.

In all experiments, the micropipette was withdrawn after the microinjection, the overlying muscle and skin layers were sutured, and the animal was allowed to recover. Postoperative analgesia was provided by subcutaneous administration of buprenorphine (0.05-0.1 mg/kg; Temgesic; Schering-Plough, Union, NJ). In cases where increased fluid excretion led to an audible respiration during surgery, atropine sulfate (0.6 mg/kg; Atrocare; Animalcare Ltd, Dunnington, UK) was administered subcutaneously. All animals recovered uneventfully and were monitored daily.

Histology

After a 7-day survival period, animals were killed by means of transcardial perfusion under deep barbiturate anesthesia (100-200 mg/kg i.p.). An initial flush of 500 ml of 0.9% saline in 0.01M phosphate buffer, pH 7.2-7.4 (PB) was given, followed by 1000 ml of fixative (4% paraformaldehyde, 0.1% glutaraldehyde, and 4% sucrose in 0.05M PB). The brain was removed from the skull and post-fixed for 1-2 hours, after which it was rinsed and stored overnight in 0.05M PB containing 10% sucrose (at 4⁰C), and subsequently embedded in 11% gelatin, 10 % sucrose. Cerebellar and caudal brainstem blocks were hardened in 10% formalin, 30% sucrose solution for 3 hours and were stored overnight in 0.05M PB containing 30% sucrose at 4⁰C.

The tissue blocks were sectioned transversally at 40 µm on a freezing microtome and collected serially in 8 glass vials containing 0.05M PB (Ruigrok, 2003). Every other vial was processed either for CTb-immunohistochemistry or for a combined CTb - zebrin immunostaining; the four remaining vials served as spares. Before processing, free-floating sections were rinsed three times in phosphate buffered saline (PBS: 0.05M PB, 0,9% NaCl, pH 7.6) and were subsequently incubated for 48 to 72 hours in a polyclonal anti-cholera toxin raised in goat (goat anti-CTb: lot #703: List Biological Laboratories) diluted 1:15,000 in PBS and containing 0.5% Triton X-100 (PBS+, pH 7.4) at 4⁰C under constant gentle stirring. After subsequent rinsing in PBS, sections were further incubated in biotinylated donkey anti-goat (1:2,000; Jackson, in PBS+) for 1-2 hours at room temperature (RT), rinsed in PBS and incubated for 1-2 hours (RT) in avidin-biotin complex (ABC Elite, Vector Laboratories, Burlingame, CA) in PBS+. After an additional rinse in 0.05M PB, two vials of sections were processed for CTb-labeling using 3,3'-diaminobenzidine tetrahydrochloride as the chromogen (DAB; 0.25% DAB and 0.005% H₂O₂ in 0.05M PB, pH 7.2 for 20 minutes), resulting in a brown reaction product. The other two vials were incubated in DAB-cobalt for 10-15 minutes (1,5 ml CoSO₄ 1% and 1,5 ml NiSO₄ 1% added to the DAB solution), resulting in a black reaction product. All vials were then rinsed in 0.05 M PB. The two vials of

sections also processed for zebrin staining were rinsed in PBS and free floating sections were incubated for 48-72 hours in zebrin II antibody (1:150 in PBS+ containing 2% normal horse serum (NHS) at 4°C). The zebrin II antibody, which was kindly provided by Dr. R. Hawkes, Calgary, was produced by immunization with a crude cerebellar homogenate of the weakly electric fish *Apteronotus* (Brochu et al., 1990). After rinsing in PBS, sections were incubated for 2 hours in rabbit anti-mouse HRP (p260 Dako, 1:200 in PBS+, containing 2% NHS). Subsequently, the sections were thoroughly rinsed in 0.05M PB, again processed (this time without heavy metal ions) with DAB and H₂O₂ (15-20 min), and rinsed in 0.05M PB. All sections were mounted serially on slides in a chromic alum solution, air dried, and counterstained with thionin, dehydrated in graded alcohol and xylene, and finally coverslipped with Permount.

Analysis

In selected cases, in which the injection site was restricted primarily (in some cases entirely, see Table 1) to one cerebellar cortical zone, as judged by the distribution of retrogradely labeled cells in the inferior olive, sections were examined and plotted using an Olympus microscope fitted with a Lucivid miniature monitor and Neurolucida™ software (MicroBrightField, Inc., Colchester, VT). A complete series of one in four transverse sections (interval 160 µm) was examined for labeled climbing fiber collaterals and mossy fiber rosettes in the cerebellar cortex. The outline of each cerebellar section was plotted with a 2.5x objective, whereas mossy and climbing fiber terminals were examined using a 20x objective and the motorized stage scan option of the plot program. A 40x objective was occasionally used if there was any doubt concerning the identity of a labeled structure. Labeled neurons within the inferior olive were also plotted using a one in four series of transverse sections (160 µm interval), resulting in a series of 14-16 plots. Cell labeling was assigned to different olivary subdivisions based on the standard diagrams of Ruigrok and Voogd (2000). Olivary areas containing labeled neurons were also indicated in standardized flattened surface maps of the individual subnuclei (Ruigrok, 1997; Ruigrok and Voogd, 2000). Similarly, labeled neurons located within the ipsi- and contralateral lateral reticular nucleus (LRn) were plotted using a 20x objective and using a description of the nucleus provided by Ruigrok (2004, also see Newman and Ginsberg, 1992). From these plots, usually consisting of 18-20 transverse levels (at 160 µm interval), three-dimensional figurines of the left and right LRn were prepared with Neurolucida software. Counts of labeled neurons within the basal pontine nuclei (Pn) were constructed in a similar way (cases 864 and AP10). Additional pontine data were also obtained from Pijpers and Ruigrok (2006).

A Leica DMR microscope equipped with a digital camera (Leica DC-300) was used to obtain photomicrographs. Photo panels were constructed in CorelDraw™ 11.0, after some correction for brightness and contrast in Corel Photopaint™ 11.0.

The individual cerebellar plots were used to construct the labeled mossy fiber terminals and climbing fiber collaterals in 2D reconstructions of the unfolded cerebellar surface (see Ruigrok, 2003 for a more detailed description). In short, the Purkinje cell layer, the underlying granular and overlying molecular layers were divided into 200- μ m-wide mediolateral 'bins'. Within each bin the number of labeled mossy fiber rosettes was charted and counted. Molecular layer bins were marked positive or negative for labeled climbing fiber terminals. Foliations and lobulations were followed throughout the transverse sections and data were entered in serial order. In this way, a 2D matrix was constructed for each experiment (on average each matrix was based on 40 transverse sections) that was visualized using MATLAB routines (The Math-Works, Inc. Natick, MA). This resulted in an interpolated and color-coded representation of the density of labeled mossy fiber rosettes over the entire unfolded cerebellar cortex. Note that these cerebellar cortical surface maps do not take into account the depth of the granular layer, which can vary considerably depending on the place and angle of sectioning. Hence, color-coding of the mossy fiber rosettes does not reflect actual density concentrations, but rather reflects a general estimate of these densities. As all cases were analyzed in the same way, the diagrams should still provide a useful means to assess and compare distributions of labeled mossy fiber rosettes. Localization of labeled climbing fiber collaterals was shown in a similarly constructed plot using MATLAB routines. Here, bins where the molecular layer contained labeled climbing fiber terminals (irrespective of their density) are indicated in red. In this way, a direct comparison was possible between the regional distribution of labeled mossy fibers and the presence of climbing fiber collaterals. Injection sites were indicated by a white box and arrow.

To further visualize how labeled mossy- and climbing fibers were distributed over- and into the depths of a folium, 3D reconstructions of the simple lobule (SL) were obtained in three cases using NeuroLucida 3D reconstruction software and using a one out of four series of sections. Section by section alignment was performed using the NeuroLucida software. The midline ventral surface of the fourth ventricle was used as a reference and new sections were shifted and rotated to obtain a best fit of contours. Three-point smoothing of contours was performed before final 3D rendering by NeuroLucida.

In two cases (AP03 and A41) 3D plots of mossy fiber and climbing fiber labeling within the simple lobule and vermal lobule VIa were constructed together with zebrin-positive Purkinje cells (also based on a 1 in 4 series of sections). The plots of the individual sections were used to determine the proportion of the total number of labeled mossy fiber rosettes in the granular layer that were directly subjacent to zebrin-positive or zebrin-negative bands. Borders between zebrin bands in the molecular layer were extrapolated into the granular layer. In order to decide if the distribution of labeled mossy fiber rosettes was biased towards a preferred position subjacent to either zebrin-positive or zebrin-negative bands, the surface areas of contours of the granular layer subjacent to these bands were determined and summed with NeuroLucida. These data indicate

that the total surface area of granular layer subjacent to zebrin-negative bands is approximately twice as large as that below zebrin-positive bands (Table 2).

In selected cases the terminal labeling of mossy and climbing fibers was also combined with a standardized surface reconstruction in which the zebrin-banding pattern was shown (Pijpers et al., 2005). Zebrin bands labeled in the sections for each case were compared with the standardized reconstruction in order to accurately position the observed terminal labeling on the standard map. In the Figures, roman numerals indicate individual lobules, and arrows are used to indicate their apices. The zebrin-positive bands are presented in gray and the numbers and letters in these bands refer to the zebrin-positive compartments as defined by Hawkes and Leclerc (1987) and modified by Voogd and Ruigrok (2004) and by Sugihara and Shinoda (2004). The corresponding negative bands are positioned directly lateral to the positive bands. Because the labeling was indicated in a standardized diagram, the resulting diagrams may reflect some minor qualitative differences with the 2D diagrams (cf. Fig. 2 with Fig. 5).

Results

Distribution of climbing and mossy fiber collateral terminals: general observations

Iontophoretic CTb injections into the cerebellar cortex of the rat typically result in small, approximately spherical, deposits of tracer (diameter approximately 500 μm , also see: Ruigrok, 2003; Voogd et al., 2003). Since injections were placed at a depth of 200-300 μm they generally included the molecular layer and the underlying granular layer. The white matter was involved only to a very limited extent or not at all (Fig. 1A). Labeled parallel fibers and corresponding extensive retrograde labeling of granule cells usually obscured the boundaries of the injection site. As a result, mossy and climbing fiber labeling directly surrounding the injection site was interpreted with caution.

Retrograde cell labeling in the contralateral inferior olive was used to determine if the site of injection was confined to a single cerebellar cortical zone and to identify that zone (Fig. 1B, inset, see arrow). Labeling confined mostly or wholly to the ventral fold of the dorsal accessory olive (vfDAO) was considered to be derived from the C1 zone (four cases), whereas the C2 zone (four cases) was targeted when the labeling was predominantly found in the rostral half of the medial accessory olive (MAO). In three additional cases most labeled neurons were located in the ventral leaf of the principal olive (PO) and/or the dorsomedial group (DM) of the PO indicating that the injection site mostly covered the D1 and/or D0 zones, respectively (Table 1). Retrograde cell labeling was also noted in several brainstem nuclei known to provide mossy fibers to cerebellar lobules VII and VIII, such as the lateral reticular nucleus (LRn), basilar pontine nuclei (Pn) and, more sparsely, the dorsal column nuclei, trigeminal nucleus and reticular formation.

Because CTb is a bi-directional tracer it was also transported to the terminal arborizations of collateral branches of the stem axons of retrogradely labeled cells; so called collateral-collateral labeling (Chen and Aston-Jones, 1998; Ruigrok, 2003; Voogd et al., 2003). Labeled terminal rosettes of mossy fiber collaterals generally displayed a more extensive distribution over the cerebellar cortex than labeled climbing fiber collaterals (Fig. 1B, D). Apart from sending collaterals ipsilateral to the injection site, labeled mossy fiber terminals were also usually found contralaterally, arranged in an approximately symmetrical pattern to the distribution on the ipsilateral side, although the density was generally lower. Terminal arborizations of labeled climbing fiber collaterals were confined ipsilaterally within the molecular layer of both the anterior and posterior cerebellum, usually in rostrocaudally oriented strips that were usually a few and up to about 10 Purkinje cells wide (Fig. 1B, C, D).

Figure 1D shows examples of transverse plots from which the two-dimensional (2D) cortical surface (Fig. 2) as well as the three-dimensional (3D) reconstructions (Figs 3, 6) were derived. The distribution of all labeled mossy fiber rosettes in the granular layer are shown as gray dots, while the general location of labeled climbing fiber collaterals in the molecular layer are shown in black (open arrows).

Distribution of climbing and mossy fiber collateral terminals: the C1 zone

Figure 2 illustrates five cases with injections into the C1 zone (Fig. 2A, B), the C2 zone (Fig. 2C,D) and into the D zone (Fig. 2E) plotted onto 2D surface maps. In case AP03 (Fig. 2A) the CTb injection involved the C1 zone of the PMD whereas C1 of the COP was injected in case GR03 (Fig. 2B). The injection in case AP03 was guided by prior recording of the distribution of climbing fiber field potentials on the surface of the cerebellum, evoked by ipsilateral forelimb stimulation. These responses identify the mediolateral boundaries of the C1 zone in PMD (cf Atkins and Apps, 1997). The exclusive C1 zone location of this injection site was confirmed by the presence of retrogradely labeled neurons confined to the medial aspect of vDAO (Fig. 2, top panel, flattened surface reconstruction of olivary subnuclei). Figure 2A, left-hand panel shows the position of labeled climbing fibers on an unfolded surface map of the cerebellar cortex (Ruigrok, 2003; Pijpers et al., 2005). From this diagram, it is evident that the climbing fiber collaterals were distributed to the paravermal cerebellum as continuous strips or, occasionally, as isolated patches that fell within a longitudinal band of cortex that was aligned with the injection site (Fig. 2A, shown in black, arrow). More specifically, from the injection site caudal-wards, labeled climbing fibers were noted in the caudal half of PMD (lobule VII) and rostral-wards in crus 2b, crus 1a, SL and caudal half of lobule V. In Figure 2A, right-hand panel, the distribution of labeled mossy fiber rosettes is depicted on the same 2D surface map in color-coded density profiles (Ruigrok, 2003). In the ipsilateral half of the cerebellar cortex, the overall distribution pattern of the mossy fiber terminals shows accumulations within three mediolateral regions. Isolated

patches of labeled mossy fibers were present within the vermis of lobules VI and VII and IX and, as a more or less continuous strip, in the hemisphere of PMD and crus 2, but were also noted in SL and crus 1. Most terminals, however, were located within the paravermal cerebellum, distributed mainly within lobules V - rostral VIII. The pattern of vermal and paravermal mossy fiber terminal labeling is approximately mirrored on the contralateral side at a lower density. However, contralateral labeling was not observed in lobules V and IX or in the lateral-most part of the hemisphere. When comparing the distributions of climbing fiber and mossy fiber terminal labeling it is also apparent that at all sites where climbing fiber collaterals are situated, a high density of labeled mossy fiber rosettes is also usually present in the subjacent granular layer (Fig. 2A, compare the location of labeling in the left- and right-hand maps).

In case GR03 (Fig. 2B) the injection, which was based on anatomical coordinates, was made into the hindlimb-related part of the C1 zone in COP (Atkins and Apps, 1997). Retrogradely labeled neurons in the contralateral inferior olive were confined to the lateral part of vfDAO (Fig. 2F, second panel), confirming that the injection site was restricted to the C1 zone. Although some labeled climbing fibers entered the dorsolateral aspect of lobule IX, most labeled climbing fiber collaterals emerged from the injection site towards the rostral part of lobule VIII. In the anterior lobe, a conspicuous and continuous rostrocaudally oriented strip of labeled climbing fibers was present in the paravermal cortex stretching from lobules V to II (Figs. 2B, left-hand panel; 5). Labeled mossy fiber rosettes (right-hand panel of Fig. 2B) were abundantly present throughout the mediolateral extent of lobule VIII, ipsilaterally whereas they were confined to vermal and paravermal parts contralaterally. In addition, patches of labeled rosettes were observed in isolated vermal, paravermal and hemispherical regions of lobules II-V ipsilaterally, and in mirror-like image in vermal and paravermal regions of the contralateral half of the anterior lobe. In contrast to the injection into the C1 zone in PMD, virtually no labeled rosettes were encountered in lobules VI and VII, including the hemispherical regions of SL, crus 1, crus 2 and PMD. Again, the correspondence between the distribution of climbing fiber collaterals and mossy fiber collaterals is striking.

Distribution of climbing and mossy fiber collateral terminals: the C2 zone

Figures 2C (case AP09) and 2D (case 981) illustrate two examples of CTb injections that were centered on the C2 zone in the PMD and in the COP, respectively (Table 1). The C2 location of both injection sites was confirmed by the fact that most of the retrogradely labeled neurons in the inferior olive were observed in the rostral part of the MAO (Fig. 2F, third and fourth panel). The few additionally labeled neurons in the medial part of vfDAO in case AP09 suggest, however, some involvement of the neighboring C1 or C3 zone. The distribution of labeled climbing fiber collaterals in this case was found within several narrow and isolated regions of the paravermis within crus 2, SL, and lobule V, which, in general were well aligned along the rostrocaudal axis

with the injection site (Fig. 2C, left-hand panel). Labeled mossy fiber rosettes (right hand panel of Fig. 2C) were mostly present in the paravermal regions of the same lobules, i.e. lobules V, VI and VII. However, patches of labeled terminals were also found in the hemispherical region of SL, both crura, lobule VIII and in the caudal parts of the proximal paraflocculus. Some vermal patches were noted in lobules V-VII and IXa. Contralateral labeling was mostly confined to paravermal regions. Note again that all places with climbing fiber terminal labeling also contained labeled mossy fiber rosettes in the subjacent granular layer.

The same observation was made for case 981 where the very small injection was centered on the C2 zone in the COP (Fig. 2D). However, here, areas of overlap of labeled climbing and labeled mossy fibers was found in paravermal regions of lobules III-V and in lobule VIII and proximal part of the paraflocculus. Isolated patches without corresponding climbing fiber labeling were also noted ipsilaterally in lobule II, lateral crus 1 and in vermal and lateral parts of the rostral half of lobule VIII. In this case, virtually no labeled mossy fiber rosettes were observed on the contralateral side.

Distribution of climbing and mossy fiber collateral terminals: D0-D1 zones

Figure 2E shows the results from an injection that aimed to target the C3 zone in PMD, but since most retrogradely labelled neurons in the olive were located in the DM group and the ventral leaf of the PO (Fig. 2F, bottom-panel), it is likely that the injection deviated laterally to involve the D1 and D0 zones, respectively (Voogd et al., 2003). A few neurons in the medial DAO suggest, however, some incorporation of the C3 zone. The distribution of labeled climbing fiber collaterals was rather dispersed mediolaterally, involving paravermal and hemispherical locations, presumably because of the involvement of multiple zones (Fig. 2E, left-hand panel). Similarly, labeled mossy fibers were also widespread and were located in vermal, paravermal and hemispherical regions of lobules V-VII. Note, however, that the hemispherical component did not have a bilateral counterpart (Fig. 2E, right hand panel). Importantly, and despite the scattered distribution of climbing fiber collaterals, they were always co-localized with labeled mossy fiber rosettes.

Distribution of climbing and mossy fiber collateral terminals: 3D reconstructions

The spatial distribution of climbing and mossy fiber collateral terminals relative to one another can be more directly appreciated in a 3D representation. Figure 3A shows a 3D reconstruction of lobule V, SL and the anterior part of crus 1 for case 979 (see also Fig. 5). In this experiment the injection site was mostly confined to the C1 zone in PMD (Fig. 4A) as was confirmed by the majority of labeled olive neurons being located in the medial aspect of vfDAO (lower panel Fig. 4A, Table 1). Cerebellar surface contours (yellow), Purkinje cell layer (cyan) and white matter contours (dark blue) indicate foliations together with the location of labeled climbing fiber collaterals (red) in the molecular layer and individual labeled mossy fiber rosettes (green). In this

example, a single more or less continuous, rostrocaudally oriented, strip of collateral climbing fiber labeling could be followed from the caudal bank of lobule V into the depths of the primary fissure and then into lobules a and b of SL. Along this whole route the location of labeled climbing fibers is closely tracked by labeled mossy fiber rosettes (double arrow), which, in addition, also form isolated strip-like clusters medial and lateral to the labeled climbing fibers (arrows). Note that although the strip of labeled mossy fibers is almost continuous throughout the depths of the primary fissure, the patches of mossy fiber rosettes at the lateral border of SL are not continuous and are found only at the apex of the two SL folia.

Figure 3B shows a 3D reconstruction for a different case (case 980), depicting labeling of climbing and mossy fiber collateral terminations in the paraflocculus. Retrograde cell labeling of olivary neurons in the ventral leaf of PO indicated that the injection site was located in the D1 zone in PMD (also see Fig. 4A). Three strip-like accumulations of labeled mossy fibers are present, which, in accordance with the specific foliation of the paraflocculus, run essentially in a mediolateral direction. The middle of these three strips is precisely accompanied by labeled climbing fiber collaterals.

Distribution of climbing and mossy fiber collateral terminals: relationship to the zebrin pattern

To further describe how the non-climbing fiber related mossy collaterals were distributed over the cerebellar cortex, labeling was also analyzed in sections that were stained for zebrin II immunohistochemistry. In Figure 4, the injection sites of all 11 cases are shown on the right side of a generalized caudal view of the cerebellar cortex in which the zebrin pattern has also been indicated. Note that in each case, the injection site was located in either a zebrin-positive or a zebrin-negative band. For example, in case A41 the injection site was considered to be within the confines of P5+ in crus 2b. Photomicrographs in Figure 4B and, in detail, in Figure 4C, illustrate how the resultant collateral labeling of climbing fiber terminations (white arrowheads in C) correlate with the zebrin-positive band P4+ in the caudal part of SL and that labeled mossy fiber rosettes are also confined to regions of the granule cell layer below the P4+ band (black arrows in C). By comparison, the photomicrographs in Figure 4D, and an enlargement shown in Figure 4E, are taken from case AP10, which was centered on the zebrin-negative band P5a- in PMD. Mossy fiber rosettes (black arrows) can be seen to be mostly located subjacent to zebrin-negative areas. Note that in Figure 4D and E no labeled climbing fiber collaterals were present in the molecular layer.

Figure 5 details for four representative cases the relation between the distribution of labeled mossy- and climbing fiber collaterals (hatched green and solid red, respectively), and the pattern of zebrin-positive and -negative Purkinje cells as shown in a generalized cortical surface map (for details, see Pijpers et al., 2005). A black circle in each diagram represents the approximate location of the injection site in each case. Parts of the diagram representing the flocculus,

paraflocculus and the lateral part of crus 1 are not shown, since these regions are fully zebrin-positive and the illustrated cases only displayed very limited mossy fiber collateral labeling in these areas.

From these diagrams it can be appreciated that C1 zone injection sites (cases 979 and AP10) resulted in accumulations of labeled mossy fiber rosettes predominantly below zebrin-negative Purkinje cells, whereas in cases with C2 zone injection sites (e.g. case AP09) they are mostly found in relation to zebrin-positive bands. The injection site in case GR03 was determined to be within the C1 zone in COP, however, it appeared to be centered on the rather weakly zebrin positive patch e1+. Climbing fiber collaterals were mostly distributed to the also weakly zebrin positive band P3+ in the anterior lobe. Both e1+ and P3+ and their bordering zebrin-negative bands have been shown to be located fully within the C1 zone (Voogd et al., 2003; Sugihara and Shinoda, 2004). Also, most additional mossy fiber patches in the anterior lobe were related to zebrin-negative bands. For these reasons, both zebrin patch e1+ as well as anterior lobe band P3+ may be considered as constituting a specific part of zebrin-negative territory. Note that, irrespective of the location of the injection site in zebrin-negative or -positive bands, all cases demonstrated at least some patches of mossy fibers within the lateral-most zebrin-positive band. The relationship between the intrinsic zebrin pattern of Purkinje cells and the distribution of climbing and mossy fiber collaterals is further illustrated in Figure 6, which shows 3D reconstructions of the SL for two cases. Case AP03 (Fig. 6A) had an injection that was centered on the C1 zone in PMD (also shown in Fig. 2A), whereas the injection in case A41 (Fig. 6B) involved the C2 zone in crus 2b. In the top two panels in both Figure 6A and B the Purkinje cell layer/granule cell layer interface is shown in cyan together with the labeled climbing fiber collaterals in the molecular layer (red). Zebrin-positive Purkinje cells (yellow) have been added in the second pair of panels. In the third pair of panels, the location of labeled mossy fiber rosettes have been added (green) and all 3 classes of labeling are shown in relation to the white matter contours (dark blue) to indicate foliations. In the bottom two cerebellar representations only the labeled climbing and mossy fiber terminals are shown either with or without zebrin-positive Purkinje cells, respectively. Finally, the retrograde cell labeling within the inferior olive is shown to indicate the zonal localization of the injection site. Note that in case AP03 strips of labeled climbing fiber collaterals are found in zebrin-negative regions on either side of the P4+ band, representing the C1 and C3 zones (Voogd et al., 2003). By contrast, in case A41 labeled climbing fiber collaterals were only found in the P4+ band, which represents the C2 zone (Voogd et al., 2003). In both cases labeled mossy fiber collaterals were most abundant directly subjacent to the labeled climbing fiber collaterals. However, collections of labeled mossy fiber rosettes were found in other regions as well. Although not exclusively, (note labeled mossy fibers within P6+ in both cases), these mossy fibers were mostly restricted to zebrin-negative bands in case AP03 and to zebrin-positive bands in case A41.

This finding was supported by quantitative analysis. Table 2 shows for the two representative cases the proportion of labeled mossy fiber rosettes in relation to zebrin-positive and -negative bands (see Materials and Methods for further details of the analysis). From inspection of Table 2 it is evident that subjacent to all zebrin-positive bands (apart from satellite band a+) the percentage of labeled rosettes was always greater in case A41 (C2 injection) than in case AP03 (C1 injection), and that this situation was essentially reversed for mossy fiber labeling subjacent to zebrin-negative bands. It is also noteworthy that in the C1 zone case, the only zebrin-positive band with a fair amount (11.2%) of labeled rosettes in the subjacent granular layer was P6+. Distributions of mossy fiber collaterals to P6+ were also noted in other cases with injections into the C1 zone (Fig. 5), highlighting the atypical status of this particular hemispherical zebrin band. In summary, mossy fiber and climbing fiber collaterals labeled after injections centered on the C1 zone in COP or PMD are mostly found in zebrin-negative bands (with the inclusion of the weakly zebrin-positive P3+ band in the anterior lobe). By contrast, mossy fiber and climbing fiber collaterals labeled after injections centered on the C2 zone are mostly located in zebrin-positive bands.

Origin of mossy fibers to different lobules and zones

The results above indicate that the distribution pattern of mossy fiber rosettes associated with the C1 zone differs from that of the C2 zone. However, lobular differences may also be present. To examine the possibility of zonal and lobular differences more fully, the distribution of retrograde cell labeling in two major sources of mossy fibers was studied: the basilar pontine nuclei (Pn, based mainly on data recently published by Pijpers and Ruigrok, 2006) and also the lateral reticular nucleus (LRn).

In Figure 7, the distributions of retrogradely labeled cells in three-dimensional views of both the ipsilateral and contralateral LRn are shown for all cases studied. Cases are presented with respect to the location of the injection site in the C1 zone in PMD or COP, the C2 zone in crus 2, PMD or COP, and the D0/D1 zones in PMD. For each case, a predominantly caudal (at 10° dorsal from the horizontal axis) as well as a predominantly dorsal view (at 70° dorsal from the horizontal axis) is shown in which similarities and differences in distribution of labeled neurons between cases can be easily appreciated.

For the C1-PMD and C2-PMD cases, labeled cells were distributed throughout the rostrocaudal extent of LRn, taking up mostly dorsal positions in its magnocellular and subtrigeminal parts, while many labeled neurons were also observed within its linear subdivision (for definition of subdivisions see Newman and Ginsberg, 1992; Ruigrok, 2004). Most labeled neurons were observed ipsilaterally (see Table 1), but labeled cells were also located at similar positions in the contralateral LRn (except the caudal aspect of the nucleus which was virtually devoid of labeled neurons). Apart from a somewhat more pronounced involvement of the caudal third of the LRn in

the C1 zone cases no clear differences were observed between C1 and C2 injections in PMD. By comparison, in the D0/D1 cases, the main magnocellular and parvocellular parts of the LRn contained only a few labeled cells. Most labeled cells were found in the subtrigeminal and linear subdivisions. The distribution of labeled neurons in case A41 (C2 zone in crus 2b) was very similar to that of the three D0/D1 cases.

Both injections in COP (GR03-C1 and 981-C2) resulted in patterns of cell labeling that differed from the PMD cases. In both cases, labeled cells were mostly found in the ventrolateral aspect of the nucleus (within the parvocellular and subtrigeminal subdivisions) with a more prominent involvement of the caudal half of contralateral LRn. However, there were no labeled cells in the linear subdivision. Like the C1 and C2 cases in PMD, some zonal differences may also be present because the caudal tip of the nucleus was more heavily involved in GR03 (a C1 zone case) as compared to case 981 (a C2 zone case).

A comparison of the number and laterality of labeled neurons observed within the Pn and LRn is presented in Figure 8 (also see Table 1). Figure 8A indicates the relation between numbers of labeled cells in the inferior olive and those within LRn and Pn. The numbers of neurons labeled within the LRn and inferior olive are positively correlated ($r=0.87$, $P<0.005$). Assuming, for different cases, a similar spread of tracer within the molecular layer and subjacent granular layer and a uniform projection density for climbing fibers (cf. Herrero et al., 2002), this suggests that the contribution from LRn is mostly related to the size of the injection site rather than to the identity of the injected cortical lobule or zone. However, when labeled cell numbers in Pn and the olive were compared, no significant correlation was noted ($r=0.47$; $P>0.05$), implying that other factors such as cortical (zonal) location may be more important factors than injection site size in determining involvement of Pn neurons. This is supported by the finding that cases with an injection in the D0/D1 zone in PMD have a significantly higher Pn/LRn ratio compared to either C2 or C1 injections in PMD or COP (for both comparisons: two-sided t-test assuming unequal variances, $P<0.05$). A significantly higher Pn/LRn ratio was also found for the C2 zone group of cases with respect to the C1 zone group (two-sided t-test, $P<0.05$). Finally, no obvious distinction could be found in the numbers of labeled neurons located in ipsi- or contralateral LRn (Fig. 8C). For the Pn however, the number of ipsilaterally labeled neurons tended to decrease when the injection was placed in more lateral zones (i.e., resulting in a higher contralateral/ipsilateral ratio) (Fig. 8D). An exception is presented by case GR03 where the C1 zone injection in COP resulted in approximately 40 times as many cells in the contralateral Pn as in the ipsilateral Pn. This contrasts with the more prominent bilateral nature of the LRn projection in this case.

Discussion

The present study makes four key observations regarding interconnectivity between functionally-related parts of the cerebellar cortex: 1) mossy fiber collaterals mostly distribute to the same cerebellar lobules as climbing fiber collaterals; 2) collaterals of labeled climbing fibers are always accompanied by labeled mossy fiber terminals in the subjacent granular layer; 3) additional mossy fiber collaterals terminate in specific, non-adjacent, strip-like regions which usually have the same zebrin-signature as the source of the collateralization; and 4) mossy fiber projections to different cortical zones are accompanied by significant differences in projection densities from two major brainstem sources. The present results therefore indicate that the mossy fiber and climbing fiber afferent systems are closely aligned and that this is a consistent and widespread feature of cerebellar cortical organization in the rat.

Due to its uniform structure, functional localization within the cerebellar cortex critically depends on the organization of its afferent systems (for review see Manni and Petrosini, 2004). On the one hand, mossy fiber input is usually characterized by multiple representations of the same body parts distributed as a mosaic of patches within the cerebellar cortex (the fractionated somatotopy of Welker, 1987), note however that some aspects of mossy fiber organization have also been described in terms of longitudinal strips, (e.g. see Ekerot and Larson, 1980; Serapide et al., 2001). On the other hand, climbing fiber inputs with similar receptive field characteristics adhere to parasagittally-arranged zones in which finer microzonal subdivisions can be recognized (Oscarsson, 1979; Apps and Garwicz, 2005). Perhaps not surprisingly then, physiological studies disagree on the extent to which the somatotopic pattern of mossy and climbing fibers are aligned to each other (Garwicz et al., 1998; Brown and Bower, 2001). Resolving this disagreement is important for understanding basic cerebellar processing (Apps and Garwicz, 2005), and the present study helps inform this debate by providing the most comprehensive description to date of the distribution of functionally-related climbing and mossy fiber collaterals.

Cerebellar somatotopy and collateralization of mossy and climbing fiber afferents

Climbing fiber somatotopic representations of the same body parts have been recognized in regions of the anterior as well as within the posterior cerebellum (for reviews see Manni and Petrosini, 2004; Apps and Garwicz, 2005). In rat, at the zonal level, representations of the ipsilateral forelimb are present in the C1 and C3 zones of PMD and SL whereas bilateral forelimb representations are present in the C2 zone of the same lobules (Atkins and Apps, 1997; Pardoe and Apps, 2002). Likewise, COP harbors zones that are characterized by ipsilateral (C1) and bilateral (C2) climbing fiber inputs from the hindlimb (Atkins and Apps, 1997), and these body representations are likely to have counterparts in the anterior lobe (Jorntell et al., 2000). The anatomical substrate for this homology has been demonstrated by Voogd and collaborators

(2003), and was confirmed in the present study. Indeed, climbing fibers collateralize from zones in PMD and COP to target similar zones in SL and anterior lobe, respectively (Pardoe and Apps, 2002). Here, we extend this finding by showing that mossy fiber collaterals, labeled from the same injection site, also exhibit a similar somatotopic distribution. Collaterals labeled from COP mostly reach the anterior lobe, whereas PMD injections result in labeled mossy fibers within SL and the crura. The present findings therefore strongly imply that these particular cerebellar regions (COP and the anterior lobe; PMD, SL and the crura) function in close association with each other.

The distribution of mossy fiber collaterals, however, was always more widespread than the climbing fiber collaterals arising from the same injection site, being clustered within multiple, essentially longitudinal patterns within vermal, paravermal and hemispherical regions of the targeted lobules. These patterns are usually mimicked contralaterally with the notable exception of patches located in the lateral-most parts of the ipsilateral cortex. The former suggests that the same information conveyed via the mossy fiber system targets a number of different cortical zones bilaterally, perhaps for the regulation of whole body movements. The latter suggests that lateral zones are more concerned with unilateral inputs.

Collateralization and zebrin pattern

The relationship between the organization of the olivocerebellar climbing fiber system and the zebrin pattern of Purkinje cells has recently been described in considerable detail (Sugihara and Shinoda, 2004; Voogd and Ruigrok, 2004; Pijpers et al., 2005). Using 2D and 3D reconstruction methods and quantitative analysis the present observations significantly extend these earlier findings by showing that the distribution of subpopulations of mossy fiber rosettes with a common lobular and zonal target (but with heterogeneous origin), also show close relations to that of the overlying zebrin pattern. If the rather weakly-positive zebrin patch 'e+' of COP and zone P3+ of the anterior lobe are considered as part of a zebrin-negative territory (see Results), then mossy fiber collaterals labeled from injections confined to the C1 zone preferentially target regions of granular layer subjacent to zebrin-negative Purkinje cells, whereas C2 zone injections result in labeled mossy fiber rosettes below zebrin-positive regions (Gravel and Hawkes, 1990; Ji and Hawkes, 1994). Our observations therefore underscore the functional differentiation of zebrin-negative versus zebrin-positive Purkinje cells (Voogd et al., 2003; Sugihara and Shinoda, 2004; Voogd and Ruigrok, 2004), and suggest that the organization of the granular layer correlates to this patterning. Interestingly, some studies have indicated that zebrin-positive and -negative Purkinje cells may operate differently (Nagao et al., 1997; Wadiche and Jahr, 2005).

Somatotopy, zones, and origin of mossy fibers

Mossy fibers terminating in COP and PMD convey somatosensory information from the periphery by way of the spinal cord, dorsal column nuclei, trigeminal nuclei and/or LRn. In addition, preprocessed information from the cerebral cortex may reach these areas via pontine relays (for review see Ruigrok, 2004). Consequently, every CTb injection site will result in retrogradely labeled neurons located within a specific combination of these precerebellar centers. We have concentrated our analysis on the LRn and the Pn (Pijpers and Ruigrok, 2006), and show that the distribution of neurons within both structures correlates closely with the lobular identity of the injection site. However, at best only subtle differences were noted in the distribution of labeled neurons arising from injections targeted at different zones within the same lobule. Since the collateral distribution of mossy fibers is strongly affected by the identity of the injected zone (see below) this suggests that either (i) cells within LRn and Pn projecting to different zones are intermingled in each structure or (ii) a subnuclear topical organization is present that could not be detected in the present experiments. The clearest differences we found related to the proportion of retrogradely labeled neurons arising from Pn as compared to LRn targeting different zones. These differences suggest at least a partly independent origin of mossy fiber terminals to the C1, C2 and D1/D0 zones. Thus, highly specific combinations of mossy fibers appear to distribute terminals to particular lobules and zones of the cerebellar cortex. Future experiments using multiple tracer techniques will be required to determine whether the observed zonal differences in collateralization patterns relate to any differences in topography in projections arising from the various precerebellar sources.

Congruence of climbing- and mossy fiber collaterals

Physiologically, convergence of mossy and climbing fiber receptive fields was first demonstrated by Eccles and collaborators (1968; Kitai et al., 1969). More recently, micromapping techniques have also focused on the importance of convergence of both afferent systems. Indeed, both for cat forelimb (Garwicz et al., 1998; Apps and Garwicz, 2005) as well as for rat peri-oral regions (Brown and Bower, 2001) a general similarity of the receptive fields of mossy fibers and climbing fibers has been noted in localized regions of the cerebellar cortex. The present data provide evidence of the anatomical substrate for this functional congruence. However, the functional implications of such a related distribution of mossy and climbing fibers remains to be resolved (see for example Ekerot and Jorntell (2001) as compared to Brown and Bower, (2001; Lu et al., 2005)).

Concluding remarks

The present study shows that labeled mossy fiber rosettes closely accompany collaterals of climbing fibers labeled from the same zonal location. A similar, but more tentative observation

was made by Voogd et al. (2003) and was also mentioned for the vestibulocerebellum (Ruigrok, 2003). Such an arrangement implies that the specific combination of mossy and climbing fiber inputs processed at a given locus within the cerebellar cortex (i.e. within PMD or COP) may be repeated (at least in part) in other cerebellar regions (such as SL or anterior lobe). This finding is consistent with the idea that the cerebellum is modular and that basic operational units are formed by multizonal microcomplexes, i.e. two or more microzones within different parts of the cortex with common climbing fiber input have output to a common group of cerebellar nuclear neurons (Apps and Garwicz, 2005). Although, originally, this was thought to enable parallel processing of information derived from different combinations of mossy fibers, the present results extend this hypothesis to suggest that microcomplexes also make use of some common mossy fiber inputs.

Acknowledgements

We thank Miss R. Bissett, Miss C. Everard, Mrs E. Sabel-Goedknegt, Mr J. van der Burg and Mr E. Dalm for their technical assistance. Supported by the Dutch Organization for Scientific Research (NWO-ALW: project number 810.37.005) and the Dutch Ministry of Health, Welfare, and Sports. Richard Apps was supported by a Senior Research Fellowship funded by the Medical Research Council (UK).

References

- Albus JS (1971) A theory on cerebellar function. *Math Biosci* 10:25-61.
- Alisky JM, Tolbert DL (1997) Quantitative analysis of converging spinal and cuneate mossy fibre afferent projections to the rat cerebellar anterior lobe. *Neuroscience* 80:373-388.
- Apps R, Garwicz M (2005) Anatomical and physiological foundations of cerebellar information processing. *Nat Rev Neurosci* 6:297-311.
- Atkins MJ, Apps R (1997) Somatotopical organisation within the climbing fibre projection to the paramedian lobule and copula pyramidis of the rat cerebellum. *J Comp Neurol* 389:249-263.
- Brochu G, Maler L, Hawkes R (1990) Zebrin II: a polypeptide antigen expressed selectively by Purkinje cells reveals compartments in rat and fish cerebellum. *J Comp Neurol* 291:538-552.
- Brown IE, Bower JM (2001) Congruence of mossy fiber and climbing fiber tactile projections in the lateral hemispheres of the rat cerebellum. *J Comp Neurol* 429:59-70.
- Chen S, Aston-Jones G (1998) Axonal collateral-collateral transport of tract tracers in brain neurons: false anterograde labelling and useful tool. *Neurosci* 82:1151-1163.
- Eccles JC, Provini L, Strata P, Taborikova H (1968) Analysis of electrical potentials evoked in the cerebellar anterior lobe by stimulation of hindlimb and forelimb nerves. *Exp Brain Res* 6:171-194.
- Ekerot CF, Jorntell H (2001) Parallel fibre receptive fields of Purkinje cells and interneurons are climbing fibre-specific. *Eur J Neurosci* 13:1303-1310.
- Ekerot C-F, Larson B (1980) Termination in overlapping sagittal zones in cerebellar anterior lobe of mossy and climbing fiber paths activated from dorsal funiculus. *Exp Brain Res* 38:163-172.
- Garwicz M, Jorntell H, Ekerot CF (1998) Cutaneous receptive fields and topography of mossy fibres and climbing fibres projecting to cat cerebellar C3 zone. *J Physiol* 512 (Pt 1):277-293.
- Gravel C, Hawkes R (1990) Parasagittal organization of the rat cerebellar cortex: direct comparison of Purkinje cell compartments and the organization of the spinocerebellar projection. *J Comp Neurol* 291:79-102.
- Hawkes R, Leclerc N (1987) Antigenic map of the rat cerebellar cortex: the distribution of parasagittal bands as revealed by monoclonal anti-Purkinje cell antibody mabQ113. *J Comp Neurol* 256:29-41.
- Herrero L, Pardoe J, Apps R (2002) Pontine and lateral reticular projections to the c1 zone in lobulus simplex and paramedian lobule of the rat cerebellar cortex. *Cerebellum* 1:185-199.
- Ito M (1984) *The cerebellum and neural control*. New York: Raven press.
- Ito M (2006) Cerebellar circuitry as a neuronal machine. *Prog Neurobiol* 78:272-303.
- Ji Z, Hawkes R (1994) Topography of Purkinje cell compartments and mossy fiber terminal fields in lobules II and III of the rat cerebellar cortex: spinocerebellar and cuneocerebellar projections. *Neuroscience* 61:935-954.
- Jorntell H, Ekerot C, Garwicz M, Luo XL (2000) Functional organization of climbing fibre projection to the cerebellar anterior lobe of the rat. *J Physiol (Lond)* 522 Pt 2:297-309.
- Kitai ST, Taborikova H, Tsukahara N, Eccles JC (1969) The distribution to the cerebellar anterior lobe of the climbing and mossy fiber inputs from the plantar and palmar cutaneous afferents. *Exp Brain Res* 7:1-10.
- Lu H, Hartmann MJ, Bower JM (2005) Correlations between Purkinje Cell Single Unit Activity and Simultaneously Recorded Field Potentials in the Immediately Underlying Granule Cell Layer. *J Neurophysiol* 94: 1849-1860.
- Manni E, Petrosini L (2004) A century of cerebellar somatotopy: a debated representation. *Nat Rev Neurosci* 5:241-249.
- Marr D (1969) A theory of cerebellar cortex. *J Physiol (Lond)* 202:437-470.
- Mihailoff G (1993) Cerebellar nuclear projections from the basilar pontine nuclei and nucleus reticularis tegmenti pontis as demonstrated with PHA-L tracing in the rat. *J Comp Neurol* 330:130-146.
- Nagao S, Kwak S, Kanazawa I (1997) EAAT4, a glutamate transporter with properties of a chloride channel, is predominantly localized in Purkinje cell dendrites, and forms parasagittal compartments in rat cerebellum. *Neuroscience* 78:929-933.
- Newman DB, Ginsberg CY (1992) Brainstem reticular nuclei that project to the cerebellum in rats: a retrograde tracer study. *Brain Behav Evol* 39:24-68.
- Odeh F, Ackerley R, Bjaalie JG, Apps R (2005) Pontine maps linking somatosensory and cerebellar cortices are in register with climbing fiber somatotopy. *J Neurosci* 25:5680-5690.
- Oscarsson O (1979) Functional units of the cerebellum - sagittal zones and microzones. *TINS* 2:143-145.
- Pardoe J, Apps R (2002) Structure-function relations of two somatotopically corresponding regions of the rat cerebellar cortex: olivo-cortico-nuclear connections. *Cerebellum* 1:165-184.
- Pijpers A, Ruigrok TJH (2006) Organization of pontocerebellar projections to identified climbing fiber zones in the rat. *J Comp Neurol* 496: 513-528.

- Pijpers A, Voogd J, Ruigrok TJH (2005) Topography of olivo-cortico-nuclear modules in the intermediate cerebellum of the rat. *J Comp Neurol* 492 in preparation:193-213.
- Ruigrok TJ (2003) Collateralization of climbing and mossy fibers projecting to the nodulus and flocculus of the rat cerebellum. *J Comp Neurol* 466:278-298.
- Ruigrok TJ, Voogd J (2000) Organization of projections from the inferior olive to the cerebellar nuclei in the rat. *J Comp Neurol* 426:209-228.
- Ruigrok TJH (1997) Cerebellar nuclei: the olivary connection. In: *The cerebellum: from structure to control* (De Zeeuw CI, Strata P, Voogd J, eds), pp 162-197. Amsterdam. Elsevier Science.
- Ruigrok TJH (2004) Precerebellar nuclei and red nucleus. In: *The rat nervous system, third edition* (Paxinos G, ed), pp 167-204. San Diego: Elsevier Academic Press.
- Ruigrok TJH, Teune TM, van der Burg J, Sabel-Goedknegt H (1995) A retrograde double labeling technique for light microscopy. A combination of axonal transport of cholera toxin B-subunit and a gold-lectin conjugate. *J Neurosci Meth* 61:127-138.
- Serapide MF, Panto MR, Parenti R, Zappala A, Cicirata F (2001) Multiple zonal projections of the basilar pontine nuclei to the cerebellar cortex of the rat. *J Comp Neurol* 430:471-484.
- Sugihara I, Shinoda Y (2004) Molecular, topographic, and functional organization of the cerebellar cortex: a study with combined aldolase C and olivocerebellar labeling. *J Neurosci* 24:8771-8785.
- Sultan F (2001) Distribution of mossy fibre rosettes in the cerebellum of cat and mice: evidence for a parasagittal organization at the single fibre level. *Eur J Neurosci* 13:2123-2130.
- Teune TM, van der Burg J, De Zeeuw CI, Voogd J, Ruigrok TJH (1998) Single Purkinje cell can innervate multiple classes of projection neurons in the cerebellar nuclei of the rat: a light microscopic and ultrastructural triple-tracer study in the rat. *J Comp Neurol* 392:164-178.
- Voogd J, Bigaré F (1980) Topographical distribution of olivary and cortico nuclear fibers in the cerebellum: a review. In: *The inferior olivary nucleus. Anatomy and physiology* (Courville J, de Montigny C, Lamarre Y, eds), pp 207-234. New York: Raven Press.
- Voogd J, Glickstein M (1998) The anatomy of the cerebellum. *Trends Neurosci* 2:305-371.
- Voogd J, Ruigrok TJ (2004) The organization of the corticonuclear and olivocerebellar climbing fiber projections to the rat cerebellar vermis: the congruence of projection zones and the zebrin pattern. *J Neurocytol* 33:5-21.
- Voogd J, Pardoe J, Ruigrok TJ, Apps R (2003) The distribution of climbing and mossy fiber collateral branches from the copula pyramidis and the paramedian lobule: congruence of climbing fiber cortical zones and the pattern of zebrin banding within the rat cerebellum. *J Neurosci* 23:4645-4656.
- Wadiche JI, Jahr CE (2005) Patterned expression of Purkinje cell glutamate transporters controls synaptic plasticity. *Nat Neurosci* 8:1329-1334.
- Welker W (1987) Spatial organization of somatosensory projections to granule cell cerebellar cortex: functional and connectional implications of fractured somatotopy (summary of Wisconsin studies). In: *New concepts in cerebellar neurobiology* (King JS, ed), pp 239-280. New York: Alan R. Liss, Inc.
- Wu HS, Sugihara I, Shinoda Y (1999) Projection patterns of single mossy fibers originating from the lateral reticular nucleus in the rat cerebellar cortex and nuclei. *J Comp Neurol* 411:97-118.
- Yatim N, Billig I, Compoint C, Buisseret P, Buisseret-Delmas C (1996) Trigemino-cerebellar and trigemino-olivary projections in rats. *Neurosci Res* 25:267-283.

Tables

Table 1. Summary of cases described in text and/or shown in figures. * Experiments performed in Bristol, all other experiments were conducted in Rotterdam. Cell counts were performed in a 1 out of 4 series of sections in all cases. co, contralateral; FL, forelimb; IO, inferior olive; ip, ipsilateral; LRn, lateral reticular nucleus; MAO, medial accessory olive; Pn, basal pontine nuclei; PO, principal olive; vfDAO, ventral fold of dorsal accessory olive.

CASE	Physiology	IOLabeling				Anatomical zone	Zebrin	LRnLabeling			PnLabeling			Ratio Pn/LRn
		MAO	vfDAO	PO	Total			ip	co	Total	ip	co	Total	
GR03	No	0	167	0	167	C1-COP	P4-(e)	358	100	458	20	778	798	1.74
979	No	8	77	4	89	C1-PMD	P5a-	241	70	311	115	594	709	2.28
AP03*	FL-ip	0	104	1	105	C1-PMD	P5a-	181	53	234	82	550	632	2.70
AP10	FL-ip	0	73	0	73	C1-PMD	P5a-	96	18	114	33	355	388	3.40
981	No	23	1	0	24	C2-COP	P5+/7+	59	14	73	17	259	276	3.78
AP09	FL-ip, FL-co	37	3	0	40	C2-PMD	P5+	103	32	135	39	573	612	4.53
864	No	93	4	0	97	C2-PMD	P5+	63	26	89	58	432	490	5.51
A41	Face-ip	29	0	0	29	C2-Crus2B	P5+	36	17	53	52	337	389	7.34
978	No	5	0	12	17	D0/D1-PMD	P6+/7+	37	10	47	13	446	459	9.77
AP02*	FL-ip	0	6	53	59	D0/D1-PMD	P6+/7+	53	18	71	42	1051	1093	15.39
980	No	0	0	20	20	D1-PMD	P6+/7+	19	9	28	20	427	447	15.96

Table 2. Distribution (expressed as a percentage of the total number) of labeled mossy fiber rosettes in the granular layer subjacent to zebrin-positive and zebrin-negative bands in simple lobule and vermal lobule VIa. Data shown for two cases: case AP03 with an injection into the C1 zone in PMD, and case A41 with an injection into the C2 zone in crus 2b (see also Fig. 6). Note that a P3+ and a P6- band are not clearly present in the simple lobule (Voogd and Ruigrok, 2004).

zebrin-positive band	zebrin-positive band		zebrin-negative band	zebrin-negative band	
	C1 (AP03)	C2 (A41)		C1 (AP03)	C2 (A41)
P1+	0.0	2.3	P1-	1.1	0.1
a+	0.6	0.2	a-	2.1	0.0
P2+	0.1	5.3	P2-	0.9	0.9
b+	0.0	3.8	b-	10.8	4.1
P4+	1.7	18.2	P4-	62.7	8.6
P5+	3.2	22.2	P5-	5.7	3.6
P6+	11.2	30.8	-	-	-
Total (%)	16.7	82.7		83.3	17.3
fraction of granular layer subjacent to zebrin-positive bands (%)	35.4	31.3	fraction of granular layer subjacent to zebrin-negative bands (%)	64.6	68.7

Figures

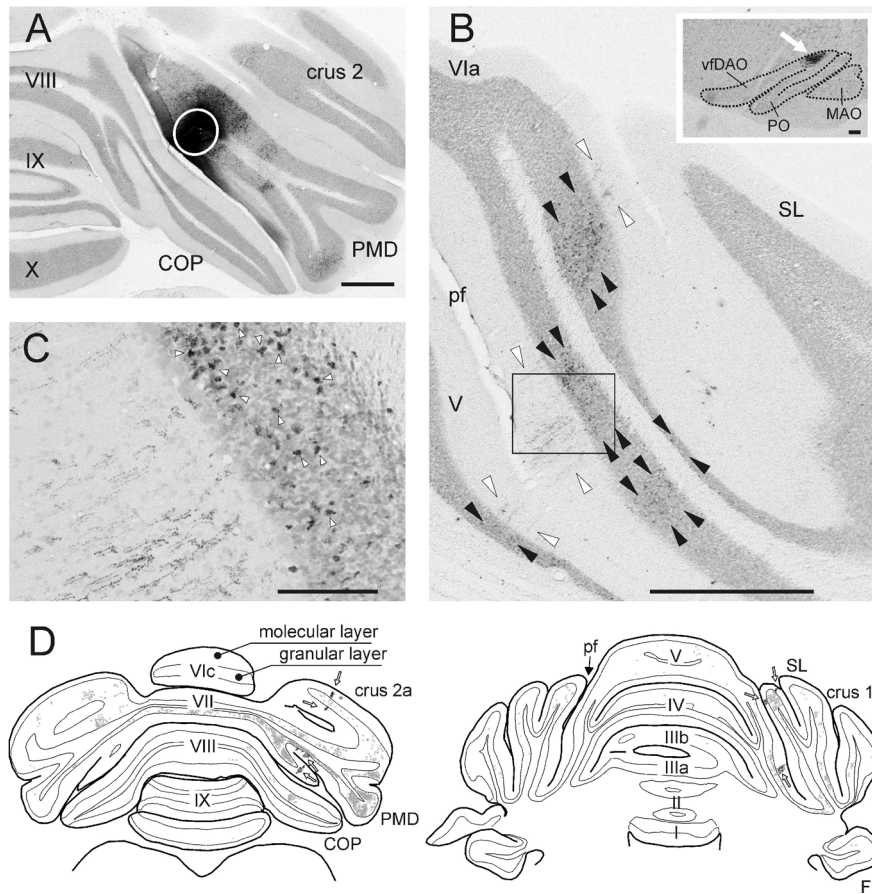


Fig. 1. Photomicrographs showing aspects of the CTb injection site and resultant labeling of climbing and mossy fiber collaterals in case AP03 together with a selection of plots of transverse sections through cerebellum of case AP09. **A**, Photomicrograph of the CTb injection site, indicated by a white circle, in the paramedian lobule. The injection was mostly restricted to the molecular and granular layers of the electrophysiologically identified c1 zone, which was verified by the presence of retrograde labeled cells in the contralateral vDAO (inset in B). **B**, Photomicrograph showing part of a section of the SL and anterior lobe of the same case. Note the characteristic appearance of CTb labeled climbing fibers in the molecular layer (between white arrowheads) and the numerous labeled mossy fiber rosettes within the granular layer (between black arrowheads). Also note that the regions with climbing fiber terminals are aligned in the mediolateral plane but that the regions with mossy fiber terminal rosettes are also found at other mediolateral positions. Inset shows retrogradely labeled cells in the DAO (arrow) of the contralateral inferior olive. **C**, Magnification of the boxed rectangle in **B** showing the boundary of granular and molecular layer. Arrowheads indicate some of the labeled mossy fiber rosettes that are located directly adjacent to labeled climbing fiber terminal arborizations. **D**, Two plots of transverse sections through the posterior and anterior cerebellum, respectively, and indicating the distribution of CTb labeling resulting from a PMD injection in the electrophysiologically identified C2 zone (case AP09). Labeled mossy fiber rosettes (small gray dots: one dot equals one rosette) and climbing fiber terminals (black dots indicated by arrows) are indicated. Scale bar equals 1 mm in A, B and 100 μ m in inset of B and C. I – X, lobules I - X; COP, copula pyramidis; vDAO, ventral fold of dorsal accessory olive; FI, flocculus; MAO, medial accessory olive; pf, primary fissure; PMD, paramedian lobule; PO, principle olive; SL, simple lobule.

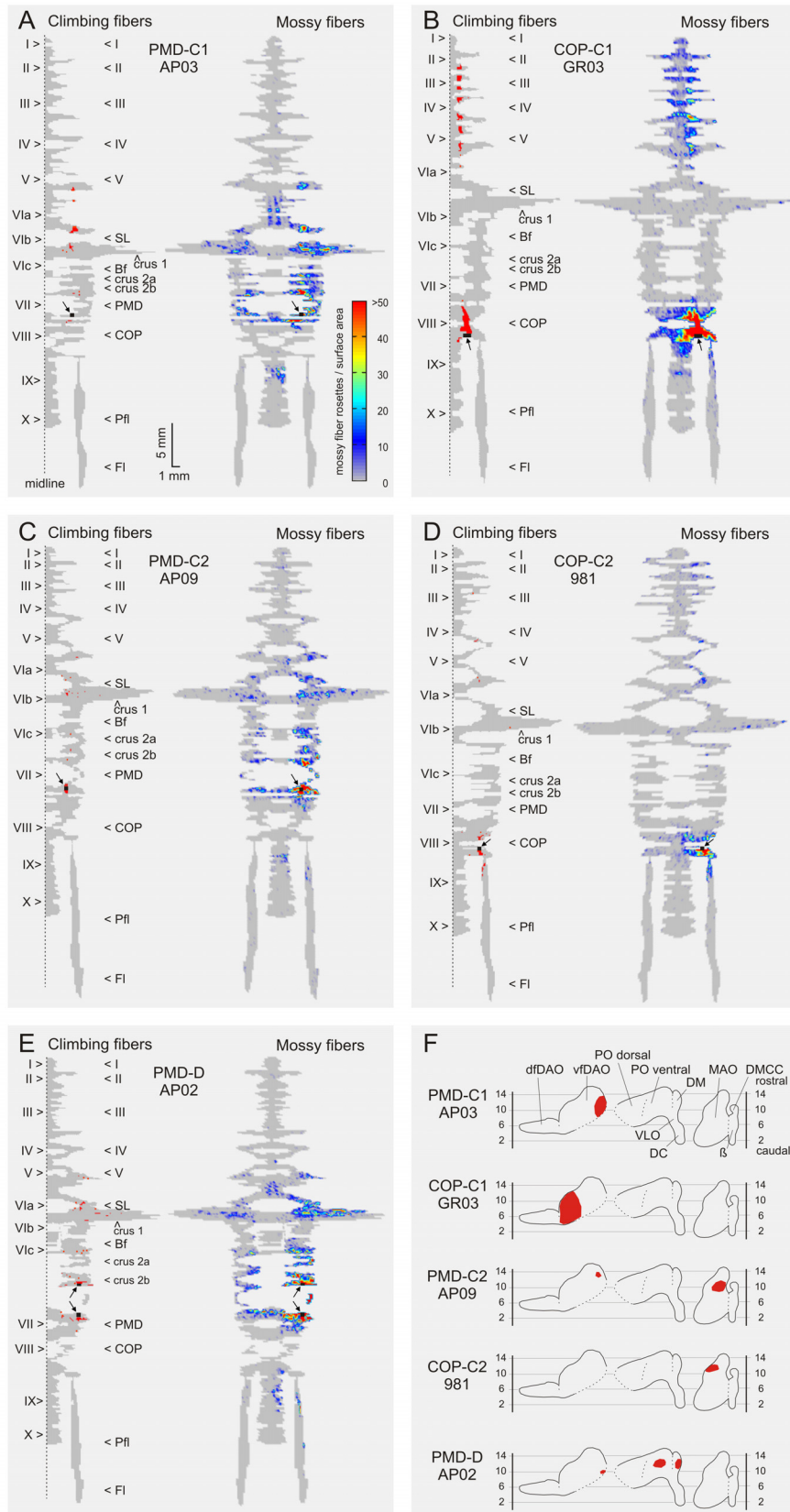


Fig. 2. Color diagrams summarizing the results of mossy and climbing fiber collateral labeling. Five cases with respectively injections in the C1 zone in PMD (case AP03: **A**), C1 zone in COP (case GR03: **B**), C2 in PMD (case AP09: **C**), C2 in COP (case 981: **D**) and the D zone in PMD (case AP02: **E**) as well as generalized flattened surface diagrams indicating the position of resultant cell labeling (red) in the inferior olivary complex (**F**). The left-hand panels show a representation of the right half of the unfolded and flattened surface diagram of the cerebellar cortex. Arrows and their roman number indicate the apex of vermal and hemispherical lobules. The injection sites are indicated by a black square and arrow. Red labeling indicates the presence of bins with labeled climbing fiber terminals in the molecular layer. The right-hand panels show a similar diagram of the whole cerebellar cortex, but now representing the granular layer. Color-coding indicates the number of labeled mossy fiber rosettes in 200 μm wide bins of the granular layer (see colorbar in A). See Ruigrok (2003) and Materials and Methods section 'Analysis' for further details on cortical reconstruction. See Results for detailed description of individual cases. I – X, lobules I – X; β , beta subnucleus; Bf, buried folium; COP, copula pyramidis; DC, dorsal cap; dfDAO, dorsal fold of dorsal accessory olive; DM, dorsomedial group of principal olive; DMCC, dorsomedial cell column; Fl, flocculus; MAO, medial accessory olive; Pfl, paraflocculus; PMD, paramedian lobule; PO, principal olive; SL, simple lobule; vfDAO, ventral fold of dorsal accessory olive; VLO, ventrolateral outgrowth.

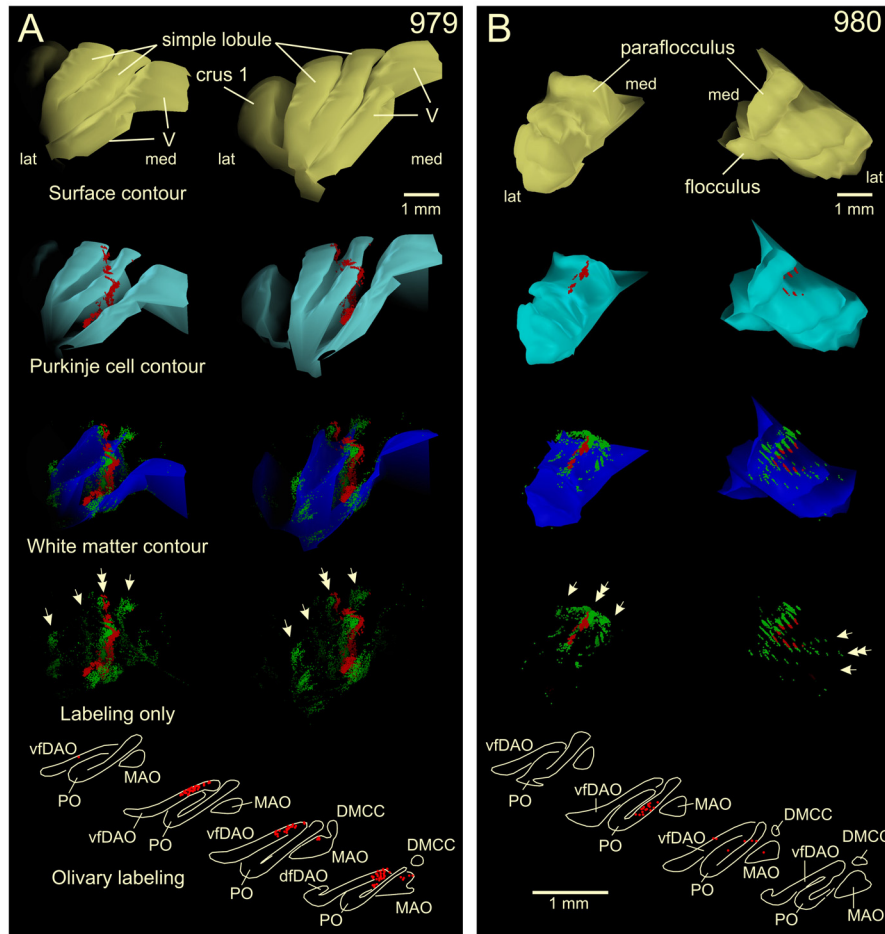


Fig. 3. 3D reconstructions of part of the cerebellar cortex showing the correspondence of mossy and climbing fiber collateral labeling. **A**, Diagrams representing case 979 with a CTb injection centered on C1 of PMD, with some involvement of C2 as judged by the distribution of retrogradely labeled neurons in the inferior olive (bottom panels). 3D reconstructions show a rostromedial (left hand column of panels) and a rostral (right-hand column of panels) view of the ipsilateral simple lobule and adjacent parts of lobule V and crus 1. From the top down the pial surface contour is shown in yellow, the contour indicating the Purkinje cell monolayer in cyan, with superimposed the labeled climbing fiber terminal labeling in red. Subsequently, the white matter contour (granular layer / white matter interface) is shown in dark-blue, with superimposed the labeled mossy fiber rosettes (green: every dot represents a single rosette) and superimposed the climbing fiber terminals (red) in the molecular layer. Finally, bottom panels indicate labeled mossy fiber rosettes and climbing fiber terminals only. Note that a strip of labeled mossy fiber rosettes (indicated by a double arrow), which, in addition also are found at other, non-adjacent, locations (single arrows), closely matches the climbing fiber labeling. **B**, Similar diagrams as shown in A showing the paraflocculus of case 980 with an injection that was centered on D1 of PMD as was judged by the distribution of labeled neurons in the ventral leaf of PO (bottom panels). Left hand panels depict the paraflocculus seen from a caudal dorsolateral view whereas the right hand panels show the paraflocculus from a rostral dorsolateral view. In the latter view the discontinuity of labeling is caused by the intermittent, non-plotted, sections (see Methods for further details on preparing the 3D reconstructions). Note that three strip-like accumulations of labeled mossy fiber rosettes were noted (arrows), the middle of which was accompanied by labeled climbing fibers (double arrow). V, lobule V; vfDAO, ventral fold of dorsal accessory olive; dfDAO, dorsal fold of dorsal accessory olive; DMCC, dorsomedial cell column; PO, principal olive; VLO, ventrolateral outgrowth.

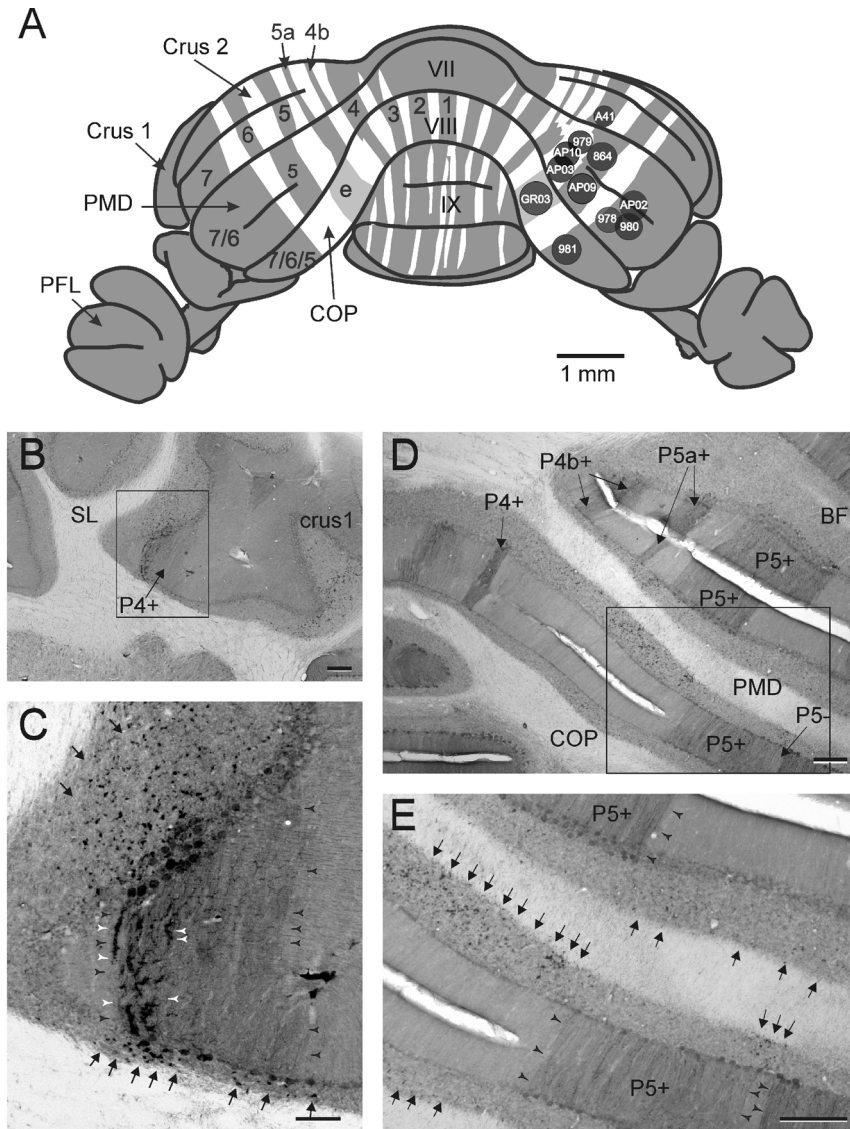


Fig. 4. Relation of injection sites and collateral labeling of climbing and mossy fibers with the intrinsic zebrin pattern of Purkinje cells. **A**, Diagram showing the approximate site and size of the CTb injections used in this study on a reconstruction of the posterior view of the rat cerebellum stained for zebrin (Voogd et al., 2003; Pijpers and Ruigrok, 2006). Note that only the positive zebrin bands are indicated by their respective numbers and letters. Patch 'e' is shaded light gray in accordance with the lightly zebrin-positive nature of this patch. **B**, Photomicrograph taken from case A41, depicting zebrin-positive band P4+ (arrow) in SL. **C**, Detail of boxed area in B. Note that darkly stained climbing fiber collaterals (white arrowheads) are found over the medial part of P4+ (width of band indicated by black arrowheads). Arrows point to labeled mossy fiber rosettes, which are found subjacent to P4+. **D**, **E**, Photomicrographs taken from case AP03 showing the relation of mossy fiber rosettes with negative zebrin bands in the posterior cerebellum. Zebrin-positive bands and band P5- are labeled (arrows in D). Note that in E (showing the boxed area of D in higher magnification) labeled rosettes (arrows) are present subjacent several zebrin-negative areas. Also note that no climbing fiber collaterals were labeled in the zebrin-negative bands. Scale bars equal 1mm in A, 100 μ m in C and 250 μ m in B,D,E. VII, VIII, IX, cerebellar lobules VII, VIII, IX; BF, buried folium; COP, copula pyramidis; PFL, paraflocculus, PMD, paramedian lobule.

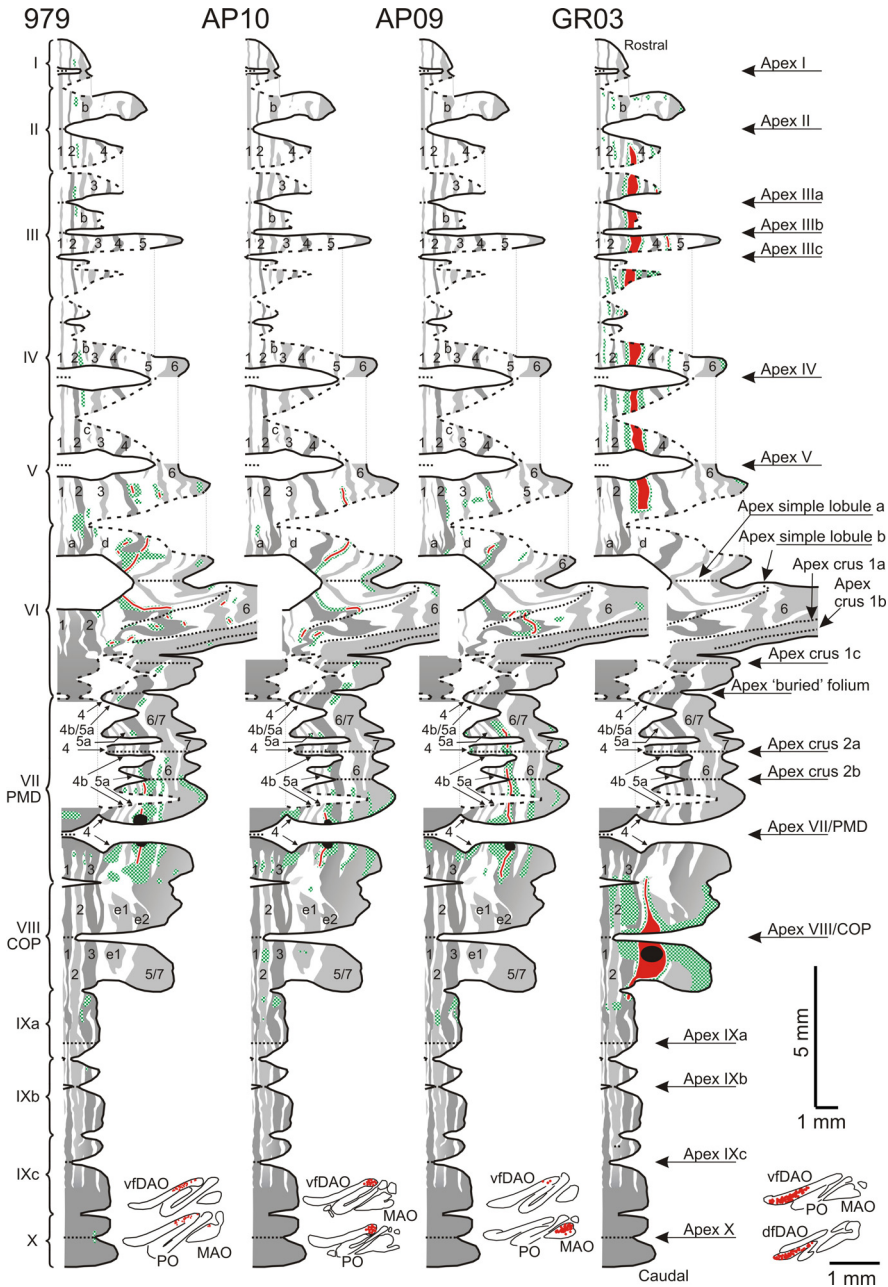


Fig. 5. Distribution of labeled mossy fiber rosettes and labeled climbing fiber collaterals of four cases plotted on a standardized surface reconstruction of the zebrin pattern of Purkinje cells (Pijpers et al., 2005). Roman numbers indicate individual lobules and arrows are used to indicate their apices. The zebrin-positive bands and their continuity over the cerebellar cortex is presented in shades of gray and the numbers and letters in these bands refer to the zebrin-positive bands from the nomenclature of Hawkes and Leclerc (1987) and modified by Voogd and Ruigrok (2004) and by Sugihara and Shinoda (2004). The corresponding negative bands lie immediately lateral to these positive bands. Labeling of both mossy and climbing fiber terminals was qualitatively entered on the standardized diagram by examining sections double labeled for zebrin and CTb and using the zebrin pattern as a reference frame. Regions in the granular layer with clustered presence of labeled mossy fiber rosettes are indicated with hatched patterns in green; climbing fiber terminal labeling is indicated in red in the same diagrams. Figurines at the bottom of each diagram show the localization of retrogradely labeled neurons in representative sections through the inferior olivary complex. See Results 'Distribution of

climbing and mossy fiber collateral terminals: relation to the zebrin pattern' for explanation of the individual diagrams. 1 – 7, zebrin-positive bands P1+ - P7+; I – X, lobules I – X; Bf, buried folium; COP, copula pyramidis; vfDAO, ventral fold of dorsal accessory olive; dfDAO, dorsal fold of dorsal accessory olive; PMD, paramedian lobule; PO, principal olive; MAO, medial accessory olive.

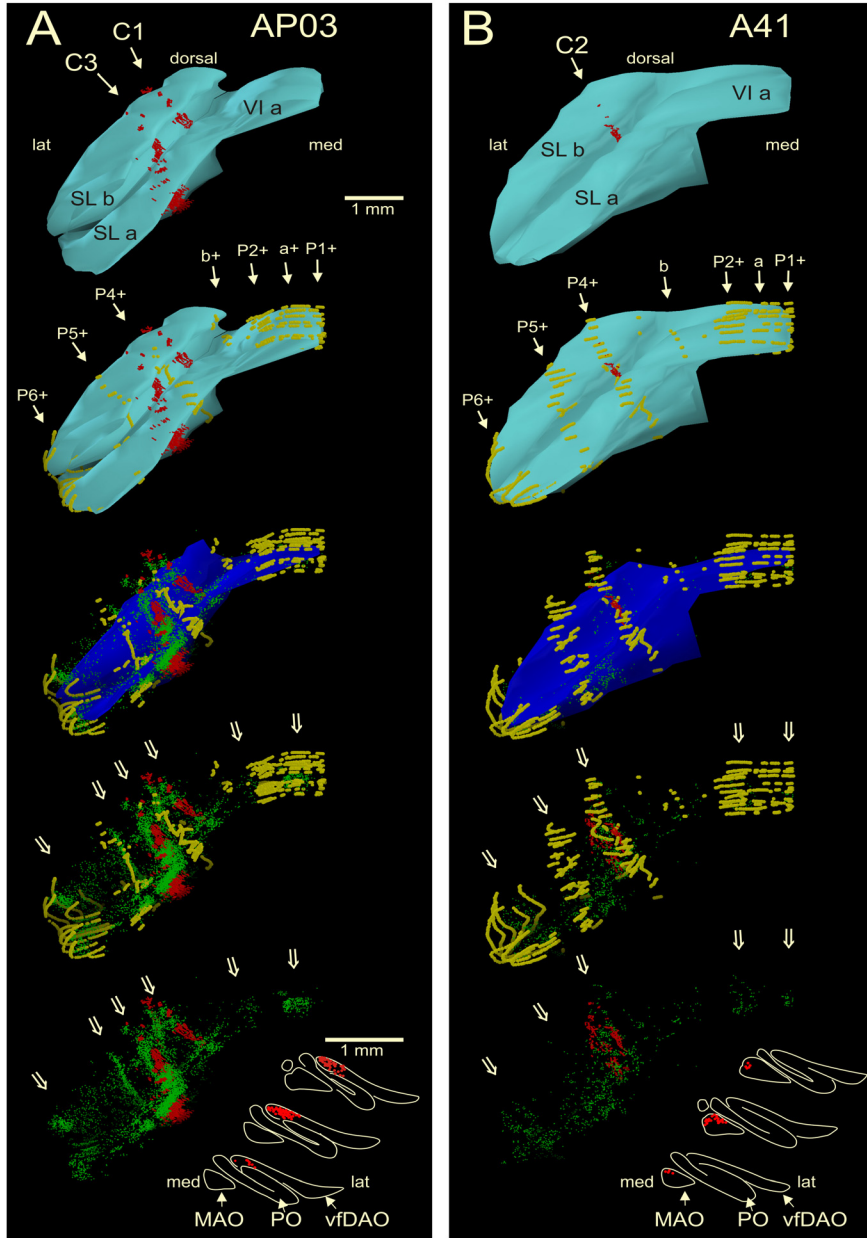


Fig. 6. Rostral view of three-dimensional color reconstructions of part of the simple lobule of cases AP03 (A) and A41 (B) showing the correspondence of mossy and climbing fiber collateral labeling in relation to the pattern of zebhrin-positive Purkinje cells (shown in brown; other conventions are similar to Fig. 3). **A**, In case AP03, the injection site was confined to the C1 zone of PMD as was evident by labeling of olivary neurons in the medial part of the vfDAO (bottom of panel). In SL, labeled climbing fiber collaterals are found in the P3- and P4- bands relating to the C1 and C3 zones (Pijpers et al., 2005). Labeled mossy fibers rosettes are found subjacent to these labeled climbing fibers, and in addition are also found at other and non-adjacent locations (open arrows). Note that most mossy fiber labeling is positioned subjacent to zebhrin-negative areas. **B**, In case A41, the injection site was centered on the C2 zone of crus 2b and resulted in labeled olivary neurons in the rostral MAO. In SL, labeled climbing fiber collaterals are found within the P4+ band that relates to the C2 zone (Pijpers et al., 2005). Labeled mossy fibers rosettes are found subjacent to these labeled climbing fibers, and in addition are also found at other non-adjacent locations (open arrows). Note that many of

them are related to zebrin-positive areas. P1+-P6+, a,b refer to zebrin bands (Voogd and Ruigrok, 2004); VIa, lobule VIa; MAO, medial accessory olive; PO, principal olive; SLa,b, simple lobule a, b; vfDAO, ventral fold of the dorsal accessory olive. Olivary panels are arranged from rostral (bottom) to caudal (top).

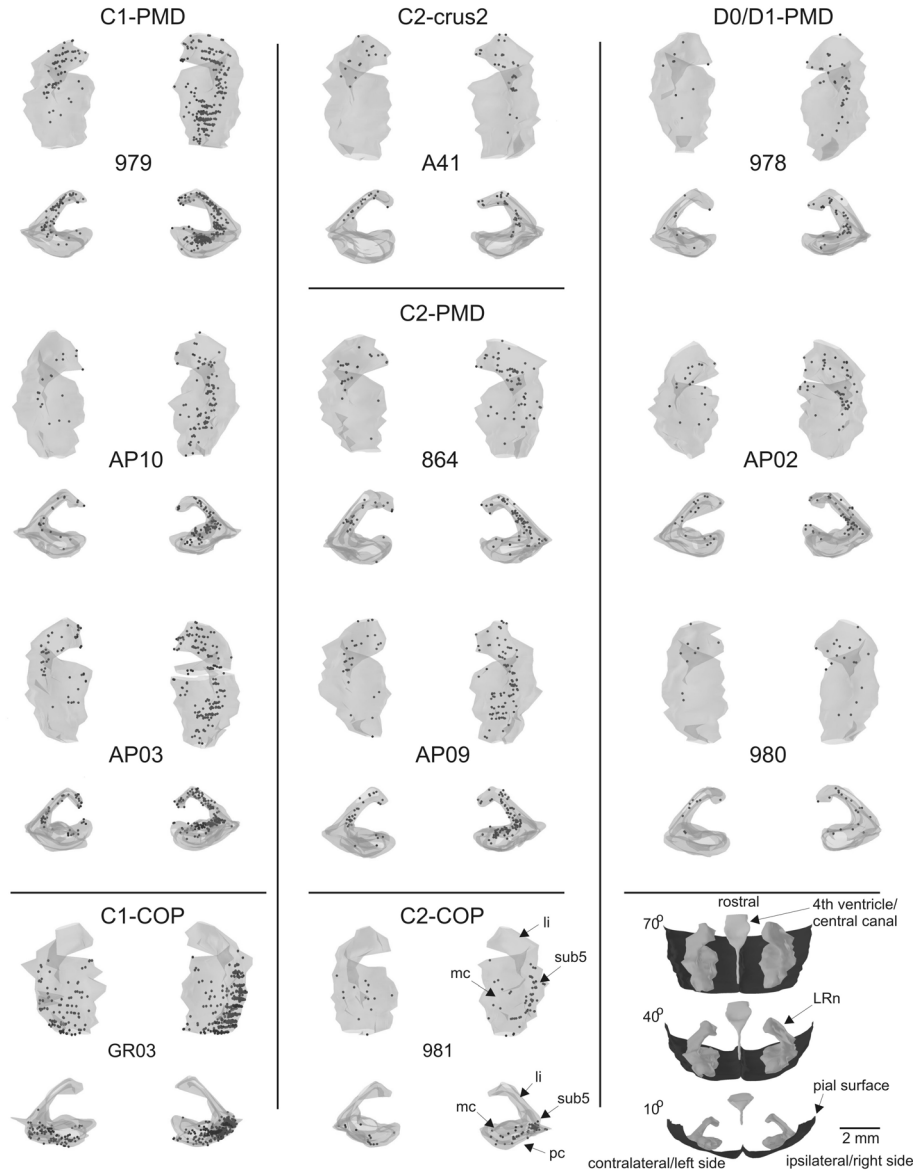


Fig. 7. Overview of the distribution of labeled precerebellar neurons in the LRn. Labeled neurons are depicted in 3D figurines prepared from plots of the ipsi- (right side) and contralateral (left side) LRn made from a one in four series of transverse sections. Every dot represents a labeled neuron. Both a caudal (10° dorsal from horizontal plane) as well as a predominantly dorsal view (70° dorsal from horizontal plane) was prepared of each case. Cases are grouped according to lobule and zone in which the injection was centered (cf. Fig. 4A). Bottom right hand panels show orientation of the figurines of ipsi- and contralateral LRn in relation to the ventral surface of the medulla and the central canal/fourth ventricle. Different subdivisions of the LRn complex are indicated for case 981 (bottom center panel). See Results 'Origin of mossy fibers to different lobules and zones' for further explanation. LRn, lateral reticular nucleus; li, linear subdivision; mc, magnocellular subdivision; pc, parvicellular subdivision; sub5, subtrigeminal subdivision.

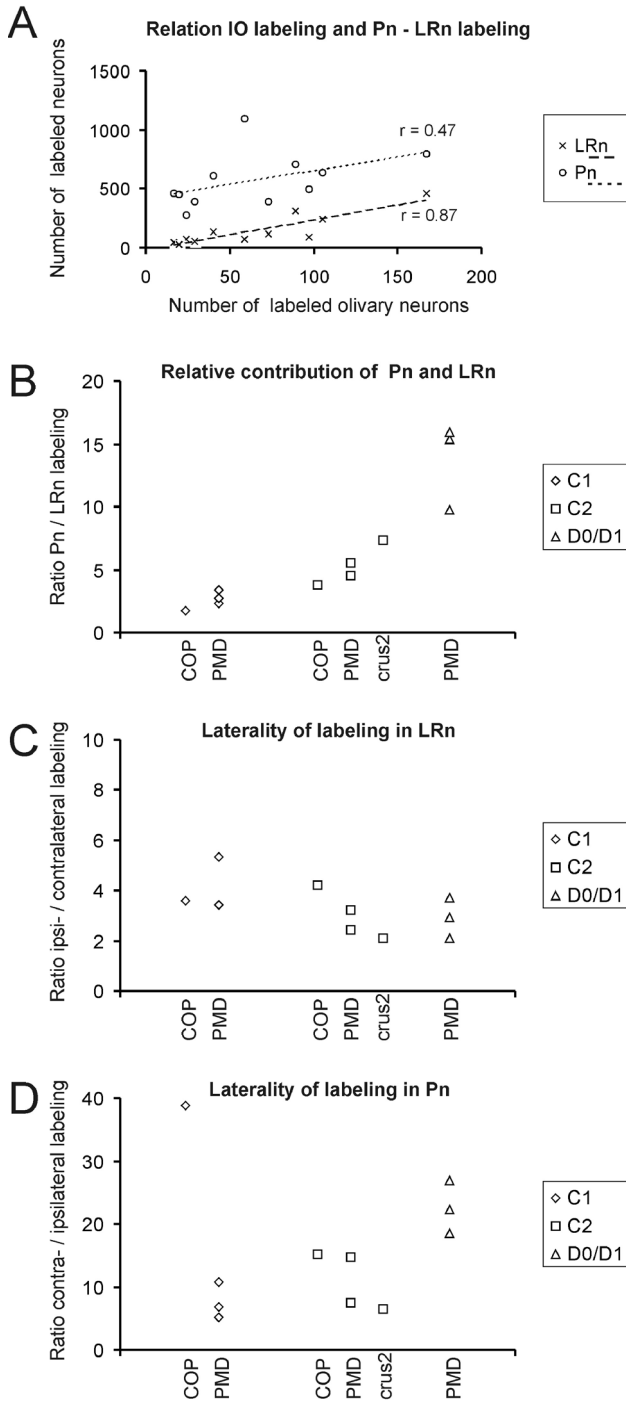


Fig. 8. A comparison of the number and laterality of labeled neurons observed within the Pn and LRn. **A**, Graph depicting the relation between number of labeled olivary neurons and number of labeled neurons in Pn and LRn. Note that the numbers of labeled LRn and IO neurons correlate better than those of PN and IO, indicating that the involvement of both precerebellar centers to provide mossy fiber afferents to the granular layer subjacent a particular climbing fiber zone differs from each other. **B**, Graph depicting the contribution of Pn and LRn to a particular injection site. Note that injections into the D0/D1 zone of PMD results in much higher ratio of labeled neurons in Pn and LRn than in cases where the injection was centered on C1. **C**, **D**, Graphs comparing the participation of ipsi- versus contralaterally labeled neurons in LRn (**C**) and Pn (**D**). Note that for the LRn, the ratio of the number of ipsi- and contralaterally labeled neurons varies only marginally between different cases, whereas notable differences are observed for the Pn. Data for Pn labeling are in part taken from Pijpers and Ruigrok (2006).

Chapter 5

Cerebellar Zones Involved In Rat Hindlimb Control -A Retrograde Transneuronal Tracing Study With Rabies Virus-



Adapted from:

Ruigrok TJH, Pijpers A, Coulon P. *Cerebellar zones involved in rat hind limb control; a retrograde transneuronal tracing study with rabies virus*. Submitted.

Abstract

To identify cerebellar regions involved in the control of individual limb muscles, rabies virus was injected into the tibialis anterior (TA), the gastrocnemius (GC) or, for comparison, into the flexor digitorum (FD) muscles. Progression of retrograde transneuronal infection at supraspinal levels was assessed after variable time spans and was divided into three phases.

Initially, infected neurons were observed in the reticular formation, red nucleus, motor cortex, and in the lateral vestibular nucleus (phase 1). In phase 2, Purkinje cells in two vermal strips were labeled throughout the anterior lobe. Double labeling with zebrin II enabled identification of these strips as the lateral part of the A1- and the B-zone. For TA both zones were ipsilateral, whereas for GC the A1 strip was present only contralaterally. Phase 3 infections were characterized by additional labeling of multiple, in part bilateral, strips of Purkinje cells, which could be related to all presently identified cortical zones apart from Ax and D1. FD injections resulted in less robust labeling of vermal strips and more pronounced labeling within paravermal and hemispherical zonal regions. Only sporadic labeling in corresponding regions of the inferior olive and no labeling of cortical interneurons or granule cells was observed. Evidence was found that motoneurons and Purkinje cells degenerate after prolonged infection.

We conclude that vermal, paravermal as well as hemispherical zones of the cerebellar cortex converge upon motoneurons that innervate a particular muscle. In addition, individual zones may control motorpools of different muscles and thus contribute to muscle synergies.

Introduction

Classic observations already established that different cerebellar regions are involved in different functions (Babinski, 1899; Holmes, 1939). E.g. the cerebellar hemispheres are thought to be mainly involved in higher order and preparatory motor processing whereas the interposed nuclei are considered to control the kinematics of ongoing movements (Thach, 1970; Strick, 1983). The uniform structure of the cerebellum suggests that the specific tasks in which the cerebellum is involved must depend on highly organized input and output relations. These relations are frequently characterized by longitudinal patterns, which can be recognized at anatomical as well as at physiological levels (Apps and Garwicz, 2005). Parasagittal arrays of Purkinje cells (PCs) have been shown to receive their climbing fiber input from specific areas of the inferior olive (IO), but also to send their axons to specific regions of the cerebellar nuclei (CN) (Sugihara and Shinoda, 2004; Voogd and Ruigrok, 2004; Pijpers et al., 2005). This organization led to the notion of olivo-cortico-nuclear modules, in which matched olivo-nuclear and nucleo-olivary projections

also participate (Ruigrok and Voogd, 1990, 2000), and that are seen as cerebellar functional entities (Apps and Garwicz, 2005).

However, as yet, little is known on how the various types of information are converted into functionally relevant signals that, via descending pathways, aid in motor control. Indeed, presently, no detailed information is available that suggests that different modules assist in the control of individual muscles or whether a single module can influence antagonistic muscle groups. Therefore, the present study was specifically designed to chart those cerebellar modules that are incorporated in the control of individual muscles and to determine if different muscles are controlled by other modules or by different parts of the same modules.

The use of rabies virus as a retrograde transneuronal tracer (Ugolini, 1995) offers a powerful tool to explore and compare the cerebellar regions that are used to control individual muscles (Graf et al., 2002). Therefore, to address the issue of cerebellar modules related to a single muscle and muscle synergies, the virus was injected into tibialis anterior (TA) and gastrocnemius (GC) of the rat, which are the main flexor and extensor muscles of the ankle, respectively. Some injections into flexor digitorum (FD) and a single injection of biceps femoris (BF) were made for validation purposes. The virus injections resulted, after several synaptic relays, in transneuronal labeling of arrays of PCs at various places of the cerebellum. The zonal, or modular, identity of these arrays was established by relating them to the intrinsic pattern of zebrin II and by assessing the labeling within the CN and IO (Voogd and Ruigrok, 2004; Pijpers et al., 2005).

We conclude that a combination of specific modules, which are located in vermal, paravermal and hemispherical regions on both sides of the cerebellum influence different aspects of control of a particular muscle. Conversely, individual modules are likely to be involved in controlling muscle synergies, but differences in zonal labeling were also observed that related to the identity of the injected muscle.

Materials and methods

Surgical procedures

Twenty-seven, female Wistar rats (weight 200-250 g) were used in this study. All procedures adhered to the European guidelines for the care and use of laboratory animals (Council Directive 86/609/EEC). Vaccinated personnel conducted all experiments at the appropriate biosafety containment level (cf. Kelly and Strick, 2000). The virus stock (2×10^9 plaque forming units/ml) of the Challenge Virus Standard 11 (CVS-11) fixed strain of rabies virus was kept frozen at -80°C until use. This strain, when injected into a muscle, has been shown to be transported in a retrograde direction to motoneurons that innervate the injected muscle (Ugolini, 1995). Moreover, recent studies in monkey show that the virus of this strain does not spread beyond its site of

injection (Ugolini et al., 2006). Therefore, single muscle injection is likely to infect only a fraction of the motoneuronpool innervating this muscle. Indeed, in 4 of our 25 cases with a rabies injection (Table 1) no signs of infection were observed in the spinal cord, which we explain by assuming that in these cases the virus was not injected in the near vicinity of endplates. In the somata of infected motoneurons the virus replicates and it has been shown to be able to pass to the presynaptic elements where it, again in retrograde direction, is transported to the soma where the cycle repeats itself. The attractiveness of the CVS strain of rabies virus is particularly formed by the fact that infected neurons have not been reported to show rapid degeneration and may survive infection for over a week (Guigoni and Coulon, 2002). Importantly, the virus does not appear to be able to infect neighboring neurons that do not have synaptic contacts (Ugolini, 1995).

Animals were initially anesthetized with an intraperitoneal (i.p.) injection of a mixture of ketamine (80mg/kg; Imalgene, Merial, Lyon, France) and xylazine (10mg/kg; Rompun, Bayer, Leverkusen, Germany). When necessary, supplementary doses were given i.p. in order to maintain surgical levels of anesthesia, as monitored by the absence of the pinch withdrawal reflex and loss of muscle tone. Body temperature was maintained and kept within physiological limits ($37 \pm 1^{\circ}\text{C}$). A small incision was made in the skin above the targeted muscle. After removal of the fascia and identification of the muscle, 5 to 30 μl of virus solution (Table 1) was slowly injected using repeated penetrations with a Hamilton syringe (1 μl / injection). Subsequently the wound was sutured and the animals were allowed to recover. All animals were carefully monitored daily for behavioral changes (such as aggressiveness or somnolence), at which point the experiment was terminated.

In order to verify the location of the pool of motoneurons that innervate the TA and GC, these muscles were injected with 10 μl of a 1% w/v cholera toxin b-subunit (CTb lot #10426A, low salt: List Biological Laboratories, Campbell, CA, 1% w/v in 0.1 M phosphate buffer, pH 7.4) into opposite sides of two rats.

Histology

After the appropriate survival time (ST) of up to six days (144 hours), or to the point at which the animals began to show symptoms of infection (in one case after 8 days), the animals were sacrificed under deep anesthesia with sodium pentobarbitone (80 mg/kg, i.p.; Nembutal, Ceva Sante Animale, Libourne, France). After an initial transcardial flush of 0.9% saline, they were perfused with 4% paraformaldehyde in phosphate buffer (PB, pH 7.4). Brain and spinal cord were removed and post-fixed for several days until further processing. Formaldehyde fixing renders the virus inactive (Kelly and Strick, 2000). Prior to being processed the tissue was stored overnight in 0.05M PB containing 10% sucrose at 4°C . Subsequently, the brain, together with the spinal cord,

was embedded in 11% gelatin with 10% sucrose. The blocks were hardened in 10% formalin and 30% sucrose solution for 3-4 hours and were stored overnight in 0.05M PB containing 30% sucrose at 4°C.

The tissue blocks were sectioned transversally at 40 µm on a freezing microtome and collected serially in 8 glass vials containing 4% paraformaldehyde in PB. Selected vials were processed either for rabies immunohistochemistry only (2 vials); for combined rabies - zebrin II immunostaining (2 vials), or for single zebrin II immunostaining (2 vials). In some cases, the remaining vials were processed for combined rabies and choline acetyl transferase (ChAT) immunohistochemistry, calbindin immunostaining, argyrophilic silver degeneration staining, or for thionin staining only. The vials designated for rabies immunohistochemistry were thoroughly rinsed with phosphate buffered saline (PBS). The free floating sections were incubated overnight at room temperature in an anti-rabies phosphoprotein mouse monoclonal antibody (Raux et al., 1997) diluted 1:5000 in PBS that contained 2% normal horse serum (NHS) and 0.5% triton X-100 (PBS+). Subsequently, sections were rinsed in PBS and incubated for 90 minutes at room temperature in rabbit anti-mouse-HRP (P260 Dako, 1:200 in PBS+). After thorough rinsing in 0.05M PB, the vials in the rabies protocol were either incubated in DAB-solution for 10-20 minutes (0.025% 3,3'-diaminobenzidine-tetrahydrochloride and 0.005% H₂O₂ in 0.05M PB at room temperature), resulting in a brown reaction product, or, in case of double labeling with zebrin II, they were incubated for 10-15 minutes in a similar DAB/H₂O₂ solution but containing cobalt/nickel ions (CoSO₄ 0.01%, NiSO₄ 0.01%), yielding a black reaction product for the rabies infected neurons. All vials were rinsed in 0.05M PB. Next, vials processed for zebrin II staining, were rinsed in PBS and the sections were incubated, free floating, for 48-72 hours at 4°C in zebrin II antibody, 1:150 in PBS+. This antibody was produced by immunization with a crude cerebellar homogenate of the weakly electric fish *Apteronotus* and recognizes a single polypeptide antigen with a molecular weight of approximately 36 kD (Brochu et al., 1990) and was kindly provided by Dr. R. Hawkes (Dept. of Cell Biology and Anatomy, University of Calgary, Canada). After rinsing in PBS, sections were incubated for 2 hours at room temperature in rabbit anti-mouse HRP (p260 Dako, 1:200 in PBS+). Subsequently, sections were thoroughly rinsed in 0.05M PB and incubated in DAB solution for 20-30 min, resulting in a brown labeling of zebrin-positive Purkinje cells (PCs).

Spare vials designated for combined immunolabeling of rabies and ChAT were heated for 30 minutes at 80 °C in 25 mM sodium citrate (pH 8.75) in order to improve antigen retrieval (Ezaki, 2000). After thorough rinsing in PBS+, sections were incubated in PBS+ containing goat anti-ChAT (1:500: Chemicon, Temecula, CA) as well as the mouse anti-rabies (1:5000) for 48-72 hours at 4°C. After rinses in PBS the sections were incubated in a cocktail containing the secondary antibodies consisting of donkey anti-goat-Cy3 (1:200) and donkey anti-mouse-FITC (1:200: both from Jackson ImmunoResearch, Newmarket, Suffolk, England) in PBS+ for 2 hours

at room temperature. After a final series of rinses in PBS and PB, sections were mounted from chromic alum and coverslipped with ProLong Gold (Invitrogen, Breda, Netherlands). Sections were stored at 4 °C and examined using with a Leica DMRBE microscope (Nussloch, Germany) equipped with a Hamamatsu camera (C4880: Hamamatsu Photonics, Hamamatsu City, Japan). Photopanel of Fig. 1C were constructed in Adobe Photoshop 7.0.

Sections from some cases were checked for agyrophilic degeneration using a modification of the Nadler silver impregnation technique (Haasdijk et al., 2002). In one of these animals, degeneration of PCs was also studied by immunohistochemistry of the calcium binding protein calbindin D28K, which is known to label PCs (Wood et al., 1988). Briefly, after an overnight incubation in rabbit anti-calbindin D28K (Swant, Bellinzona, Switzerland: diluted 1:10,000 in PBS+), sections were rinsed in PBS, incubated for 2 hours in biotinylated goat-anti-rabbit (Vector Laboratories: 1:200 in PBS+), rinsed and incubated in avidin-biotin-complex (ABC-Elite, Vector Laboratories, Burlingame, Ca) for 2 hours. Finally, sections were incubated in DAB-solution (see above). All incubations were performed at room temperature.

The spinal cord and lower brainstem of the two rats that received CTb injections into TA and GC were blocked, embedded in gelatin and sectioned transversally at 40 µm and also collected serially in eight vials. Two vials were incubated consecutively overnight with a high-titer polyclonal anti-cholera toxin antibody raised in goat (goat anti-CTb: lot #703, List Biological Laboratories Campbell, CA, 1:15,000 in PBS containing 0.5 % Triton X-100 for 48-72 hours at 4 °C), a biotinylated donkey anti-goat antibody (List Biological Laboratories, 1:2000 in PBS, containing 0.5% triton-X100 for 1½ hours at room temperature), avidine-biotin complex (ABC Elite, Vector Laboratories for 1½ hours at room temperature) and, finally, in DAB and H₂O₂ (see above) in PB at room temperature.

After the immunohistochemical procedures, sections were mounted serially on slides in a chromic alum solution, air dried, and lightly counterstained with thionin, dehydrated in graded alcohol and xylene baths, and coverslipped with Permount. Sections stained for silver degeneration were mounted on gelatinized slides; air-dried and coverslipped with Permount without passing alcohol and xylene baths.

Analysis

Assessment of the progress of viral infection was done by careful analysis of labeled structures in thionin-counterstained and non-zebrin stained sections. Photomicrographs were made with a Leica DMR microscope (Nussloch, Germany) equipped with a digital camera (Leica DC-300). Photo panels were constructed in CorelDraw™ 11.0, after some correction for brightness and contrast in Corel Photopaint™ 11.0.

Labeled neurons in the IO and CN were plotted serially from a one out of four series (160 µm intervals = two vials) of sections using an Olympus microscope equipped with a Lucivid™

miniature monitor, and using NeuroLucida™ software (MicroBrightfield, Inc., Colchester, VT). This package was also used to construct three-dimensional plots of labeled structures and motoneuron-like profiles in the spinal cord using a one out of four series of sections as were three-dimensional plots of PCs and zebrin II-positive PCs. In preparing these plots, contours of the spinal gray matter (spinal cord) or fourth ventricle and cerebellar cortex including boundaries of the molecular and granular layer, were plotted at low magnification (2.5x objective) and rabies-positive and motoneuron-like profiles (spinal cord) or zebrin-positive PCs (cerebellum) were subsequently indicated at high power magnification (10-20x objective). Individual sections were aligned using the central canal (spinal cord) or midline of the bottom of the 4th ventricle as a reference. Point to point measurements used to prepare Figure 7F were also made with NeuroLucida.

For some cases, the relation of the retrograde Purkinje cell labeling with rabies virus and the zebrin-banding pattern was indicated in a standardized reconstruction of the unfolded surface reconstruction of the cerebellar cortex with the superimposed zebrin-banding pattern (Fig. 9: for details Pijpers et al., 2005). In these figures, roman numbers indicate individual lobules and arrows were used to indicate their apices. The zebrin-positive bands are presented in gray and the numbers and letters in these bands refer to the zebrin-positive compartments from the nomenclature of Hawkes and Leclerc (1987) and as modified by Voogd et al. (2003) and Sugihara and Shinoda (2004). The corresponding negative compartments lie immediately lateral to the positive compartments. All final plots were constructed in CorelDraw™ 11.0.

Results

Table 1 provides an overview of all our cases with injection of rabies virus. Note that in five out of twenty cases with injection of rabies into either the TA or GC no signs of rabies infection or transport could be detected in the central nervous system. In the remaining cases (n=15) viral uptake in the lumbosacral spinal cord was evident and consisted of labeling of large neuronal profiles that were located within lamina IX as well as of labeling of usually massive numbers of interneurons. In all but one of these cases, labeling of neurons was also noted at supraspinal levels. PCs were included as labeled neuronal structures in eleven cases. Five additional cases, four with an injection into the FD (a distal forelimb muscle) and one with an injection into the BF (proximal hindlimb) also resulted, apart from labeling in the spinal cord, in infection of supraspinal neurons, which in some cases also included PCs (Table 1).

Spinal cord

The location of motoneurons supplying TA and GC was determined using injections of CTb, a non-transneuronal tracer, into these muscles. Motoneurons innervating GC occupied central regions of lamina IX at L5-L6 levels, whereas TA motoneurons take up positions at somewhat more dorsolateral aspects of the L4-L5 segments (Fig. 1A1, 1B1). The position of large rabies-positive neurons and neuron-like profiles was very similar to the location of the motoneurons labeled from CTb injection into the TA or GC (cf. Fig. 1A1-3 and Fig. 1B1-3). Note however, that with an ST of 4 days many of these rabies-infected motoneuron-like contours appear disintegrated as evidenced by the absence of sharp soma borders (Fig. 1A3 and 1B3). In several experiments with rabies injections of the flexor digitorum muscle (FD: Table 1), motoneuron-like labeling was observed medially within the dorsolateral-most aspect of lamina IX of the caudal cervical intumescence. Similar to the TA and GC cases, these motoneurons also had a fuzzy appearance and were already observed at 78 hours post-injection (Fig. 1C1-3, E), but could also be recognized at longer STs. These damaged, rabies-labeled, neuronal contours were all ChAT-negative, although occasionally a usually small but normal appearing rabies-positive and ChAT-positive neuronal profile was observed within the cluster of motoneurons (Fig. 1C1-C3). Although alpha- and gamma- motoneurons have been reported to be susceptible to infection after rabies injection into a muscle, no information is available on potential differences in vulnerability of different types of motoneurons to infection with rabies virus (Buttner-Ennever et al., 2002; Rathelot and Strick, 2006). Due to the early degeneration of the infected motoneurons it was not possible to reliably assess their number, especially in experiments with more advanced STs. For the objective of the present study, however, it is important to note that at the STs shown in Fig. 1, but also in the spinal cords of animals with more prolonged STs (not shown), most large lamina IX neurons remain uninfected with the rabies virus indicating that inadvertent spread of the virus due to degeneration of infected neurons was not likely to take place. The distributions of all of these motoneuronal-like profiles were in good accordance with our CTb results and with earlier descriptions of rat motoneuronal pools (Nicolopoulos-Stournaras and Iles, 1983; Curfs et al., 1993).

In addition to lamina IX labeling, many small- and medium-sized neurons were observed in other laminae (Fig. 1). Initially, most neurons were noted ipsilaterally in laminae IV-VII (Fig. 1D). At a somewhat later stage, the number of neurons in these laminae increased dramatically, especially in the medial part of laminae IV-VI. Additional labeling was noted in lamina I (Fig. 1E) and within the contralateral cord, where they were most abundant in the medial part of lamina VII/VIII (Fig. 1D,E). At longer STs, the number of labeled neurons in lamina IV-VIII increased dramatically resulting in labeling of virtually all neurons within these laminae. Labeling within lamina II/III and, as noted above, within lamina IX remained rather sparse even after 120 or 144 hours of survival.

Spinal labeling was also observed at thoracic and cervical levels (in case of TA and GC injections) but its analysis was beyond the scope of the present study.

Supraspinal labeling

In all infected animals but one (Table 1), labeled neurons were found at supraspinal levels. In two cases (1015, GC, ST 120 hours and 1055, FD, ST 78 hours), this labeling was limited to some cells of the ventromedial medulla. In all other cases, apart from sometimes intense labeling of the ventromedial reticular formation (VMRF), additional labeling was prominent in the lateral vestibular nucleus (LVN), red nucleus (RN) and within layer V of the sensorimotor cortex (Fig. 2 A-G). Apart from the VMRF, where labeling was abundantly present bilaterally (not shown), labeling was only slightly more pronounced ipsilateral to the injection site for the LVN and nearly completely contralateral for the RN and the motor cortex (Rathelot and Strick, 2006).

At a more advanced phase of infection, which was usually observed with a ST of 120 or 144 hours for TA and GC injections, labeling within these premotor areas became considerably more pronounced as was the bilateral nature of this labeling (Fig. 2J). In addition, marked labeling was observed throughout virtually all regions of the reticular formation, deep layers of the superior colliculus, deep mesencephalic nucleus including the interstitial nucleus of the medial longitudinal fascicle, vestibular nuclei, raphe nuclei and in some cells of the locus coeruleus. Within the cerebral cortex, labeling within the sensorimotor regions included layers II-VI but also involved labeling within premotor and secondary somatosensory cortices. Labeling was also noted in the ventrolateral and ventral anterior part of the thalamus and even in the entopeduncular nucleus (not shown).

Labeling in the cerebellum was noted in the CN before labeling of PCs in two cases only (cases 1006 and 1008, Table 1). In other cases labeling within the CN coincided with labeling of the cerebellar cortex. In one hindlimb case, labeling in nuclei and cortex was noted as early as 101 hours post-injection (case 1016), whereas in others still only relatively sparse labeling was observed after 144 hours (Table 1, e.g. cases 1009, 1021). Usually however, robust staining of PCs was noted after an ST of 120 or 144 hours, which were arranged into one or several strip-like patterns (Fig. 2H,I, Fig. 5). Labeling of PCs coincided with sparse labeling of neurons in the IO (Fig. 4C,D). Surprisingly, even after 144 hours (and up to 192 hours), no labeling was observed of cerebellar cortical interneurons that are known to contact PCs such as basket and stellate cells. Also, labeled granule cells were never observed.

The progression of infection was arbitrarily categorized into phases. Cases with a phase 0 infection only displayed spinal cord labeling without sign of any supraspinally infected neurons. Phase 1 infection was designated to cases with supraspinal labeling, which was usually present in VMRF, RN and LVN but without any obvious involvement of the CN. Phase 2 infected cases displayed prominent involvement of labeling within the CN and of up to two strips of infected PCs.

Finally, phase 3 infection was assigned to cases which had developed heavy labeling within multiple PC zones. Several cases were classified using an intermediary phase. Although prolonged STs generally resulted in a more advanced infection phases, the relation was not absolute (Fig. 2K, Table 1). For this reason we have ordered our cases with respect to the observed progression of infection rather than according to ST (Table 1).

Validation of the selectivity of transneuronal transport

In order to further establish and demonstrate the confinement of the rabies virus within well-established pathways (cf. Ugolini, 1995; Kelly and Strick, 2000), the TA and GC cases were compared with results obtained in several cases with FD injections (Table 1). Apart from the obvious differences in location in the spinal cord, at supraspinal level the most conspicuous difference with labeling resulting from both hindlimb muscles was observed in the RN. Labeling resulting from either TA or GC injection was confined to the ventrolateral aspect of the magnocellular part of the contralateral RN whereas FD labeling was restricted to its dorsomedial part (cf. Fig. 2A, D, G). The dorsomedial and ventrolateral parts of the caudal RN specifically connect to the cervical and lumbosacral cord, respectively (Huisman et al., 1981; for review Ruigrok, 2004). Although labeling intensity, number of labeled neurons as well as the bilateral nature of the labeling in the RN generally increased with longer STs it is important to note that the overall distribution of labeled neurons within the RN did not significantly change (cf. Fig. 2A with Fig. 2J).

With FD injections, labeled layer V pyramidal neurons were found mostly rostral to the level of the anterior commissure, whereas initial labeling resulting from TA and GC was observed mostly caudal to the anterior commissure. In addition, FD injections resulted in a considerably more lateral extension of the involved sensorimotor cortex as compared to TA and GC injected cases (cf. Fig. 2B, E; for review on corticospinal connections in rat Tracey, 2004).

Finally, when comparing labeling within the CN, it was noted that hindlimb muscle injections resulted in more prominent labeling of the ipsilateral LVN compared to the FD cases, which showed rather abundant labeling in the contralateral dorsolateral protuberance of the medial cerebellar nucleus (MCN: cf. double arrows in Fig. 2C and 2F). Most important however, was the observation that the labeling within the AIN (arrows in Fig. 2C,F) was in complete agreement with the known topography of the rat AIN projections to the RN (Daniel et al., 1987). Based on these results we conclude that within these early phases of infection the virus remains confined within anatomically connected networks.

Distribution of labeled neurons within the cerebellar nuclei and inferior olive

Figure 3 shows, for both the GC and TA, the distribution of retrogradely labeled cells within the ipsi- and contralateral CN for each of the three phases that were considered typical for progression of the supraspinal infection (Table 1). In the earliest phase (1016 for GC and 1008 for TA), labeled neurons were only found in the LVN bilaterally and, only very sporadically, in the CN where they were located in the medial part of the posterior and anterior interposed nucleus (PIN and AIN, respectively), interstitial cell groups (ICG: Buisseret-Delmas et al., 1993a) and rostral part of the MCN. Phase 2 cases displayed many prominently labeled cells bilaterally within the LVN while labeling in the CN was considerably more robust in the areas mentioned above (i.e. medial AIN and PIN, ICG and rostral MCN). Labeling was only slightly more prominent at the ipsilateral (=right) side but, in case of the GC injections, the rostral and medial parts of the MCN were more densely packed with labeled cells at the contralateral side. In addition, a few scattered cells were noted bilaterally in the dorsolateral hump (DLH), which lies interspersed between the interposed and lateral cerebellar nucleus (LCN). In the last investigated phase of infection (phase 3), the LVN, most of the MCN (its dorsolateral protuberance usually showed the lowest density of infected neurons) and the medial AIN and PIN (including the ICG) were heavily labeled at both sides of the brain. AIN involvement was more extensive ipsilaterally. In addition the DLH at both sides as well as isolated spots of labeling in the lateral cerebellar nucleus (LCN) became visible. Hence, in phase 3 aspects of all main cerebellar nuclear divisions (i.e. MCN, PIN, AIN and LCN) contained labeled neurons. Note that, apart for the preponderance of labeling in the contralateral MCN at phase 2 in the GC case, consistent differences in rate of infection or in distribution of labeled neurons between GC and TA cases could not be determined. Three cases (TA-case 1020 and GC-cases 1016 and 1017) were considered to be intermittent between phase 1 and 2, and phases 2 and 3, respectively, as based on the number and position of zones of labeled PCs (see below and Table 1).

The CN as well as the LVN receive a collateral innervation from the IO, which also provides the climbing fibers that terminate upon the PCs. Because the organization of the olivo-nuclear and olivo-cortical connections reflects the parallel modular organization of the cerebellum (Ruigrok and Voogd, 2000; Apps and Garwicz, 2005; Pijpers et al., 2005), special interest was paid to the labeling within the IO complex. Earliest viral labeling of IO neurons was observed in animals with phase 2 infection (Table 1). Plots illustrating the distribution of labeled olivary neurons at phases 2 and 3 for both GC and TA injections are shown in Figure 4. Note that at phase 2 most infected neurons were noted within the dorsal fold of the dorsal accessory olive (dfDAO: Fig. 4A-C). This correlates well with the phase 1 labeling within the LVN, which is known to receive its collateral innervation from the dfDAO (Ruigrok and Voogd, 2000). However, although LVN labeling was noted bilaterally (with an ipsilateral preponderance), labeling in the dfDAO at phase 2 was observed at the contralateral side only. Labeled cells were not clustered but were found

intermingled between many unlabeled neurons (Fig. 4D). In addition to dfDAO labeling, some labeled neurons were found in the caudolateral-most aspect of the medial accessory olive (cMAO: Fig. 4). For GC injections, neurons were mostly labeled in the ipsilateral olive, whereas they occurred exclusively contralaterally in case of TA injections. Because the timing and location of these earliest infected olivary neurons correspond nicely to that of the beginning and location of infected PCs (see below and Table 1), these results suggest it seems likely that olivary infection indeed can be initiated by way of their collaterals to infected neurons of the LVN and CN and do not necessarily require the route through the climbing fibers that terminate on infected PCs. However, the rate of progression of infection within the IO is clearly dissimilar from that observed in CN or of PCs. This is illustrated by the phase 3 cases where the number of labeled neurons had increased somewhat, as had the bilateral nature of the labeling (Fig. 4A,B). However, no additional areas of the IO complex showed signs of labeling. This is remarkable because the distribution of infected areas within LVN and CN clearly progressed in every following phase. E.g. phase 2 shows many labeled neurons in medial AIN and PIN, areas known to receive collaterals from the ventral fold of the DAO (vfDAO) and more rostral areas of the MAO, respectively (Ruigrok and Voogd, 2000). Also, additional cases with injections of BF (case 1037) and FD (case 1036), both with phase 3 infections, showed only limited incorporation of dfDAO and cMAO (cf. Table 1). Finally, counts of infected IO and CN (and LVN) neurons and of infected anterior lobe PCs, based on plots made from a one out of four series of sections, showed a phase-related exponential increase in labeled neurons of the CN and of PCs but not so of IO neurons (Fig. 4E). Olivary collaterals are known to terminate with fine terminal arborizations on the distal dendrites of cerebellar nuclear neurons (van der Want and Voogd, 1987; Ruigrok and Voogd, 2000). This specific synaptic organization may thwart adequate uptake of the virus from infected cerebellar nuclear neurons. However, even if olivary infection could only take place via their climbing fibers contacting infected PCs, the timing, number and distribution of labeled olivary neurons does not nearly seem related to the amount and location of labeled PCs. We conclude that olivary neurons show an unexpected resilience against infection by rabies virus.

Distribution of labeled PCs within the cerebellar cortex

Labeling of rabies-infected neurons within the cerebellar cortex was only observed in PCs of cases that were classified as a phase 2 or 3 infection. Figure 2H shows a rabies-infected Purkinje cell (case 1006), with its typical round inclusions that were confined to the soma and proximal dendrites. However, note that the fine distal dendrites are also clearly labeled. PCs were usually labeled in tightly packed bands (Fig. 2I). Although the width of these bands varied (see below), PCs within a band usually all showed the same level of infection.

Strips of labeled PCs were continuous throughout several lobules forming one or several strips of labeling in transversally cut sections. Figure 5 shows microphotographs of individual cases

illustrating the progression of the location and number of strips in the anterior lobe in both GC and TA cases. Figure 5A1 and 5B1-2 depict cases with phase 2 infections; Figure 5A2 shows a phase 2/3 case, whereas Figure 5A3-4, B3-4, C and D all illustrate phase 3 infections. Case 1009 with a GC injection resulted in a strip of labeling of PCs at the lateral vermal region at the right (=ipsilateral) side of lobules III and IV (Fig. 5A1) but was also present in lobule V. In addition, a thin strip of PCs was seen in the contralateral midvermal region of the same lobules. Note that both strips are only one or two PCs wide. The TA injection of case 1020 resulted in similarly positioned strips of labeled PCs; however here both were positioned ipsilaterally (Fig. 5B1). Cases 1004, also with a TA injection, showed labeling of strips of PCs at approximately the same position but both strips were somewhat wider and were more robustly stained (Fig. 5B2). Labeling with a similar intensity was noted in GC case 1017 (Fig. 5A2). Here, 4 strips of labeling can be observed throughout lobules III to V. Note that the position of the strips is symmetrical with respect to the midline, however note that the left hand medial strip and the lateral right hand strip (double arrows) are more robustly stained compared to the other two (single arrow). These more robustly stained strips were at the same approximate position as in case 1009 shown in Figure 5A1. Apart from labeling in the anterior lobe, small bands of labeled PCs were also observed within lobule VIII (Fig. 9B).

The bilateral nature of the labeling progressed in cases with a phase 3 infection. Apart from the four strips mentioned above, additional strips became visible. E.g. in GC cases 1013 and 1011 and TA cases 1032 and 1031 labeled PCs were located both medial as well as lateral to the formerly described strips (arrows in Fig. 5A3-4 and Fig. 5B3-4, respectively). Labeling in the paravermal regions was mostly noted ipsilateral to the injected side. In contrast, hemispherical labeling was very prominent contralaterally (Fig. 5A3-4 and B3-4). The newly added strips, especially the paravermal ones, tended to be less well characterized. However, despite the additional labeling, the strip-like character of labeling is maintained in all cases, indicating that strips of unlabeled PCs remain interspersed between strips of labeled ones. In addition to labeling within the anterior lobe and lobule VIII, sparse Purkinje cell labeling was noted in other cerebellar lobules (cf. Fig. 9).

Phase 3 labeling in the anterior lobe after injection of a distal forelimb flexor (FD) is seen in Figure 5C. Note that the strips in the lateral vermis are also labeled in this animal but seem to take up a somewhat more medial position. Midvermal labeling was only very limited in this case whereas, in contrast, dense mostly ipsilateral labeling was located in the paravermal regions of lobules IV/V and simple lobule (cf. Fig. 9F). Labeling in the anterior lobe after injection of the virus in a more proximal hindlimb muscle (BF) is shown in Figure 5D. Despite the fact that the ST of this animal was 192 hours, only relatively limited labeling was observed in the cerebellar cortex. In vermal regions essentially the same strips of PCs were labeled but the midvermal region was more completely labeled compared to phase 3 labeling in GC and TA cases. The difference was

exceptionally obvious when comparing the vermal labeling with the FD case (case 1036: Fig. 5C). Labeling of the paravermal strips in the BF case, however, was very limited, whereas the hemispherical strips of labeled PCs again were rather prominent (Fig. 5D).

Case 1037 demonstrates that prolonged STs eventually can result in degeneration of labeled PCs. This can be seen in Fig. 5D where the asterisks indicate the position of the ipsilaterally placed strip in the lateral vermis, which was found labeled in all cases with cortical labeling, but was not conspicuous in case 1037. Figure 6 shows additional evidence that many PCs in this strip in fact were degenerated. Increased gliosis and disappearance of Purkinje cell somata in thionin stained sections (Fig. 6A) coincided with only occasional rabies labeling of PCs (Fig. 6B). Furthermore, treating adjacent sections with anti-calbindin, which is known to label all PCs (Wood et al., 1988), shows a conspicuous strip-like gap of labeling (Fig. 6C). Note that within this gap a number of calbindin-positive Purkinje cells were still present. Finally, staining sections for argyrophilic degeneration revealed a strip-like region of silver deposit that reflects the position of the degenerated PCs (Fig. 6D,E). In agreement with this notion is the observation of degenerating debris within the confines of the LVN (Fig. 6F). Because the earliest labeling of PCs was found after 101 hours (case 1016: Table 2), it would seem that PCs might start to degenerate after 4 days of infection. However, because in case 1037, only at day 8 neurological symptoms started to develop in this particular animal while 6 or 7 days would be normal following hindlimb injection, it seems likely that the whole infection process may have been delayed by 1 or 2 days suggesting that Purkinje cell degeneration could already begin 2 or 3 days post infection.

Identification of labeled Purkinje cell strips – correspondence with the intrinsic zebrin pattern

From the above, it was evident that the strips of labeled PCs were noted at rather fixed positions of the cerebellar cortex and are likely to be related to the areas of infection of the vestibular and CN. A fixed and independent reference frame of the cerebellar cortex is represented by the zebrin pattern of PCs. Zebrin (aldolase C) positive PCs are located in a number of parasagittally organized strip-like bands (Hawkes and Leclerc, 1987; Sugihara and Shinoda, 2004). The correspondence of these zebrin bands with the zonal organizations of olivo-cortical as well as with the cortico-nuclear projections have recently been described in detail (e.g. Sugihara and Shinoda, 2004; Voogd and Ruigrok, 2004; Pijpers et al., 2005). Therefore, analyzing the material in combination with the zebrin pattern enables the zonal identification of the rabies labeled strips in the present experiments. For this reason, selected vials were either treated with zebrin (brown reaction product) and rabies (black) antibodies or incubated for zebrin only. Figure 7 shows microphotographs of such a double labeling experiment. Microphotographs in Figure 7A-C are taken from TA case 1004 and depict labeling of both the medial and lateral strips of ipsilaterally labeled PCs (Fig. 7A). In an adjacent section, shown in Figure 7B, the rabies labeled neurons are

shown in black and brownish labeling reflects the zebrin-positive PCs, which can be identified according to their position from the midline. In this case, the two rabies-labeled PCs strips are located directly medial and somewhat lateral to the p2+ band of zebrin-positive PCs (Fig. 7C). Figure 7D,E show that the rabies-labeled strip in GC case 1010 takes up a position midway between the p2+ and p3+ zebrin bands. The position of this strip of labeled PCs relative to the zebrin bands is very similar to the position of retrograde Purkinje cell labeling after an tracer injection into the LVN and also corresponds to the location of labeled climbing fibers after injection of an anterograde tracer in the dfDAO (Voogd and Ruigrok, 2004). Therefore, this rabies-labeled zone is considered to represent part of the B-zone (Voogd and Glickstein, 1998). Likewise, labeling of the thin strip of PCs directly medial to p2+ was also noted after injection of the LVN and has been shown to receive climbing fibers from the caudolateral MAO (Sugihara and Shinoda, 2004; Voogd and Ruigrok, 2004). This zone has been referred to as lateral A1 by Voogd and Ruigrok (2004).

When comparing the relative position of the B-zone in TA case 1004 and GC case 1010 (cf. Fig. 7B and 7E) it would seem that the distance between the lateral margin of p2+ and medial margin of the rabies-labeled Purkinje cell strip is larger for the GC case. Because this might indicate that the GC is controlled by a different part of the B-zone compared to TA, we have measured the width of the rabies-labeled part of the B-zone together with its position lateral to the p2+ band in lobules I–V. For all phase 2 and phase 2/3 infections at least 5 measurements in every lobule were, after controlling for shrinkage in every specific case, averaged at various rostrocaudal levels and the results are shown in Figure 7F. Horizontal bars indicate for three TA cases and four GC cases, the average position and width of the band of rabies-labeled PCs in every lobule (Fig. 7F1 and F2, respectively). Cases are arranged from bottom to top in increasing width of the B-zone labeling. From these diagrams it can be noted that the position of the rabies labeled cells in TA and GC cases is approximately similar in lobules I to III but is diverging in lobules IV and V, where the GC injections overall result in a more lateral position of the rabies labeled strip compared to TA injection. This difference is especially clear in cases with wide B-zone labeling (cf. TA case 1004 and GC case 1017 in Fig. 7F1 and F2). The overall position of the labeled strip within the B-zone for TA and GC cases was determined by averaging data from the three relevant TA and four GC cases (Fig. 7F3). Although there was a tendency that the zone of labeled PCs in the GC cases was generally shifted laterally relative to the TA cases, it will be obvious that most PCs of the B-zone, and especially those located within lobules I-III, will become infected after injection of either the TA or GC.

The position of rabies-labeled strips of PCs relative to the zebrin pattern in both phase 2 and 3 infected cases can be further appreciated in 3D plots of the anterior lobe as shown in Figure 8. Note in Figure 8A, showing two phase 2 cases, that the position of the B-zone labeling in the GC case (1010) is slightly more lateral with respect to the p2+ and p3+ bands as compared to the B-

zone labeling in case 1004 (TA). Furthermore, in both cases, the labeling of the lateral-most part of the A1-zone seems to be identical with respect to the zebrin pattern, but is located on opposite sites of the brain (contralateral for GC, ipsilateral for TA). Two phase 3 cases are shown in Figure 8B. Here, labeled PCs were plotted in sections that were alternately labeled for rabies and zebrin. Apart from massive bilateral vermal labeling of the A1- and B-zones, additional strips of labeling now become discernable in the paravermal and hemispherical parts of the cortex. At the ipsilateral side, labeling of strips of PCs directly lateral to the B-zone and covering the lateral parts of the P2-, as well as P3+ and P3- was noted and can be considered to relate to the C1-zone. PCs within the lateral-most aspects of p3- but also extending to the medial parts of p4+ have been defined as Cx and C2, respectively. Some labeling lateral to p4+, corresponding to the C3-zone, was noted in most cases. The D1-zone, believed to match the p5+ band, was devoid of labeled cells. Prominent labeling, however, was noted within p5- corresponding to the D0-zone. In GC case 1011 infected PCs were also observed within p6+/7+ at the very lateral aspect of the cerebellar cortex. Contralaterally, strips of labeled PCs were noted to cover lateral p3- and medial p4+ (Cx/C2-zones) and, rather robustly, within p5- (D0-zone), but were not obvious within C1 or C3 territories. Note that the labeling of the vermal A1-zone includes a lateral component (also seen in Fig. 8A) as well as a medial component (arrowheads in Fig. 8B) that, in lobules IV and V, becomes interspersed between p1+ and the satellite zebrin band 'a' (Voogd et al., 2003; Voogd and Ruigrok, 2004). Finally, it was noted that in lobules IV and V a wedge-like region intercalated between p2+ and the medial border of the B-zone labeling can still be recognized contralaterally (double arrowheads) but not ipsilaterally, which suggests that the X-zone, which has been shown to fill this gap (Buisseret-Delmas et al., 1993a; Voogd and Ruigrok, 2004), is labeled ipsilaterally but not, or not fully, contralaterally.

Table 2 provides an overview of the zebrin bands in the anterior lobe; their relation to the zonation of PCs as based on corticonuclear and olivocortical projections and the presence of rabies infected PCs within these zones. Note that in cases with more advanced phases of infection a rather similar and reproducible pattern emerges with no obvious differences between GC and TA cases. From Figure 8 and Table 2 is noted that, even at more advanced phases of infection, by far most labeled PCs occupy zebrin-negative territories. The exceptions are presented by incorporation of the rather lightly positive p3+ band ipsilaterally (Pijpers and Ruigrok, 2006), the medial-most aspects of the p4+ bands (C2-zone) and some involvement of p6/7+ (D2-zone) in two TA cases (Table 2).

An overview of the position of rabies infected PCs relative to the pattern of zebrin positive and – negative bands is shown for the whole cerebellar cortex in Figure 9. The cerebellar cortex is shown as a single elongated outstretched and flattened sheet on which the position of the zebrin pattern has been indicated (for details Ruigrok, 2003; Pijpers et al., 2005). The approximate position of major labeled strips of PCs has been entered using the zebrin pattern as a frame of

reference. Both a phase 2 as well as a phase 3 infection is shown for GC (Fig. 9B, D, respectively) and TA cases (Fig. 9C, E). For comparison, the pattern of a phase 3 infection after FD injection is shown in Figure 9F. A recently published key showing the olivo-cortico-nuclear modules relative to the zebrin pattern (Pijpers et al., 2005) is shown in Figure 9A. Note that for both phase 2 cases (Fig. 9 B,C), the B-zone labeling coincides with a small strip of labeling within the medial part of p4- of lobule VIII (Voogd and Ruigrok, 2004). Similarly, labeling of the lateral part of A1 is matched by labeling of within p2- of lobule VIII, though for GC this p2- labeling, like the A1 labeling in the anterior lobe, is found at the side contralateral to the injection. These observations suggest that the zones in anterior lobe and lobule VIII are functionally related. This notion can also be recognized in the plots of the phase 3 infections of Fig. 9D and E, where the paravermal strips are found both within the anterior lobe as well as in lobule VIII. Note however, that in the FD case most paravermal labeling was found within lobules V and simple lobule and lobule VII (cf. Fig. 9D, E, F). The modular relation between parts of the anterior and posterior parts of the cerebellum are in line with earlier observations on the somatotopy of climbing fiber zones (Pardoe and Apps, 2002; Voogd et al., 2003; Apps and Garwicz, 2005; Pijpers et al., 2005).

We conclude that the patterns of labeled zones of PCs among cases show marked similarities but also differences that can be related to the muscle that served as the origin of the spreading rabies infection.

Discussion

Retrograde transneuronal infection of rabies virus from two antagonistic ankle joint muscles and a forelimb muscle was studied to identify cerebellar cortical regions that participate in the control of individual muscles. We have made three key observations: 1) injection of a single muscle results in infection-rate related labeling of strips of PCs in vermal, paravermal and hemispherical parts at both sides of the cerebellum; 2) these strips were identified as part of specific, mostly zebrin-negative, cortical zones, and 3) order, localization, and specific combination of infected strips, at least partly, are related to muscle identity.

Technical considerations

Lack of neuronal degeneration, among other properties, is considered a major improvement of rabies virus over other transneuronally transported viruses (Ugolini, 1995; Tang et al., 1999; Graf et al., 2002). However, we found evidence that motoneurons degenerate starting 78 hours after injection. Because it takes at least 48 hours for the virus to reach the motoneurons (Graf et al.,

2002), degeneration of these cells may already begin 30 hours after the virus reaches the soma. This contrasts the observation that in cell cultures motoneurons may survive infection for up to 7 days (Guigoni and Coulon, 2002), and suggests that survival may depend on environmental factors. Similarly, degeneration of PCs, which may start 2 or 3 days after they become infected, has not yet been reported. Interestingly, other calbindin-positive neurons, found in the mouse telencephalon, have been reported to possess an increased vulnerability to rabies-infection (Torres-Fernandez et al., 2005). Increased vulnerability of these neurons may reflect infection-related triggering of specific apoptotic processes or relate to enhanced susceptibility to immune responses (Jackson, 2003).

Some neuronal types seem to be characterized by successfully resisting infection. E.g. neurons of the locus coeruleus have been reported to unexpectedly remain unlabeled (Astic et al., 1993; Ugolini, 1995). Here, we have noted an unexpected and as yet unexplained resilience of inferior olivary neurons against infection. Moreover, complete failure of infection, not reported earlier, was noted for the cerebellar cortical interneurons such as basket and stellate cells. Especially basket cells, with their strong synaptic connections with soma and axon hillock of PCs (King et al., 1993), would be a likely next step following infection of PCs. However, even two or more days after appearance of the first labeled PCs, no labeled basket cells were detected in the cerebellar cortex. Likewise, granule cells failed to become labeled. Potential explanations might include a lack of the necessary receptor apparatus with which the virus needs to interact in order to gain access to the presynaptic structure (Lafon, 2005). Using a different strain of rabies virus, retrograde transneuronal infection of granule cells was reported in the primate cerebellum to occur one day after infection of PCs after virus injection into the primate motor cortex (Kelly and Strick, 2003).

We conclude that differences in susceptibility to infection and viability may exist between different neuronal types and properties may be dissimilar among various viral strains and host species and requires careful consideration.

Identification of rabies-infected Purkinje cell zones

Labeling of strips of PCs resulting from rabies injections into orbicularis oculi or oculomotor muscles has been mentioned earlier (Graf et al., 2002; Morcuende et al., 2002) and was also reported after rabies injections into the primate motor cortex (Kelly and Strick, 2003). However, using the zebrin pattern as a reference frame we have characterized these strips in considerable detail and evaluated differences and similarities of the emerging patterns resulting from injections into different muscles.

In order to understand and discuss the selective labeling of cerebellar zones, we refer to Figure 10, which depicts suggested routes along which PCs may become infected. Our results show that

labeling of strips of PCs nicely follows the progression of infection within the CN and LVN. Of these PC targets, the LVN is the only nucleus with projections to the lumbar spinal cord. Indeed, LVN, together with RN and VMRF, were the first structures to contain rabies labeled neurons. Hence, it is not surprising that the B-zone and lateral A1-zone, which both connect to LVN (Voogd and Ruigrok, 2004), were the first zones containing infected PCs. However, the initial differences in laterality of the A1-zone between TA and GC cases was unexpected and points to differences in the organization of cerebello-vestibulospinal pathways towards ankle extensor and flexor muscles.

Closely following A1- and B-zone labeling, labeling of PCs in the D0-zone was noted bilaterally. Infection of these cells should be related to the early labeling of the DLH (Pijpers et al., 2005). Although DLH neurons are known to project ipsilaterally to the lateral medullary reticular formation (Teune et al., 2000), its relation with the lumbar cord was unexpected (e.g. Jones, 1995). Phase 3 labeling was characterized by the additional appearance of multiple strips of PCs. Vermal labeling of narrow PC strips likely relates to labeling of the MCN and its connection with the vestibular nuclei and medial reticular formation (Fig. 10, e.g. Teune et al., 2000; Voogd and Ruigrok, 2004). Simultaneously, paravermal labeling of the C2- and Cx-zone, which project to the PIN and ICG, respectively (Buisseret-Delmas et al., 1993b; Voogd and Ruigrok, 2004) was recognized bilaterally, whereas labeling of PCs within C1- and C3-zones, known to be connected to the AIN, was mostly noted ipsilaterally. Infection of the RN constitutes the most likely intermediary in the route of infection to these paravermal zones (Fig. 10, for review Ruigrok, 2004). Finally, labeling of the ipsilateral D2-zone in two TA cases may relate to phase 3 infection of the dorsocaudal aspect of the LCN which projects to the ventromedial part of the medullar and pontine reticular formation (Teune et al., 2000). However, no obvious differences were noted in the distribution of infected cells within LCN between TA and GC cases.

Apart from the infection of PCs in the zebrin-positive C2 and, in some cases, D2-zones, phases 2 and 3 mostly affect zebrin-negative PCs. It was noted before that the subnuclei of the IO that supply the climbing fibers to these zebrin-negative PCs receive a somatotopically organized input from the periphery, whereas zebrin-positive PCs seem to be controlled by olivary cells that receive their connections from higher levels of the brainstem (Voogd et al., 2003). Recent evidence indicates that zebrin-positive and zebrin-negative PCs may operate differently (Wadiche and Jahr, 2005).

Functional implications

We show that rabies injection of single muscles eventually results in the labeling of specific strips of PCs located within identified cortical zones. Some strips, like that in the B-zone, cover most of their zonal extent whereas others, e.g. in C1/C3, take up more restricted zonal parts. Purkinje

cells of the B-zone inhibit the LVN, which is implicated in the control of ipsilateral antigravity muscles (Arshavsky et al., 1986). The observed overlap in coverage of the infected PC strips between antagonists such as the TA and GC suggests B-zone involvement in controlling muscle synergies. Moreover, the early robust bilateral labeling of this zone indicates it is managing muscles on both sides of the body (e.g. Matsuyama and Drew, 2000; Jankowska et al., 2005). Although the bilateral nature of hindlimb input to the B-zone via spino-olivocerebellar pathways has been well characterized (Oscarsson, 1980), its specific role (or that of the lateral A-zone) in motor control is less well established (Pompeiano et al., 1995; Jankowska et al., 2005). In this respect the initial difference between both ankle antagonists in laterality of the A1-zone, which also controls LVN or directly adjacent areas, is highly interesting and warrants further study (cf. Matsuyama and Drew, 2000; Jankowska et al., 2005).

Rather enigmatic is the specific nature of bilateral muscle control by the D0-zones. Their relevance is highlighted by robust staining of DLH, being the target of D0, reported after rabies injection of tongue, bulbospongiosus, orbicularis oculi, and oculomotor muscles (Ugolini, 1995; Tang et al., 1999; Graf et al., 2002; Morcuende et al., 2002). Behaviorally however, DLH has been specifically implicated in motor activities requiring related oral and forelimb movements only (Cicirata et al., 1992). Additional bilateral labeling of thin vermal strips of the A-zone may reflect cerebellar control over reticulospinal pathways (e.g. Matsuyama and Drew, 2000). The C1/C3-zones are implicated in controlling aspects of actual movement execution (Apps and Garwicz, 2005). Climbing fiber input to these zones is characterized by an ipsilateral origin (Oscarsson, 1980), which ties in with the observation that ipsilateral AIN contained the highest concentration of rabies-infected cells and ipsilateral C1/C3-zone labeling of PCs predominated. Contrasting labeling of A1- and B-zones, the specific lobular involvement of C1/C3 infection is correlated with the general location of the injected muscles (i.e. fore- or hindlimb).

We conclude that rabies injection into limb muscles results in infection of strips of PCs that belong to specific zones located in vermal, paravermal and hemispherical parts of the cerebellum. The nature and timing of these strips to a degree depend on the identity of the injected muscle. Involvement of multiple zones is likely to reflect multiple, but as yet largely unspecified, roles for cerebellar modular control of muscles.

Acknowledgements

We thank Mrs E. Sabel-Goedknecht, Mr E. Dalm for their technical assistance. Supported by the Dutch Organization for Scientific Research (NOW-ALW: project number 810.37.005; A.P.), the Dutch Ministry of Health, Welfare, and Sports (T.R.) and by CNRS through FRE 2722 (P.C.).

References

- Apps R, Garwicz M (2005) Anatomical and physiological foundations of cerebellar information processing. *Nat Rev Neurosci* 6:297-311.
- Arshavsky YI, Gelfand IM, Orlovsky GN (1986) *Cerebellum and rhythmical movements*. Berlin Heidelberg: Springer-Verlag.
- Astic L, Saucier D, Coulon P, Lafay F, Flamand A (1993) The CVS strain of rabies virus as transneuronal tracer in the olfactory system of mice. *Brain Res* 619:146-156.
- Babinski J (1899) De l'asynergie cerebelleuse. *Rev Neurol (Paris)* 7:806-816.
- Brochu G, Maler L, Hawkes R (1990) Zebrin II: a polypeptide antigen expressed selectively by Purkinje cells reveals compartments in rat and fish cerebellum. *J Comp Neurol* 291:538-552.
- Buisseret-Delmas C, Yatim N, Buisseret P, Angaut P (1993a) The X zone and CX subzone of the cerebellum in the rat. *Neurosci Res* 16:195-207.
- Buisseret-Delmas C, Yatim N, Buisseret P, Angaut P (1993b) The X zone and CX subzone of the cerebellum in the rat. *Neurosci Res* 16:195-207.
- Buttner-Ennever JA, Horn AK, Graf W, Ugolini G (2002) Modern concepts of brainstem anatomy: from extraocular motoneurons to proprioceptive pathways. *Ann N Y Acad Sci* 956:75-84.
- Cicirata F, Angaut P, Serapide MF, Panto MR, Nicotra G (1992) Multiple representation in the nucleus lateralis of the cerebellum: an electrophysiologic study in the rat. *Exp Brain Res* 89:352-362.
- Curfs MH, Gribnau AA, Dederen PJ (1993) Postnatal maturation of the dendritic fields of motoneuron pools supplying flexor and extensor muscles of the distal forelimb in the rat. *Development* 117:535-541.
- Daniel H, Billard JM, Angaut P, Batini C (1987) The interposito-rubrospinal system. Anatomical tracing of a motor control pathway in the rat. *Neurosci Res* 5:87-112.
- Ezaki T (2000) Antigen retrieval on formaldehyde-fixed paraffin sections: its potential drawbacks and optimization for double immunostaining. *Micron* 31:639-649.
- Graf W, Gerrits N, Yatim-Dhiba N, Ugolini G (2002) Mapping the oculomotor system: the power of transneuronal labeling with rabies virus. *Eur J Neurosci* 15:1557-1562.
- Guigoni C, Coulon P (2002) Rabies virus is not cytolytic for rat spinal motoneurons in vitro. *J Neurovirol* 8:306-317.
- Haasdijk ED, Vlug A, Mulder MT, Jaarsma D (2002) Increased apolipoprotein E expression correlates with the onset of neuronal degeneration in the spinal cord of G93A-SOD1 mice. *Neurosci Lett* 335:29-33.
- Hawkes R, Leclerc N (1987) Antigenic map of the rat cerebellar cortex: the distribution of parasagittal bands as revealed by monoclonal anti-Purkinje cell antibody mabQ113. *J Comp Neurol* 256:29-41.
- Holmes G (1939) The cerebellum of man. *Brain* 62:1-30.
- Huisman AM, Kuypers HGJM, Verburgh CA (1981) Quantitative differences in collateralization of the descending spinal pathways from red nucleus and other brain stem cell groups in rat as demonstrated with the multiple fluorescent retrograde tracer technique. *Brain Res* 209:271-286.
- Jackson AC (2003) Rabies virus infection: an update. *J Neurovirol* 9:253-258.
- Jankowska E, Krutki P, Matsuyama K (2005) Relative contribution of Ia inhibitory interneurons to inhibition of feline contralateral motoneurons evoked via commissural interneurons. *J Physiol* 568:617-628.
- Jones BE (1995) Reticular formation: cytoarchitecture, transmitters, and projections. In: *The rat central nervous system*, 2 Edition (Paxinos G, ed), pp 155-171. New York: Academic Press.
- Kelly RM, Strick PL (2000) Rabies as a transneuronal tracer of circuits in the central nervous system. *J Neurosci Methods* 103:63-71.
- Kelly RM, Strick PL (2003) Cerebellar loops with motor cortex and prefrontal cortex of a nonhuman primate. *J Neurosci* 23:8432-8444.
- King JS, Chen YF, Bishop GA (1993) An analysis of HRP-filled basket cell axons in the cat's cerebellum .2. axonal distribution. *Anat Embryol* 188:299-305.
- Lafon M (2005) Rabies virus receptors. *J Neurovirol* 11:82-87.
- Matsuyama K, Drew T (2000) Vestibulospinal and reticulospinal neuronal activity during locomotion in the intact cat. I. Walking on a level surface. *J Neurophysiol* 84:2237-2256.
- Morcuende S, Delgado-Garcia JM, Ugolini G (2002) Neuronal premotor networks involved in eyelid responses: retrograde transneuronal tracing with rabies virus from the orbicularis oculi muscle in the rat. *J Neurosci* 22:8808-8818.
- Nicolopoulos-Stourmaras S, Iles JF (1983) Motor neuron columns in the lumbar spinal cord of the rat. *J Comp Neurol* 217:75-85.
- Oscarsson O (1980) Functional organization of olivary projections to the cerebellar anterior lobe. In: *The inferior olivary nucleus, anatomy and physiology* (Courville J, de Montigny C, Lamarre Y, eds), pp 279-289. New York: Raven Press.
- Pardoe J, Apps R (2002) Structure-function relations of two somatotopically corresponding regions of the rat cerebellar cortex: olivo-cortico-nuclear connections. *Cerebellum* 1:165-184.
- Pijpers A, Ruigrok TJ (2006) Organization of pontocerebellar projections to identified climbing fiber zones in the rat. *J Comp Neurol* 496:513-528.
- Pijpers A, Voogd J, Ruigrok TJ (2005) Topography of olivo-cortico-nuclear modules in the intermediate cerebellum of the rat. *J Comp Neurol* 492:193-213.
- Pompeiano O, Andre P, D'Ascanio P, Manzoni D (1995) Role of the spinocerebellum in adaptive gain control of cat's vestibulospinal reflex. *Acta Otolaryngol Suppl.* 520:82-86.
- Rathelot JA, Strick PL (2006) Muscle representation in the macaque motor cortex: an anatomical perspective. *Proc Natl Acad Sci U S A* 103:8257-8262.
- Raux H, Iseni F, Lafay F, Blondel D (1997) Mapping of monoclonal antibody epitopes of the rabies virus P protein. *J Gen Virol* 78 (Pt 1):119-124.

- Ruigrok TJ (2003) Collateralization of climbing and mossy fibers projecting to the nodulus and flocculus of the rat cerebellum. *J Comp Neurol* 466:278-298.
- Ruigrok TJ, Voogd J (1990) Cerebellar nucleo-olivary projections in the rat: an anterograde tracing study with Phaseolus vulgaris-leucoagglutinin (PHA-L). *J Comp Neurol* 298:315-333.
- Ruigrok TJ, Voogd J (2000) Organization of projections from the inferior olive to the cerebellar nuclei in the rat. *J Comp Neurol* 426:209-228.
- Ruigrok TJH (2004) Precerebellar nuclei and red nucleus. In: *The rat nervous system, third edition* (Paxinos G, ed), pp 167-204. San Diego: Elsevier Academic Press.
- Strick PL (1983) The influence of motor preparation on the response of cerebellar neurons to limb displacements. *J Neurosci* 3:2007-2020.
- Sugihara I, Shinoda Y (2004) Molecular, topographic, and functional organization of the cerebellar cortex: a study with combined aldolase C and olivocerebellar labeling. *J Neurosci* 24:8771-8785.
- Tang Y, Rampin O, Giuliano F, Ugolini G (1999) Spinal and brain circuits to motoneurons of the bulbospongiosus muscle: retrograde transneuronal tracing with rabies virus. *J Comp Neurol* 414:167-192.
- Teune TM, van der Burg J, van der Moer J, Voogd J, Ruigrok TJH (2000) Topography of cerebellar nuclear projections to the brain stem in the rat. In: *Cerebellar modules: molecules, morphology and function* (Gerrits NM, Ruigrok TJH, De Zeeuw CI, eds), pp 141-172. Amsterdam: Elsevier Science B.V.
- Thach WT (1970) Discharge of cerebellar neurons related to two maintained postures and two prompt movements. I. Nuclear cell output. *J Neurophysiol* 33:527-536.
- Torres-Fernandez O, Yepes GE, Gomez JE, Pimienta HJ (2005) Calbindin distribution in cortical and subcortical brain structures of normal and rabies-infected mice. *Int J Neurosci* 115:1375-1382.
- Tracey DJ (2004) Ascending and descending pathways in the spinal cord. In: *The rat nervous system, 3 Edition* (Paxinos G, ed), pp 149-164. San Diego: Elsevier Academic Press.
- Ugolini G (1995) Specificity of rabies virus as a transneuronal tracer of motor networks: transfer from hypoglossal motoneurons to connected second-order and higher order central nervous system cell groups. *J Comp Neurol* 356:457-480.
- Ugolini G, Klam F, Doldan Dans M, Dubayle D, Brandi AM, Buttner-Ennever J, Graf W (2006) Horizontal eye movement networks in primates as revealed by retrograde transneuronal transfer of rabies virus: differences in monosynaptic input to "slow" and "fast" abducens motoneurons. *J Comp Neurol* 498:762-785.
- van der Want JJL, Voogd J (1987) Ultrastructural identification and localization of climbing fiber terminals in the fastigial nucleus of the cat. *J Comp Neurol* 258:81-90.
- Voogd J, Glickstein M (1998) The anatomy of the cerebellum. *Trends Neurosci* 21:370-375.
- Voogd J, Ruigrok TJ (2004) The organization of the corticonuclear and olivocerebellar climbing fiber projections to the rat cerebellar vermis: The congruence of projection zones and the zebrin pattern. *J Neurocytol* 33:5-21.
- Voogd J, Pardoe J, Ruigrok TJ, Apps R (2003) The distribution of climbing and mossy fiber collateral branches from the copula pyramidis and the paramedian lobule: congruence of climbing fiber cortical zones and the pattern of zebrin banding within the rat cerebellum. *J Neurosci* 23:4645-4656.
- Wadiche JI, Jahr CE (2005) Patterned expression of Purkinje cell glutamate transporters controls synaptic plasticity. *Nat Neurosci* 8:1329-1334.
- Wood TL, Kobayashi Y, Frantz G, Varghese S, Christakos S, Tobin AJ (1988) Molecular cloning of mammalian 28,000 Mr vitamin D-dependent calcium binding protein (calbindin-D28K): expression of calbindin-D28K RNAs in rodent brain and kidney. *DNA* 7:585-593.

Tables

Table 1. Summary of the results of studied cases with rabies injection into limb muscles

Case	Muscle	Injection * dilution 1/3	PFU / animal (x 10 ⁷)	ST (hrs)	Spinal cord labeling	Med Ret. form	Motor cortex	RN	LVN	Cbl. nuclei	Inferior olive	PC's	Zones	Infection phase
1019	TA	2 x 5 µl	2	120	-	-	-	-	-	-	-	-	-	-
1012	TA	10 x 1 µl	2	144	-	-	-	-	-	-	-	-	-	-
1006	TA	5 x 1 µl	1	100	++	+	+	+	+	-	-	-	-	1
1008	TA	5 x 1 µl	1	120	++	++	+	+	+	-	-	-	-	1
1021	TA	2 x 5 µl	2	144	++	++	++	+	++	++	+	+	A1/B	2
1004	TA	5 x 1 µl	1	120	+++	++	++	++	++	+	+	+	A1/B	2
1020	TA	2 x 5 µl	2	144	++	++	++	++	+	++	+	+	A1/B/D0	2/3
1031	TA	2 x 5 µl	2	144	+++	+++	+++	++	+++	+++	+	+++	multiple	3
1032	TA	2 x 5 µl	2	171	+++	++	++	++	++	++	+	+++	multiple	3
1007	GC	5 x 1 µl	1	100	-	-	-	-	-	-	-	-	-	-
1003	GC	5 x 1 µl	1	120	-	-	-	-	-	-	-	-	-	-
1005	GC	5 x 1 µl	1	120	-	-	-	-	-	-	-	-	-	-
1014	GC	6 x 5 µl *	2	96	+	-	-	-	-	-	-	-	-	0
1015	GC	6 x 5 µl *	2	96	+	+	-	-	-	-	-	-	-	1
1016	GC	6 x 5 µl *	2	101	++	++	+	++	+	+	-	+	B	1/2
1009	GC	5 x 2 µl	2	120	++	++	++	++	++	++	+	+	A1/B	2
1010	GC	30 x 1 µl *	2	120	++	++	++	++	++	++	+	++	A1/B	2
1017	GC	6 x 5 µl *	2	120	+++	+++	++	++	++	++	+	++	A1/B/D0	2/3
1013	GC	6 x 5 µl *	2	144	+++	+++	++	++	+++	+++	+	+++	multiple	3
1011	GC	30 x 1 µl *	2	144	+++	+++	+++	+++	+++	+++	+	+++	multiple	3
1055	FD	2 x 5 µl	2	76	+	+	-	-	-	-	-	-	-	1
1056	FD	2 x 5 µl	2	96	+++	++	++	++	++	+	-	-	-	1
1057	FD	2 x 5 µ	2	104	+++	+++	++	++	++	++	+	+	B	2
1036	FD	2 x 5 µl	2	120	++	+++	+++	+++	+++	+++	+	+++	multiple	3
1037	BF	6 x 5 µl *	2	192	++	++	+++	+	++	+++	+	+++	multiple	3

Density of infected neurons in the listed areas was subjectively judged to be sparse (+), fair (++) are abundant (+++).

Table 2. Overview of labeled strips of PCs within the pattern of zebrin bands and its relation to zones of the anterior cerebellum

Zebrin band	contralateral												midline				ipsilateral										
	p6+	p5-	p5+	p4-	p4+	p3-	p3-	p3+	p2-	p2-	p2-	p2+	p1-	p1+	p1-	p2+	p2-	p2-	p2-	p3+	p3-	p3-	p4+	p4-	p5+	p5-	p6+
Cortical zone	D2	D0	D1	C3	C2	Cx	C1	C1	C1	B	X	Ax	A1	A1	A1	Ax	X	B	C1	C1	C1	Cx	C2	C3	D1	D0	D2
TA cases																											
1021-phase 2															+				++								
1004-phase 2															++				+++								
1020-phase2/3		+													++				+++								+
1031-phase 3		++			+	+				++			+		++		+	+++	++	++	++	+	+	+	+		+
1032-phase 3		++			+	+				++	+		++		++		+	+++	++	++	++	+	+	+		++	+
GC cases																											
1016-phase1/2																			+								
1009-phase 2													+						++								
1010-phase 2													+						++								
1017-phase2/3		+								++			++		+				+++								
1013-phase 3		+++								+++			++		++				+++	++	+	+	+				+
1011-phase 3		++			+	+				+++	+		+++		+++		+	+++	++	++	+	+	+	+	+		+

Relation of zebrin bands and PC zones is based on earlier reports (Sugihara and Shinoda, 2004; Voogd and Ruigrok, 2004; Pijpers et al., 2005). Coverage of infected PCs within the listed zones was subjectively judged to be sparse (+), intermediate (++), or over nearly the full width of the zone (+++).

Figures

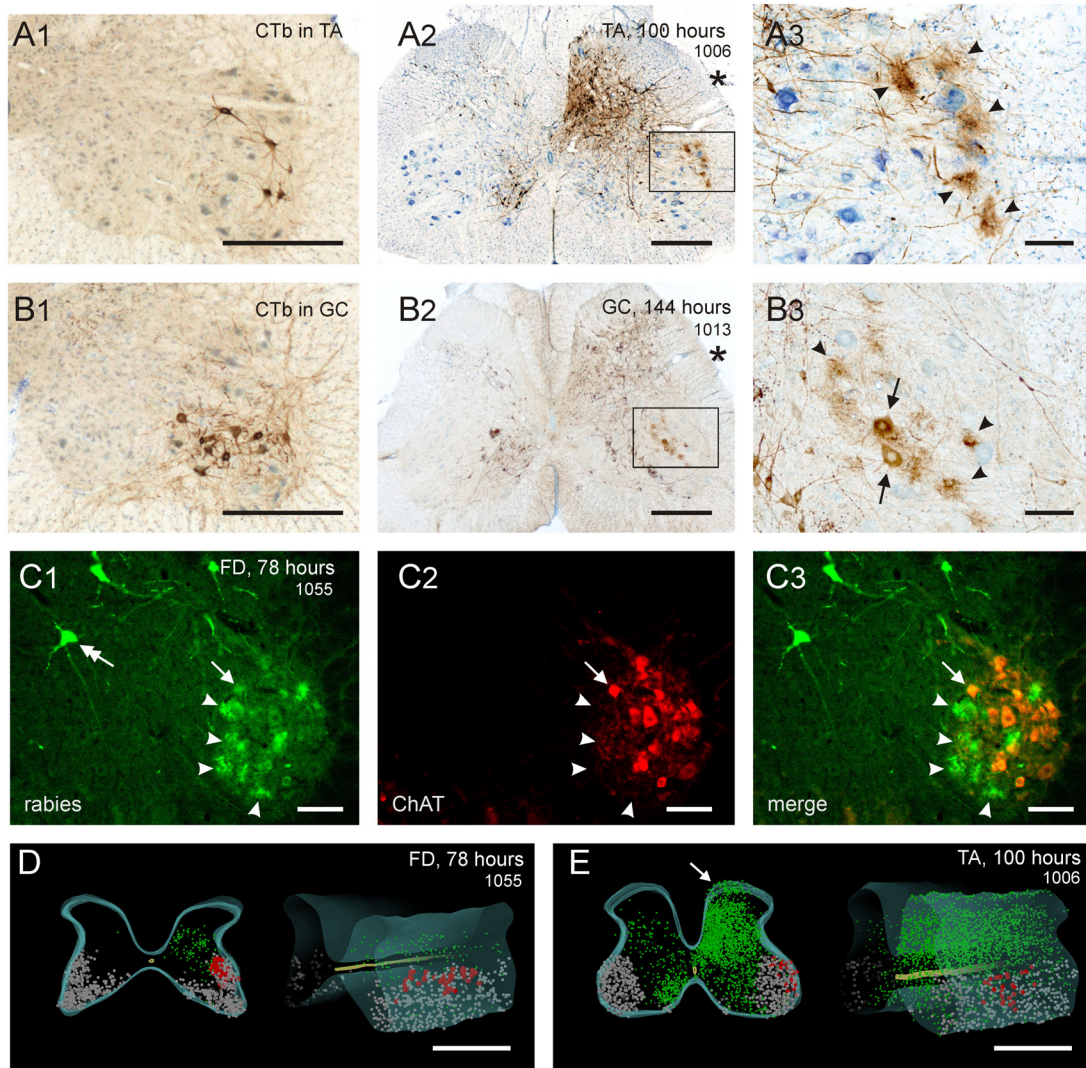


Fig. 1. Spinal labeling after rabies injection into limb muscles. **A1**, Localization of labeled motoneurons within the L5 segment after injection of CTb into the TA. Note that TA motoneurons are positioned dorsolaterally within lamina IX. **A2-3**, Overview and detail of the L5 spinal segment of case 1006 with a rabies injection of right TA and a ST of 96 hours. Note the profuse labeling of interneurons in the ipsilateral dorsal horn (laminae III-V) and contralateral ventromedial ventral horn (lamina VIII). The boxed area is shown enlarged in **A3**. Note that the labeled brown spots (arrowheads) resemble motoneurons but have 'fuzzy' boundaries, and are in approximately the same position as shown in **A1**. **B1**, Similar to **A1** but after a CTb injection into GC. Labeled motoneurons take up a central position within lamina IX. **B2-3**, Similar to **A2-3** but with a rabies injection into GC (case 1013, ST 144 hours). Note that rabies labeling of motoneuronal structures is found at approximately similar positions as shown for GC in **B1**. Apart from two clear motoneuronal contours in which nuclei can be recognized (arrows), several 'fuzzy' brown structures (arrowheads) interpreted as degenerating motoneurons can be recognized. Also note that most motoneuronal structures are not labeled with the rabies antibody, even after the prolonged ST. **C1-3**, Fluorescent microphotographs showing rabies (**C1**) and ChAT (**C2**) labeling of part of the ventral horn in a section from segment C8 after injection of rabies into FD (case 1055, ST 78 hours). **C3** shows a merged image of **C1** and **C2**. Note that the rabies-positive 'fuzzy' contours (arrowheads) are ChAT-negative, but fit well

within the motoneuronal column. The arrow points to a rabies-positive and ChAT-positive neuronal contour, which may reflect a small motoneuron. The double arrow in **C1** points to a rabies-labeled interneuron exhibiting sharp contours. **D**, 3D reconstruction of part of the caudal cervical cord of case 1055 (FD injection, ST 78 hours), as based on a one out of four series of plots showing large lamina IX neurons as gray dots, rabies-infected neurons with 'fuzzy' boundaries as red dots, whereas green dots reflect rabies-labeled neurons at other locations. Both a caudal as well as a caudolateral view is shown. Note the consistent position of the red dots within the dorsolateral part of the spinal cord. Virtually no rabies labeling was present at the side contralateral to the injection. **E**, Similar 3D reconstructions of lumbar segment L5 of case 1006 (TA injection, ST 100 hours). Note enormous increase in labeling of interneurons, which now includes labeling within lamina I (arrow) and contralaterally of lamina VIII. Sections shown in **A** and **B** are counterstained with thionin. Scale bars: **A1-2, B1-2, D, E**, 500 μm ; **A3, B3, C1-3**, 100 μm .

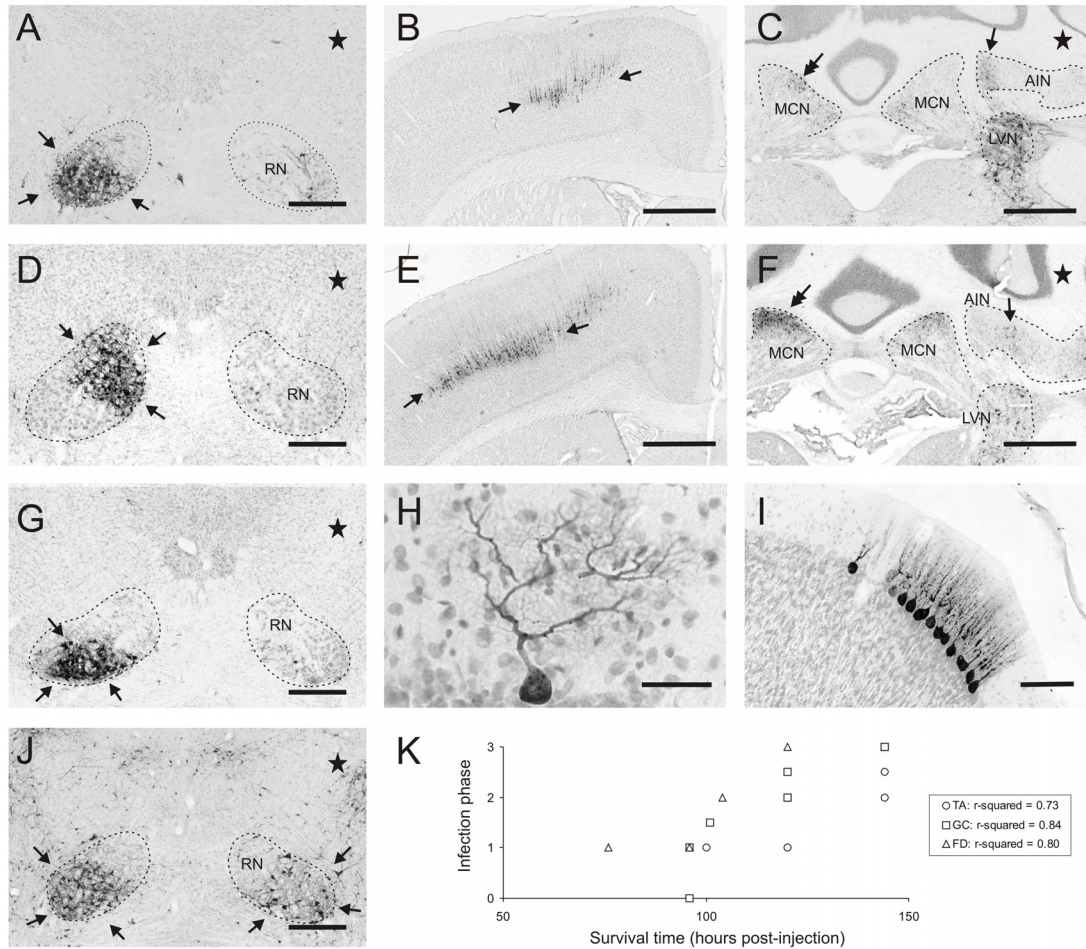


Fig. 2. Progression of supraspinal labeling of neuronal structures after injection of rabies virus into various limb muscles. **A, B, C,** Microphotographs showing labeling (arrows) of the RN (**A**), layer V pyramidal cells of the sensorimotor cortex (**B**) and LVN and CN (**C**) in case 1004 (TA injection, ST 120 hours). **D, E, F,** Microphotographs of similar levels in case 1057 (FD injection, ST 104 hours). Note the differences in distribution of labeled neurons (arrows) as compared to TA injection. See Results section Validation of the selectivity of transneuronal transport for further information. **G,** Distribution of labeled neurons within the RN in case 1010 (GC injection, ST 120 hours). Distribution of labeling is rather similar to that shown in **A**. **H,** Labeling of an isolated rabies-infected Purkinje cell in the ventral paraflocculus of case 1004. Note the labeling of fine dendritic arborizations. **I,** Labeling of a cluster of Purkinje cells in the lateral vermis. Note that all PCs within the cluster display a uniform level of infection. **J,** Distribution of labeled neurons at the level of the magnocellular RN in case 1031 (TA injection, ST 144 hours). Note the increase in number of labeled neurons surrounding the RN and within the ipsilateral RN. However, the general distribution of labeled neurons within the RN is similar to that shown in **A**. **K,** Relation between ST and infection phase. Although increased STs generally result in more advanced progression of infection, the relation is not absolute. Hatched lines in **A, B, C, G,** indicate nuclear contours. Star: injection side. Scale bars: **A-G, J,** 500 μ m; **H,** 50 μ m; **I,** 100 μ m.

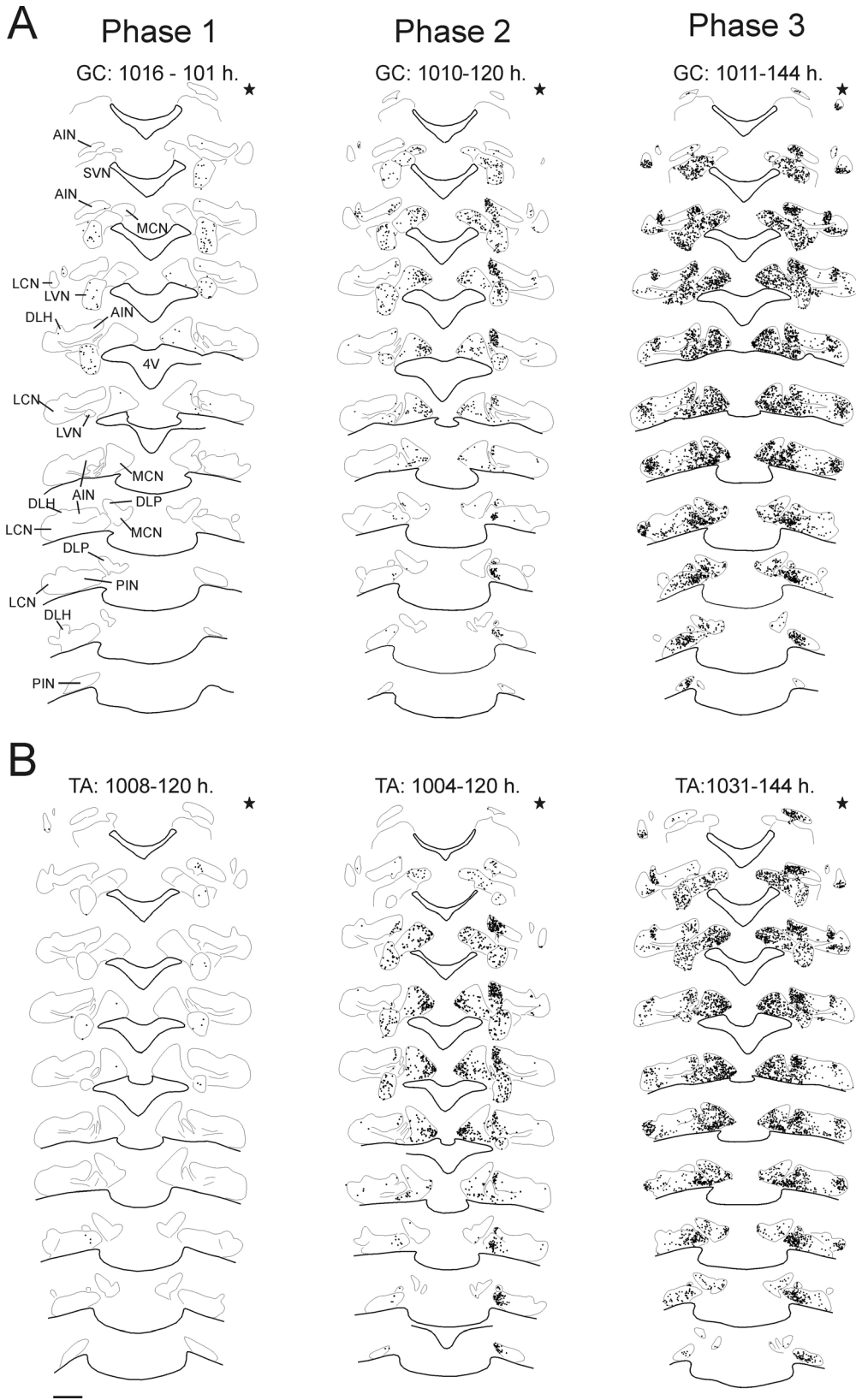


Fig. 3. Plots of equidistant sections (1 out of 4) depicting progression of rabies infection in the CN and LVN. *A*, Left hand, middle and right hand panels, respectively, show phase 1/2 (case 1016), phase 2 (case 1010) and phase 3 (case 1011) labeling after injection of GC. Note that phase 2 labeling is most prominent within the medial AIN and PIN ipsilaterally, but in medial MCN contralaterally. Also note that even in phase 3 the labeling remains restricted to rather circumscribed areas of the nuclei. ***B*,** Left hand, middle and right hand panels, respectively show phase 1 (case 1008), phase 2 (case 1004) and phase 3 infections (case 1031) after injection of TA. In contrast to the GC injection phase 2 infection for TA cases result in more prominent labeling of MCN ipsilaterally. Every dot represents a single labeled neuron. Star: injected side. Scale bar: 1mm. 4V, 4th ventricle; DLP, dorsolateral protuberance; SV, superior vestibular nucleus.

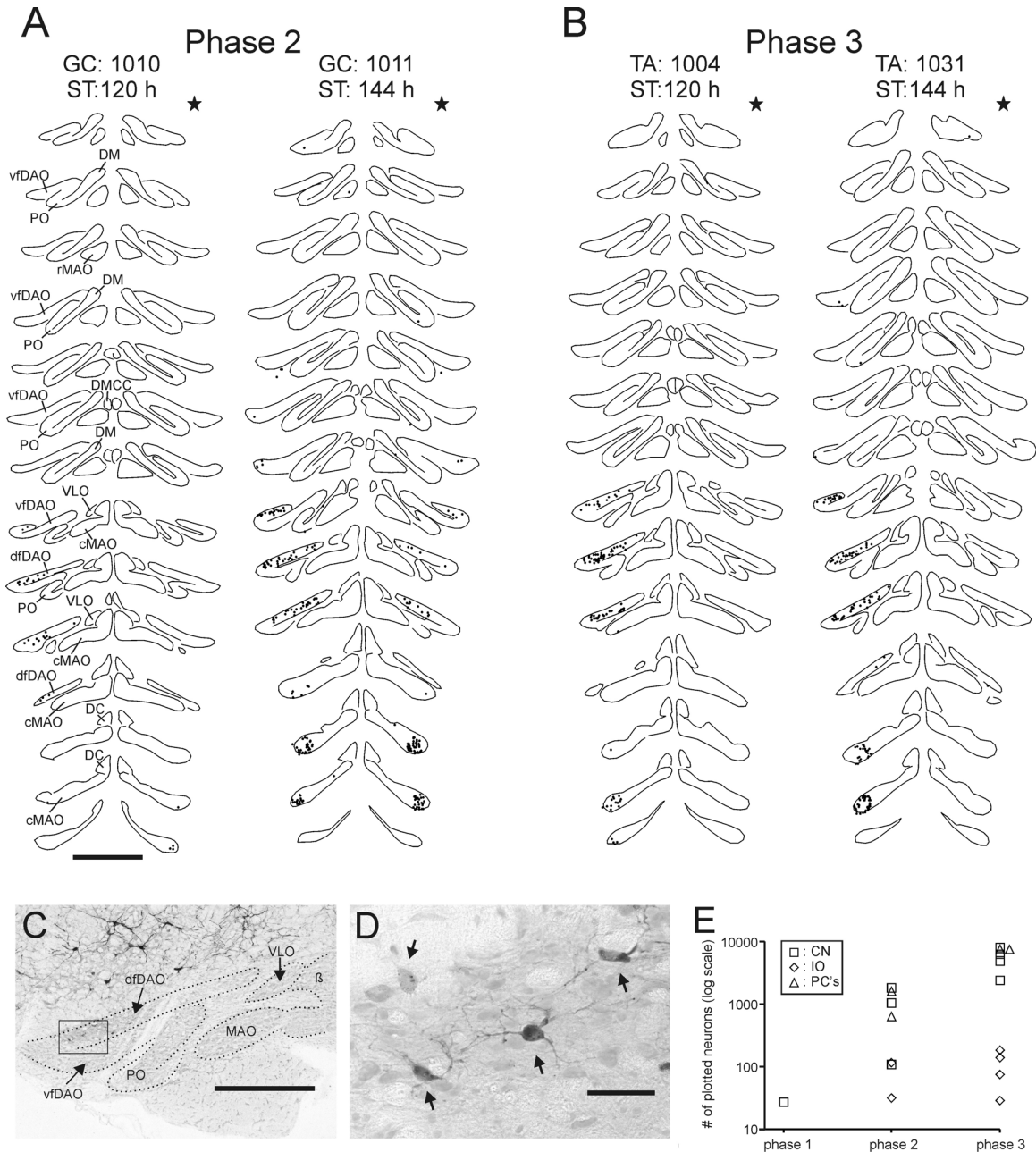


Fig. 4. Plots of equidistant sections (1 out of 4) depicting rabies labeling in the inferior olivary complex of phase 2 and phase 3 infected rats. A, Left and right hand panels show phase 2 and phase 3 labeling after injection of GC, respectively. **B,** Left and right hand panels show phase 2 and phase 3 labeling after injection of TA, respectively. In both GC and TA cases and for both phases most labeled cells are found in the dfDAO and lateral part of cMAO but labeling within the ipsilateral cMAO is absent in TA cases. Note that the progression of infection is dissimilar to that shown for the CN (cf. Fig. 3). Every dot represents a single labeled neuron. **C, D,** Microphotographs showing an overview and detail of labeling in the IO contralateral to the injected side in case 1004 (TA injection, ST 120 hours). Note that labeling of olivary neurons is rather sparse. **E,** Counts of labeled neurons in IO, CN (including LVN) and of infected PC cells in the anterior lobe in cases with different phases of infection. Note that a phase-related exponential increase in number of infected neurons as seen for CN and PC's is not obvious for IO neurons. Hatched lines: nuclear contours. Star: injected side.

Scale bars: **A, B**, 1mm; **C**, 500 μm , **D**, 50 μm . DC, dorsal cap; DM, dorsomedial group; DMCC, dorsomedial cell column; PO, principal olive; rMAO, rostral part of medial accessory olive; VLO, ventrolateral outgrowth.

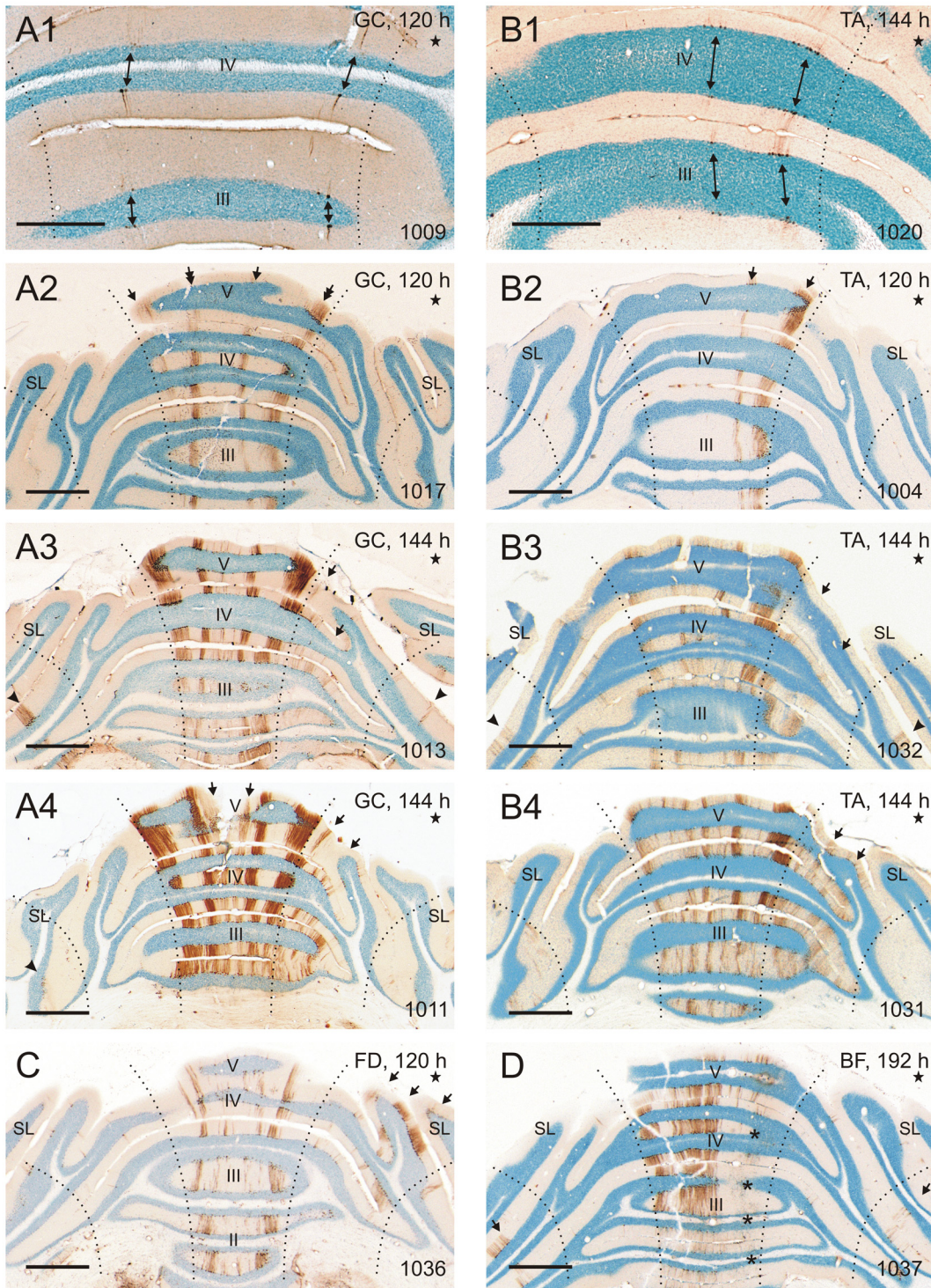


Fig. 5. Microphotographs showing localization and progression of Purkinje cell labeling resulting from muscle injections with rabies virus. A1-4, Progression of infection after GC injection in case 1009 (ST: 120 hours), case 1017 (ST: 120 hours), case 1013 (ST: 144 hours) and case 1011 (ST: 144 hours), respectively. Note that in **A1** labeling starts in the lateral vermis ipsilaterally and intermediate vermis contralaterally (arrows). These bands are more pronounced in **A2** (double arrows), but two additional and apparently 'mirror' strips appear as well (single arrows). In **A3** and **A4** the bilateral nature of the vermal nature becomes more obvious, but labeling in the paravermal region is mostly ipsilateral (arrows). In addition, bilateral labeling is noted in hemispherical regions (arrowheads). In **A4** two additional strips on either side of the midline can be recognized (vermal arrows). **B1-4**, show progression of infection after TA injection in case 1020 (ST: 144 hours), case 1004 (ST: 120 hours), 1032 (ST: 171 hours) and 1031 (ST: 144 hours), respectively. Note that in **B1** labeling starts in the intermediate and lateral vermis (arrows) of the ipsilateral cerebellar cortex only. Both zones are more pronounced and can be recognized throughout the entire anterior lobe in **B2** (arrows). In **B3**, these zones are also labeled but in addition comprise 'mirror' images contralaterally. Also note labeling in ipsilateral paravermal regions (arrows) and hemispherical regions bilaterally (arrowheads). In **B4**, several additional vermal strips may be recognized, and the paravermal labeling has considerably advanced. Note that the level of infection is not directly related to the ST (cf. B1 and B4, both with a ST of 144 hours). **C**, Phase 3 labeling after injection of FD (case 1036, ST: 120 hours). Note that a lateral vermal strip is present bilaterally. Paravermal labeling is conspicuous in lobules IV, V and SL (arrows). **D**, Phase 3 labeling after injection of BF (case 1037, ST: 192 hours). Note the very prominent labeling of the vermal regions while the paravermal region is almost devoid of labeling. Bilateral labeling of the hemispheres is clearly present (arrows). Asterisks denote regions with degenerated PCs (cf. Fig. 6). Star: injected side. Stippled lines: approximate borders of vermal, paravermal and hemispherical parts of the rat cerebellum. Scale bars: **A1, B1**, 500 μ m; all other, 1 mm. II, III, IV, V: cerebellar lobules II, III, IV and V; SL, simple lobule.

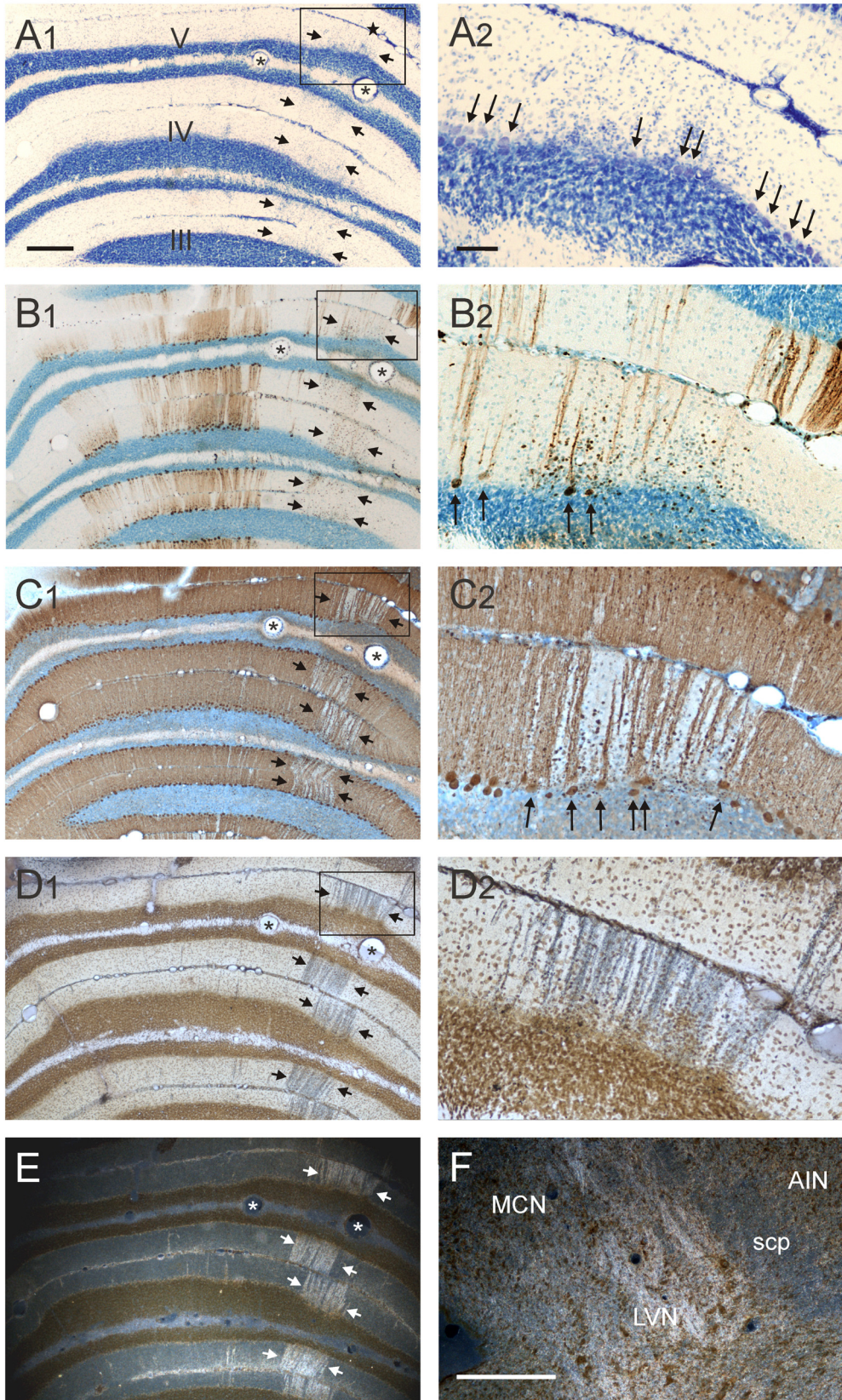


Fig. 6. Microphotographs showing zonal degeneration of infected PCs in case 1037 (BF injection, ST 192 hours). **A1, A2**, Overview and detail of boxed area showing degeneration and gliosis in thionin stained sections. Arrows in **A1** denote strip with degeneration. Arrows in **A2** indicate Purkinje somata. **B1, B2**, Overview and detail of rabies labeling in an adjacent section. Note increased glial activity depicted by non-specific DAB staining. Arrows in **B2** point to rabies infected surviving PCs. **C1, C2**, Overview and detail of calbindin labeling. Note the gap indicated by arrows in **C1** in the otherwise evenly distributed labeling of PCs. In line with **A2** and **B2**, several PCs within this strip remain labeled (arrows in **C2**). Also note non-specific glial labeling (cf. **B2**). **D1, D2**, Overview and detail of an adjacent section depicting neuronal degeneration as shown by silver impregnation. **E**, Darkfield exposure of the section shown in **D1**. **F**, Darkfield exposure of degenerating fibers within the LVN, indicating that the degenerating strip of PCs is part of the B-zone. Asterisks: capillaries. Star in **A1**: injected side. Scale bars: **A1, F**, 500 μm ; **A2**, 100 μm . Scp, superior cerebellar peduncle.

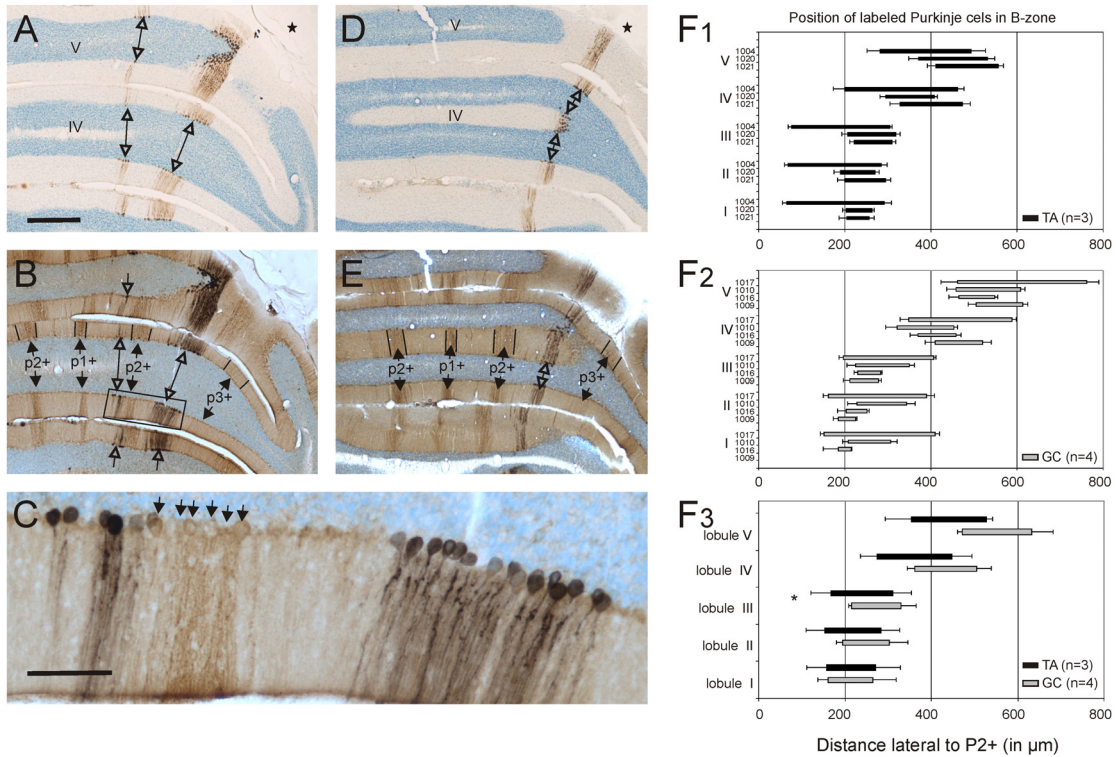


Fig. 7. Relation between strips of rabies-infected PCs and the intrinsic pattern of zebrin II immunohistochemistry. **A**, Microphotograph of two vermal strips (open arrows) of rabies labeling in case 1004 (TA injection: ST 120 hours). **B**, Adjacent section processed for rabies immunohistochemistry (black reactionproduct and indicated by open arrows) and zebrin II immunohistochemistry (brown reactionproduct). The individual zebrin-positive bands are indicated by p1+, p2+ and p3+ (solid arrows). Note that the rabies labeling is found just medial to p2+ and midway between p2+ and p3+. **C**, Enlargement of the boxed area shown in **B**. Zebrin-positive PCs of the p2+ band are indicated by arrows. **D**, **E**, Similar to **A** and **B** for case 1010 with an injection of GC. Note that the overall position of the rabies-labeled PC strip seems to be somewhat more lateral compared to case 1004. **F1-3**, Position of rabies-infected PCs relative to p2+ zebrin band after TA and GC injections. **F1**, Average position of labeled neurons in cerebellar lobules I to V in three phase 2 (including one phase 2/3) cases with injection of TA. Note that wider strips tend to be closer to p2+. Position (with standard error bars) with respect to the p2+ zebrin band and width of rabies-infected strip of PCs is indicated by the left hand and right hand margins of bars, based on at least 5 and up to 24 individual measurements in each lobule. **F2**, Similar plot of the average position and width of labeled neurons in cerebellar lobules I to V in four phase 2 (including one phase 2/3) cases with injection of GC. Note that wider strips tend to end farther from p2+. **F3**, Average of lobular position of labeled PCs relative to p2+ in TA and GC cases. Note that GC injections result in a somewhat more lateral position of labeled Purkinje cell in lobules IV and V, but are largely overlapping in lobules I to III. Left and right hand error bars denote standard error of mean of the distance to p2+ and width of labeled strip, respectively. Only for lobule III a significant difference between TA and GC cases was established concerning lateral positioning of the labeled strip of PCs (F-test, $p < 0.05$). Star in **A** and **D**: injected side. Scale bars: **A**, **B**, **D**, **E**, 500 µm; **C**, 100 µm.

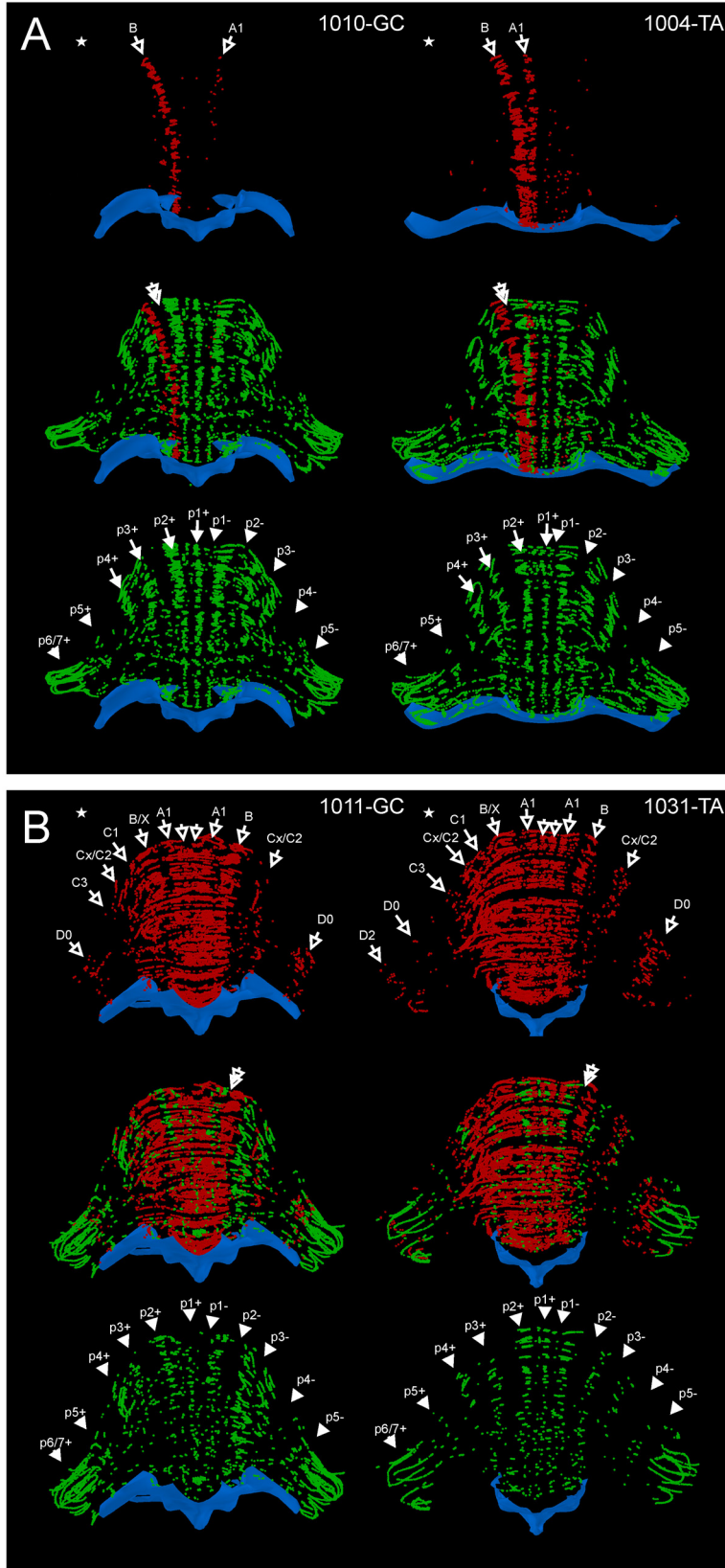


Fig. 8. Rostral views of 3D reconstructions of the anterior lobe showing positions of rabies-infected PCs relative to zebrin II bands. A, Left hand panels show a phase 2 infection resulting from a GC injection (case 1010, ST: 120 hours); right hand panels show a phase 2 infection resulting from a TA injection (case 1004; ST: 120 hours). Top figurines depict rabies-labeled PCs (red dots) only, bottom panels only show zebrin-positive PCs (green dots). In the middle figurines, both views are merged. Identification of zebrin bands is indicated in the bottom figurines. Identification of the rabies-infected zones was possible by examination of rabies-strips relative to the zebrin-bands (cf. Sugihara and Shinoda, 2004; Voogd and Ruigrok, 2004; Pijpers et al., 2005). **B,** Similar to A for two phase 3 cases: case 1011 (GC: left hand panels) and case 1031 (TA: right hand panels). Note that most rabies-infected neurons were found in zebrin-negative bands. Blue contours mark dorsal aspect of brainstem. Star: injected side. ; A1, B, C1, C2, C3, Cx, D0, D2, X, refer to olivocorticonuclear zones.

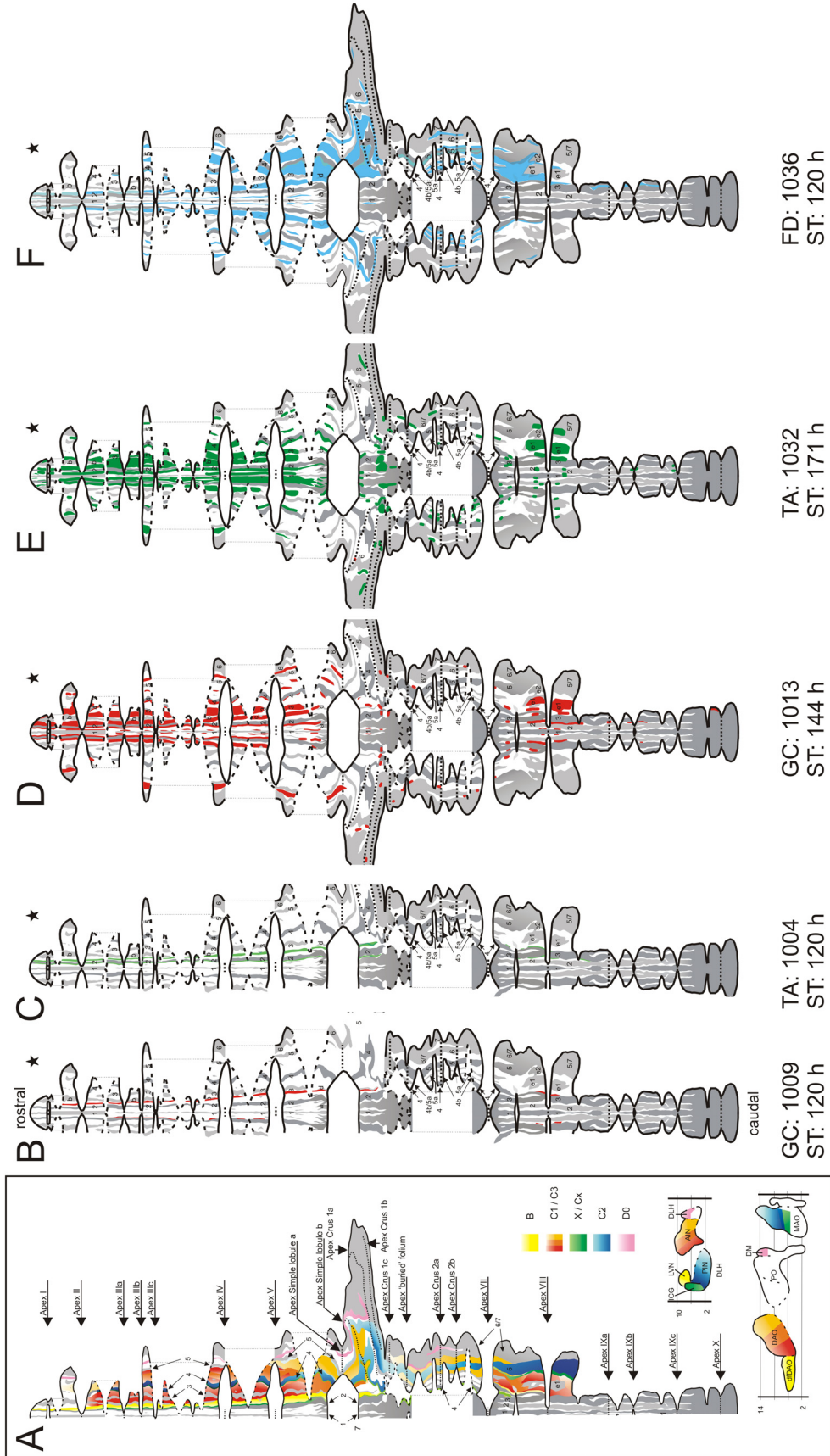


Fig. 9. Labeling of rabies-infected PCs as indicated on a standardized unfolded and flattened diagram of the rat cerebellar cortex with zebrin pattern (Pijpers et al., 2005). **A**, Relation of olivocorticonuclear projections adapted from Pijpers et al. (2005). **B**, Labeling in GC case 1009 (phase 2 infection). Note that apart from labeling shown in the anterior lobe, additional labeling was observed in the vermis of lobule VI and within lobule VIII, where it was found in p4- ipsilaterally, but in p3- contralaterally. **C**, Similar to A for TA case 1004. Here also, labeling was present in lobule VI and VIII. Note that, contrary to the GC case in **B**, p4- and p3- labeling was both found ipsilaterally. **D**, Similar to **B** for a phase 3 infection after injection of GC (case 1013). Note the abundance of bilateral labeling in vermis and hemispheres, but that paravermal labeling is mostly found ipsilaterally in the anterior lobe and lobule VIII. **E**, Phase 3 infection after injection of TA (case 1032). Note the abundant overlap of labeled areas with **D**. **F**, Case 1036 shows phase 3 labeling resulting from an injection in FD (ST: 120 hours). Here robust labeling is seen in paravermal regions (i.e. in p3- and p4-) of lobule IV, V, SL and of lobules VII and dorsal half of VIII (i.e. lateral of p4+ and medial to P5+).

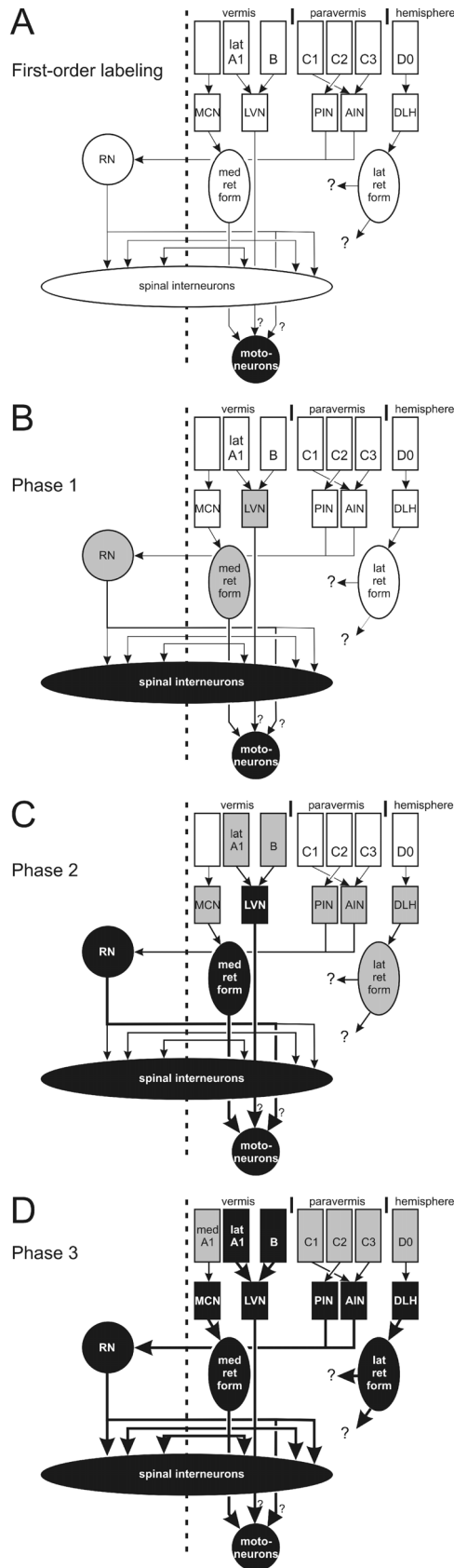


Fig. 10. Diagram illustrating suggested major routes along which progression of rabies infection may be routed from spinal motoneurons to PCs of cerebellar zones. Only the routes leading to the ipsilateral cerebellum are shown for simplicity. **A**, Basic diagram indicating anatomical relations between cerebellar zones, their target nuclei, three brainstem regions (RN, and medial and lateral divisions of the medullary reticular formation) and the spinal cord, represented as the group of motoneurons innervating a particular muscle and as spinal interneurons on both sides of the cord, are shown. In **A** only the first order motoneurons are labeled as indicated by the blackened circle. **B**, Diagram showing progression of infection to supraspinal structures that were typical for phase 1 infection. RN, LVN and VMRF contain some labeled neurons that may result from potential monosynaptic contacts to distal motoneuronal dendrites but may also originate from labeled spinal interneurons (Tang et al., 1999). The early arrival of first labeled structures is indicated by gray shading of the relevant boxes. **C**, In phase 2 labeling an additional step results in early labeling of lateral A1- and B-zones as well as labeling of MCN and interposed and DLH subdivisions of the CN (gray shaded boxes). Blackening of the formerly shaded boxes indicates progression of infection within RN, LVN and VMRF. **D**, Third recognized phase of infection resulting in further blackening of formerly gray shaded boxes and the appearance of early labeling of PCs in medial A1-, C- and D0-zones. Route via which the lateral reticular formation and DLH become labeled at early phases is not known. Hatched line: midline. ?, unknown or sparse connections.

Chapter Six

Selective Impairment Of The C1 Module Involved In Rat Hindlimb Control Has Specific Effects On Locomotion



Adapted from:

Pijpers A, Winkelman BHJ, Ruigrok TJH. *Selective impairment of the cerebellar C1 module involved in rat in hind limb control has specific effects on locomotion.* To be submitted.

Abstract

The cerebellum is divided into multiple functional modules. However, the way in which different modules participate in the various aspects of cerebellar controlled behavior remains largely unknown. Furthermore, although cerebellar control of compensatory eye movements is well established, little is known about its control of peripherally induced cutaneous reflexes during locomotion. By applying cortical injections of a retrogradely transported neurotoxin, CTb-saporin (CTb-S), this study is the first to present a method for inducing selective dysfunction of spatially separated parts of particular cerebellar modules.

Injections of CTb-S into the C1 zone of the copula pyramidis (C1-COP) or paramedian lobule resulted in degeneration of neurons within well-circumscribed regions within the contralateral inferior olive and of anterograde degeneration of the ipsilateral cerebellar nuclei. In addition retrograde degeneration of precerebellar mossy fiber systems was seen in the basal pontine nuclei. Furthermore, corresponding anterograde degeneration of mossy and climbing fiber collaterals was noted in the paravermal regions of the anterior lobe. It was concluded that the CTb-S injections had a significant effect on the integrity of a functionally related module without affecting adjacent modules.

Behavioral analysis of rats with C1-COP injection with CTb-S showed that there was no significant impact on skilled walking. However, the modulation of peripherally induced cutaneous reflexes was severely altered since the facilitation of this reflex during the swing phase of the step cycle was significantly diminished. We propose that the C1/C3 hind limb module of the cerebellum is able to adaptively control the modulation of peripheral reflexes in order to optimally meet the requirements of a changing environment.

Introduction

Within the uniform structure of the cerebellar cortex, a series of parasagittally-organized modules can be recognized due to the specific distribution of its efferent and afferent connections. These modules are comprised of longitudinally arranged strips or zones of Purkinje cells that receive their climbing fiber input from specific parts of the inferior olive and project to a specific part of the cerebellar nuclei (Voogd and Bigaré, 1980; Voogd and Glickstein, 1998; Pijpers et al., 2005). Since, in addition, the receptive fields of at least some of these modules seem to possess similar characteristics it is believed that different modules subservise different functional roles (Apps and Garwicz, 2005; Pijpers et al., 2005; Pijpers and Ruigrok, 2006). In order to allow parallel processing of information, modules are believed to be interconnected through the mossy fiber system (Armstrong et al., 1973; Ekerot and Larson, 1982; Wu et al., 1999; Brown and Bower,

2001; Apps and Garwicz, 2005). Although, cerebellar function is usually described in terms of serving motor control, coordination and motor learning (Bloedel, 1992; Bloedel and Bracha, 1995), the precise way in which different modules contribute to different aspects of such behavior is still largely unclear.

Of course, since the time of Dow and Moruzzi (1958), a multitude of cerebellar lesion studies were able to attribute different functional roles in movement control to different parts of the cerebellar cortex (e.g. see Yeo and Hardiman, 1992; Barmack et al., 2002). However, recent studies also revealed that the modular arrangement comprises multiple thin and non-continuous cortical zones that have similar afferent and efferent connections (Apps and Garwicz, 2000; Voogd et al., 2003; Apps and Garwicz, 2005). Therefore, attempts to selectively affect the functionality of specific modules by necessity need to selectively interfere with the output of the modules, i.e. the cerebellar nuclei (Welsh and Harvey, 1991; Nordholm et al., 1993; Bastian and Thach, 1995; Koekkoek et al., 2003), or by selective inactivation of parts of the inferior olive (Barmack and Simpson, 1980; Welsh and Harvey, 1998; Seoane et al., 2005). However, due to the size and location of these nuclei interference in these areas will either be subtotal or may affect surrounding regions, i.e. other functional modules. Here, we present a new method for inducing selective dysfunction of spatially separated parts of a particular cerebellar module. This method is based on the observation that the climbing fibers that reach a specific part of the module provide collaterals to the other regions of the same module (Voogd et al., 2003). Similar observations have been made for the mossy fibers that target a specific part of a module. Therefore, by injecting a retrogradely transported neurotoxin into an identified part of the modular complex, subsequent transport of the toxin towards their cells of origin followed by death of these cells and accompanied by anterograde degeneration of all their collaterals to spatially distinct, but functionally related, parts of the injected locus, a large part of a functional module will become affected.

We have evaluated this technique and its functional effects on the C1/C3 hindlimb module of the rat. A major zonal component of this module is present as the C1 zone in the copula pyramidis (COP). Related regions are found in the C1 and C3 zones of lobules II-V of the anterior lobe (Buisseret-Delmas and Angaut, 1993; Atkins and Apps, 1997; Voogd et al., 2003; Pijpers et al., 2005). C1 and C3 in these lobules mainly receive input from the ipsilateral hindlimb and projects to the medial part of the anterior interposed nucleus, which is connected to various premotor regions in brainstem and thalamus (Teune et al., 2000a; for review, see Ruigrok, 2004).

We show that a targeted injection of a conjugate of cholera toxin b subunit (CTb) and saporin (CTb-S: Llewellyn-Smith et al., 2000b) into C1 of COP results in selective degeneration of olivary neurons in the caudolateral aspect of the dorsal accessory olive. Corresponding degeneration of fibers in the anterior lobe further established the selectively expanded effect of the induced lesion. The induced lesions resulted in no or very mild effects on motor skills and biceps femoris EMG

pattern during locomotion, respectively. However, the lesions diminished the modulation of cutaneously induced reflexes during locomotion. We conclude that CTB-S is an attractive tool for studying functions of individual cerebellar modules and present evidence that the C1/C3 hindlimb module may be specifically involved in adaptive control of peripheral hindlimb reflexes.

Materials and methods

Animals and neurotoxic agent

Sixty adult, male Wistar rats (weight 200-300 g) were used in this study. All experiments were carried out in accordance with NIH guidelines for the care and use of laboratory animals and with permission from the national committee overseeing animal experiments.

As a targeted toxin Cholera Toxin subunit b conjugated to saporin (CTb-S) was used (Advanced Targeting Systems, San Diego, California, USA). The ribosome-inactivating protein, saporin (derived from seeds of the plant *Saponaria officinalis*) cannot be internalized by itself and therefore needs a targeting agent such as CTb. CTb binds to the galactosyl-N-acetylgalactosaminyl-1 receptor that is present on most neuronal types and has proven to be a reliable neuronal tracer (Luppi et al., 1995; Ruigrok et al., 1995; Voogd et al., 2003). After internalization and transport, saporin dissociates from the CTb and inactivates the ribosomes thereby eventually causing cell death. Because now the neurotoxin is not bound to a targeting agent risks of subsequent internalization by surrounding cells will be minimal. Usage and storage protocols were followed according the manufacturers details.

Experimental design

Forty animals were used to develop a reliable method to lesion selective modules and to monitor histological effects over-time (group 1). To investigate if a selected module could be targeted a small quantity (approximately 50nl) of CTb-S at full concentration was pressure injected into either the C1 zone of the copula pyramidis (COP) or into the C1 zone of the paramedian lobule (PMD) of the right cerebellar hemisphere. This should result initial labeling with CTb and subsequent cell death caused by saporin of neurons in clearly different and distinguishable regions of the contralateral inferior olivary complex and therefore indicate if the selected module was specifically targeted (Voogd et al., 2003; Pijpers et al., 2005). Injections were placed on the basis of the electrophysiological mapping of climbing fiber zones (Atkins and Apps, 1997; Pardoe and Apps, 2002; Voogd et al., 2003; Pijpers and Ruigrok, 2006). Animals were sacrificed at various time intervals after injection in order to establish a time course of the resultant CTb labeling. Neuronal degeneration was followed by a suppressed silver degeneration technique and

cell counts of the dorsal accessory olive. Within this group, two-sham operations with saline injections were performed.

The behavioral effect of CTb-S injection was assessed in 14 animals (group 2, see table 1) by evaluating their skilled walking in the ladder rung walking test as described by Metz and Wishaw (2002). A few alterations were made to their testing paradigm. Firstly, during testing trials, the animals had to cross the ladder in 10 different irregular patterns, rather than of 5. Second, a mirror was placed at an angle behind the ladder enabling videotaping both sides of the animal in one shot. After two days of training, to get acquired to walk the apparatus on regular patterns, and subsequent three days of testing the animals underwent their surgery. The following eleven days the animals were tested again under the same experimental conditions. In this group, eight animals were injected with conjugate into the C1 hind limb receiving area of the COP in the right cerebellar hemisphere. Two animals receiving C1 saline injections were used as controls. Two additional animals received an injection with saporin alone into the COP. Finally, in two cases a CTb-S injection was made into the motor cortex.

In order to evaluate the effects of a selective lesion on normal locomotion and on the modulation of peripherally induced reflexes during locomotion, a third group of six animals (group 3, see table 1) underwent daily sessions in which they learned to walk on a walking belt for at least 1 minute at constant speed (approximately 10 m/min) and in which they got used to handling. Usually, this took about two weeks after which they underwent instrumentation with EMG electrodes in the left m. biceps femoris (BF) and subcutaneously stimulation electrodes near the left lateral malleolus (for surgery details see section below).

Animals were allowed to recover for two days and were subsequently exposed to recording sessions once a day for a period of up to two weeks (Bronsing et al., 2005). Several minutes of non-stimulated (normal) walking were recorded prior to each actual test session and reflex threshold was determined in a rest situation. Subsequently, a minimum of twelve minutes of stimulated walking was recorded. Usually, this was achieved by several alternating cycles of walking and resting. Single stimuli lasted 0.1 ms and thresholds were usually found between 80 and 250 μ A and were quite constant between various days. The stimuli were generated using the stimulus sequencer of the 1401 PlusTM (Cambridge electronic design, Cambridge, UK) that triggered a PG4000 digital pulse generator and isolated stimulation unit (SIU; both Neuro Data Instruments Corp., New York, USA). These stimuli were randomly delivered with an intensity of 1.5 times threshold using two Gaussian clocks programmed to generate stimuli with an average frequency of 0.4 HZ and with a minimum inter-stimulus interval of 0.5 second. EMG signals were amplified (5000x) and band pass filtered (30 Hz-10 kHz; Axon CyberAmp 380). A humbug device (Quest Scientific, North Vancouver, British Columbia, Canada) was used to eliminate 50 Hz electrical interference. EMG signals were sampled with the 1401 PlusTM at 8.333 kHz and stored

for off-line analysis using the Spike 2™ data acquisition and analysis software (CED, Cambridge, UK).

In this group four animals were injected in the left cerebellar hemisphere with CTb-S into the C1 zone of COP and two animals received a sham lesion with 0.9% saline (see table 1)

Surgical procedures

In the first two experimental groups, animals were initially anesthetized by an intraperitoneal (i.p.) injection of 60 mg/kg pentobarbital (Nembutal, CEVA SANTE ANIMALE B.V., Maassluis, the Netherlands). In addition, supplementary doses were given i.p. in order to maintain deep levels of anesthesia. This anesthetic was chosen because it allows the extra-cellular recording of evoked climbing fiber field potentials with glass-coated tungsten microelectrodes (tip approximately 50µm; impedance, 50-140 kΩ; (Atkins and Apps, 1997)). The responses were recorded on the cerebellar surface as the result of brief (0.1 ms) electrical percutaneous stimulation of the ipsi- or contralateral forelimb or hindlimb with pairs of needle electrodes (for detailed description, see Atkins and Apps (1997)). In this way the C1 zone of the COP or PMD was identified, that responds with short latency field potentials to respectively ipsi- hindlimb and ipsi-forelimb stimulation. In the third experimental group, the animals were anesthetized with halothane (5% initial, 0.5% to 2% maintenance in 0.5 L/min oxygen and 1 L/min nitrous oxide). In all cases the depth of anesthesia was monitored by absence of the pinch withdrawal reflex and loss of muscle tone. Body temperature was maintained and regulated within physiological limits with a thermostatically controlled heated blanket ($37 \pm 1^{\circ}\text{C}$).

Animals were subsequently placed in a stereotaxic head holder and a small craniotomy exposed the posterior part of the cerebellum. The atlanto-occipital membrane and the dura were opened and the exposed cerebellar surface was kept moist by periodic flushing with sterile saline solution. Micro-injections were made in the first two groups in the electrophysiologically identified C1- zone at the site where a maximum response could be evoked. This site was situated at a rather fixed distance to the midline and therefore no electrophysiology was considered to be required in the third experimental group. All injections were placed at a depth of 200-300 µm from the cerebellar surface. In all experiments the micropipette was withdrawn and the surface was flushed with saline. Subsequently, the overlying muscle and skin layers were sutured and the animal was allowed to recover. However, in the third experimental group, the skin was not yet sutured and the animals remained under anesthesia in order to implant customized bipolar EMG electrodes, made of Teflon isolated multi-strand stainless steel wire (diameter 150 µm; exposed tip length ~1 mm; Advent Research Materials Inc., Oxford, UK). Through a small skin incision (2 cm) three of these electrodes were implanted along the posterior BF of the left hind limb just below the muscle fascia, to which they were secured by a single suture (Ethicon 6.0). In addition,

two similar stimulation electrodes were implanted on either side of the left lateral malleolus. Next, the leads were tunneled to the small incision over the BF and fixed with a single suture to the subcutaneous fascia (Ethicon 6.0). From there all leads were looped to allow sufficient slack and were tunneled subcutaneously to the incision in the neck. Here the wires were looped again and attached to a connector, which was secured in a pedestal of dental cement, which in turn was fixed to the skull with screws (Bronsing et al., 2005). The skin incisions were carefully closed with single sutures (Ethicon 6.0) and the animals were allowed to recover.

In all cases, postoperative analgesia was provided by subcutaneous administration of buprenorphine (0.05-0.1 mg/kg; Temgesic; Schering-Plough). All animals recovered uneventfully and were monitored daily for signs of stress or discomfort.

Analysis

Histology

At the end of each experiment, animals were sacrificed by means of transcardial perfusion under deep barbiturate anesthesia (240 mg/kg, i.p.; Nembutal, CEVA SANTE ANIMALE B.V., Maassluis, the Netherlands). An initial flush of 500 ml of 0.9% saline was given, followed by 1000 ml of fixative (4% paraformaldehyde, 0.1% glutaraldehyde, and 4% sucrose in 0.05M phosphate buffer, PB, pH 7.2-7.4). The brain was removed from the skull and post-fixed for 3 hours, after which it was rinsed and stored overnight in 0.05M PB containing 10% sucrose (at 4°C). The collected brain was embedded in 11% gelatin, 10% sucrose. Cerebellar- and caudal brainstem blocks were hardened in a 30% formalin, 30% sucrose solution for 3 hours and were stored overnight at 4°C in 0.05M PB containing 30% sucrose.

The tissue blocks were sectioned transversally at 40 µm on a freezing microtome and collected serially in 8 glass vials containing 0.05M PB (Ruigrok, 2003). Every other vial was processed free-floating either for CTb-histochemistry (for details, see Ruigrok et al., 1995) or for silver degeneration (see Haasdijk et al., 2002).

A Leica DMR microscope equipped with a digital camera (Leica DC-300) was used to evaluate sections and for acquiring photomicrographs. Photo panels were constructed in CorelDraw™ 11.0, after correction for brightness and contrast in Corel Photopaint™ 11.0.

A quantitative analysis of cells in the inferior olive was obtained by examining and plotting a one in four series of transverse sections (160 µm interval) using an Olympus microscope fitted with a Lucivid miniature monitor and NeuroLucida™ software (MicroBrightField, Inc., Colchester, VT). The outlines of each inferior olive were plotted with a 2.5x objective, whereas individual neurons were examined using a 20x objective and the motorized stage scan option of the plot program. With the automated cell count option, the number of olivary neurons per section (100 µm wide bins running perpendicular to the direction of the DAO) could be assessed. From these plots a

color-coded density profiles of the DAO were constructed with standard MATLAB routines (The Mathworks, Natick, MA: Pijpers and Ruigrok, 2006).

Video analysis

The skilled walking tests of group 2 rats were videotaped with a Sony Digital Handycam (DCR-PC8E) at 30 frames/s. In each case, the number of errors in foot placement accuracy was counted for both hind limbs. The video recordings were inspected at low speeds (0.2 times normal speed). The percentage of steps with foot faults, defined as a slip or a total miss was determined (also see Metz and Whishaw, 2002).

EMG preprocessing

Custom MATLAB™ (The Mathworks, Natick, MA) routines were used to import and analyze the stimulation times and EMG data. The raw EMG signal was pre-processed by masking stimulation artifacts for a period of 4 ms from the onset of stimulation followed by digital band pass-filtering (100-3000 Hz) using a 5th order Butterworth filter. The EMG amplitude was computed by root-mean-square (RMS) rectification using a 20 ms window.

Step identification

Biceps femoris EMG activity of a single step cycle was partitioned into three distinct phases: a burst of activity (BA), a silent period (SP) and a period of sustained activity (SA). The onset of BA was chosen as the start and end of a step cycle (Bronsing et al., 2005). Cursors delineating the step phases were placed on the basis of visual inspection of the EMG and EMG amplitude signals. Step cycles with a shorter duration than 0.4 s or longer than 1.4 s were discarded.

Step standardization

In order to allow averaging and comparison of EMG activity from steps with different lengths, EMG amplitude data was extracted and step duration was normalized to 100%. Accordingly, the duration of all step cycle phases was normalized to step cycle fractions. Ideally, EMG activity of all steps at a particular point (%) in the step cycle should all belong to the same step cycle phase (BA, SP or SA). Therefore, a standard step cycle was computed by averaging the step cycle fractions over all rats and all days (BA=9.83%, SP=13.08%, SA=77.09%). Subsequently, EMG amplitude data from all steps was time-rescaled so that the step cycle fractions of each step equaled the standard step. This time-rescaling was achieved by calculating the projection of the integrated step fractions of the standard step onto the integrated step fractions of each actual

step using piecewise cubic spline interpolation of 1000 linearly spaced time bins, followed by linear interpolation of the EMG amplitude data onto the 1000 time-rescaled bins. This procedure produced a gradual deformation of the time axis and on average equal time per bin.

EMG normalization

Because EMG data from different rats vary in gain and noise levels EMG amplitude data per rat for each day was normalized to the range of the average step cycle EMG, computed for each rat per day from all steps not including stimulation, and the minimum average step cycle EMG was subtracted.

Reflex comparison

The height of the normalized EMG amplitude 15 ms after a stimulus (corresponding to the RMS activity from 5-25 ms after stimulation) was used to obtain a measure of the reflex magnitude. The value of the previously computed and normalized average step cycle EMG at the same point in the step cycle was subtracted from the reflex magnitudes to obtain the net reflex magnitudes, which in turn were averaged in 5% step cycle bins for each day or in step phase bins over all days. Error bars indicate the standard error of the mean (σ_M). Between the sham and lesion group, the mean reflex response per step cycle bin was compared using a two sample Student's t-test and Bonferroni correction for multiple comparisons ($P=0.0005$ for the per day comparison, $P=0.015$ for the step cycle phase comparison).

Results

Modular effects of CTb-S injection

The group 1 experiments demonstrated that the optimal histological results were obtained by pressure injecting approximately 50 nl of the CTb-S conjugate. These injections, directed at the C1 zones of either the COP or PMD, display the selective transport and accompanying degeneration characteristics of the conjugate tracer. Twenty-four hours after injection, the injection site was clearly demarcated by CTb immunohistochemistry (Fig. 1A1,B1) and had a diameter of 300-500 micron (Ruigrok and Voogd, 2000; Pijpers et al., 2005). No degeneration of cortical structures could be observed within or around the injection site at this time with either thionin or silver degeneration staining. Evidence for uptake and transport of the conjugate, however, was clearly noted since CTb immunohistochemistry revealed many retrogradely labeled neurons at various places in the brainstem, such as the pontine nuclei, lateral reticular nucleus

and inferior olive. Since the precise locations of labeling in the inferior olive provide identification of the targeted cerebellar module (Ruigrok and Voogd, 2000; Voogd et al., 2003; Pijpers et al., 2005; Pijpers and Ruigrok, 2006), our description will focus on the source of climbing fibers. Injections of the conjugate in COP, retrogradely labeled neurons, as recognized by CTb immunohistochemistry, were confined to the caudolateral aspect of the ventral fold of the dorsal accessory olive (vfDAO: Fig. 1A). However, injecting C1 of PMD resulted in CTb-labeled neurons restricted to the medial aspect of the vfDAO (Fig. 1B). These locations are in perfect agreement with earlier data on topography of olivo-cortical connections (Atkins and Apps, 1997; Voogd et al., 2003; Sugihara and Shinoda, 2004; Pijpers et al., 2005; Pijpers and Ruigrok, 2006).

Because CTb is also transported in an anterograde direction, labeling of Purkinje cell axons from the injection site to the cerebellar nuclei was noted at the same survival time. In accordance with the notion of modular cerebellar circuitry (Pijpers et al., 2005), these terminal projections were noted in the medial-most aspect of the anterior interposed nucleus (AIN) for C1-COP injections (Fig. 1A2-3) but within more central regions of AIN after injection of the C1-PMD (Fig. 1B2-3). The medial and central AIN regions are known to receive collateral input from the caudolateral vfDAO and medial vfDAO, respectively (Ruigrok and Voogd, 2000; Pijpers et al., 2005). Finally, both types of injections also resulted in early retrograde neuronal labeling of nucleo-cortical neurons, which were mostly confined to regions also harboring anterograde terminal labeling (Fig. 1A2-3 and B2-3).

Signs of cortical degeneration were noted with survival times of two days or more (Fig. 1C1, D1). Agyrophilic degeneration was specifically prominent at survival times of at least 4 days and up to two weeks. Silver staining was most prominent over degenerating fibers as was seen in the medial and central AIN for C1-COP and C1-PMD injections respectively (Fig. 1C3 and D3). Agyrophilic degeneration was less prominently visible in the inferior olive, but higher magnifications usually revealed enhanced accumulations of silver deposits at expected regions (Fig. 1C5, D5). The intensity of labeled olivary structures as examined with CTb immunohistochemistry was somewhat diminished at 4 days survival. (cf. Fig. 1C6 and D6 with Fig. 1A5 and D5). Moreover, labeled neuronal profiles in the inferior olive were small without a clearly identifiable nuclei and showed proliferation of glial structures (Fig. 1C6, D6). CTb labeled structures were not seen within the AIN regions that contained silver degeneration (Fig. 1C2, D2). After 10 days, apart from faint labeling near the injection site, no CTb label could be recovered using immunohistochemistry.

Figure 2 provides an overview of the agyrophilic staining of degenerated structures in an animal (case R5) from experimental group 3, with a CTb-S injection that was targeted at C1-COP and having a survival time of 21 days. It shows that massive degeneration of fiber structures in the

white matter of COP, but also within the white matter of adjacent lobules such as PMD and lobule IX. Degenerated debris could be followed to the medial half of the AIN with some involvement of the interstitial cell groups (ICG), which are intercalated between the interposed nuclei and the medial cerebellar nucleus (MCN). Degeneration was noted in the contralateral vfDAO (Fig. 2C, D), but also within the ipsilateral lateral reticular nucleus (LRN: not shown). Degeneration of olivary and LRN neurons was also reflected by many degenerated fibers within the ipsilateral inferior cerebellar peduncle (icp: Fig. 2E). However, the other cerebellar peduncles also carried degenerated fibers. Degenerated precerebellar neurons in the pontine nuclei resulted in axonal degeneration of the middle cerebellar peduncle (mcp: Fig. 2F). Numerous degenerating fibers were also found in the dorsal region of the central superior cerebellar peduncle of the ipsilateral site (Fig. 2I,J). This region is known to contain the efferent fibers from the AIN (Haroian et al., 1981). Presumably, they consist of the bulbar projection fibers from AIN neurons with nucleo-cortical collaterals (McCrea et al., 1978; Tolbert et al., 1978). The degenerating fibers could be followed to a field of terminal degeneration in the ventral part of the contralateral magnocellular red nucleus (Fig. 2K,L). It is important to note that evidence that the neurons of origin of the climbing and mossy fibers to the C1-COP injection site had died, is provided by the degeneration of fibers in the paravermal white matter of lobules II-V of the anterior lobe (Fig. 2G). These fibers can only reflect the collaterals of climbing and mossy fibers that possessed terminals within the injection site (Voogd et al., 2003). In accordance with the bilateral nature of the collateralization of the mossy fiber system, some fibers were also noted at the contralateral side. Unfortunately, only relatively sparse terminal labeling was noted in the granular and molecular layer of the ipsilateral paravermis of lobules II-V (Fig. 2H), which did not justify the abundance of collateral projections of both climbing and mossy fibers from the same cortical regions and using unconjugated CTb as a tracer (Voogd et al., 2003). The difficulty of demonstrating robust terminal degeneration of climbing fibers has been noted repeatedly in the classic literature (e.g. see Desclin and Escubi, 1975). Therefore, in order to verify the modular effect of small localized lobular injections with CTb-S, it was essential to verify and chart the degeneration of olivary neurons in the appropriate places. For this reason, cell counts of both the vfDAO and dfDAO were made of the contra- and ipsilateral side of the injection in all animals of experimental group 3 (including the two sham operated animals) and of a single PMD injection (group 1, case 61). The results are presented in color-coded diagrams that reflect the density of neuronal cell bodies in flattened and unfolded plots of the ipsi- and contralateral DAO (Fig. 3). These diagrams show that CTb-S injection into C1-COP results in low densities of neurons within the caudolateral aspect of the right vfDAO. In several animals virtually no neuronal contours were noted within this region (e.g. cases R5, R6). Densities of neurons in the other regions of the DAO were similar to those seen at the side ipsilateral to the injection (left side). The average reduction of total number of neurons in the DAO was estimated at 85.8% (range: 80.1%-89.4%), which would equal an

degeneration of approximately 1650 neurons in the whole DAO. Injection into the C1-PMD zone (responsive to ipsilateral forelimb stimulation) resulted in a reduction of neuronal density that was specifically noted at the caudomedial aspect of the vfDAO (Fig. 3, case 61). Sham-operated animals (saline injections into C1-COP) evidently did not result in changes in cell densities within the DAO (Fig. 3, cases R7 and L2).

We conclude that early immunohistochemical labeling with CTb and later silver degeneration staining as well as the location of diminished cell counts within the DAO are in line with previously conducted studies establishing the modular connections of paravermal zones (Atkins and Apps, 1997; Voogd et al., 2003; Voogd and Ruigrok, 2004; Pijpers et al., 2005; Pijpers and Ruigrok, 2006). Importantly, the well-circumscribed area of cell loss within the inferior olive indicates that a single and specific cerebellar module can be targeted resulting in deafferentation of a major part of the climbing fiber input to the whole module.

Effects on skilled walking

To validate the experimental set-up for testing skilled walking of 12 animals with a CTb-S injection of C1-COP, two additional animals (L13, 14 Table 1) received a CTb-S injection into the hind limb region of the right motor cortex (asterisks; Fig. 4A). This resulted in degeneration of fibers in the corpus callosum (cc) and the capsula interna (ic; arrows Fig. 4A). In addition, degeneration was noted in the ipsilateral pontine nuclei, the pyramidal tract and the contralateral dorsal corticospinal tract (Fig. 4B,C and D, respectively) as well as in neuronal cell loss within the ventrolateral thalamus (not shown). Histology of the cerebella of the C1-COP injected animals all revealed degeneration of paravermal parts of the COP as well as signs of neuronal degeneration of olivary neurons within the caudolateral parts of the contralateral vfDAO.

Figure 5 shows the percentage of scored foot faults collected from the ladder rung walking apparatus in a series of three test days before and a series of test days after the CTb-S injection. Because there were no significant differences in the number of foot faults over consecutive days before or after lesion (except for cases L13 and 14), data before and after surgery was pooled. Injections into the right cerebellar cortex should predominantly affect the ipsilateral side whereas injections into the motor cortex are expected to predominantly affect the contralateral side. Our results show that the only significant increase in number of foot faults after an injection with CTb-S was seen in cases L13 and L14. The number of induced errors was similar to those obtained by (Metz et al., 2002) after mechanical lesions of the motor cortex or the pyramidal tracts. However, unexpectedly, CTb-S injection of C1-COP did not result in a worsening of skilled walking using this specific test.

Effects of lesions on the walking pattern and reflex modulation

In order to further study potential behavioral effects of C1-COP injections with CTb-S, 6 rats, trained to walk steadily on a walking belt at 10 m/min were chronically instrumented with EMG electrodes in the ipsilateral biceps femoris (BF) muscle as well as with subcutaneously placed stimulation electrode near the lateral malleolus of the same foot (Bronsing et al., 2005). During the surgery four rats received a CTb-S injection into C1-COP and two rats a saline injection in the same area). After a two day recovery period, performance of the animals on the walking belt was examined. Figure 6 A, B show examples of raw EMG traces of BF in sham and CTb-S injected animals. Note that the activity of the BF during a step cycle of sham-operated animals consists of a short burst of activity (BA: darkly shaded areas), followed by a relatively silent period (SP, shaded areas) and a second, sustained and less intense, period of BF activity (sustained activity: SA, light areas). The onset of the BA was taken as the beginning of the step cycle, as it reflects the onset of knee flexion at the beginning of the swing phase. SA activity is thought to be related to the extension of the hip during the stance phase (English and Weeks, 1987; Chanaud and Macpherson, 1991). In this way a single step can be divided into three phases, which are coded from dark to light gray.

Our first goal was to investigate if the CTb-S induced lesion induced differences in durations of the steps during normal walking (i.e. no cutaneous stimulation: unstimulated steps). For both the sham (Fig. 6C) and lesioned (Fig. 6D) rats the distribution of all measured step durations (in seconds) are shown for each postoperative day. Note that although the mean step durations are virtually similar (Fig. 6E, values range between 0.77 and 0.83 s), the shape of the step duration distribution is more peaked amongst the lesioned animals as compared to the controls. This 'peakedness' as measured by the sample kurtosis (Fig. 6F) is maximal at postoperative day 4 for the lesioned animals and indicates a more regular gait.

Peripheral stimulation triggered within a step produced on average a small but significant ($P < 0.05$) difference in step duration in both sham ($\Delta\mu = 23$ ms) and lesioned animals ($\Delta\mu = 25$ ms). The step following a stimulated step also did show a small but significant ($P < 0.05$) shortening of mean step duration for the sham animals only ($\Delta\mu = -18$ ms). However, the effects of stimulation on the step duration distribution were so marginal that it was concluded that stimulation itself did not disrupt normal walking behavior.

Subsequently, the size of the BF reflex response to the cutaneous stimulation was analyzed. Figure 7A shows an EMG trace of sham-operated animal R7 during walking with randomly triggered stimulations of the subcutaneously placed electrodes (stimulated walk). Again the three phases of the step cycle are coded in gray scale. In this specific trace two stimuli are present, which are indicated by the red dotted lines. The same trace is displayed in Figure 7B as a rectified signal. Within this bout of walking two stimulation pulses were triggered (red lines). The

first fell within the SA phase and hardly resulted in a visible reflex response within the BF EMG. In contrast, the second stimulation, triggered within the SP phase, produced a marked reflex response in the BF EMG (Fig. 7B,C).

Next, the steps were isolated and, after standardization (Fig. 7D) and amplitude normalization, sorted into groups of normal steps (Fig. 7E) and groups of steps that contained a stimulus (Fig. 7F). By averaging the EMG amplitude data for those without stimulation the average 'standard' step EMG was calculated (Fig. 7E, red line). Per day, the number of normal steps ranged between 722 and 1218 ($\mu=959.0$) in the sham group and between 680 and 1881 ($\mu=1115.8$) in the lesion group. The number of stimulus steps ranged between 240 and 336 ($\mu=293.2$) in the sham group and between 437 and 686 ($\mu=558.2$) in the lesion group. For figure 7E, the EMG recordings of 513 non-stimulated steps were used (shown in black traces), to produce the average BF EMG at day 4 of case R7. The standardized step of every experimental day was taken as a reference for base line EMG activity on which the reflex responses could be superimposed from the stimulated steps (Fig. 7F, black traces labeled with yellow dots at the time of the triggered cutaneous stimulation) of the same animal on the same post-operative day. From these two values the relative reflex magnitude was calculated and plotted against the moment of triggering within the step cycle (Fig. 7G, step cycle was divided into 20 5% bins). In this way, it was obvious that in the two sham animals cutaneously induced reflexes are most pronounced during the BA and SP period whereas they are suppressed during the SA phase. These observations are in line with a recent report by Bronsing et al (2005).

Data obtained from the four animals with a C1-COP injection of CTb-S was processed in a similar way and compared to the sham animals. The mean reflex responses per step cycle bin as obtained for each animal and for each post-operative day as well as the summed results of these plots (sham, white bars vs. lesion, gray bars) are shown in Figure 8A. From these plots it can be seen that the depth of modulation is considerably reduced in the lesioned animals. Especially during the initial 20% of the step cycle the size of the reflex response was reduced as compared to the sham-operated rats. The effects appear less pronounced at postoperative day 3, when the internalized CTb-S may not have resulted in adequate degeneration, and at day 7, where other adaptive or compensating processes may have begun to take effect. When all reflex responses between postoperative day 3 and 7 are grouped into the three identified phases of BF activity significant differences between the lesioned and sham animals were found for all phases. The BF and SP phases showed a diminishing reflex response whereas a slight increase (i.e. a disinhibition of the normally suppressed reflex during this phase) was observed in the SA phase (Fig. 8B). We conclude that the CTb-S injection into C1-COP considerably changed the modulation of BF reflex responses during locomotion.

Discussion

The data presented in this study show that selective and specific cerebellar modules can be affected with the neurotoxic agent CTb-S. By injecting this neurotoxin into the cerebellar cortex of the rat we could successfully lesion cells of origin of the C1 module of the COP, which has been implicated in hind limb control (Atkins and Apps, 1997). Behavioral tests showed that inducing such a lesion did not produce a significant impact on skilled walking. However, the modulation of peripherally induced cutaneously triggered reflexes was severely altered. Based on these experiments, we propose that the C1 hind limb module of the cerebellum is able to adaptively control peripherally induced reflexes of the hind limb.

Methodological considerations

As has been pointed out by Bloedel and Bracha (1995), a lesion study does not unequivocally prove the function of that specific part of the CNS, however it is generally accepted that lesion studies at least can provide important clues or insights for normal functioning. It was the main goal of the present study to obtain clues on the function of a single cerebellar module. The Purkinje cells of the targeted module, i.e. the C1 hind limb module, receive their climbing fiber input from the caudolateral part of the vfDAO, which have been shown to possess receptive fields from the ipsilateral hind limb (Atkins and Apps, 1997). Olivary neurons of this part of the vfDAO distribute their climbing fibers to C1 and C3 zones of Purkinje cells in the anterior lobe and to the C1 zone of COP (Sugihara et al., 2004; Pijpers et al., 2005). Indeed, many climbing fibers collateralize to reach both the COP as well as the anterior lobe parts of this module (Voogd et al., 2003). Purkinje cells of these related zones seem to project to the medial part of the AIN (Pijpers et al., 2005; Apps and Garwicz, 2005). Our results depend critically of the effectiveness of the suicide tracer to impact both regions without affecting adjacent cerebellar modules. Llewellyn-Smith and collaborators (1999; 2000a) injected CTb-saporin into either the superior cervical ganglion or the facial nerve and compared its neurotoxic effects on sympathetic preganglionic or motor neurons with injections of unconjugated saporin. They concluded that, since CTb binds to GM1 ganglioside, the conjugate is effective in eliminating all neurons that express this molecule in their membranes. Previously anatomical tracing studies have already proved the susceptibility for CTb for neurons within the cerebellar modular system (Voogd et al., 2003; Voogd and Ruigrok, 2004). Hence, CTb-S injection is likely not only to result in degeneration of Purkinje cells located at and directly surrounding the injection site, but also of the mossy and climbing fiber sources that reach the injected area. Following degeneration of the parent soma climbing as well as mossy fiber afferents to other cerebellar regions will degenerate as well. Climbing fiber deafferentation of Purkinje cells has been reported to severely affect their functional

characteristics (Benedetti et al., 1984). Thus, a single injection of CTb-S in C1-COP is expected, by degeneration of a largely common olivary source of climbing fibers affect a major part of the module as a whole. The olivary cell counts and the suppressed silver staining fully support this notion and provide us with enough evidence that the function of an individual module that is distributed over multiple sites, can be effectively impaired (Ruigrok and Voogd, 2000; Sugihara and Shinoda, 2004; Pijpers et al., 2005).

It may be important to realize the implications of these lesions on the whole system of modules. Within the targeted module both climbing- and mossy fiber inputs are abolished, but only the Purkinje cells and interneurons at the site of injection are eliminated. This is expected to lead to a disinhibition of the cerebellar nuclear neurons that receive their input from these Purkinje cells. However, climbing fiber deafferentation has been reported to result in enhanced activity of the zonally related Purkinje cells in the anterior lobe (Benedetti et al., 1984). The resultant effect on the AIN is hard to predict but is not likely to result in a meaningful signal learning (Tarnecki et al., 2001; Tarnecki, 2003).

In this respect, it is also important to realize that recurrent cortico-nucleo-cortical loops, as evidenced by the CTb - and silver stainings, are operative within these modules. Here, we provide some evidence that at least some of the nucleocortical neurons within the AIN, in addition to the cortical axon to the C1-COP, also possess a projection axon directed to the magnocellular red nucleus. This suggests that CTb-S injections not only result in changed firing patterns of AIN neurons but that a specific part of its output is completely abolished. In our view, this further stresses the great potential of this suicide tracer since the cortical application warrants a degree of selectivity that cannot be obtained by making selective nuclear or olivary injections (Pijpers et al., 2005).

Behavioral effects of CTb-S injections in C1-COP

Problems with locomotion are usually one of the first and major signs of cerebellar disease (Dow and Moruzzi, 1958). Therefore, it was quite unexpected that none of the C1-hindlimb module impaired animals showed any overt signs of walking disability. Also, with the more sophisticated analysis using the ladder rung test no obvious problems with skilled stepping came to light. This was in marked contrast to the effects of motor cortex lesions, which did result in frequent misplacements of the contralateral hind paw. Hence, lesions do not necessarily have to lead to easily recognizable deficits as long as they are well targeted and specific. E.g. marginal walking problems were found in cats with deprivation of cutaneous hind limb input (Bouyer and Rossignol, 2003). Also, lesions of the magnocellular red nucleus (mRN) do not lead to major alterations in locomotion (Muir and Whishaw, 2000). Since the mRN constitutes one of the major output sources of the AIN (Daniel et al, 1987; Teune et al., 2000; Ruigrok, 2004) this observation is in

general agreement with our own findings. However, in trying to get a handle on the specific functioning of the C1 module in locomotion our subsequent studies on reflex modulation pointed to processes that may be specifically controlled by the C1 hindlimb module.

Modulation of cutaneous reflexes during locomotion

In human, responses to electrical stimulation of the cutaneous nerve have been shown to be similar to obstacle contact with the foot, thereby eliciting a stumbling corrective response (Eng et al., 1994; Schillings et al., 1996). However, human studies have shown different gait adjustments in response to an obstacle depending on the phase of the step cycle favoring either step-lengthening or shortening (Weerdesteyn et al., 2004; Weerdesteyn et al., 2005). Our data in the rat does not appear to show any such adaptations nor in the sham or lesion animals.

At the level of the spinal cord, central pattern generators are thought to produce the basic walking rhythm (Juvin et al., 2005). However, because walking has to be adapted to be functionally relevant environmental requirements, this behavior cannot be stereotyped and sensory modalities are continuously used to regulate stepping by means of phase- and task-dependent modulation of reflexes (Forssberg et al., 1975; Duysens et al., 1990; Pearson, 1995; Zehr et al., 1997). For instance, Drew and Rossignol (1987) already showed in cats that during the swing phase cutaneous receptors correct and modify locomotive limb movements. In a recent study, Bronsing et al. (2005) showed that modulation of cutaneously induced reflexes are also found in BF and gastrocnemius EMG recordings in walking rats. Furthermore, there is a powerful modulation of the input to the intermediate cerebellum of the cat during locomotion and this input is facilitated during the swing phase and suppressed during stance phase (Apps and Lee, 2002; Pardoe et al., 2004). Therefore, the intermediate cerebellum, where peripheral somatosensory and motor inputs are combined, would be an ideal candidate to monitor and modulate these reflexes (Brown and Bower, 2002; Jorntell and Ekerot, 2003). The present results show that inducing a selective impairment of the hind limb related C1-zone and its in- and output connections has specific and profound effects on the modulation of these reflexes.

Functional implications

Although the role of the cerebellum in controlling movement has extensively been studied in case of compensatory eye movements and eye blink conditioning paradigms, we have only just begun to appreciate and elucidate its function during voluntary movements and locomotion (Ito, 2006). Eye blink conditioning paradigms have implicated that the cerebellar cortex modulates the timing and amplitude of the reflex and facilitates its acquisition and can thereby aid in motor learning and motor performance (Koekoek et al., 2003). The AIN, by way of its strong projections to the mRN (Courville, 1966; Teune et al., 2000b) has also been implicated in cerebellar learning during eye

blink conditioning (De Zeeuw and Yeo, 2006). We propose that during locomotion the C1-hindlimb module can fulfill a similar role by optimally adjusting peripherally evoked reflexes of hindlimb muscles to environmental clues.

Due to complex anatomical connections (involving e.g. central pattern generator, reflexes and various supraspinal control systems) the specific cerebellar participation on aspects of motor control has been difficult to establish. The currently applied technique of inducing a modularly restricted impairment of cerebellar function provides a new and promising tool to investigate modular cerebellar function in locomotion.

Acknowledgements

We thank Mrs. E. Sabel-Goedknecht and Mr. E. Dalm for their technical assistance. Supported by the Dutch Organization for Scientific Research (NWO-ALW: project number 810.37.005, A.P., NWO-VIDI: project number 016.048.306, B.W.), the Dutch Ministry of Health, Welfare, and Sports (T.R.).

References

- Apps R, Garwicz M (2000) Precise matching of olivo-cortical divergence and cortico-nuclear convergence between somatotopically corresponding areas in the medial C1 and medial C3 zones of the paravermal cerebellum. *Europ J Neurosci* 12:205-214.
- Apps R, Lee S (2002) Central regulation of cerebellar climbing fibre input during motor learning. *J Physiol* 541:301-317.
- Apps R, Garwicz M (2005) Anatomical and physiological foundations of cerebellar information processing. *Nat Rev Neurosci* 6:297-311.
- Armstrong DM, Harvey RJ, Schild RF (1973) Cerebello-cerebellar responses mediated via climbing fibers. *Exp Brain Res* 18:19-39.
- Atkins MJ, Apps R (1997) Somatotopical organisation within the climbing fibre projection to the paramedian lobule and copula pyramidis of the rat cerebellum. *J Comp Neurol* 389:249-263.
- Bardin JM, Batini C, Billard JM, Buisseret-Delmas C, Conrath-Verrier M, Corvaja N (1983) Cerebellar output regulation by the climbing and mossy fibers with and without the inferior olive. *J Comp Neurol* 213:464-477.
- Barmack NH, Simpson JI (1980) Effects of microlesions of dorsal cap of inferior olive of rabbits on optokinetic and vestibuloocular reflexes. *J Neurophysiol* 43:182-206.
- Barmack NH, Errico P, Ferraresi A, Fushiki H, Pettorossi VE, Yakhnitsa V (2002) Cerebellar nodulectomy impairs spatial memory of vestibular and optokinetic stimulation in rabbits. *J Neurophysiol* 87:962-975.
- Bastian AJ, Thach WT (1995) Cerebellar outflow lesions: a comparison of movement deficits resulting from lesions at the levels of the cerebellum and thalamus. *Ann Neurol* 38:881-892.
- Bastian AJ, Zackowski KM, Thach WT (2000) Cerebellar ataxia: torque deficiency or torque mismatch between joints? *J Neurophysiol* 83:3019-3030.
- Bastian AJ, Martin TA, Keating JG, Thach WT (1996) Cerebellar ataxia: abnormal control of interaction torques across multiple joints. *J Neurophysiol* 76:492-509.
- Benedetti F, Montarolo PG, Rabacchi S (1984) Inferior olive lesion induces long-lasting functional modification in the Purkinje cells. *Exp Brain Res* 55:368-371.
- Bloedel JR (1992) Functional heterogeneity with structural homogeneity: How does the cerebellum operate? *Behav Brain Sci* 15:666-678.
- Bloedel JR, Bracha V (1995) On the cerebellum, cutaneomuscular reflexes, movement control and the elusive engrams of memory. *Behavioral Brain Research* 68:1-44.
- Bouyer LJ, Rossignol S (2003) Contribution of cutaneous inputs from the hindpaw to the control of locomotion. II. Spinal cats. *J Neurophysiol* 90:3640-3653.
- Bronsing R, van der Burg J, Ruigrok TJ (2005) Modulation of cutaneous reflexes in hindlimb muscles during locomotion in the freely walking rat: A model for studying cerebellar involvement in the adaptive control of reflexes during rhythmic movements. *Prog Brain Res* 148:243-257.
- Brown IE, Bower JM (2001) Congruence of mossy fiber and climbing fiber tactile projections in the lateral hemispheres of the rat cerebellum. *J Comp Neurol* 429:59-70.
- Brown IE, Bower JM (2002) The influence of somatosensory cortex on climbing fiber responses in the lateral hemispheres of the rat cerebellum after peripheral tactile stimulation. *J Neurosci* 22:6819-6829.
- Buisseret-Delmas C, Angaut P (1993) The cerebellar olivo-cortico-nuclear connections in the rat. *Progr Neurobiol* 40:63-87.
- Caughell KA, Flumerfelt BA (1977) The organization of the cerebellorubral projection: an experimental study in the rat. *J Comp Neurol* 176:295-306.
- Chanaud CM, Macpherson JM (1991) Functionally complex muscles of the cat hindlimb. III. Differential activation within biceps femoris during postural perturbations. *Exp Brain Res* 85:271-280.
- Cooper SE, Martin JH, Ghez C (2000) Effects of inactivation of the anterior interpositus nucleus on the kinematic and dynamic control of multijoint movement. *J Neurophysiol* 84:1988-2000.
- Courville J (1966) Somatotopical organization of the projection from the nucleus interpositus anterior of the cerebellum to the red nucleus. An experimental study in the cat with silver impregnation methods. *Exp Brain Res* 2:191-215.
- Daniel H, Billard JM, Angaut P, Batini C (1987) The interposito-rubrospinal system. Anatomical tracing of a motor control pathway in the rat. *Neurosci Res* 5:87-112.
- Dow RS, Moruzzi G (1958) *The physiology and pathology of the cerebellum*. Minneapolis: University of Minnesota Press.
- Drew T, Rossignol S (1987) A kinematic and electromyographic study of cutaneous reflexes evoked from the forelimb of unrestrained walking cats. *J Neurophysiol* 57:1160-1184.
- Duysens J, Trippel M, Horstmann GA, Dietz V (1990) Gating and reversal of reflexes in ankle muscles during human walking. *Exp Brain Res* 82:351-358.
- Ekerot C-F, Larson B (1982) Branching of olivary axons to innervate pairs of sagittal zones in the cerebellar anterior lobe of the cat. *Exp Brain Res* 48:185-198.
- Eng JJ, Winter DA, Patla AE (1994) Strategies for recovery from a trip in early and late swing during human walking. *Exp Brain Res* 102:339-349.
- English AW, Weeks OI (1987) An anatomical and functional analysis of cat biceps femoris and semitendinosus muscles. *J Morphol* 191:161-175.
- Forsberg H, Grillner S, Rossignol S (1975) Phase dependent reflex reversal during walking in chronic spinal cats. *Brain Res* 85:103-107.
- Gasbarri A, Pompili A, Pacitti C, Cicirata F (2003) Comparative effects of lesions to the ponto-cerebellar and olivo-cerebellar pathways on motor and spatial learning in the rat. *Neuroscience* 116:1131-1140.

- Haasdijk ED, Vlug A, Mulder MT, Jaarsma D (2002) Increased apolipoprotein E expression correlates with the onset of neuronal degeneration in the spinal cord of G93A-SOD1 mice. *Neurosci Lett* 335:29-33.
- Hallett M, Shahani BT, Young RR (1975) EMG analysis of patients with cerebellar deficits. *J Neurol Neurosurg Psychiatry* 38:1163-1169.
- Hore J, Wild B, Diener HC (1991) Cerebellar dysmetria at the elbow, wrist, and fingers. *J Neurophysiol* 65:563-571.
- Ito M (2006) Cerebellar circuitry as a neuronal machine. *Prog Neurobiol* 78:272-303.
- Jornetell H, Ekerot CF (2003) Receptive field plasticity profoundly alters the cutaneous parallel fiber synaptic input to cerebellar interneurons in vivo. *J Neurosci* 23:9620-9631.
- Juvin L, Simmers J, Morin D (2005) Propriospinal circuitry underlying interlimb coordination in mammalian quadrupedal locomotion. *J Neurosci* 25:6025-6035.
- Koekkoek SK, Hulscher HC, Dortland BR, Hensbroek RA, Elgersma Y, Ruigrok TJ, De Zeeuw CI (2003) Cerebellar LTD and learning-dependent timing of conditioned eyelid responses. *Science* 301:1736-1739.
- Llewellyn-Smith IJ, Martin CL, Arnolda LF, Minson JB (1999) Retrogradely transported CTB-saporin kills sympathetic preganglionic neurons. *Neuroreport* 10:307-312.
- Llewellyn-Smith IJ, Martin CL, Arnolda LF, Minson JB (2000a) Tracer-toxins: cholera toxin B-saporin as a model. *J Neurosci Methods* 103:83-90.
- Llewellyn-Smith IJ, Martin CL, Arnolda LF, Minson JB (2000b) Tracer-toxins: cholera toxin B-saporin as a model. *J Neurosci Methods* 103:83-90.
- Luppi P-H, Aston-Jones G, Akaoka H, Chouvet G, Jouvet M (1995) Afferent projections to the rat locus coeruleus demonstrated by retrograde and anterograde tracing with cholera-toxin B subunit and Phaseolus Vulgaris Leucoagglutinin. *Neuroscience* 65:119-160.
- Martin JH, Cooper SE, Hacking A, Ghez C (2000) Differential effects of deep cerebellar nuclei inactivation on reaching and adaptive control. *J Neurophysiol* 83:1886-1899.
- Metz GA, Whishaw IQ (2002) Cortical and subcortical lesions impair skilled walking in the ladder rung walking test: a new task to evaluate fore- and hindlimb stepping, placing, and co-ordination. *J Neurosci Methods* 115:169-179.
- Muir GD, Whishaw IQ (2000) Red nucleus lesions impair overground locomotion in rats: a kinetic analysis. *Eur J Neurosci* 12:1113-1122.
- Nordholm AF, Thompson JK, Dersarkissian C, Thompson RF (1993) Lidocaine infusion in a critical region of cerebellum completely prevents learning of the conditioned eyeblink response. *Behav Neurosci* 107:882-886.
- Pardoe J, Apps R (2002) Structure-function relations of two somatotopically corresponding regions of the rat cerebellar cortex: olivo-cortico-nuclear connections. *Cerebellum* 1:165-184.
- Pardoe J, Edgley SA, Drew T, Apps R (2004) Changes in excitability of ascending and descending inputs to cerebellar climbing fibers during locomotion. *J Neurosci* 24:2656-2666.
- Pearson (1995) Proprioceptive regulation of locomotion. *Curr Opin Neurobiol* 5:786-791.
- Pijpers A, Ruigrok TJ (2006) Organization of pontocerebellar projections to identified climbing fiber zones in the rat. *J Comp Neurol* 496:513-528.
- Pijpers A, Voogd J, Ruigrok TJ (2005) Topography of olivo-cortico-nuclear modules in the intermediate cerebellum of the rat. *J Comp Neurol* 492:193-213.
- Ruigrok TJ (2003) Collateralization of climbing and mossy fibers projecting to the nodulus and flocculus of the rat cerebellum. *J Comp Neurol* 466:278-298.
- Ruigrok TJ, Voogd J (2000) Organization of projections from the inferior olive to the cerebellar nuclei in the rat. *J Comp Neurol* 426:209-228.
- Ruigrok TJH (2004) Precerebellar nuclei and red nucleus. In: *The rat nervous system*, third edition (Paxinos G, ed), pp 167-204. San Diego: Elsevier Academic Press.
- Ruigrok TJH, Teune TM, van der Burg J, Sabel-Goedknegt H (1995) A retrograde double labeling technique for light microscopy. A combination of axonal transport of cholera toxin B-subunit and a gold-lectin conjugate. *J Neurosci Meth* 61:127-138.
- Schillings AM, Van Wezel BM, Duysens J (1996) Mechanically induced stumbling during human treadmill walking. *J Neurosci Methods* 67:11-17.
- Seoane A, Apps R, Balbuena E, Herrero L, Llorens J (2005) Differential effects of trans-crotononitrile and 3-acetylpyridine on inferior olive integrity and behavioral performance in the rat. *Eur J Neurosci* 22:880-894.
- Sugihara I, Shinoda Y (2004) Molecular, topographic, and functional organization of the cerebellar cortex: a study with combined aldolase C and olivocerebellar labeling. *J Neurosci* 24:8771-8785.
- Tarnecki R (2003) Responses of the red nucleus neurons to limb stimulation after cerebellar lesions. *Cerebellum* 2:96-100.
- Tarnecki R, Lupa K, Niechaj A (2001) Responses of the red nucleus neurons to stimulation of the paw pads of forelimbs before and after cerebellar lesions. *J Physiol Pharmacol* 52:423-436.
- Teune TM, van der Burg J, van der Moer J, Voogd J, Ruigrok TJH (2000a) Topography of cerebellar nuclear projections to the brain stem in the rat. In: *Cerebellar modules: molecules, morphology and function* (Gerrits NM, Ruigrok TJH, De Zeeuw CI, eds), pp 141-172. Amsterdam: Elsevier Science B.V.
- Teune TM, van der Burg J, van der Moer J, Voogd J, Ruigrok TJ (2000b) Topography of cerebellar nuclear projections to the brain stem in the rat. *Prog Brain Res* 124:141-172.
- Voogd J, Bigaré F (1980) Topographical distribution of olivary and cortico nuclear fibers in the cerebellum: a review. In: *The inferior olivary nucleus. Anatomy and physiology* (Courville J, de Montigny C, Lamarre Y, eds), pp 207-234. New York: Raven Press.
- Voogd J, Glickstein M (1998) The anatomy of the cerebellum. *Trends Neurosci* 2:305-371.
- Voogd J, Ruigrok TJ (2004) The organization of the corticonuclear and olivocerebellar climbing fiber projections to the rat cerebellar vermis: the congruence of projection zones and the zebrin pattern. *J Neurocytol* 33:5-21.

- Voogd J, Pardoe J, Ruigrok TJ, Apps R (2003) The distribution of climbing and mossy fiber collateral branches from the copula pyramidis and the paramedian lobule: congruence of climbing fiber cortical zones and the pattern of zebrin banding within the rat cerebellum. *J Neurosci* 23:4645-4656.
- Weerdesteyn V, Nienhuis B, Hampsink B, Duysens J (2004) Gait adjustments in response to an obstacle are faster than voluntary reactions. *Hum Mov Sci* 23:351-363.
- Weerdesteyn V, Nienhuis B, Mulder T, Duysens J (2005) Older women strongly prefer stride lengthening to shortening in avoiding obstacles. *Exp Brain Res* 161:39-46.
- Welsh JP, Harvey JA (1991) Pavlovian conditioning in the rabbit during inactivation of the interpositus nucleus. *J Physiol (Lond)* 444:459-480.
- Welsh JP, Harvey JA (1998) Acute inactivation of the inferior olive blocks associative learning. *Eur J Neurosci* 10:3321-3332.
- Wu HS, Sugihara I, Shinoda Y (1999) Projection patterns of single mossy fibers originating from the lateral reticular nucleus in the rat cerebellar cortex and nuclei. *J Comp Neurol* 411:97-118.
- Yeo CH, Hardiman MJ (1992) Cerebellar cortex and eyeblink conditioning: a reexamination. *Exp Brain Res* 88:623-638.
- Zehr EP, Komiyama T, Stein RB (1997) Cutaneous reflexes during human gait: electromyographic and kinematic responses to electrical stimulation. *J Neurophysiol* 77:3311-3325.

Tables

Table 1. Description of injection protocols in experimental groups 2 and 3.

Ladder rung walking test; group 2	Injection into right hemisphere	Injection of approximately 50 nl
L1	C1 - COP	CTb - S
L2	C1 - COP	0.9 % NaCl
L3	C1 - COP	CTb - S
L4	C1 - COP	CTb - S
L5	C1 - COP	CTb - S
L6	C1 - COP	CTb - S
L7	C1 - COP	0.9 % NaCl
R1	C1 - COP	CTb - S
L9	C1 - COP	CTb - S
L10	C1 - COP	Saporin
L11	C1 - COP	Saporin
L12	C1 - COP	Saporin
L13	Motor cortex	CTb - S
L14	Motor cortex	CTb - S
Tread mill; group 3	Injection into left hemisphere	
R8	C1 - COP	CTb - S
R6	C1 - COP	CTb - S
R5	C1 - COP	CTb - S
L8	C1 - COP	CTb - S
R7	C1 - COP	0.9 % NaCl
L2	C1 - COP	0.9 % NaCl

C1 - COP, cerebellar C1 zone related to the C1 hind limb module of the copula pyramidis; CTb - S, the conjugate of cholera toxin subunit b and the ribosome inactivating protein saporin; L1 - L14 and R1 - R8, the respective cases L1 - L14 and R1 - R8.

Figures

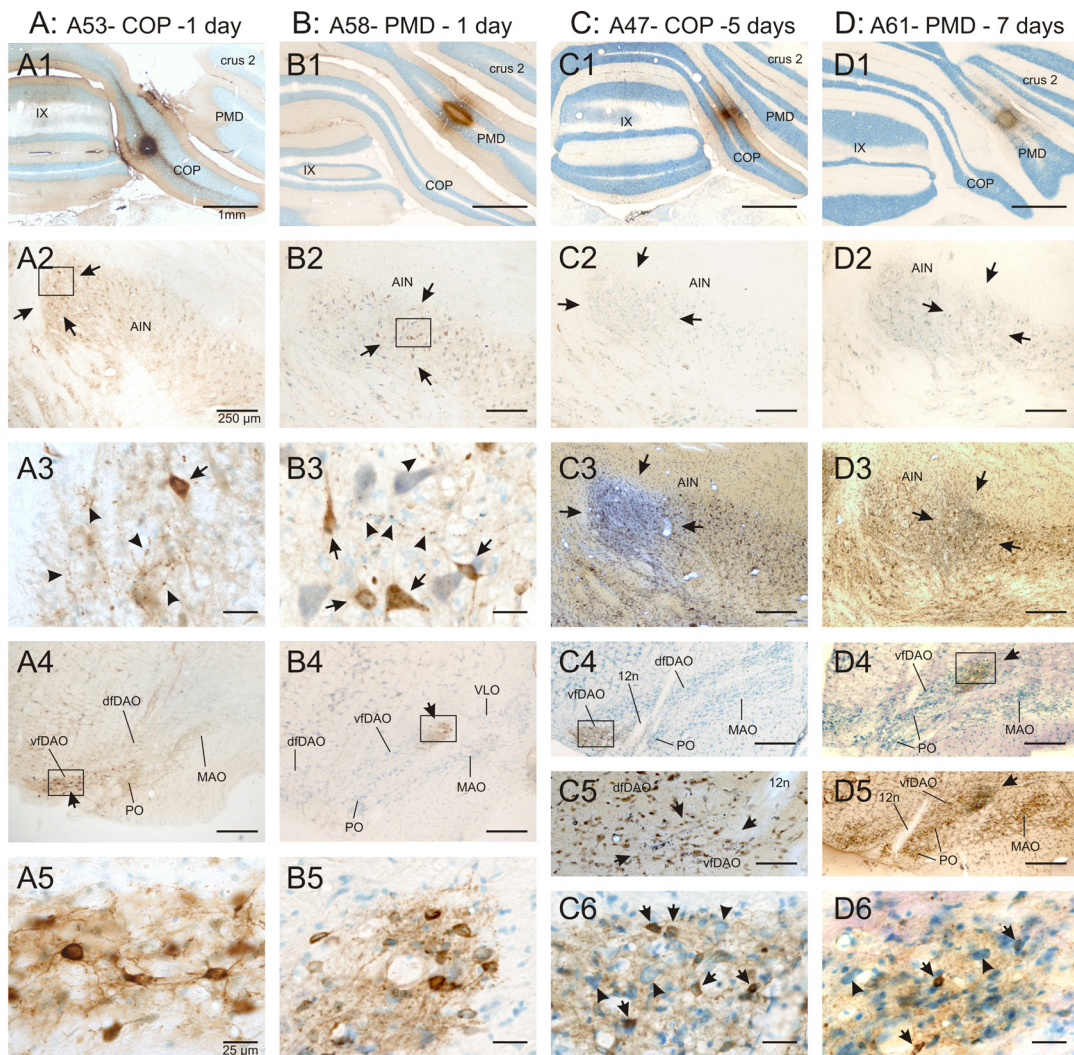


Fig. 1. Microphotographs showing CTb-S injection sites and resultant labeling after various survival times. A. Case A53 was injected in the C1 zone of COP and was sacrificed after 1 day. The injection site was visualized with CTb immunocytochemistry. Virtually no degeneration was observed at this stage (**A1**). Anterograde transport of the CTb-S by Purkinje cell axons was indicated by labeling of fibers with varicosities (arrowheads in **A3**) in the medial aspect of the AIN (arrows in **A2**). Retrograde transport was implied by labeling of several nucleo-cortical projecting neurons (arrow in **A3**) in the medial AIN (**A2, A3**) and of olivary neurons in the caudolateral part of the vfDAO (**A4, A5**). **A3** and **A5** show enlargements of the boxed areas in **A2** and **A4**, respectively. **B.** Similar to **A**, but now for case A58 with a CTb-S injection in the C1 region of PMD (**B1**). Note that anterograde (arrowheads in **B3**) and retrograde labeling (arrows in **B3**) in the AIN is located in a more central region of the AIN (between arrows in **B2**), whereas retrograde labeling within the vfDAO was restricted to its medial aspect (**B4, B5**). **C.** CTb labeling revealed only scant labeling of neurons and fibers within the AIN after a survival time of 5 days (**C2, C3**), with an injection in C1 of COP (**C1**). However reduced silver staining of an adjacent section revealed abundant agyrophilic degeneration confined to the medial AIN (**C3** cf. **A2**). In the inferior olive both CTb labeling (in the caudolateral vfDAO: **C4, C6**) and silver degeneration in a similar region (**C5**, arrows) was noted. **C6** is an enlargement of the boxed area in

C4. Note, that the size of the neuronal somata is reduced compared to **A5** and **B5**. **D.** Similar set of photographs as in **C**, but now for case A61 with an injection of C1 in PMD and a survival time of 7 days. Note failure of CTb labeling in AIN (**D2**) and scant labeling within the inferior olive (**D4, D6**). Silver degeneration within the central AIN (**D3**, cf. **B2**) and medial vfDAO (**D5**, cf. **B4**) indicates degeneration of neuronal structures. **D6** is an enlargement of the boxed area of **D4** and shows, apart from labeling of neuropil, some sparse labeling of small neuronal profiles (arrows). Scale bars equal 1 mm for A1, B1, C1 and D1; 250 μm for A2-D2, C3, D3, A4-D4, C5 and D5; 25 μm for A3, A5, B3, B5, C6 and D6. Abbreviations: IX, cerebellar lobule IX; 12n, hypoglossal nerve; AIN, anterior interposed nucleus; COP, copula pyramidis; crus 2, cerebellar lobule crus 2; dfDAO, dorsal fold of dorsal accessory olive; MAO, medial accessory olive; PMD, paramedian lobule; PO, principal olive; vfDAO, ventral fold of dorsal accessory olive.

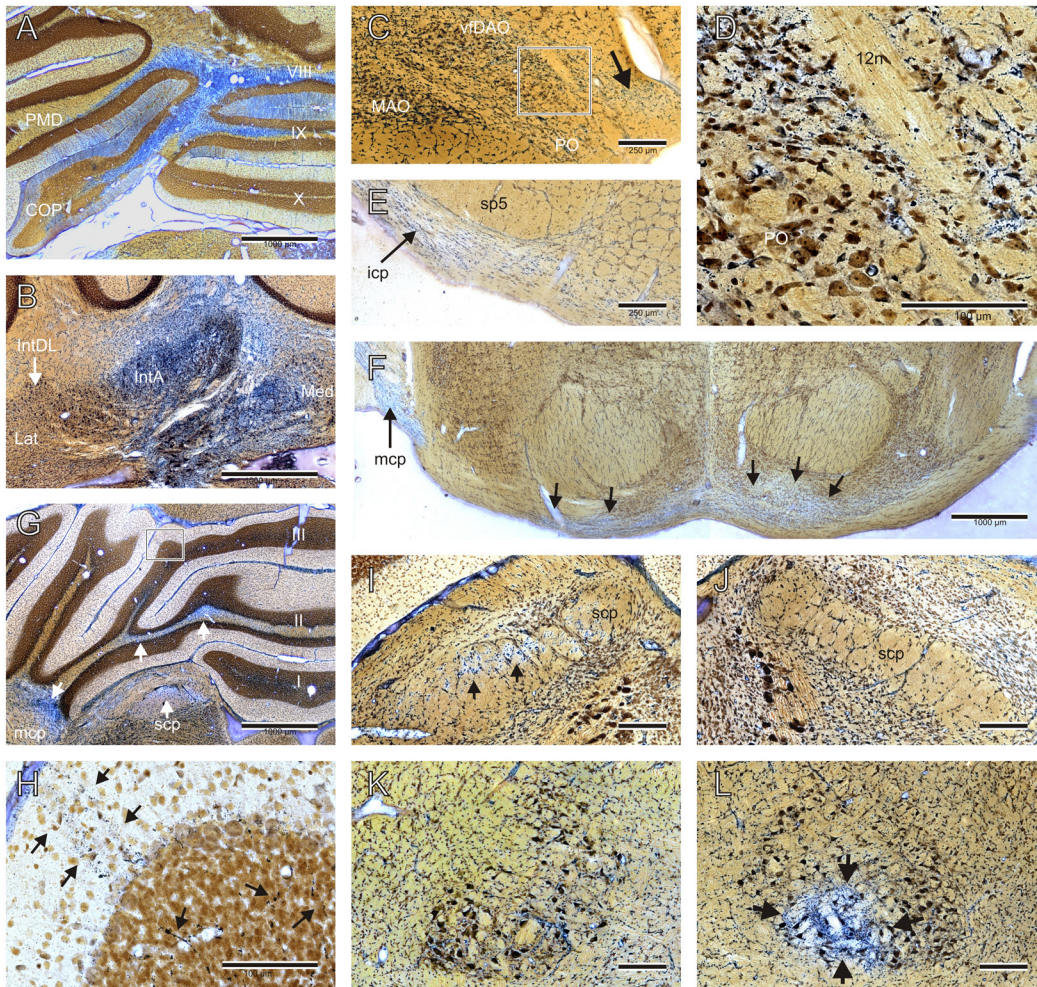


Fig. 2. Agyrophylic degeneration in case R5 with an injection of C1 in COP and a survival time of 21 days. A. Degeneration within the white matter of COP and adjacent white matter of PMD and lobule IX. **B.** Degeneration in the white matter en within the medial part of AIN. **C.** Degenerating debris (arrow) in the caudolateral part of the vfDAO. **D.** Enlargement of the boxed area in C. Note the agyrophilic degeneration of structures surrounding the hypoglossal nerve (12n). Also note that neuronal somata positioned within the silver debris are distinctly smaller compared to the somata found within the PO. **E.** Degeneration of fibers in the icp. **F.** Degeneration of axons and neurons was also noted within the caudal part of the basilar pontine nuclei and ipsilateral mcp. **G.** White matter degeneration in the anterior lobe and cerebellar peduncles (white arrows). **H.** Enlargement of the boxed area is enlarged in **G**, showing degeneration in granular and molecular layers (arrows) of the area corresponding to C1. **I, J.** Degeneration of nucleo-bulbar fibers in the ipsilateral scp (arrows; **I**) but not in the contralateral scp (**J**). **K, L.** Degeneration of nucleobulbar fibers in ventral part of contralateral red nucleus (**L**, arrows) but not in ipsilateral red nucleus (**K**). Scale bars equal 1 mm in A,B, F, G; 250 μ m in C, E, I, J, K, L and 100 μ m in D, H. Abbreviations: I-X, cerebellar lobules I-X; AIN, anterior interposed nucleus; COP, copula pyramidis; DLH, dorsolateral hump; icp, inferior cerebellar peduncle; LCN, lateral cerebellar nucleus; MAO, medial cerebellar nucleus; MCN, medial cerebellar nucleus; mcp, medial cerebellar peduncle; PMD, paramedian lobule; PO, principal olive; scp, superior cerebellar peduncle; sp5, spinal tract of the trigeminal nerve; vfDAO, ventral fold of dorsal accessory olive.

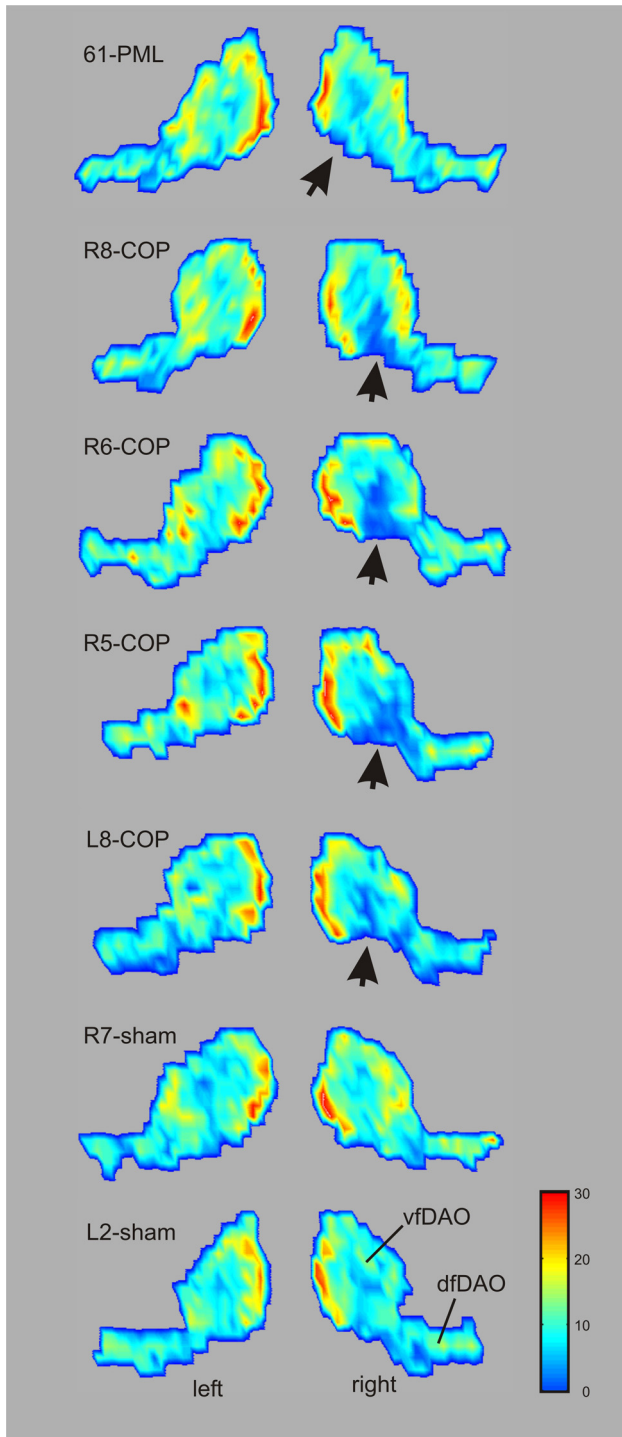


Fig. 3. Color-coded density plots of neuronal profiles in the flattened and unfolded dorsal accessory olives (DAO) after CTb-S or saline (sham) injection in the right COP of all group 3 animals. For comparison a case with a C1 injection of PMD (case A61, survival time 7 days) was included. Diagrams were prepared by counting the number of neuronal profiles in 100-micron wide bins, running perpendicular to the direction of the DAO. Note that the density profiles of the vfDAO of the left side reveal an unequal distribution of neurons throughout the dorsal accessory olive. Highest densities were found at the medial and lateral aspects of the nucleus. Occasional, small patches with few cells in the center of the nucleus were due to traversing bundles of the hypoglossal nerve. Note that the CTb-S injections in COP resulted in diminished density of neurons in the caudolateral part of the vfDAO (arrows). No such change was observed after saline injections (R7-sham and L2-sham, bottom panels). PMD injection resulted in a decrease of neurons in the caudomedial part of the vfDAO.(arrow in top panel: 61-PMD). Dotted lines marks approximate position of folding line between dfDAO and vfDAO. Abbreviations: dfDAO, dorsal fold of accessory olive; vfDAO, ventral fold of dorsal accessory olive.

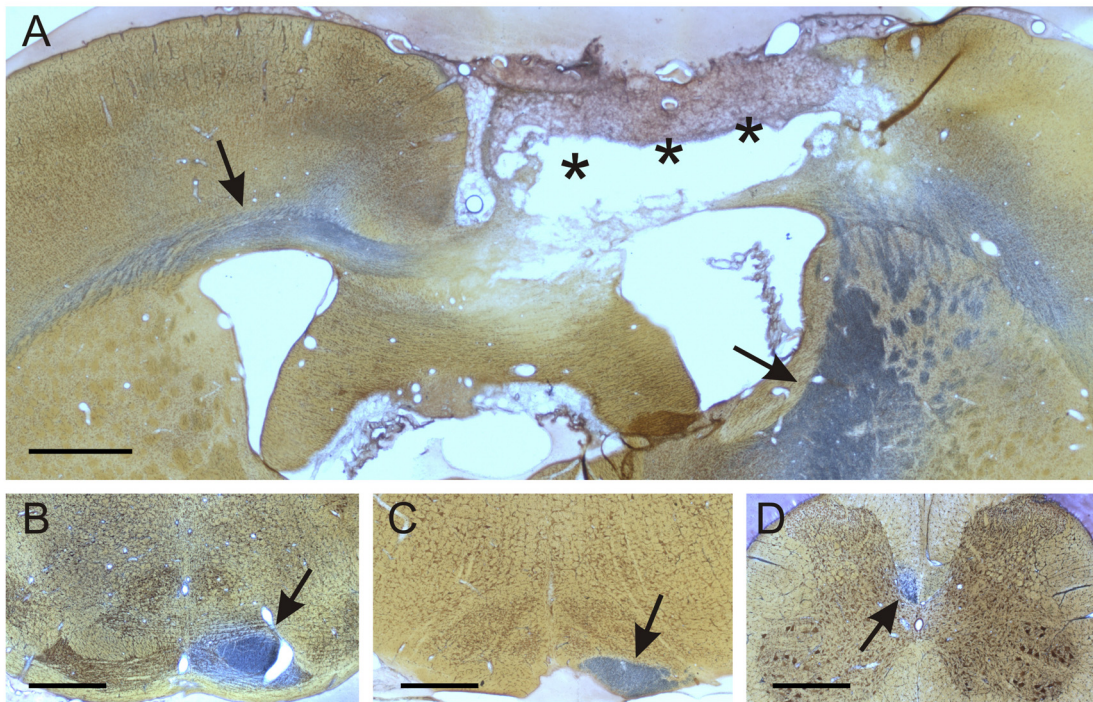


Fig. 4. Microphotographs of sections treated with reduced silver staining after an injection with CTB-S in the hindlimb region of the right motor cortex of case L13 (A). Apart from the virtual complete disappearance of the injected region (asterisks), note the massive anterograde degeneration of fibers in the corpus callosum (cc) and capsula interna (ic: arrows). B. Degeneration was also noted in the ipsilateral basal pontine nuclei, pyramidal tract (C) and contralateral dorsal corticospinal tract (arrows), which reached lumbosacral levels (D). Scale bars equal 1 mm in all panels.

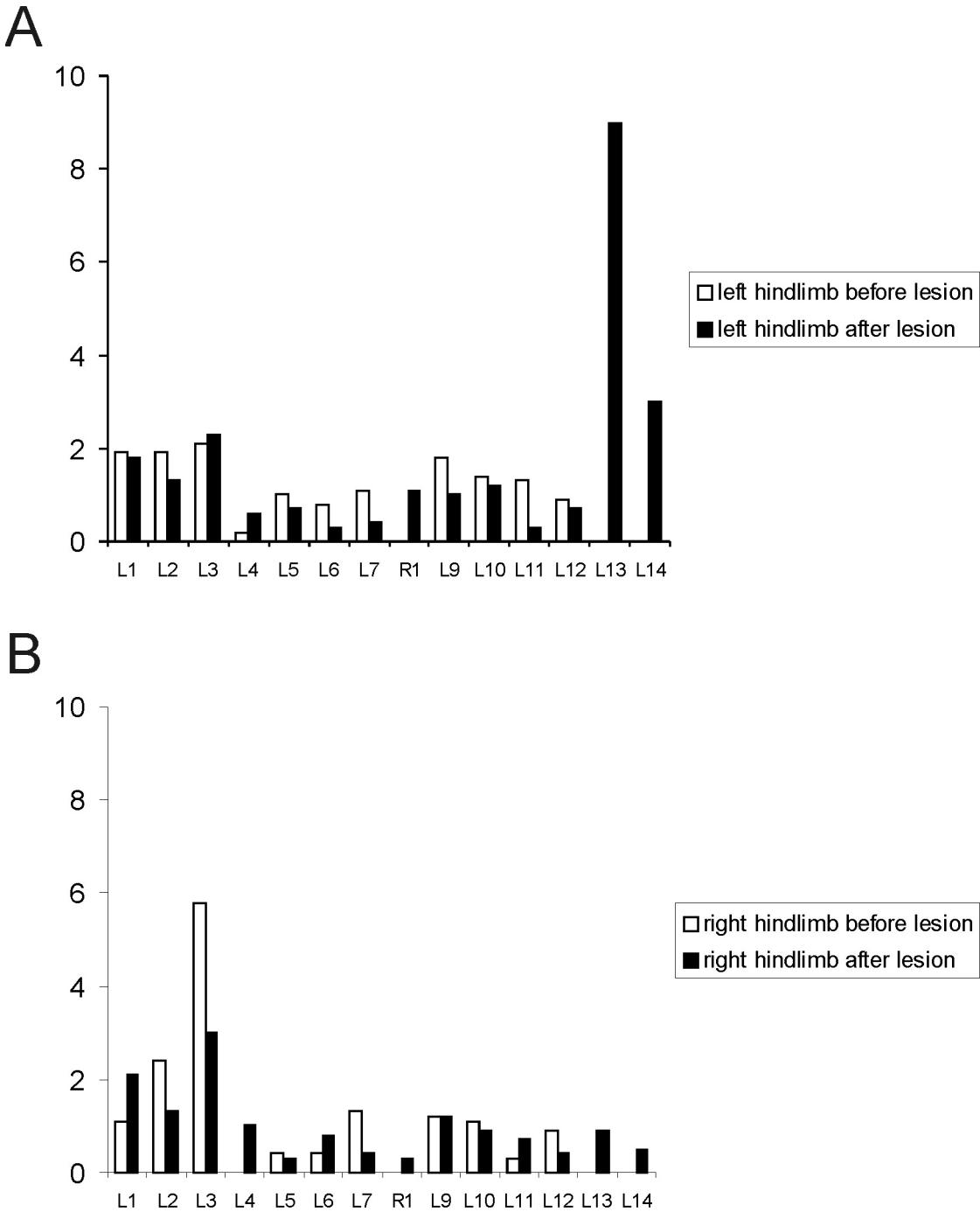


Fig. 5. Evaluation of skilled walking before (white bars) and after (black bars) lesioning on the ladder rung walking test. A. Data obtained from the left hind limb. **B.** Data obtained from the right hind limb. X-axis represent the individual cases (L1,2,3,4,5,6,7,9,10,11,12,13,14 and R1; see table 1 for specifics on the received injection). Y-axis represents the percentage of steps with a scored foot fault, defined as a slip or total miss. Data of consecutive days before and after surgery was pooled for each case. Note that the only marked post-injection decline of walking efficiency (as seen by an increase in number of foot faults of specifically the left hind limb) were seen in cases L13 and L14, which both received an injection of CTb-S into the hind limb related area of the contralateral motor cortex.

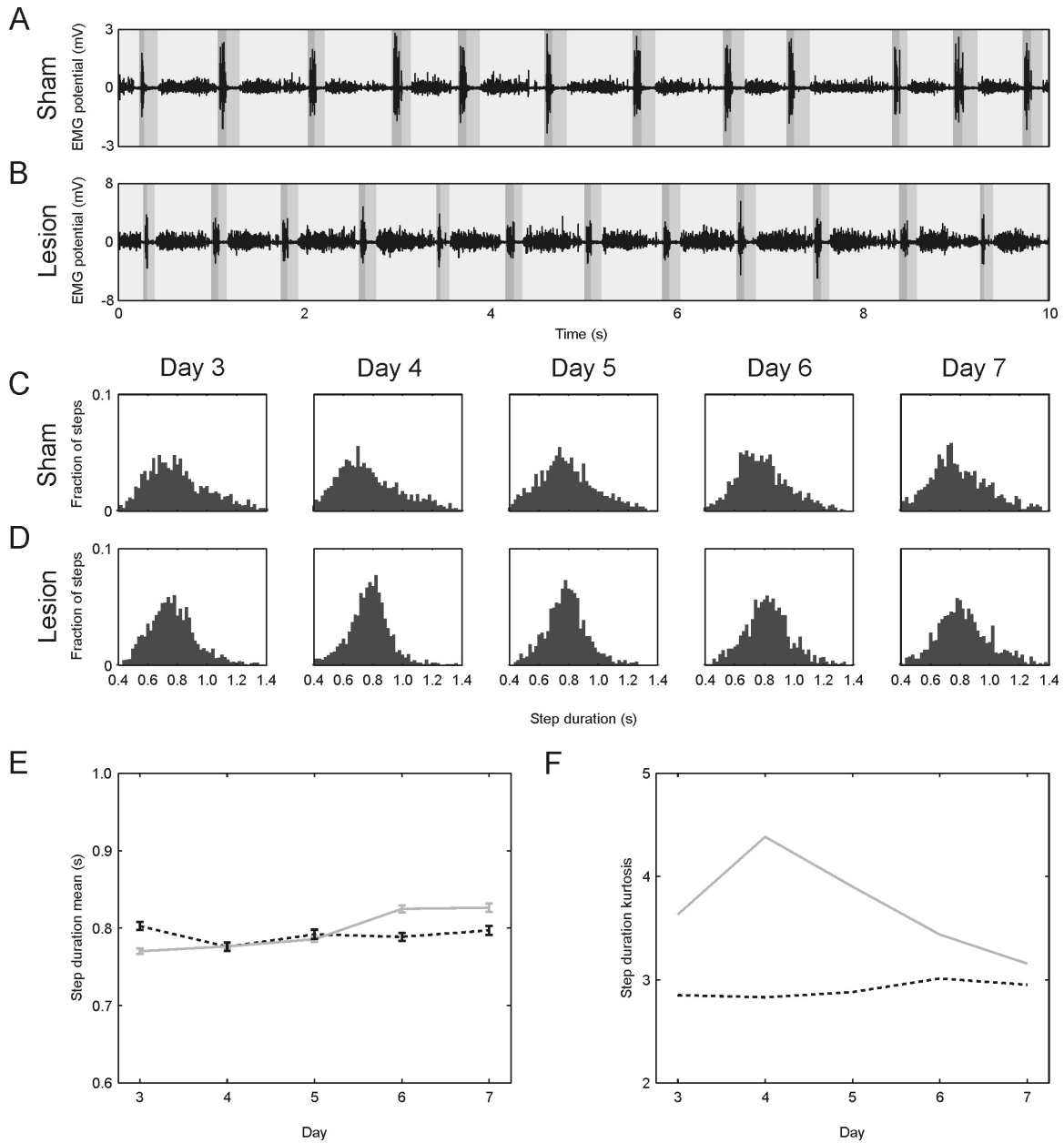


Fig. 6. Analysis of step cycle related EMG activity of the m. biceps femoris of the left hind limb in normal unperturbed steps of sham and lesion animals. **A.** 10 seconds of EMG activity (mV) recorded in an unstimulated session of a sham animal. **B.** 10 seconds of EMG activity (mV) recorded in an unstimulated session of a lesion animal. Both traces show a subdivision of the step cycles into three phases. In dark gray the burst of activity (BA phase). In intermediate gray the silent period (SP phase). In light gray the period of the step cycle were there is sustained EMG activity (SA phase). The beginning and end of each step cycle was defined by the onset of each BA phase. **C, D.** Distribution (pooled data) of total step cycle durations for sham (C) and lesion (D) animals for post-operative days 3 – 7. Step cycles with a longer duration than 1.4 s or shorter than 0.4 s were discarded. Note the more peaked distribution amongst the lesion animals. **E.** Mean step duration for sham (black dashed line) and lesion animals (gray line). Error bars indicate standard error of the mean. **F.** Sample kurtosis of the step duration distributions. Note that the kurtosis for the lesioned animals (gray line) exceeds the sham animals (black dashed line), indicating a more regular gait. The kurtosis for the lesioned animals is maximal at day 4.

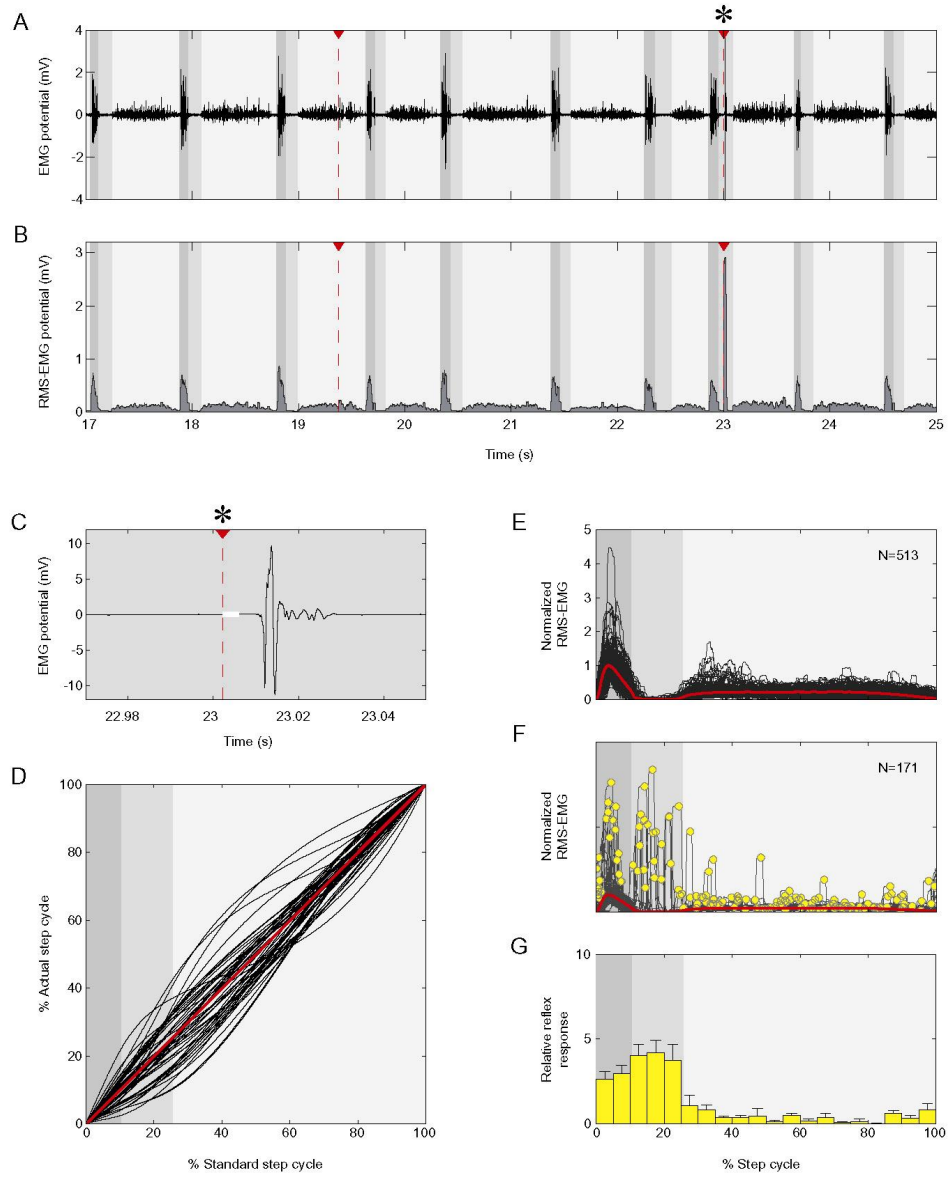


Fig. 7. Step standardization and analysis of relative reflex responses derived from EMG activity of the m. biceps femoris of the left hind limb in stimulated steps. **A.** Trace of recorded EMG activity (mV) during a session with randomly induced peripherally cutaneous reflexes, which are indicated by the red dashed lines. Step phases are delineated as in Figure 6. **B.** EMG amplitude (mV) computed by root-mean-square (RMS) rectification using a 20 ms window. **C.** Enlargement of the reflex response as part of the EMG potential (mV) derived from the starred stimulus in **A.** The white bar shows the masked area of the stimulus artifact. **D.** Step standardization by time rescaling of 50 example steps (randomly drawn). The relative time axis of each step (black lines) was smoothly rescaled to fit the standard step phase lengths (gray shaded areas). Time is compressed where slopes exceed 1 and stretched where slopes are smaller than 1. The red line indicates no rescaling. **E, F.** Normalized RMS-EMG amplitude data were divided into groups of normal, unstimulated steps (**E**) and stimulated steps (**F**). The red trace reflects the EMG amplitude data of the normal step group, which was averaged per rat for each day. The yellow dots in **F** represent the reflex magnitude as the height of the normalized EMG amplitude 15 ms after a stimulus. **G.** Relative reflex responses averaged in 5% step cycle bins. Net reflex magnitudes were calculated by subtracting the corresponding value of the average step cycle EMG activity from the reflex magnitude observed in **F**. Error bars indicate standard error of the mean.

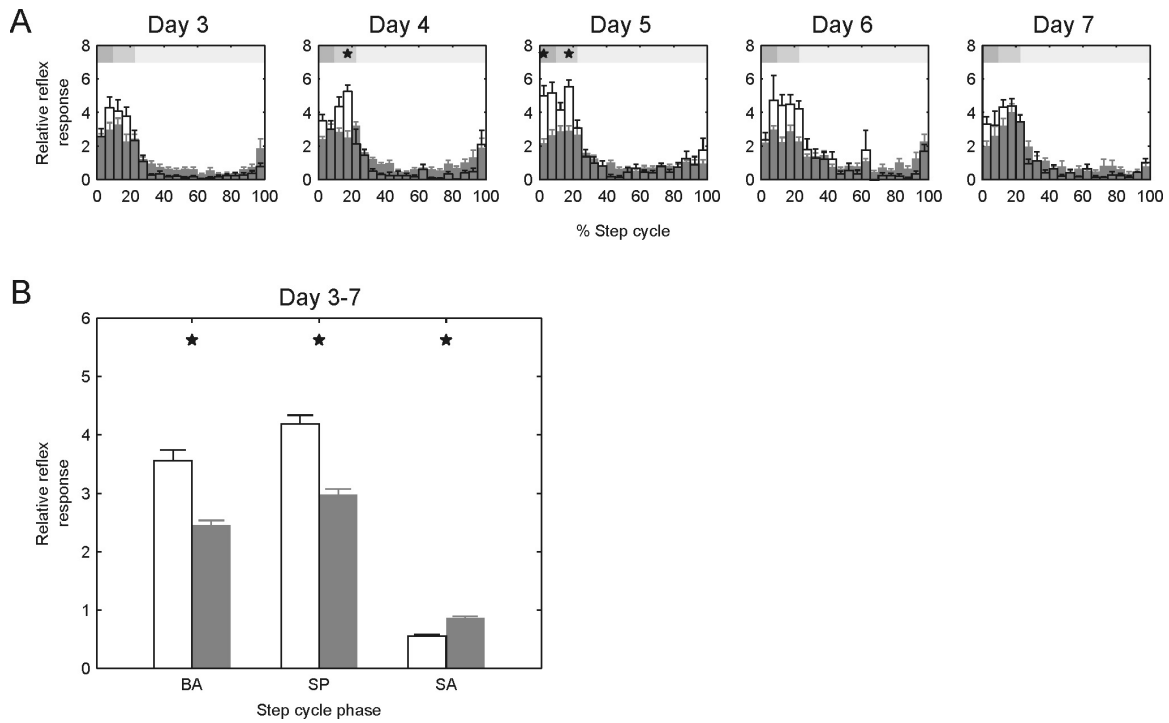
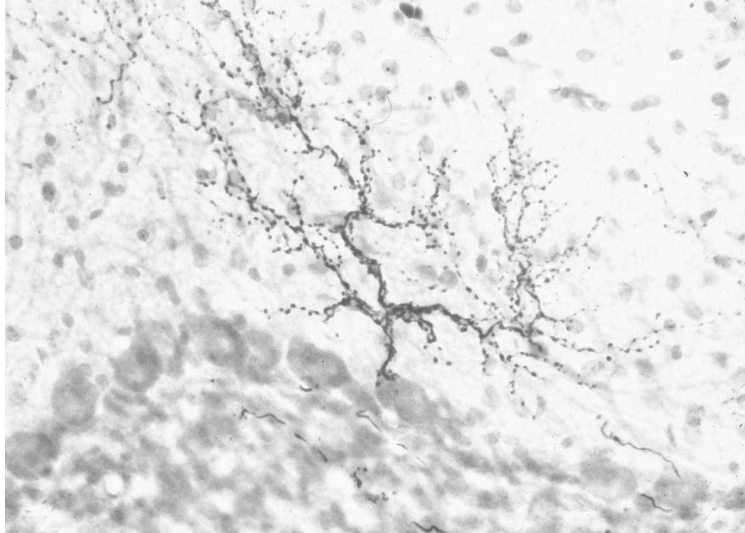


Fig. 8. Comparison of relative reflex magnitudes between the sham (white bars) and lesion (gray bars) group. A. Relative reflex responses averaged in 5% step cycle bins as a function of the step cycle for postoperative days 3 to 7. **B.** Relative reflex responses averaged in the three step cycle phases with data pooled for all postoperative days. Stars represent significant differences (A: $P < 0.0005$, B: $P < 0.015$).

Chapter Seven

General Discussion



7.1 Introduction

This chapter will present the data described in this thesis in a larger perspective. In particular we will discuss our results in relation to the questions that were posed in the General Introduction (1.6: Aims of this thesis). In succession we will review the organization of the olivo-cortico-nuclear connections to the paravermis in relation to the zebrin pattern and the concept of cerebellar modules (question 1); the relation between organization of climbing fiber and mossy fiber systems (question 2); the identification of modules that participate in the control of single muscles (question 3) and the potential role of individual modules in this control (question 4). The chapter will finish with a recommendation for further experiments.

7.2 Organization of olivo-cortico-nuclear projections in the intermediate cerebellum

The experiments described in chapter 2 have provided additional detail of the organization of the paravermal modules in the rat (Pijpers et al., 2005). This study also provides the first actual demonstration of the concept of modular connections between inferior olive, Purkinje cells and cerebellar nuclei has been provided by simultaneous visualization of matching olivo-cortical, olivo-nuclear, cortico-nuclear and nucleo-olivary projections.

In order to begin understanding the functional significance of the functional significance of the modular organizational pattern, the original work done by Oscarsson, Voogd and Buisseret-Delmas and all their co-workers needed to be detailed in some depth. This was realized by relating climbing fiber projections to the zebrin banding pattern (Hawkes and Leclerc, 1987), which can be used as an internal frame of reference in- and between rats. Originally the vermis and paravermis were divided into the A, B, C1, C2 and C3 zones (Voogd, 1964; Oscarsson, 1967; Voogd et al., 1969; Oscarsson and Sjolund, 1977; Buisseret-Delmas, 1988a). Later, anatomical and electrophysiological studies further detailed this subdivision in the anterior lobe of the cat, by showing the existence of a X- and a Cx- zone (respectively located between the A-B zones and the C1-C2 zones; (Ekerot and Larson, 1982a; Campbell and Armstrong, 1985; Trott and Armstrong, 1987; Pardoe and Apps, 2002). In the rat, Buisseret-Delmas found similar zones in (1993), which were partially confirmed in the anterior lobe by electrophysiological studies by Jorntell et al. (2000). However, the presence of these zones within the posterior lobe remained controversial. The PCs in the X-Cx zones receive climbing fiber input from an oblique band in the i-MAO and project to the ICG. In Chapter 2, we provide some evidence for the existence of a X-Cx zone in the posterior lobe was found, based on olivo-cortico-nuclear projections, but anatomically establishing a sharp cortical border between the Cx and C2 zones was not possible.

Buisseret-Delmas (1988b) was the first to describe the C1- and C3 zones in the rat, which had previously been described in the cat by Voogd (1964) and Groenewegen et al. (1977). In contrast to their proposal that both the anterior and posterior interposed nuclei (AIN and PIN, respectively) receive inputs from the C1 zone, our data, and that of Ruigrok and Voogd (2000), showed exclusive projections from the C1/C3 zone to the AIN and not to the PIN. The C1 zone extends from the anterior lobe to the COP and runs mainly in the zebrin negative P3- and P4-bands respectively, whereas the C3 zone runs from the anterior lobe to the PMD in the P4-/P5-bands respectively (this thesis). With regard to the P3+ band in the anterior lobe, which receives its climbing fiber input from the junctional area of the df- and vf- DAO and is probably linked to the posterior e+ patch, is most likely also part of the C1 zone, based on the results of chapter 3 and the results of previous studies (Voogd et al., 2003; Sugihara and Shinoda, 2004). Its PCs project to the area within the CN where the AIN, ICG and PIN meet, possibly explaining why initially C1 was thought to project to both the AIN and PIN.

A third zone, described by Buisseret-Delmas and Angaut in (1989) is the D0 zone, which, we suggest, may be the rat equivalent of the γ -zone in the cat (Ekerot and Larson, 1979, 1982b). The PCs of this zone receive climbing fiber input from the DM and possibly, in case of the anterior lobe, from the rostro-medial DAO, which characterizes mediolateral branching of climbing fibers between C3 and the D0-zone. The cortical output is targeted at the DLH. Originally, this zone was located between the C3/D1 zones, but recent studies support the suggestion made by Voogd et al (2003) that this zone is actually located between the D1/D2 zones (Sugihara and Shinoda, 2004). Like the C1 and C3 zones, the D0 zone is interrupted at the level of Crus I.

The anatomy of the C2 zone, running from lobule II to the caudal half of the COP in the P4+/P5+ band, was further detailed in this study. Rather than being the only continuous zone in the cerebellum, we propose that the C2 zone is interrupted at the level of crus I as well. Furthermore, caudo-rostral projection lines within the r-MAO are converted into medio-lateral projections within the C2 zone and caudo-lateral shifts within the cortico nuclear projections to the PIN.

Moreover, the present findings anatomically underscore the concept of multizonal microcomplexes (MZMCs) as the operational units of the cerebellum. The concept of MZMCs was put forward by Apps and Garwicz in(2005), and elaborates the ideas of Oscarsson (Oscarsson, 1979) and Ito (Ito, 1984), where a strict correspondence is maintained between in- and output in spatially separated microzones, that converge their output to the same region in a given cerebellar nucleus; thus facilitating parallel processing of information. These MZMCs are supposed to control multiple muscles or muscle synergies.

In conclusion, olivo-cerebellar and cortico-nuclear reciprocal connections form a series of cerebellar modules and although the concept of modular connections is not a new one, the present study provides additional detail specifically in relation to the intermediate cerebellum and which served as a basis for the rest of the thesis.

7.3 Relation of mossy fiber organization with the cerebellar modular concept

When cerebellar modules are considered as the operational entities of the cerebellum, it is important to understand their relation to the other main cerebellar input system; the mossy fibers. Data presented in chapter 3 and 4 provide evidence that the mossy fiber system, to some degree, adheres to the modular concept. This is surprising since the mossy fiber system, especially when seen in conjunction with the parallel fiber system is classically seen as widely diverging in order to spread its information over large regions of cerebellar cortex. The strict and strip-like termination patterns of mossy fibers that, at least partly, relate to that of climbing fibers suggest that 1) the ascending and parallel parts of the granule cell axons may subserve different functions and 2) the organization of related climbing and mossy fibers are tailored to each other 3) mossy fibers provide similar input to different zonal regions, thereby further linking different modules. Furthermore, it is noteworthy that in the paravermis cortical injections into zebrin positive zones results in mossy fiber collateralization to mostly zebrin-positive zones and those in zebrin-negative zones are restricted to zebrin-negative zones.

One of the main pathways by which the cerebellum receives its mossy fiber input is the cerebro-pontine-cerebellar connection. Initially, it was thought that there was no clear somatopic pattern of projections from the cerebral cortex to the pons. Recently, at least for the somatosensory cortex (SI), a shell like map of SI projections to the basilar pontine nuclei (Pn) was observed, where a core representing the head is surrounded by shells of projections reflecting the forelimbs, body, hind limbs and tail (Bjaalie and Brodal, 1997; Bjaalie and Leergaard, 2000; Leergaard et al., 2000a; Leergaard et al., 2000b). Furthermore, tracer injections into the Pn result in multiple strip-like patterns of labeled mossy fibers, which in part correspond to the climbing fiber zones and at least preserve some of their somatotopic organization (Serapide et al., 1994; Serapide et al., 2001; Voogd et al., 2003; Odeh et al., 2005).

Apparently, corticopontine projections from the SI are maintained in the pontocerebellar projection (Chapter 3). This study suggests that for instance, within one cerebellar lobule, the face related regions receive pontine mossy fiber input from the same area within the Pn, but differ in the origin and therefore the modality of their climbing fiber input (A2 vs. C2 vs. D0). Zonal differences of pontine mossy fiber input to one lobule mostly consider the degree of bilateral pontine labeling, which was higher for C2 injections, presumably reflecting its bilateral nature. These observations extend previous knowledge on cerebellar modules and suggest that they may incorporate cerebro-cerebellar-cerebral loops as well. For instance, the motorcortex receives cerebellar cortical information through the AIN and the ventrolateral nucleus of the thalamus. Recently, using neurotropic viruses, Peter Strick and collaborators showed that the arm area of the motor cortex receives input from arm-related Purkinje cells in the cerebellar cortex. These cerebral neurons project back to the same area within the cerebellar cortex through mossy fiber

projections originating from the pons, thus forming an internal feedback loop for the motor cortex (Kelly and Strick, 2003). It is now attractive to assume a similar arrangement may hold for the sensory cortex (also see (Leergaard et al., 2000b)). It seems likely that the current level of detail used in our analysis was not refined enough to detect further interzonal differences. On the other hand it could be possible that a zonal distribution of mossy fiber projections related to the climbing fiber zones is only present for mossy fibers from non-pontine regions (King et al., 1998; Herrero et al., 2002), or that pontine neurons do project to specific zones, but that these neurons are intermingled with each other.

Although the mossy/parallel fiber system is characterized by a divergent projection pattern, there is a close relation between this system and the climbing fiber system based on physiological studies and recently a close spatial relationship was observed on the anatomical level as well (Yatim et al., 1996; Yeo and Hesslow, 1998; Wu et al., 1999; Brown and Bower, 2001; Ekerot and Jorntell, 2001b; Sultan, 2001; Voogd et al., 2003). As was mentioned above, not all mossy fiber sources necessarily project to the cerebellum in the same organizational manner. However, based on zonal cortical injections with cholera toxin b-subunit (CTb), the whole spectrum of mossy fiber projections to a given climbing fiber zone collateralizes to areas subjacent to collaterals of climbing fibers and, in addition, to non-adjacent strip-like regions mostly restricted to the lobules containing labeled climbing fibers collaterals and which often have the same zebrin signature as the injection site. This implies that, inline with data from Chapter 2, mossy fibers originating from COP mainly collateralize to the anterior lobe, and those originating from the PMD, mainly collateralize to the SL and both crura. Furthermore, within these specific lobules, mossy fibers collateralize bilateral to a number of (climbing fiber) zones in both the vermis and paravermis, whereas the hemispherical regions are mostly concerned with ipsilateral inputs.

A current debate on cerebellar functioning forms the question what mossy- and climbing fibers actually signal to the cerebellum. Popular hypotheses state that climbing fibers convey some sort of peripheral sensory information that could serve as an error signal (Marr, 1969; Albus, 1971) . However, it has now become clear that the information carried by the climbing fiber activity may reflect a pre-integrated signal of both sensory- and movement related modalities (Ekerot et al., 1987b; Ekerot et al., 1987a; Bosco and Poppele, 2001; Dean et al., 2004; Highstein et al., 2005; Winkelman and Frens, 2006; Xu et al., 2006). Furthermore, both main afferent systems converging on a PC have, at least in part, similar or related peripheral receptive fields from the extremities (Brown and Bower, 2001; Ekerot and Jorntell, 2001a). However, the functional implications of such a related distribution of mossy and climbing fibers remain to be resolved (see for example Ekerot and Jorntell (2001b) as compared to Brown and Bower, (2001) and Lu et al. (2005a) and will be further detailed below.

Motor adaptation and motor learning, at least to some extent, are likely to depend on the induction of synaptic plasticity. One of the sites, where synaptic plasticity is known to take place is

at the PC dendrite through the interaction of the mossy/parallel fiber system with the climbing fiber system. Ekerot and Jorntell (2001b) have noted that the Purkinje cell simple spike receptive fields (induced by parallel fibers) differed from the climbing fiber receptive fields of the same cells and the subjacent located mossy fibers. They therefore suggested that the simple spike activity of Purkinje cells might be governed by parallel fibers originating from non-local mossy fibers. In contrast, activation of local mossy fibers would, by a combination of long-term depression (LTD) and climbing fiber activation of local inhibitory interneurons, result in a general depression of simple spike firing (also see Apps and Garwicz, 2005). Brown and Bower (2001), however, reported a similarity in receptive fields of complex and simple spikes, which both matched the responses of subjacent granule cells (Lu et al., 2005b). The ascending part of the parallel fiber, activated by local mossy fibers, is suggested to play a major role in activating Purkinje cells (Llinas, 1982; Gundappa-Sulur et al., 1999; Lu et al., 2005b). This issue is further complicated by recently observed differences in long term effects between the ascending and parallel parts of granule cell axons (Sims and Hartell, 2006). These studies all highlight the important implications for further understanding of aligned and non-aligned climbing and mossy fiber collaterals may have for grasping cerebellar functioning

In addition, from Chapter 6 another interesting observation was made concerning the nucleocortical projections. In the cat, the paravermal zones differ in extend to which they receive these nucleocortical projections, which most probably terminate as mossy fibers in the granular layer. The c1 zone in the anterior lobe receives very little of these projections, whereas in the posterior lobe, the same zone receives an appreciable input, especially from the PIN. Furthermore, it is thought that there is a certain degree of non-reciprocity in the topography of these projections (Tolbert et al., 1976; Trott et al., 1990, 1998). However, from Chapter 6 it was concluded that the AIN has numerous projections to the C1 zone in the posterior lobe as well. Teune et al. (1998) established that a single PC cell could project to both types of nuclear projection neurons (the GABAergic, nucleo-olivary neurons and the non-GABAergic neurons that project to subnuclear specific targets). These nucleocortical projections can serve as an additional feedback controller within the modular system, possibly allowing for further adapting and parallel processing of information by their local interneurons. This might implicate that in addition to the linkage of cerebellar modules through the parallel fiber system and the formation of multizonal microcomplexes, there is another track for parallel processing through the cerebellar nuclei.

7.4 Cerebellar modules associated to single muscles

Employing transneuronal retrograde transport with rabies virus it is shown in Chapter 5 that multiple cerebellar modules may affect a single muscle (Ruigrok et al. submitted). The longitudinal character of modules was clearly visualized and several zones of Purkinje cells were labeled in vermal, paravermal but also in hemispherical regions of the cerebellum.

Due to simultaneous labeling of the zebrin pattern and correlating the data with our previous work on the olivocerebellar en corticonuclear connections, we could identify the individual modules that are obviously participating in the control of single muscles. Although prior studies also mention labeling of Purkinje cells after injections of facial or extraocular muscles, no attempts were made to further identify this labeling (Graf et al., 2002; Morcuende et al., 2002). Small but consistent zonal differences in cerebellar cortical labeling were obtained when injecting different muscles. Although the pathways by which Purkinje cells become labeled could not be established unequivocally, the obtained results indicate that multiple cerebellar modules participate in a parallel fashion in motor control. We hypothesize that each module will provide a specific aspect of this control. Surprisingly, labeling was nearly identical at both sides of the cerebellum indicating some kind of bilateral control.

7.5 The C1 module and adaptive control of reflex modulation

Chapter 6 shows how the specific aspects of modular control of muscles can be studied. Already in classic studies, lesions were popular to determine the role of specific brain regions. However, due to the structure of cerebellar modules, many of which may spread out over multiple lobules in the rostral and caudal parts of the cerebellum, isolated lesions of specific modules were hardly possible. We have tackled this problem by employing a retrogradely transported suicide tracer. Small, targeted injections of such a tracer in the cerebellar cortex not only will result in local destruction of neurons but also in the degeneration of their afferent neurons. Hence, due to the accompanying extensive degeneration of both climbing and mossy fiber collateral fibers to related parts of the module under study, this whole functional module will be largely deafferented and rendered dysfunctional. We have employed this technique in the C1 hind limb zone, which is easily accessible from the copula pyramidis of the rat posterior lobe. The retrograde and anterograde degeneration of linked parts of the injected module could be verified.

Although the anatomical evidence indicated that the effect of the lesion extended beyond the C1 part of the copula pyramidis, remarkably little effects were noted in skilled walking of the rat. However, the step-phase dependent modulation of cutaneously induced reflexes during locomotion was clearly diminished after lesion. Interestingly, we noted that lesioned rats tended to

walk in a more regular pattern, possibly because their locomotion pattern more significantly depends on intrinsic pattern generation and are not or less able to rely on adaptive behavioral responses. We propose that C1 hind limb module is involved in the adaptive control of these reflexes enabling an optimal use of peripheral reflexes during locomotion.

7.6 Future experiments and final conclusion

On the level of functional anatomy there are at least five issues arising from this thesis that require further study.

First, the cortical morphology and cerebellar nuclear organization need to be detailed even further. For a considerable period of time cerebellar function has focused on the convergence of the climbing fiber- and mossy/parallel fiber systems on the Purkinje cell and the processing of their inputs into LTD or LTP. However, it has now become apparent that interneurons play crucial roles in cerebellar processing and that they too might store information (Jorntell and Ekerot, 2002, 2003; Simpson et al., 2005). The interplay between the anatomical, modular, organization of afferent and efferent connections and the cortical interneurons require considerable additional attention.

A second question that arises considers the differences in projections of different mossy fiber sources to specific zones. These differences were already observed in the cat by King et al. (1998), who noted that cortical areas in lobule V and VII that receive similar climbing fiber input, receive markedly different projection densities from various mossy fiber sources. Furthermore, it would be interesting to investigate what the detailed projections of mossy fiber rosettes are; do they terminate on different subsets of cortical interneurons at different cortical locations?

A third intriguing concept is the observation from chapter 5 that predominantly zebrin-negative Purkinje cells get labeled after injection of a transneuronal virus in to peripheral muscles. This raises the question if zebrin-positive and zebrin-negative Purkinje cells have different behavioral properties, which may have considerable consequences for cerebellar functioning. Sarna et al (Sarna et al., 2006) have addressed this issue in a recent paper confirming this question.

Finally, the functional role(s) of hind limb related modules need to be explored further. The specificity of the modulatory effects of these modules on different types of hindlimb muscles has to be explored in detail. Moreover, since the C1 zone, by way of the AIN, strongly connects to the magnocellular part of the red nucleus (Courville, 1966; Teune et al., 2000), the role of the red nucleus in mediating the adaptive control of reflexes need to be further established (Tarnecki, 2003). Finally, the functional differences between A, B, C1, C2 and D0 zone control of hindlimb muscles need to be established. The techniques used in the present thesis may provide the

necessary tools to investigate the modular function of the cerebellum not only in locomotion, but for instance also in forelimb-withdrawal paradigms (Apps and Lee, 2002).

Ultimately, this line of research may contribute to a better understanding of postural- and gait-disorders that occur in the elderly. Although elderly people are not necessarily more frequently subjected to falls, they are less capable of preventing an actual fall (Lockhart et al., 2005). However, these gait- and balance disorders cannot simply be ascribed to impairments in muscular, sensory or joint kinematics alone, but must be seen in union with disorders of central motor programming and the dysfunction of muscle synergies (Serratrice, 1994). Alterations in step-phase-dependent reflex modulation, therefore, might be related to gait disorders in the elderly or persons suffering from neurodegenerative diseases (Dietz et al., 1997; Zehr and Stein, 1999; Chalmers and Knutzen, 2000). Although, the vermal regions are considered mostly with posture and the intermediate cerebellum is related to locomotion in novel contexts (Armstrong and Edgley, 1988; Armstrong and Marple-Horvat, 1996), it can be concluded from this thesis that relations are not straight forward. In summary, during locomotion there are potential roles for all cerebellar regions, most probably all with unique specifications. In this respect it is interesting to note that during ageing there is a considerable loss of PCs in the anterior lobe (Andersen et al., 2003). In addition, the significance of the third, usually unmentioned, afferent input system to the cerebellum, the monoaminergic connections, comes into play. As is lined out in the introduction, this type of input is considered to have a modulatory role and these types of input may actually enhance learning (van Neerven et al., 1990; Schweighofer et al., 2004). Bickford and co-workers (1995; 1999) implicate a role for noradrenergic interactions facilitating cerebellar plasticity and that these interactions importantly diminish during ageing (Van Neerven et al., 1989). Therefore, the cerebellum might be able to adaptively control the modulation of peripherally induced reflexes during rhythmical movements in a learning-dependent way, in order to meet environmental requirements.

References

- Albus JS (1971) A theory on cerebellar function. *Math Biosci* 10:25-61.
- Andersen BB, Gundersen HJ, Pakkenberg B (2003) Aging of the human cerebellum: a stereological study. *J Comp Neurol* 466:356-365.
- Apps R, Lee S (2002) Central regulation of cerebellar climbing fibre input during motor learning. *J Physiol* 541:301-317.
- Apps R, Garwicz M (2005) Anatomical and physiological foundations of cerebellar information processing. *Nat Rev Neurosci* 6:297-311.
- Armstrong DM, Edgley SA (1988) Discharges of interpositus and Purkinje cells of the cat cerebellum during locomotion under different conditions. *J Physiol* 400:425-445.
- Armstrong DM, Marple-Horvat DE (1996) Role of the cerebellum and motor cortex in the regulation of visually controlled locomotion. *Can J Physiol Pharmacol* 74:443-455.
- Bickford P (1995) Aging and motor learning: a possible role for norepinephrine in cerebellar plasticity. *Rev Neurosci* 6:35-46.
- Bickford PC, Shukitt-Hale B, Joseph J (1999) Effects of aging on cerebellar noradrenergic function and motor learning: nutritional interventions. *Mech Ageing Dev* 111:141-154.
- Bjaalie JG, Brodal P (1997) Cat pontocerebellar network: numerical capacity and axonal collateral branching of neurones in the pontine nuclei projecting to individual parafloccular folia. *Neurosci Res* 27:199-210.
- Bjaalie JG, Leergaard TB (2000) Functions of the pontine nuclei in cerebro-cerebellar communication. *Trends Neurosci* 23:152-153.
- Bosco G, Poppele RE (2001) Proprioception from a spinocerebellar perspective. *Physiol Rev* 81:539-568.
- Brown IE, Bower JM (2001) Congruence of mossy fiber and climbing fiber tactile projections in the lateral hemispheres of the rat cerebellum. *J Comp Neurol* 429:59-70.
- Buisseret-Delmas C (1988a) Sagittal organization of the olivocerebellonuclear pathway in the rat. I. Connections with the nucleus fastigii and the nucleus vestibularis lateralis. *Neurosci Res* 5:475-493.
- Buisseret-Delmas C (1988b) Sagittal organization of the olivocerebellonuclear pathway in the rat. II. Connections with the nucleus interpositus. *Neurosci Res* 5:494-512.
- Buisseret-Delmas C, Angaut P (1989) Anatomical mapping of the cerebellar nucleocortical projections in the rat: a retrograde labeling study. *J Comp Neurol* 288:297-310.
- Buisseret-Delmas C, Yatim N, Buisseret P, Angaut P (1993) The X zone and CX subzone of the cerebellum in the rat. *Neurosci Res* 16:195-207.
- Campbell NC, Armstrong DM (1985) Origin in the medial accessory olive of climbing fibers to the x and lateral c1 zones of the cat cerebellum: a combined electrophysiological / WGA-HRP investigation. *Exp Brain Res* 58:520-531.
- Chalmers GR, Knutzen KM (2000) Soleus Hoffmann-reflex modulation during walking in healthy elderly and young adults. *J Gerontol A Biol Sci Med Sci* 55:B570-579.
- Courville J (1966) Somatotopical organization of the projection from the nucleus interpositus anterior of the cerebellum to the red nucleus. An experimental study in the cat with silver impregnation methods. *Exp Brain Research* 2:191-215.
- Dean P, Porrill J, Stone JV (2004) Visual awareness and the cerebellum: possible role of decorrelation control. *Prog Brain Res* 144:61-75.
- Dietz V, Wirz M, Jensen L (1997) Locomotion in patients with spinal cord injuries. *Phys Ther* 77:508-516.
- Ekerot C-F, Larson B (1982a) Branching of olivary axons to innervate pairs of sagittal zones in the cerebellar anterior lobe of the cat. *Exp Brain Res* 48:185-198.
- Ekerot C-F, Oscarsson O, Schouenborg J (1987a) Stimulation of cat cutaneous nociceptive C fibres causing tonic and synchronous activity in climbing fibres. *J Physiol (Lond)* 386:539-546.
- Ekerot C-F, Gustavsson P, Oscarsson O, Schouenborg J (1987b) Climbing fibres projecting to cat cerebellar anterior lobe activated by cutaneous A and C fibres. *J Physiol (Lond)* 386:529-538.
- Ekerot CF, Larson B (1979) The dorsal spino-olivocerebellar system in the cat. II. Somatotopical organization. *Exp Brain Res* 36:219-232.
- Ekerot CF, Larson B (1982b) Branching of olivary axons to innervate pairs of sagittal zones in the cerebellar anterior lobe of the cat. *Exp Brain Res* 48:185-198.
- Ekerot CF, Jorntell H (2001a) Parallel fibre receptive fields of Purkinje cells and interneurons are climbing fibre-specific. *Eur J Neurosci* 13:1303-1310.
- Ekerot CF, Jorntell H (2001b) Parallel fibre receptive fields of Purkinje cells and interneurons are climbing fibre-specific. *Eur J Neurosci* 13:1303-1310.
- Graf W, Gerrits N, Yatim-Dhiba N, Ugolini G (2002) Mapping the oculomotor system: the power of transneuronal labelling with rabies virus. *Eur J Neurosci* 15:1557-1562.
- Groenewegen HJ, Voogd J (1977) The parasagittal zonation within the olivocerebellar projection. I. Climbing fiber distribution in the vermis of cat cerebellum. *J Comp Neurol* 174:417-488.
- Gundappa-Sulur G, De Schutter E, Bower JM (1999) Ascending granule cell axon: an important component of cerebellar cortical circuitry. *J Comp Neurol* 408:580-596.
- Hawkes R, Leclerc N (1987) Antigenic map of the rat cerebellar cortex: the distribution of parasagittal bands as revealed by monoclonal anti-Purkinje cell antibody mabQ113. *J Comp Neurol* 256:29-41.
- Herrero L, Pardoe J, Apps R (2002) Pontine and lateral reticular projections to the c1 zone in lobulus simplex and paramedian lobule of the rat cerebellar cortex. *Cerebellum* 1:185-199.
- Highstein SM, Porrill J, Dean P (2005) Report on a workshop concerning the cerebellum and motor learning, held in St Louis October 2004. *Cerebellum* 4:140-150.
- Ito M (1984) *The cerebellum and neural control*. New York: Raven press.

- Jorntell H, Ekerot CF (2002) Reciprocal bidirectional plasticity of parallel fiber receptive fields in cerebellar Purkinje cells and their afferent interneurons. *Neuron* 34:797-806.
- Jorntell H, Ekerot CF (2003) Receptive field plasticity profoundly alters the cutaneous parallel fiber synaptic input to cerebellar interneurons in vivo. *J Neurosci* 23:9620-9631.
- Jorntell H, Ekerot C, Garwicz M, Luo XL (2000) Functional organization of climbing fibre projection to the cerebellar anterior lobe of the rat. *J Physiol (Lond)* 522 Pt 2:297-309.
- Kelly RM, Strick PL (2003) Cerebellar loops with motor cortex and prefrontal cortex of a nonhuman primate. *J Neurosci* 23:8432-8444.
- King VM, Armstrong DM, Apps R, Trott JR (1998) Numerical aspects of pontine, lateral reticular, and inferior olivary projections to two paravermal cortical zones of the cat cerebellum. *J Comp Neurol* 390:537-551.
- Leergaard TB, Alloway KD, Mutic JJ, Bjaalie JG (2000a) Three-dimensional topography of corticopontine projections from rat barrel cortex: correlations with corticostriatal organization. *J Neurosci* 20:8474-8484.
- Leergaard TB, Lyngstad KA, Thompson JH, Taeymans S, Vos BP, De Schutter E, Bower JM, Bjaalie JG (2000b) Rat somatosensory cerebropontocerebellar pathways: spatial relationships of the somatotopic map of the primary somatosensory cortex are preserved in a three-dimensional clustered pontine map. *J Comp Neurol* 422:246-266.
- Llinas R (1982) Radial connectivity in the cerebellar cortex: a novel view regarding the functional organization of the molecular layer. *Exp Brain Res suppl* 6:189.
- Lockhart TE, Smith JL, Woldstad JC (2005) Effects of aging on the biomechanics of slips and falls. *Hum Factors* 47:708-729.
- Lu H, Hartmann MJ, Bower JM (2005a) Correlations between purkinje cell single-unit activity and simultaneously recorded field potentials in the immediately underlying granule cell layer. *J Neurophysiol* 94:1849-1860.
- Lu H, Hartmann MJ, Bower JM (2005b) Correlations between Purkinje Cell Single Unit Activity and Simultaneously Recorded Field Potentials in the Immediately Underlying Granule Cell Layer. *J Neurophysiol*.
- Marr D (1969) A theory of cerebellar cortex. *J Physiol (Lond)* 202:437-470.
- Morcuende S, Delgado-Garcia JM, Ugolini G (2002) Neuronal premotor networks involved in eyelid responses: retrograde transneuronal tracing with rabies virus from the orbicularis oculi muscle in the rat. *J Neurosci* 22:8808-8818.
- Odeh F, Ackerley R, Bjaalie JG, Apps R (2005) Pontine maps linking somatosensory and cerebellar cortices are in register with climbing fiber somatotopy. *J Neurosci* 25:5680-5690.
- Oscarsson O (1967) Termination and functional organization of a dorsal spino-olivocerebellar path. *Brain Res* 5:531-534.
- Oscarsson O (1979) Functional units of the cerebellum - sagittal zones and microzones. *TINS* 2:143-145.
- Oscarsson O, Sjolund B (1977) The ventral spine-olivocerebellar system in the cat. II. Termination zones in the cerebellar posterior lobe. *Exp Brain Res* 28:487-503.
- Pardoe J, Apps R (2002) Structure-function relations of two somatotopically corresponding regions of the rat cerebellar cortex: olivo-cortico-nuclear connections. *Cerebellum* 1:165-184.
- Pijpers A, Voogd J, Ruigrok TJ (2005) Topography of olivo-cortico-nuclear modules in the intermediate cerebellum of the rat. *J Comp Neurol* 492:193-213.
- Ruigrok TJ, Voogd J (2000) Organization of projections from the inferior olive to the cerebellar nuclei in the rat. *J Comp Neurol* 426:209-228.
- Sarna JR, Marzban H, Watanabe M, Hawkes R (2006) Complementary stripes of phospholipase Cbeta3 and Cbeta4 expression by Purkinje cell subsets in the mouse cerebellum. *J Comp Neurol* 496:303-313.
- Schweighofer N, Doya K, Kuroda S (2004) Cerebellar aminergic neuromodulation: towards a functional understanding. *Brain Res Brain Res Rev* 44:103-116.
- Serapide MF, Cicirata F, Sotelo C, Panto MR, Parenti R (1994) The pontocerebellar projection: longitudinal zonal distribution of fibers from discrete regions of the pontine nuclei to vermal and parafloccular cortices in the rat. *Brain Res* 644:175-180.
- Serapide MF, Panto MR, Parenti R, Zappala A, Cicirata F (2001) Multiple zonal projections of the basilar pontine nuclei to the cerebellar cortex of the rat. *J Comp Neurol* 430:471-484.
- Serratrice G (1994) [Disorders of walking in elderly subjects: towards new concepts]. *Presse Med* 23:1014-1016.
- Simpson JI, Hulscher HC, Sabel-Goedknegt E, Ruigrok TJ (2005) Between in and out: linking morphology and physiology of cerebellar cortical interneurons. *Prog Brain Res* 148:329-340.
- Sims RE, Hartell NA (2006) Differential susceptibility to synaptic plasticity reveals a functional specialization of ascending axon and parallel fiber synapses to cerebellar Purkinje cells. *J Neurosci* 26:5153-5159.
- Sugihara I, Shinoda Y (2004) Molecular, topographic, and functional organization of the cerebellar cortex: a study with combined aldolase C and olivocerebellar labeling. *J Neurosci* 24:8771-8785.
- Sultan F (2001) Distribution of mossy fibre rosettes in the cerebellum of cat and mice: evidence for a parasagittal organization at the single fibre level. *Eur J Neurosci* 13:2123-2130.
- Tarnecki R (2003) Responses of the red nucleus neurons to limb stimulation after cerebellar lesions. *Cerebellum* 2:96-100.
- Teune TM, van der Burg J, de Zeeuw CI, Voogd J, Ruigrok TJ (1998) Single Purkinje cell can innervate multiple classes of projection neurons in the cerebellar nuclei of the rat: a light microscopic and ultrastructural triple-tracer study in the rat. *J Comp Neurol* 392:164-178.
- Teune TM, van der Burg J, van der Moer J, Voogd J, Ruigrok TJH (2000) Topography of cerebellar nuclear projections to the brain stem in the rat. In: *Cerebellar modules: molecules, morphology and function* (Gerrits NM, Ruigrok TJH, De Zeeuw CI, eds), pp 141-172. Amsterdam: Elsevier Science B.V.
- Tolbert DL, Massopust LC, Murphy MG, Young PA (1976) The anatomical organization of the cerebello-olivary projection in the cat. *J Comp Neurol* 170:525-544.
- Trott JR, Armstrong DM (1987) The cerebellar corticonuclear projection from lobule Vb/c of the cat anterior lobe: a combined electrophysiological and autoradiographic study. II. Projections from the vermis. *Exp Brain Res* 68:339-354.

- Trott JR, Apps R, Armstrong DM (1990) Topographical organisation within the cerebellar nucleocortical projection to the paravermal cortex of lobule Vb/c in the cat. *Exp Brain Res* 80:415-428.
- Trott JR, Apps R, Armstrong DM (1998) Zonal organization of cortico-nuclear and nucleo-cortical projections of the paramedian lobule of the cat cerebellum. 2. the C2 zone. *Exp Brain Res* 118:316-330.
- Van Neerven J, Pompeiano O, Collewijn H (1989) Depression of the vestibulo-ocular and optokinetic responses by intrafloccular microinjection of GABA-A and GABA-B agonists in the rabbit. *Arch Ital Biol* 127:243-263.
- van Neerven J, Pompeiano O, Collewijn H, van der Steen J (1990) Injections of beta-noradrenergic substances in the flocculus of rabbits affect adaptation of the VOR gain. *Exp Brain Res* 79:249-260.
- Voogd J (1964) *The cerebellum of the cat: Structure and fiber connections*. Assen: Van Gorcum.
- Voogd J, Broere G, van Rossum J (1969) The medio-lateral distribution of the spinocerebellar projection in the anterior lobe and the simple lobule in the cat and a comparison with some other afferent fibre systems. *Psychiatr Neurol Neurochir* 72:137-151.
- Voogd J, Pardoe J, Ruigrok TJ, Apps R (2003) The distribution of climbing and mossy fiber collateral branches from the copula pyramidis and the paramedian lobule: congruence of climbing fiber cortical zones and the pattern of zebrin banding within the rat cerebellum. *J Neurosci* 23:4645-4656.
- Winkelman B, Frens M (2006) Motor coding in floccular climbing fibers. *J Neurophysiol* 95:2342-2351.
- Wu HS, Sugihara I, Shinoda Y (1999) Projection patterns of single mossy fibers originating from the lateral reticular nucleus in the rat cerebellar cortex and nuclei. *J Comp Neurol* 411:97-118.
- Xu D, Liu T, Ashe J, Bushara KO (2006) Role of the olivo-cerebellar system in timing. *J Neurosci* 26:5990-5995.
- Yatim N, Billig I, Compoin C, Buisseret P, Buisseret-Delmas C (1996) Trigemino-cerebellar and trigemino-olivary projections in rats. *Neurosci Res* 25:267-283.
- Yeo CH, Hesslow G (1998) Cerebellum and conditioned responses. *Trends Neurosci* 2:322-330.
- Zehr EP, Stein RB (1999) What functions do reflexes serve during human locomotion? *Prog Neurobiol* 58:185-205.

Summary

This thesis studies the functional organization of the intermediate cerebellum in the rat, with a special emphasis on the part that is involved in hind limb control. In *Chapter 1*, the fundamentals of cerebellar organization and function are reviewed. The intermediate cerebellum is thought to be involved in the coordination and control of the execution of movements. Furthermore, it is important in the process of acquiring new motor skills. One could say that the cerebellum operates in automating movements, in order to allow the cerebrum concern itself with other tasks. For example, when we are learning to write, we first have to focus completely on the shape of individual letters and in the sequence of fine movements to get these letters in writing. Later on, only when these movements are automated, we are able to pay attention to the meaning of combination of letters, into words and sentences. Similar processes may take place when we learn to walk and locomotion is applied to everyday living, when we are able to eat an apple or have a conversation while walking.

Although it is clear that the cerebellum is instrumental in fulfilling these requirements it is not known how its operations result in this process. While strong evidence suggests that certain structures within the cerebellum have a learning capacity through synaptic plasticity, our knowledge is lacking in understanding how the cerebellum organizes afferent information and processes this into automatic adaptive and meaningful output signals.

A thorough understanding of the flows of different modalities of information to, within and from the cerebellum is therefore a prerogative to understand cerebellar functioning. The primary topic of this thesis was to detail the organization of afferent signals to the intermediate cerebellum or paravermis (Chapters 2,3 and 4). Subsequently, it was investigated which parts of the cerebellum are involved in the control of a single muscle (Chapter 5) and what the consequences on motor behavior are after impairing one of these well-defined areas of the cerebellum (Chapter 6).

The results described in this thesis provide us with new concepts for defining and understanding problems associated with degeneration and disease of the intermediate cerebellum.

Organization of the intermediate cerebellum

In short, two types of afferent signals reach the cerebellum from the spinal cord and brainstem. Climbing fibers are all derived from the inferior olive and make direct synaptical contacts with the Purkinje cells (PCs) in the cerebellar cortex. Mossy fibers, on the other hand, sprout from various centers within the central nervous system and synapse on the granule cells, who are located in a layer of the cerebellar cortex below the PCs. Granule cells contact the PCs through their parallel fibers. A single PC receives input from only one climbing fiber and up to hundreds of thousand parallel fibers. PCs are the sole output system of the cerebellar cortex and influence the neurons in the deep cerebellar nuclei to which they project. The neurons within these nuclei form the sole

output system of the cerebellum and project to various premotor areas within the brainstem. So far, it was generally accepted that the organization of climbing- and mossy fiber systems was rather different.

In *Chapter 2* we have further detailed the present knowledge on the organization of olivo-cortico-nuclear modules in the intermediate cerebellum of the rat. These modules were identified by relating different cerebellar zones to the zebrin banding pattern (an internal frame of reference) on new 2D-surface reconstructions of the cerebellar cortex. Furthermore, using a triple labeling technique, we are the first to provide direct anatomical evidence of the interconnectivity of these modules.

In *Chapter 3* it is shown that the distribution of pontine neurons, a major source of mossy fibers, is closely related to climbing fiber somatotopy, but not so clear to climbing fiber zones (areas of cerebellar cortex based on the olivary origin of these climbing fibers). Within the pontine nuclei there is a core of neurons projecting to face-related cerebellar regions. Shells of neurons projecting to forelimb and hindlimb related cerebellar regions surround this core. These observations are similar to projections from the primary sensory cortex (S1) to the pontine nuclei. Despite the clear interlobular differences, no clear zonal differences could be made based on the present data.

Chapter 4 studies the anatomical interrelationship of functionally linked climbing and mossy fiber collaterals by relating the cortical distributions of both systems to each other as well as to the zebrin banding pattern. It was shown that both systems preferentially collateralize to cortical areas with similar zebrin characteristics as the injection site. Furthermore, the mossy fibers, like the climbing fibers, have a highly organized projection pattern and these patterns are closely related to climbing fiber somatotopy. This relation, presented in two- and three-dimensional reconstructions, thereby further details the modular organization of the cerebellum. In addition, the projections of a second mossy fiber source, the lateral reticular nucleus (LRn), were explored in a similar way as the pontine nuclei in Chapter 3. Again interlobular differences were found but no clear interzonal differences. The observed differences between the zonal distribution of mossy fiber collaterals but the non-zonal distribution of pontine and LRn neurons suggest a highly organized patterning of in- and output relations of these precerebellar centers, which warrants further exploration.

Cerebellar involvement in individual muscles

The above-mentioned chapters exemplified and elaborated the modular character of cerebellar organization. So far, it was not known to what extent modules are involved in the control of a

certain muscle. In *Chapter 5* we have tackled this problem in a series of experiments using a transsynaptic viral tracer as a marker. The (rabies) virus is, once injected into a muscle, taken up by the motor end plate and transported to the cell soma of the motoneuron belonging to that particular end plate. Here, the virus replicates, the neuron gets infected and subsequently the virus can pass the synaptic cleft of nerve fibers that project to this motoneuron. From here on, the cycle repeats itself and finally after passing three or four of those synapses PCs can get infected and labeled. This resulted in the labeling of nearly complete cerebellar modules after injection of the virus into a single hind limb muscle. Because of the previous experiments described in chapter 2, these modules could be identified. The injection of a single muscle resulted in an infection-related bilateral labeling of different cortical zones of PCs in vermal, paravermal and hemispherical areas. Slight differences between the two antagonistic ankle joint muscles were observed. Clear differences were seen when these muscles were compared to other muscles. Based on these results it is hypothesized that different cerebellar modules regulate specific aspects in the control of hind limb muscles. Interestingly, the majority of the earliest infected PCs were situated in zebrin negative cortical zones. In addition, remarkably few labeled neurons were observed in the inferior olive and none of the cortical interneurons showed any signs of infection. Furthermore, evidence was found that PCs might degenerate after prolonged infection.

Function of the C1 hind limb module

In *Chapter 6* the hypothesis that different cerebellar modules regulate specific aspects in the control of hind limb muscles was further explored. A new application of ribosome inactivating proteins made it feasible to impair a specific module and to evaluate the effects on locomotion in the rat. In these experiments the module (C1/C3) known to be involved in hind limb control, more particular the flexor muscles was injected with CTb-saporin. The results showed that there were hardly any clear alterations in locomotion or in the activity pattern (EMG) of a knee flexor, the m. biceps femoris after injection. However, it did result in a clear alteration in the gain of cutaneously-induced reflexes. In the intact animal the strength of these reflexes is highly dependent on the phase of the step cycle in which they are induced. However, after impairment of the C1/C3 hind limb module this step cycle dependent reflex modulation is sharply diminished. The results of these experiments are in line with the hypothesis that the C1/C3 module is involved in the adaptation of peripheral induced reflexes required for automatic processes involved in locomotion and adaptive responses to unexpected perturbations. Thereby the cerebellum is able to continuously adapt reflexes required in locomotion to meet biological demands.

Samenvatting

Dit proefschrift onderzoekt de functionele organisatie van het intermediaire deel van de kleine hersenen (cerebellum, paravermis) van de rat, met de nadruk op dat deel wat betrokken is bij de controle van de achterpoot. In *Hoofdstuk 1* wordt een overzicht gegeven van de beginselen van de organisatie en functie van het cerebellum. De paravermis wordt in verband gebracht met het coördineren en controleren van de bewegingen die wij uitvoeren. Daarnaast is het cerebellum belangrijk bij het aanleren van nieuwe bewegingen. Je zou kunnen zeggen dat het cerebellum betrokken is bij het automatiseren van bewegingen waardoor onze grote hersenen andere taken kunnen uitvoeren. Zo moeten wij bijvoorbeeld bij het leren schrijven eerst onze aandacht volledig richten op de vorm van de letters en de volgorde van de bewegingen die nodig zijn om die letters op papier te krijgen. Pas later, wanneer die bewegingen geautomatiseerd zijn, kan aandacht worden gegeven aan de inhoud van het geschrevene. Iets dergelijks kan ook gezegd worden over het aanleren van onze loopbewegingen en het lopen in het dagelijkse leven, wanneer we in staat zijn naast het lopen b.v. een gesprek te voeren of een appel te eten.

Het is niet duidelijk hoe het cerebellum deze automatiseringstaak uitvoert. Hoewel er sterke aanwijzingen zijn dat structuren binnen het cerebellum leervermogen hebben (de synaptische contacten tussen bepaalde typen cellen kunnen bijvoorbeeld onder invloed van deze leerprocessen blijvend veranderd worden), is het nog grotendeels onduidelijk hoe het cerebellum de aangeboden informatie structureert en aanpast tot een signaal dat tot die automatisering kan leiden.

Een goed begrip van het kanaliseren van verschillende soorten van informatie naar, binnen, en vanuit het cerebellum is daarom een vereiste om te begrijpen wat voor processen er binnen het cerebellum plaatsvinden. Het in dit proefschrift beschreven onderzoek is in de eerste plaats een zeer nauwkeurige beschrijving van de organisatie van aanvoerende signalen naar het intermediaire cerebellum van de rat (Hoofdstukken 2, 3 en 4). Vervolgens is onderzocht welke delen van het cerebellum betrokken zijn bij het controleren van de activiteit van een enkele spier (Hoofdstuk 5). Ten slotte is nagegaan wat de gevolgen zijn het buitenwerking stellen van één van deze nauw gedefinieerde delen van het cerebellum (Hoofdstuk 6).

Als zodanig verschaffen de resultaten van dit onderzoek ons belangrijke aanknopingspunten voor het begrijpen van problemen die kunnen optreden bij een verminderd functioneren van deze intermediaire delen van het cerebellum.

Organisatie van het intermediaire cerebellum

In principe lopen vanuit ruggenmerg en hersenstam twee soorten signalen naar het cerebellum. De zgn. klimvezels komen allen uit de onderste olijf en maken direct synaptisch contact met de Purkinje cellen van de cerebellaire schors. De zgn. mosvezels ontspringen van verschillende

centra en eindigen op de korrelcellen van de schors. Korrelcellen kunnen, middels hun parallel vezel contact maken met Purkinje cellen. Een enkele Purkinje cel ontvangt informatie van slechts een klimvezel maar van vele honderdduizenden parallel vezels. Purkinje cellen vormen vervolgens het output station van de cerebellaire schors en beïnvloeden de activiteit van diep in het cerebellum gelegen cerebellaire kernen waarvan de zenuwuitlopers vervolgens premotor centra van de hersenstam bereiken. Tot op heden is altijd gedacht dat de organisatie van het klimvezelsysteem en die van het mosvezelsysteem totaal van elkaar verschilde.

In *Hoofdstuk 2* wordt de bestaande kennis van de organisatie van de olivo-cortico-nucleaire modules in het intermediaire cerebellum verder gedetailleerd. Deze modules werden geïdentificeerd door verschillende zones van het cerebellum te relateren aan het zogenaamde zebrin patroon (een intrinsiek referentie kader) op 2-dimensionale reconstructies van de cerebellaire cortex. Bovendien werd het bestaan van deze modules voor het eerst direct aangetoond met behulp van een drievoudige labeling techniek.

Hoofdstuk 3 laat zien dat de distributie van neuronen in de pons, een van de belangrijkste bronnen van mosvezels, nauw gerelateerd is aan de klimvezel somatotpie, maar niet zo duidelijk aan de klimvezel zones (gebieden in de cortex gebaseerd op de specifieke oorsprong van de klimvezels). In de pons bevindt zich een kern van cellen die projecteren naar aangezicht gerelateerde gebieden in de cerebellaire cortex, omgeven door schillen van cellen welke respectievelijk projecteren naar voor- en achterpoot gebieden. Vanuit de primaire sensibele cortex (S1) worden vergelijkbare projecties gevonden naar de pons. Hoewel er duidelijke verschillen waren in interlobaire projecties werd er geen verschil gevonden tussen de verschillende zones binnen 1 lobje.

In *Hoofdstuk 4* wordt de anatomische relatie tussen functioneel gerelateerde klim- en mosvezel collateralen nauwkeurig bestudeerd door de corticale verdeling van beide systemen te relateren aan elkaar en aan het zebrin patroon. Hierbij blijkt dat beide systemen bij voorkeur projecteren naar corticale gebieden met dezelfde zebrin karakteristieken als die van de injectie plaats. Bovendien blijkt dat mosvezels, net als klimvezels, een hoge mate van organisatie kennen en dat deze organisatiepatronen sterk overeenkomen met die van de klimvezels. Deze relatie tussen deze twee systemen wordt duidelijk gemaakt in twee- en drie-dimensionale reconstructies en benadrukt nogmaals de modulaire organisatie van het cerebellum. Tot slot wordt in dit hoofdstuk het projectiepatroon van een tweede bron van mosvezels (de laterale reticulair kern) geanalyseerd zoals voor de pons werd gedaan in Hoofdstuk 3. Ook hier worden geen duidelijke interzonale, maar wel interlobulaire verschillen waargenomen. Aangezien de verdeling van mosvezelcollateralen wel duidelijke zonale karakteristieken vertoont, suggereert dit een zeer

hoge mate van organisatie in de aan- en afvoerende verbindingen van deze precerebellaire centra welke nader onderzoek behoeven.

Cerebellaire betrokkenheid bij individuele spieren

Uit het bovenstaande onderzoek is duidelijk geworden dat het cerebellum bestaat uit een aantal parallel georganiseerde modules. Het is niet precies bekend welke van deze modules betrokken zijn bij de controle van één enkele spier. In *Hoofdstuk 5* is getracht hierover informatie te krijgen door een serie experimenten uit te voeren met een transsynapische virale tracer. Het virus (rabiës virus) wordt, indien ingespoten in een achterpootspier, opgenomen door een zenuwuiteinde en getransporteerd naar het motoneuron van waaruit de zenuwvezel ontsprong. Hier kan het virus zich vermenigvuldigen en kan daarna de synapsspleet passeren van vezels die dit motoneuron beïnvloeden. Op deze manier kan het virus een volgende schakel passeren, waarna de cyclus zich herhaalt, enzovoort. Uiteindelijk, na passage van drie of vier synapsen kan het virus Purkinje cellen labelen. Dit resulteerde in de labeling van min of meer complete cerebellaire modules na injectie van het virus in een enkele spier. Dankzij de gedetailleerde informatie beschreven in *Hoofdstuk 2* was het mogelijk deze modules precies te identificeren. Injecties in een enkele spier resulteerde in een infectie-gerelateerde bilaterale labeling van verschillende corticale zones van Purkinje cellen in de vermis paravermis en hemisferen. Kleine verschillen werden gezien in het labelingspatroon van twee verschillende spieren die aangrijpen op het enkelgewricht en duidelijke verschillen ten opzichte van labeling ontstaan uit andere spieren. Op basis van deze informatie is een hypothese opgesteld die aangeeft dat verschillende cerebellaire modules verschillende aspecten van de controle van een achterpootspier zullen reguleren. Het was opvallend dat de meerderheid van de initieel geïnfecteerde Purkinje cellen gelegen was in zebra-negatieve gebieden. Bovendien werd er geen labeling gezien van de interneuronen en relatief weinig labeling in de oliva inferior. Ten slotte werd gezien dat bij langdurige infectie een deel van de Purkinje cellen kan degenereren.

Functie van de achter poot module C1

In *Hoofdstuk 6* werd vervolgens de hypothese dat verschillende cerebellaire modules verschillende aspecten van de controle van een achterpootspier zullen reguleren deels getoetst. Door een nieuwe toepassing van ribosoom inactiverende eiwitten werd het mogelijk om een specifieke module grotendeels uit te schakelen en het effect hiervan op loopgedrag in de rat te bestuderen. Bij deze experimenten werd de C1/C3 module, waarvan bekend is dat deze betrokken is bij de controle van bewegingen van de achterpoot (in het bijzonder die van de flexoren), geïnjecteerd met CTb-saporin. Dit resulteerde in nauwelijks zichtbare veranderingen in het lopen van de ratten en effecten in het activiteitspatroon (EMG) van de m. biceps femoris, een flexor van de knie. De aangebrachte laesie resulteerde echter wel in een verandering van de

sterkte van huidreflexen. Het effect van deze reflexen is normaal genomen sterk afhankelijk van het moment in de stapcyclus waarop deze geïnduceerd worden. In de dieren met een inactivering van de zgn. C1/C3 achterpoot module was deze stapcyclus afhankelijke reflexmodulatie echter sterk verminderd.

De resultaten van deze experimenten zijn in overeenstemming met de door ons opgestelde hypothese dat de C1/C3 module verantwoordelijk is voor het optimaal afstemmen van reflexen die benodigd zijn voor het automatisch laten verlopen van de stapcyclus, en/of die er voor zorgen dat de rat adequaat kan reageren indien er onverwachte obstakels voorkomen. Het cerebellum kan aldus het functioneren van reflexen die belangrijk zijn tijdens het lopen continue variëren en daarmee optimaal afstemmen op de situatie die voor het individu van toepassing is.

Dankwoord

Na vele zonnige middagen te hebben geschreven aan het proefschrift c.q. de artikelen, is het me deze zonnige middag dan toch eindelijk gelukt om aan te belanden bij het schrijven van het dankwoord.

Een proefschrift schrijven doe je niet alleen! Gelukkig maar, want anders was ik een hele boel leuke, interessante, bijzondere mensen in die 6 (!) jaar niet tegengekomen. Een ieder, die de moeite heeft genomen om dit proefschrift in meer of mindere mate door te nemen, heeft waarschijnlijk op zijn eigen wijze bijgedragen aan de tot standkoming ervan. Jullie waren de randvoorwaarden om dit mogelijk te maken. Vooral de verandering in het laatste jaar van de belangstellende vraag “hoe is het met je proefschrift?” in “wanneer is het feest?” typeert de kracht die jullie hebben om voor mij alles in het juiste perspectief te plaatsen. Ik hoop dat jullie daar nog lang mee doorgaan en tot zover alvast bedankt! Een klein aantal van deze mensen wil ik op deze plaats echter in het bijzonder bedanken.

Om te beginnen Tom: Beste Tom, mijn copromotor, plot-koning en “baas,” Ruigrok. Het is jouw enthousiasme waarmee je onderwijs geeft waardoor ik überhaupt ooit overwogen heb om OIO te worden. Zonder jouw grenzeloze vertrouwen, geduld en kennis zou dit onderzoek niet gelukt zijn. Jij hebt mij de mogelijkheid gegeven om te groeien en daarvoor kan ik je onmogelijk genoeg bedanken. Ik hoop dat je net als ik een beetje trots bent op wat nu voor je ligt.

Hierbij wil ik ook mijn promotor Chris de Zeeuw heel hartelijk bedanken. Ook zonder jouw (wetenschappelijke) inspiratie, uitstekende begeleiding en natuurlijk het verzorgen van de onontbeerlijke partij handtekeningen was dit proefschrift niet mogelijk geweest; hiervoor mijn hartelijke dank.

Beste Jan, iedereen zou willen dat hij (of zij) ooit zo veel weet van 1 onderwerp als jij weet van het cerebellum. Ik dus ook. Bedankt voor het leggen van verbanden als ik ze niet meer zag en voor alles wat je me geleerd hebt. En ja! Anatomie is wonderlijk en kan ook best hip zijn!

De volgende is Hans (vd B), alias Handige Hans. Sinds je naam in een ander proefschrift al tot werkwoord verheven is wordt het enigszins moeilijk hier nog wat aan toe te voegen. Ik denk dat er op de afdeling weinig opstellingen zijn die jij niet in elkaar geHanst, dan wel verHanst hebt. Zo ook de mijne, maar Hans kan meer dan dat! Hij is ook onmisbaar wanneer je hak is afgebroken of je bril of fiets stuk is en meer van dat soort (vrouwen?) dingen. Bovendien is er op jouw wipstoel altijd plaats en tijd voor een goed gesprek of gewoon gezellige onzin. In ieder geval, voor alles, Bedankt!

Logische volgende stap is het lab: Erika, Mandy en Elize, bedankt voor het helpen met het fixeren, snijden, spoelen, inzetten, spoelen (x oneindig), kleuren, plakken, afdekken en het

kletsen, geinen, koffiedrinken en de enorme gezelligheid. In het bijzonder jouw speciale touch Eer leidde altijd tot verbluffende resultaten.

Phebe, Bjorn en Alexander bedankt voor de broodnodige afleiding als er ik weer eens een AIO-dip of writers block had. Ook zonder jullie was dit nooit gelukt.

Beste Edith en Loes, jullie wil ik graag bedanken voor jullie zorg dat alles op de juiste tijd en plaats werd ingeleverd en m.n. ook als leverancier van koffie, chocolade, snoep, zoutjes en printer.

Bas, Arjan en Michiel jullie als drie-eenheid van 'de oude garde' hebben uiteindelijk de doorslag gegeven om mijn handtekening te zetten onder dat OIO contract. Toegegeven ik heb wel eens getwijfeld, maar toch: Ontzettend bedankt hiervoor!

Freek, later gekomen, doch niet minder belangrijk. Ook jij bedankt voor het vertrouwen dat je in me had ;-). Het is er nu dus toch van gekomen en ik wacht met spanning af op wat komen gaat! Ik wens jou en Elza veel geluk in jullie nieuwe woning.

Beste Beerend, jouw inzet was van onschatbare waarde in hoofdstuk 6. Zonder jouw matlabroutines was ik nu nog bezig met het handmatig uitwerken van de files. Bedankt!

Ook Maarten wil ik langs deze weg bedanken voor zijn advies in de analyses van dit hoofdstuk en voor het zitting nemen in de promotiecommissie.

Beste Ludo wat jij voor je medemens over hebt is gewoon weg onbeschrijflijk! Ik wil ook jou en Bernard hartelijk bedanken voor het precisie werk.

Eddie, bedankt voor het printen van de figuren en het leveren van de benodigde software.

Dear Jerry, your visits were always something to look forward to, your comments on my research a gift and no one I know can belly bump like you;-). Thank you for the great times we had and for those to come.

Of course I am also grateful to Richard and Joanne. Thank you for the learning opportunity and a wonderful time in Bristol. I had a really nice birthday!

Beste Virgil en Gerard in dit promotie traject nemen ook jullie een bijzondere plaats in. Dat begon eigenlijk al toen we 6 jaar geleden alledrie begonnen aan een promotie onderzoek. Virgil, jij als dokter, doctor en ervaren paranimf zal ongetwijfeld een grote steun zijn op de dag zelf. Gerard, als mede promovendus zitten we nu een beetje in hetzelfde schuitje. Heel veel succes op jouw promotie en een fijne tijd in Boston.

Tot slot wil ik mijn ouders en broer bedanken voor het onvoorwaardelijke vertrouwen in mij en hun steun in dit project.

Curriculum Vitae

Personalialia

Naam	Wilhemina Catharina Theodora Maria Pijpers
Geboortedatum	12 juni 1977
Geboorteplaats	Nieuw-Ginneken

Opleidingen / Aanstellingen

September 1989 – juni 1995	VWO, Nassau-Scholengemeenschap te Breda.
September 1995 – juni 1996	1 ^e kandidatuur Geneeskunde aan de Rijks Universiteit Gent
September 1996 – januari 2004	W.O. Geneeskunde aan de Erasmus Universiteit Rotterdam
September 2000 – september 2005	Promotieonderzoek getiteld: Functional anatomy of the intermediate cerebellum in the rat. Afdeling Neurowetenschappen, Erasmus MC Rotterdam
November 2005 – heden	AGNIO neurologie. Amphia Ziekenhuis Breda

List of publications

Pijpers A, Voogd J, Ruigrok TJH. 2005. *Topography of olivo-cortico-nuclear modules in the intermediate cerebellum of the rat*. J Comp Neurol, 492 (2): 193-213.

Pijpers A and Ruigrok TJH. 2006. *Organization of pontocerebellar projections to identified climbing fiber zones in the rat*. J Comp Neurol, 464 (4): 513-528.

Pijpers A, Pardoe J, Apps R, Voogd J, Ruigrok TJH. *Precise spatial relationships between mossy fibers and climbing fibers in rat cerebellar cortical zones*. Accepted J Neurosci.

Ruigrok TJH, Pijpers A, Coulon P. *Cerebellar zones involved in rat hind limb control; a retrograde transneuronal tracing study with rabies virus*. Submitted.

Pijpers A, Winkelman BHJ, Ruigrok TJH. *Selective impairment of the cerebellar C1 module involved in rat in hind limb control has specific effects on locomotion*. To be submitted.